Sveučilište u Zagrebu

FACULTY OF MECHANICAL ENGINEERING AND NAVAL ARCHITECTURE

HRVOJE DOROTIĆ

MULTI CRITERIA METHOD FOR EVALUATION OF DISTRICT HEATING AND COOLING WITH REGARD TO INDIVIDUAL SYSTEMS

DOCTORAL THESIS

Zagreb, 2022

Sveučilište u Zagrebu

FAKULTET STROJARSTVA I BRODOGRADNJE

HRVOJE DOROTIĆ

VIŠEKRITERIJSKA METODA PROCJENE VALJANOSTI CENTRALIZIRANIH TOPLINSKIH I RASHLADNIH SUSTAVA U ODNOSU NA INDIVIDUALNE

DOKTORSKI RAD

Zagreb, 2022

Sveučilište u Zagrebu

FACULTY OF MECHANICAL ENGINEERING AND NAVAL ARCHITECTURE

HRVOJE DOROTIĆ

MULTI CRITERIA METHOD FOR EVALUATION OF DISTRICT HEATING AND COOLING WITH REGARD TO INDIVIDUAL SYSTEMS

DOCTORAL THESIS

SUPERVISOR:

Prof.dr.sc. NEVEN DUIĆ

Zagreb, 2022

Sveučilište u Zagrebu

FAKULTET STROJARSTVA I BRODOGRADNJE

HRVOJE DOROTIĆ

VIŠEKRITERIJSKA METODA PROCJENE VALJANOSTI CENTRALIZIRANIH TOPLINSKIH I RASHLADNIH SUSTAVA U ODNOSU NA INDIVIDUALNE

DOKTORSKI RAD

Mentor:

Prof.dr.sc. Neven Duić

Zagreb, 2022

BIBLIOGRAPHY DATA

UDC: **620.9**
681.52
621.039.534

Keywords: district heating, energy planning, multi-objective optimisation, cogeneration, exergy, natural gas

Scientific area: TECHNICAL SCIENCES

Scientific field: Mechanical engineering

Institution: Faculty of Mechanical Engineering and Naval Architecture

Thesis supervisor: Prof. Neven Duić, PhD

Number of pages: 242

*Number of figures:*43

Number of tables: 0

*Number of references:*136

Date of examination: 09.05.2022.

Thesis defence commission:

Asst. prof. Tomislav Pukšec, PhD – Chairman of defence commission

Prof. Andrej Jokić, PhD – member

Prof. Poul Alberg Østergaard, PhD – external member

Archive: Faculty of Mechanical Engineering and Naval Architecture

TABLE OF CONTENTS

ACKNOWLEDGEMENT

The research presented in this thesis was carried out at the Department of Energy, Power Engineering and Environment, Faculty of Mechanical Engineering and Naval Architecture, University of Zagreb. Firstly, I would like to express my gratitude to my mentor and supervisor prof. Neven Duić, who introduced me to the world of research and gave me the opportunity to join his group.

I would also like to thank prof. Goran Krajačić and prof. Tomislav Pukšec who introduced me to energy planning. The research and professional advice shared with me in the past years were always highly appreciated.

My thanks goes to the whole *Powerlab*, the best research group, and the most wonderful office in the world. I would like to give my thanks to: Borna Doračić, Ana Lovrak, Matija Pavičević, Tomislav Novosel, Tibor Bešenić, Filip Jurić, Nikola Matak, Antun Pfeifer, Marko Mimica, Goran Stunjek, Hrvoje Stančin, Danijela Španović, Ivan Pađen, Tena Maruševac, Iva Gavran, Robert Bedoić, Romano Grbić, Hrvoje Mikulčić and Marko Ban. Thank you for all your exceptional research advice, philosophical discussions, for all the laughs, and the best conferences ever held.

Most importantly, I would like to express my gratitude to my mother and father who have been supportive in all my decisions and made me the person I am today. My mother was looking forward to the day of my PhD thesis defence, but unfortunately, she did not see it happen. She will always be in my thoughts…

Special thanks goes to my family and friends – for all the love, laughs and support. This would not be possible without you.

Finally, I would like to thank my fiancée and future wife Maja. You were with me during all the ups and downs in this journey. Looking forward to the next one…

PREFACE

“Do, or do not. There is no try.”

Yoda

SUMMARY

According to EU climate strategies, district heating and cooling technologies will have an important role in energy transition by contributing to energy efficiency and decarbonisation targets defined for 2030 and reaching climate neutrality by 2050. District heating and cooling systems can integrate renewable energy sources and low-temperature waste heat by utilising heat pumps combined with thermal storage. This makes them a crucial component in future energy systems where power system balancing will have a vital role. Despite these qualities, district heating is still not recognized as the primary heating source in dense urban areas. Due to its relatively low price and the distribution of existing networks in numerous EU member states, a natural gas boiler is usually the preferred heating source. The utilization of natural gas for space heating results in high exergy destruction and represents poor resource management. Due to this, its use in energy transition should be reserved for industrial processes challenging to decarbonise or the production of electrical energy in cogeneration power plants.

The main objective of this doctoral thesis is to define the energy market conditions where district systems are superior to individual natural gas solutions by considering economic, environmental and exergetic criteria. It should be mentioned that exergy is usually used for detailed thermodynamic analyses and is rarely considered in energy planning. For this purpose, a novel multi-objective optimisation method was developed based on mixed-integer linear programming capable of finding optimal system capacities and hourly operation for a whole year. Objective functions are defined as minimisation of total cost, minimisation of carbon emissions and maximisation of exergy efficiency. To deal with the multi-objective optimisation, the epsilon constraint method was utilised. Cost and carbon allocation in cogeneration units has been implemented by using a power-loss method. It is based on the reduction of a power output due to heat production. The power-loss is then translated to cost and carbon emissions allocated to heat in cogeneration units.

The obtained results have shown the importance of utilising district heating in future energy systems. Firstly, the integration of intermittent renewable energy sources in power markets will have a positive impact on district heating systems, since it will enable larger power-to-heat capacities which are becoming an economically suitable solution. The incorporation of heat prosumers and the deployment of a heat market can provide a price reduction. Secondly, the thesis quantifies the benefits of integrating district heating and cooling systems by using a multi-objective optimisation approach. Thirdly, a district heating model has been developed, which

considers the exergy destruction of a system. Exergy destruction in heat-only boilers has been calculated as the system cost. The impact of exergy taxing on the displacement of natural gas heat-only boilers has been assessed. Finally, the impact of carbon and cost allocation in cogeneration units has been evaluated. The thesis determines the range of natural gas prices for which district systems are superior to individual heating. It has been shown that cogeneration-based district heating is economically, environmentally and exergy-wise better than individual natural-gas boilers, even for low households' natural gas prices.

SAŽETAK

Centralizirani toplinski sustavi imat će važnu ulogu u energetskoj tranziciji EU-a i postizanju ciljeva energetske učinkovitosti i dekarbonizacije definiranih za 2030. te ostvarivanju klimatske neutralnosti do 2050. Centralizirani toplinski sustavi mogu integrirati obnovljive izvore energije i niskotemperaturnu otpadnu toplinu korištenjem dizalica topline u kombinaciji sa spremnicima topline. To ih čini ključnom komponentom u budućim energetskim sustavima gdje će balansiranje elektroenergetskih mreža imati važnu ulogu. Unatoč ovim kvalitetama, centralizirani toplinski sustavi još uvijek nisu prepoznati kao primarni izvor grijanja u gusto naseljenim urbanim područjima. Zbog relativno niske cijene i razvijenih distribucijskih mreža, prirodni plin često je glavni izvor grijanja u brojnim gradovima EU-a. Korištenje prirodnog plina za grijanje prostora rezultira visokim eksergetskim gubicima i predstavlja loše upravljanje energetskim resursima. Zbog toga bi njegova upotreba u energetskoj tranziciji trebala biti rezervirana za industrijske procese koji je teško dekarbonizirati ili za proizvodnju električne energije u kogeneracijskim elektranama.

Glavni je cilj ove doktorske disertacije definirati tržišne uvjete u kojima su centralizirani sustavi bolji od individualnih plinskih bojlera uzimajući u obzir ekonomske, ekološke i eksergetske kriterije. Treba spomenuti da se eksergijska analiza obično koristi za proučavanje termodinamičkih procesa, ali se rijetko uzima u obzir u energetskom planiranju. U tu svrhu razvijena je nova metoda višeciljne optimizacije koja se temelji na mješovitom cjelobrojnom linearnom programiranju, kojom se mogu pronaći optimalni kapaciteti proizvodnih jedinica i optimalno satno vođenje sustava za čitavu godine. Funkcije cilja definirane su kao minimiziranje ukupnih troškova, minimiziranje emisija ugljikova dioksida i maksimiziranje eksergetske učinkovitosti. Za rješavanje problema višeciljne optimizacije korištena je metoda epsilon ograničenja. Alokacija troškova i emisija u kogeneracijskim jedinicama provedena je metodom gubitka snage. Ona se temelji na smanjenju električne snage uslijed proizvodnje topline. Gubitak snage se zatim prevodi u troškove i emisije ugljikovog dioksida alocirane proizvodnji topline u kogeneracijskim jedinicama.

Dobiveni rezultati pokazali su da integracija varijabilnih obnovljivih izvora na tržištima električne energije ima pozitivan utjecaj na sustave daljinskog grijanja jer će omogućiti veće kapacitete dizalica topline koji su ujedno i troškovno prihvatljivi. Nadalje, uključivanje aktivnih kupaca topline i razvoj tržišta topline mogu osigurati smanjenje cijena toplinske energije. Uz to, doktorski rad je kvantificirao prednosti integracije sustava daljinskog grijanja i hlađenja

korištenjem višeciljne optimizacije. Također, razvijen je model centraliziranog toplinskog sustava koji uzima u obzir eksergijske gubitke prevedene u trošak sustava. Procijenjen je utjecaj troška eksergije na istiskivanje kotlova na prirodni plin iz troškovno optimalnog rješenja. Konačno, analiziran je utjecaj alokacije emisija i troškova u kogeneracijskim jedinicama. U disertaciji se definirao raspon cijena prirodnog plina za koje su daljinska rješenja superiornija od individualnog grijanja. Pokazano je da su centralizirani toplinski sustavi temeljeni na kogeneraciji ekonomski, ekološki i eksergijski bolji od individualnih kotlova na prirodni plin, čak i za niske cijene prirodnog plina u kućanstvima.

PROŠIRENI SAŽETAK

Ključne riječi:
centralizirani toplinski sustavi, energetsko planiranje, višeciljna optimizacija, kogeneracija, eksergija, prirodni plin

Antropogene emisije stakleničkih plinova glavni su uzročnik klimatskih promjena koje predstavljaju najveći izazov stavljen pred čovječanstvo. Premda su klimatske promjene i njihov uzrok poznate desetljećima, države svijeta tek su 2015. službeno prepoznale ovaj problem prihvaćanjem tzv. Pariškog sporazuma. On predstavlja pravno obvezujući dokument kojim se želi ograničiti povećanje srednje temperature na 2°C, s težnjom da se ne premaši vrijednost od 1.5°C. Većina istraživača slaže se da je to moguće postići dubokom dekarbonizacijom svih sektora, povećanjem energetske učinkovitosti i masovnom integracijom obnovljivih izvora energije.

Europska Unija je prepoznala problem klimatskih promjena mnogo prije potpisivanja Pariškog sporazuma, definirajući energetsko-klimatske ciljeve za 2020. koji se sastoje od: povećanja energetske učinkovitosti na 20%, povećanja udjela obnovljivih izvora energije na 20% te smanjenja emisija ugljikovog dioksida u odnosu na 1990. godinu za 20%. Ciljevi su ažurirani za nadolazeći vremenski okvir do 2030. Nadalje, EU je odredio cilj za 2050. – postići klimatsku neutralnost.

Navedeni planovi, kao što je i očekivano, temelje se na integraciji obnovljivih izvora energije, posebice vjetra i sunčeve energije korištenjem vjetroelektrana i fotonaponskih panela. Premda su ove tehnologije tržišno prihvatljive, potrebno ih je pravilno uklopiti u sektor proizvodnje električne energije. Kao potencijalno rješenje nameće se integracija sektora proizvodnje i potrošnje električne i toplinske energije, plina i sektora transporta. Jedan je od troškovno najdostupnijih načina integracija sektora električne i toplinske energije putem postojećih centraliziranih toplinskih sustava baziranih na kogeneraciji (istovremena proizvodnja električne i toplinske energije) i dizalicama topline u kombinaciji sa spremnicima toplinske energije. Na ovaj način se viškovi električne energije mogu visokoučinkovito pretvoriti u toplinsku i koristiti za pokrivanje toplinskih potreba. Dodatno, centralizirani toplinski sustavi mogu integrirati niskotemperaturnu otpadnu toplinu i obnovljive izvore energije te na taj način osigurati povećanje energetske učinkovitosti. Centralizirani toplinski sustavi sastoje se od centralnog toplinskog izvora, toplinske mreže i krajnjih korisnika (grijanje prostora, priprema potrošne

tople vode i hlađenje). Kroz povijest razvoja ovakvih sustava moguće je razlikovati četiri generacije ovisno o temperaturnim režimima i korištenim tehnologijama, pri čemu svaka sljedeća generacija ima veću učinkovitost i mogućnost integracije obnovljivih izvora energije te otpadne topline.

Premda je Europska Unija prepoznala važnost centraliziranih toplinskih sustava i predlaže njihovo korištenje, oni još uvijek nisu primarni izvor grijanja u gusto naseljenim urbanim područjima mnogih zemalja članica EU-a. Premda je uzrok tome složeni sociološki, ekonomski i tehnološki splet okolnosti, važno je spomenuti da individualni bojleri na prirodni plin ipak predstavljaju najkorišteniju tehnologiju u sektoru grijanja kućanstva EU-a. Ovu činjenicu podupire i rasprostranjenost plinske mreže te relativno niske cijene goriva u mnogim zemljama članicama EU-a. Premda prirodni plin ima relativno niske specifične emisije ugljikovog dioksida, čestica i ostalih štetnih tvari u odnosu na ugljen i loživo ulje, on i dalje predstavlja fosilno gorivo. Pri tome je bitno napomenuti da se usporedba s ostalim fosilnim gorivima mijenja ako se u obzir uzmu i fugitivne emisije metana u proizvodnji, transportu i distribuciji. Važno je napomenuti da korištenje prirodnog plina, kao visokokvalitetnog goriva, za grijanje prostora predstavlja loše upravljanje resursima. Naime, korištenje visokotemperaturne topline za dobivanje tople vode u svrhu grijanja rezultira velikim eksergijskim gubicima. Uloga prirodnog plina u energetskoj tranziciji trebala bi biti rezervirana za industrijske procese koje je prezahtjevno dekarbonizirati i za proizvodnju električne energije u visokoučinkovitim kogeneracijskim postrojenjima. Toplina iz kogeneracijskih postrojenja većinom predstavlja otpadnu toplinu koja bi bila bačena u atmosferu u slučaju da nema centraliziranog toplinskog sustava. Jedan od ključnih problema leži u činjenici da je ona rijetko tako i prezentirana.

Centralizirani toplinski sustavi često su modelirani korištenjem različitih optimizacijskih metoda. Unatoč tome, u razvijenim modelima često nedostaju određene ključne tehnologije, ne obuhvaćaju istovremenu optimizaciju kapaciteta i vođenje sustava ili ne uzimaju u obzir satnu vremensku razinu za čitavu godinu. Višeciljna optimizacija uglavnom je fokusirana na minimizaciju ukupnog troška i emisija ugljikovog dioksida. Nadalje, eksergijska analiza uglavnom je rezervirana za detaljne termodinamičke proračune industrijskih procesa, dok je njena upotreba u energetskom planiranju rijetka. Alokacija troška i emisija u kogeneracijskim postrojenjima nije česta u istraživačkim radovima i uglavnom se bazira na analizi već postojećih postrojenja te nije provedena za slučaj višeciljne optimizacije. Konačno, istraživački radovi rijetko uspoređuju rezultate optimizacije s drugim rješenjima, poput individualnih bojlera na prirodni plin.

CILJ I HIPOTEZA

Ciljevi ovoga istraživanja su sljedeći:

1. Razviti višeciljni optimizacijski model centraliziranog toplinskog sustava pri čemu su funkcije cilja definirane kao minimum ukupnog troška, minimum ekološkog utjecaja te maksimum eksergetske učinkovitosti.

2. Izraditi metodu za analizu potencijala integracije centraliziranih toplinskih i rashladnih sustava koja, osim potražnje za toplinskom energijom, uzima u obzir i tržišne uvjete te proizvodne tehnologije i kapacitete.

3. Odrediti raspon tržišnih cijena energije pri kojima centralizirani toplinski i rashladni sustavi imaju veću eksergetsku učinkovitost i manji ekološki utjecaj u usporedbi s individualnim sustavima grijanja i hlađenja, pri čemu su i ekonomski isplativi.

Hipoteza ovoga istraživanja je da se metodom višeciljne optimizacije centraliziranih toplinskih sustava može pronaći prostor rješenja gdje su centralizirani sustavi bolji od individualnih u smislu ekološkog utjecaja i eksergetske učinkovitosti, a da su pritom i ekonomski isplativi, u funkciji tržišnih cijena energije.

ZNANSTVENI DOPRINOS

Očekivani znanstveni doprinosi ovog istraživanja su sljedeći:

1) Višeciljni optimizacijski model centraliziranog toplinskog sustava koji je u mogućnosti odrediti kapacitete proizvodnih postrojenja i njihov rad pritom uzimajući u obzir ukupni trošak, ekološki utjecaj te eksergetsku učinkovitost sustava.

2) Tržišni uvjeti pri kojima su centralizirani toplinski sustavi istovremeno bolji od individualnih u smislu ekološkog utjecaja i eksergetske učinkovitosti, a ujedno i ekonomski isplativi.

METODE I POSTUPCI

Za potrebe doktorskoga rada je razvijen višeciljni optimizacijski model kojim se mogu dobiti optimalni kapaciteti proizvodnih postrojenja i toplinskih spremnika, uključujući vođenje sustava na satnoj razini za čitavu godinu. Alokacija emisija i troška u kogeneracijskom postrojenju modelirana je pomoću metode gubitka električne snage. Naime, uslijed povećanja proizvodnje topline u kogeneracijskome postrojenju dolazi do gubitka električne snage na

turbini. Taj gubitak električne snage preveden je u trošak i emisije uslijed proizvodnje topline. Funkcije cilja definirane su kao minimum ukupnog troška, minimum emisija ugljikovog dioksida te maksimum eksergetske učinkovitosti. Važno je navesti da konačno rješenje višeciljne optimizacije nije jedan broj, već čitav niz rezultata koji čine tzv. Pareto frontu. Ona predstavlja kompromis između svih funkcija cilja jer se optimumi često ne poklapaju. Problem višeciljne optimizacije riješen je korištenjem metode epsilon ograničenja. Pomoću nje je moguće problem višeciljne optimizacije svesti na problem jednociljne optimizacije uz dodatna, tzv. epsilon, ograničenja. Variranjem različitih epsilon ograničenja uz optimizaciju definirane funkcije cilja moguće je vizualizirati čitavu Pareto frontu. U ovome slučaju zapravo se radi o Pareto površini pošto je problem definiran s tri funkcije cilja. Optimizacijski problem modeliran je koristeći mješovito cjelobrojno linearno programiranje u besplatnome programskome jeziku otvorenog koda *Julia*, odnosno paketu za optimizaciju pod nazivom *JuMP*. Kao optimizacijski rješavač korišten je komercijalni rješavač s akademskom licencom zvan *Gurobi*.

KEYWORDS

District heating

Energy planning

Multi-objective optimisation

Cogeneration

Exergy

Natural gas

KLJUČNE RIJEČI

Centralizirani toplinski sustavi

Energetsko planiranje

Višeciljna optimizacija

Kogeneracija

Eksergija

Prirodni plin

LIST OF ABBREVIATIONS

CHP	cogeneration
DH	district heating
DHW	domestic hot water
DC	district cooling
EH	electrical heater
EU	European Union
GHG	greenhouse gasses
HOB	heat-only boiler
HP	heat pump
P2H	power-to-heat
RES	renewable energy sources
ST	solar thermal

NOMENCLATURE

Chemical formulas

CO_2	carbon dioxide

Variables and parameters

A_{ST}	area of solar thermal collectors [m^2]
a_1	first order heat loss coefficient [W/K]
a_2	second order heat loss coefficient [W/K^2]
b	binary variable, technology selection [-]
C	cost [EUR]
$Cost_{CHP}$	total cost of CHP unit [EUR]
$Cost^*_{CHP}$	cost of CHP unit allocated to heat [EUR]
$CO_{2_{CHP}}$	Total carbon emissions of CHP unit [tonnes of CO_2]
$CO^*_{2_{CHP}}$	Carbon emissions of CHP unit allocated to heat [tonnes of CO_2]
DEM	district heating demand [MW]
e_{Exe}	exergy factor of the fuel [-]
e_{CO_2}	Specific carbon emissions of a fuel [tonnes of CO_2/MWh]
E	electrical energy production in CHP unit [MWh]
Ex_{in}	exergy input [MWh]
Ex_{out}	exergy output [MWh]
f_{eco}	ecological objective function [tonnes of CO_2]
f_{econ}	economical objective function (EUR)
f_{exe}	exergetic objective function [-]
$f_{Lorentz}$	Lorentz factor of the heat pump [-]
G	global solar radiation [W/m^2]
P	supply capacity [MW]
Q	thermal energy [MWh]
$r_{up-down}$	ramping limit of technology [h^{-1}]
SOC	state-of-charge [MWh]
T	temperature [°C]
TES	thermal storage
TES_{in-out}	thermal storage charge and discharge [MW]

Greek letters

β_{CHP}	power-loss factor of CHP unit [-]
η	technology efficiency [-]
η_0	optical efficiency of solar thermal collector [-]
ε_{eco}	epsilon constraint for ecological objective function [tonnes of CO_2]
ε_{exe}	epsilon constraint for exergetic objective function [-]
σ_{CHP}	power-to-heat factor of CHP unit [-]

Subscripts

eco	ecological
econ	economical
exe	exergetic
fix	fixed
i	technology type
inv	investment
t	time
var	variable

LIST OF FIGURES

1 INTRODUCTION

This section provides the background of the topic and a driving motivation for this thesis. This is followed by the definition of district heating and cooling systems. Then, the literature review is presented, which provides a knowledge gap analysis of the introduced topic, while focusing on optimisation techniques in general, exergy analysis in energy planning, a multi-objective optimisation in district heating systems and different allocation methods in cogeneration units.

1.1 Background

In this section, an overview of the climate change problem is given, and its potential solution is briefly explained. This is followed by a definition of a district heating system and its role in reaching climate neutrality. The most important characteristics of district technologies are introduced. Finally, the prospects of district heating and cooling are discussed.

1.1.1 Global warming and climate change

Anthropogenic greenhouse gas (GHG) emissions are the main cause of global warming and climate change [1]. The humankind has been constantly emitting carbon dioxide (CO_2), and other GHG since the industrial era, thus increasing their concentration in the atmosphere [2]. Consequently, this resulted in an average global temperature rise [3]. Scientists agree that an increase of 2°C presents a threshold which will result in irreversible climate change [4]. Tackling this issue presents one of the greatest challenges that humankind has ever faced since all nations will have to cooperate swiftly and efficiently.

Most countries have officially recognized this problem and undertaken to face this challenge during the 21st Conference of the Parties (COP 21) in 2015, organized in Paris, by adopting the so-called Paris Agreement [5]. It is a legally binding climate change agreement which sets a framework to avoid the 2°C temperature increase with ambition to curb it below 1.5°C. Most researchers and policy developers agree that this could be achieved through deep decarbonisation of all energy related sectors and large-scale integration of renewable energy sources (RES) [6], [7].

It should be mentioned that the European Union (EU) has officially and legally identified this problem before the signing of the Paris Agreement by developing energy and climate strategies for 2020 [8]. The goals of the 2020 strategy are the reduction of CO_2 emissions by 20% (when

compared to 1990 levels), as well as an increase in energy efficiency and renewable energy share by 20%. All these goals were achieved by the end of 2020 [9]. The energy and climate strategy for 2030 is pushing these goals even further: a 40% GHG reduction (when compared to 1990 levels), achieving at least a 32% share of renewable energy and at least a 32.5% improvement in energy efficiency [10]. All EU member states had to develop National Energy and Climate Plans (NECP) which define how they will contribute to reaching the abovementioned goals. Even so, the EU went one step further in its decarbonisation policy by developing a long-term strategy which will make the EU climate-neutral by 2050 [11]. This implies achieving net-zero GHG emissions in all sectors: energy, industry, transport, buildings, agriculture and forestry.

At the heart of all decarbonisation policies is an energy efficiency increase and a large-scale integration of RES, primarily wind and solar, by using wind turbines and solar photovoltaics. Although these technologies already reached market maturity and are becoming an economically feasible option for an electrical energy production [12], [13], they are challenging to integrate in power sectors due to their intermittency and variability in electricity production [14]. Nevertheless, researchers are already suggesting that a potential solution for this challenge is a integration of different energy sectors, usually referred to as sector coupling [15]. The main idea behind this is that variable RES production could be balanced by transforming the excess of electricity production to various energy vectors such as hydrogen, synthetic gasses, heat or cold and storing it for later use. This solution has already been recognized by the EU since the Strategy for energy system integration was proposed [16]. In order to deploy capacities for a large-scale sector coupling, the EU's industrial sector will have to scale-up and reduce the cost of technologies such as electrolysers [17], fuel-cells and batteries [18]. However, one of the most recognizable technologies for energy efficient and low-cost sector coupling is already available – heat pumps and electrical heaters in combination with thermal storage [19], [20], [21], [22]. These technologies enable power and heating sector coupling, thus they are usually called power-to-heat (P2H) technologies [23]. Their large-scale implementation is already possible by using district heating (DH) systems. Furthermore, DH can enable an additional connection between the power and the heating sector by using another proven technology - cogeneration (CHP) units, which can simultaneously produce electricity and heat [24]. Besides sector coupling, district heating has additional benefits such as efficient energy utilization through the integration of a low-temperature RES [25] and waste heat [26],

thus contributing to all EU's energy and climate policy targets [27]. District heating and cooling systems and their benefits are explained in a detail below.

1.1.2 Definition of district heating and cooling

District heating systems provide thermal energy to final customers [28]. The thermal energy is usually produced at a central location and then distributed to end-users by the use of a thermal network. There are various network types depending on coverage area, the number of pipes, pressure and temperature levels, but they can be usually divided in two groups – ring or meshed networks. Starting at the central location, a supply line feeds the medium (hot water) at the supply temperature to the final users. Thermal energy from the thermal network (primary loop) is commonly transferred to the end-user (secondary loop) by using a heat exchanger at the heating substation. Here, the thermal network medium is cooled down to the return temperature and is pumped back to the central location through the return pipe. At the building level (secondary loop), thermal energy is used for space heating (SH) and domestic hot water (DHW) preparation. The temperature levels of the space heating demand must be correlated to the thermal network temperature. In other words, new or retrofitted buildings usually require lower temperature levels and older and non-renovated building blocks usually require higher temperature for space heating [29]. Sometimes, the final customers require thermal energy at a higher temperature, or even have a steam demand, such as industrial plants [30]. In that case both a thermal network and a supply unit at the central location must respond appropriately to these requirements. The temperature level of the district heating is a crucial parameter since it affects the system configuration and efficiency, available RES utilization potential, running and investment costs, GHG emissions and primary energy consumption. In fact, the temperature levels of the system are used when describing the technological progression of district heating.

1.1.3 Generations of district heating

Throughout the history of DH systems, four generations can be defined [28], [31] as shown in Figure 1. The first generation used steam as the energy carrier which resulted in extremely high system temperatures (more than 200°C) and a low energy efficiency. A thermal network consisted of steam pipes and massive concrete ducts, while supply technologies usually involved only coal or waste heat-only boilers. Although these systems were predominantly used at the beginning of the 20th century, they are still used today in old and large DH networks. The second generation used pressurized water as the energy carrier at temperatures higher than 100°C. Although system temperatures were lower than in the first generation, thermal

losses were still relatively high. In the second generation, coal and oil CHP in combination with thermal storage were dominantly used, while the thermal network still used heavy equipment and built-on site stations. In the third generation, thermal network temperatures were reduced below 100°C, thus achieving an even lower thermal losses in the network and, more importantly, providing the possibility of integrating renewable energy sources such as solar thermal or geothermal. Furthermore, these system temperatures enabled the utilization of industrial surplus heat which would otherwise have been wasted and emitted into the ambient air. Besides new heat supply options, the thermal network also evolved by using pre-insulated pipes, including substations, data metering and demand monitoring. Finally, in the fourth generation of district heating (4DH), temperatures were additionally reduced, below 70°C (50-60°C), while energy efficiency of the thermal networks are higher than 90%. This generation is characterized by low temperature space heating demand combined with low temperature sources. At such network temperatures, heat pumps could be effectively utilised to boost low-temperature thermal energy source and inject it to the thermal network grid. This way, power and heating sector coupling can easily be achieved. The system could be additionally upgraded if P2H units are coupled with thermal storage. This enables flexible production of thermal energy and utilisation of low electricity market prices. In general, 4DH is usually used along the term "smart energy system", which enables the integration of multiple energy sectors such as electricity, gas, transport, heat and cold grids [32]. To enable an optimal operation of all sectors, on both an individual and system level, energy metering and data analysis must be incorporated by using smart meters. This should enable bidirectional metering, thus making the final user (consumer) also a producer (provider), i.e. a "prosumer".

Similarly to the district heating, district cooling (DC) systems provide cooling energy to a final customer by using, similarly to DH, cooling networks. The energy carrier is usually water, chilled to around 8°C. As it passes through end user's substation, it is heated up to around 12°C and then returned to the cold supply unit. Cooling technology usually includes absorption or compression heat pumps, combined with cold storage. Although district cooling is dominantly used in hot climates such as the Middle East, there are numerous DC systems in northern EU countries [33]. Unlike district heating, district cooling is not categorized according to temperature levels.

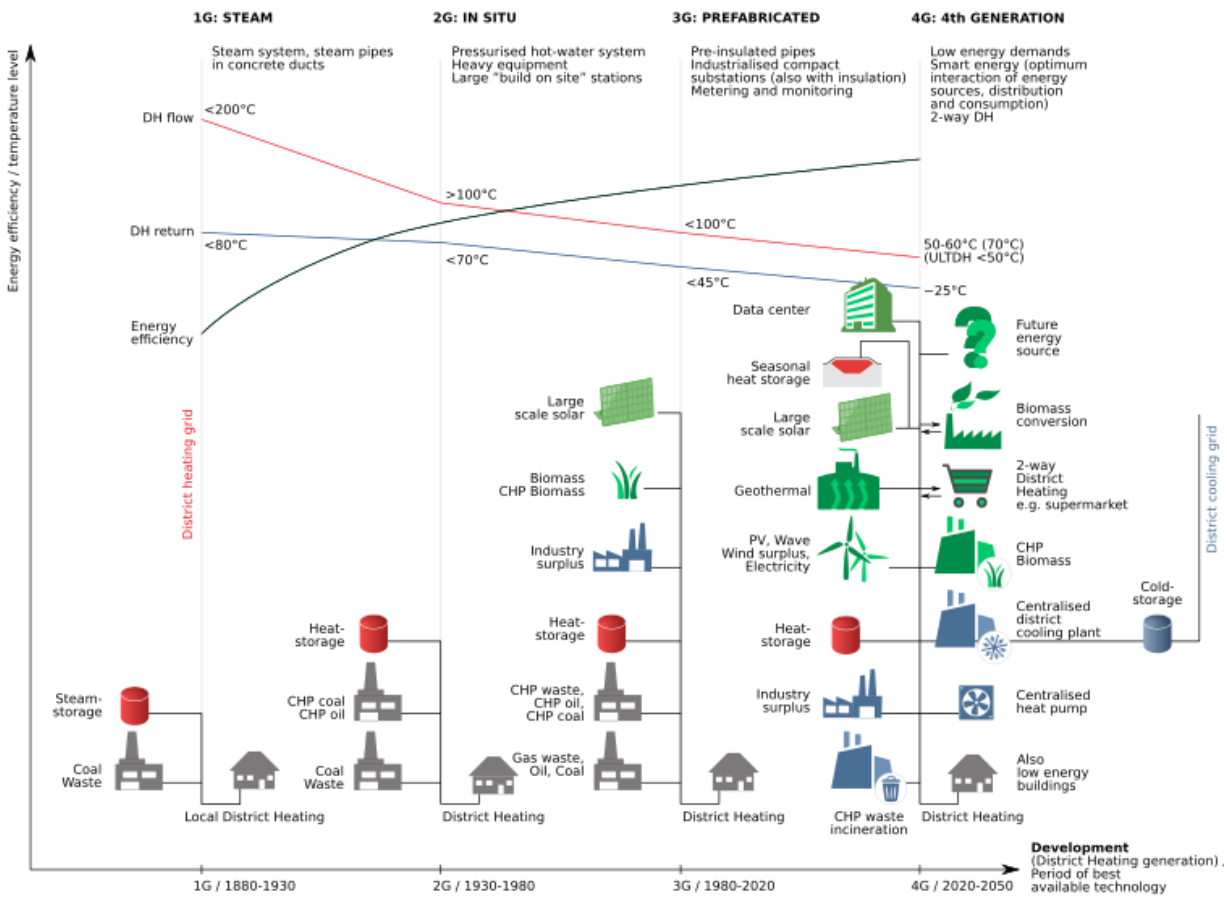

Figure 1 District heating generations [31]

Although the categorization of district heating systems by using a specific generation is relatively simplified, certain trends can be recognized [28]. The refurbishment of buildings and the development of building stock with lower space heating demand enables a reduction in supply temperature in the thermal network, which results in the following:

- reduction of thermal losses in the thermal network and thermal storage units;
- increase in energy efficiency of supply units such as: cogeneration, heat pumps, solar thermal collectors, heat-only boilers;
- increased potential for the utilization of low temperature renewable and waste heat sources;
- enabling more efficient coupling of power, heating and cooling sectors;
- enabling a bidirectional flow of energy in district heating and cooling grids, i.e. encouraging the integration of prosumers in the network.

Although most of the current DH systems belong to the second or third generation, researchers are already exploring next, i.e. 5th generation sometimes called the ultra-low temperature, neutral temperature or low-exergy DH networks [34]. They tend to bring energy and exergy

losses to as low level as possible by using even lower temperature in the networks – less than 55°C for ultra-low temperature and around 20°C for neutral temperature DH networks. However, with supply temperature reduction additional challenges arise, which should be considered. Although the supply temperature for space heating demand can be low, for DHW preparation it still has to be relatively high, around 60°C, to eliminate the risk of *Legionella* [35]. For this reason, such networks have booster heat pumps, usually installed at the end-user substation, to reach higher temperatures needed for DHW. In the case of neutral temperature DH networks, individual booster heat pumps are also usually needed to cover the space heating demand. Basically, in such systems the district heating network serves as a thermal source for individual booster heat pumps, thus increasing installed P2H capacities and providing an additional source of flexibility through power and heating sector coupling.

1.1.4 Cogeneration systems

Cogeneration, or combined heat and power, can provide the simultaneous production of electrical and thermal energy. It is a crucial technology in DH systems since it utilizes heat that would usually be wasted in the ambient air through cooling towers, as is the case in non-CHP condensation power plants. Furthermore, it has relatively high energy and exergy efficiency and consequently can provide a high-quality transformation of energy. These systems can be generally divided in two main groups: back-pressure cogeneration and extraction CHP plants. In back-pressure CHP units, power and heat production are directly correlated, i.e. heat production follows power and vice-versa. The total output of heat, i.e. power, is proportional to the steam flow in the turbine. It should be mentioned that steam does not expand to the lowest possible pressure, since it must provide thermal energy for district heating through the heat exchanger, while satisfying the minimum temperature difference. For this reason, a small part of the power output in the turbine is lost at the expense of district heating. Extraction cogeneration units are more complex systems where steam is extracted at different pressure levels (and different temperatures) from the turbine to cover the district heating load. As a result, the operation of CHP units is more flexible since electricity production does not strictly follow heat production and vice versa. The reduction of the supply temperature in both back-pressure and extraction CHP units results in higher power for the same heat generation. This can be directly translated into higher efficiency, lower carbon emissions and lower primary energy consumption.

1.1.5 Integration of waste heat and low-temperature thermal sources

As previously mentioned, district heating systems can offer a large-scale integration of low-temperature renewable energy and urban waste heat sources. There are already numerous DH systems in the EU that successfully combine solar energy and classical heat supply units to increase the RES share and reduce carbon emissions of their system. Solar district heating operates as follows. Solar energy is transformed into heat by using solar thermal collectors. In the case of a high solar fraction (share of demand covered by solar), large thermal storage, or even seasonal, can be used.

The second most common RES, except biomass, which is used in heat-only boilers or CHP units, is geothermal energy. Different renewable energy sources are often coupled [36]. To directly use geothermal energy and feed it to the DH system, soil and underwater geothermal potential must be analysed. Once the location is defined, geothermal water is brought to the surface through production wells and thermal energy is transferred to the thermal network by using heat exchangers while geothermal water is returned to the soil through the injection well.

Besides renewable energy, there are numerous urban waste heat sources that can be successfully utilized in the DH networks. The most obvious heat sources are industrial or chemical facilities which involve high-temperature processes [37]. Although such heat is suitable for integration in the DH networks, there is a high possibility that it has already been utilised at the location. Furthermore, such facilities are often located far away from the urban, densely populated regions, where a DH system is usually located. Due to this, it could be challenging to connect such a heat source with a thermal network. On the other hand, there are numerous low-temperature heat sources in urban areas such as supermarkets and shopping malls [38], data centres [39], etc. All these facilities have relatively high cooling demands, which means that large amount of heat must be ejected into the atmosphere. Once again, this energy could be utilized in a district heating system. However, such waste heat is usually available at a relatively low temperature, which means it cannot be injected directly into the high-temperature DH networks. In order to boost the temperature of the heat source, heat pumps can be used [40], [41].

1.1.6 Power-to-heat technologies

The heat pump is a power-to-heat technology that uses electricity to provide thermal energy [42]. The simplified heat pump cycle is as follows. Electrical energy is used to drive the compressor and compresses an evaporated working medium, thus also increasing its

temperature. In the condenser, the working medium is cooled down and condenses, while giving away its heat to the heat sink. In case of DH systems, the heat sink is the supply line of the thermal network. Then, the working medium expands in the expansion valve, thus decreasing its pressure. The working medium is afterwards heated up in the evaporator, i.e. evaporates by using a heat source and is finally brought back to the compressor. In DH networks, heat sources may differ from renewable energy, industrial or other urban waste heat sources. The efficiency of the cycle is defined by using the term *Coefficient of Performance* (COP), which is higher than unity [43]. COP is the ratio of electrical energy used at the compressor and the heat transferred to the heat sink at the evaporator.

The temperature difference between the heat source and the heat sink temperature is a crucial parameter when discussing a successful integration of heat pumps in DH systems, since it impacts the COP of a heat pump, i.e. the running costs of the system. The heat sink and source temperature difference are directly correlated to the *temperature lift* of a heat pump. The smaller the temperature lift is, the higher the COP of a heat pump is. This means that heat pump integration potential is higher if the temperatures of a heat sink and heat source are as close as possible. In other words, the reduction of district heating's supply temperature provides significant potential for heat pump integration.

Besides the heat pump, there is additional technology, which is using electrical energy as a fuel. We are talking about electrical heaters, or sometimes called resistant heaters. They operate on the Joule heating principle: electrical current flows through an electrical resistor and turns electrical energy into heat. Although energy efficiency of such transformation is relatively high, reaching up to 99%, it is rather low when compared to heat pumps' COP which is usually higher than 250%. This means that operating costs of electrical heaters [44] are at least two times higher than those of heat pumps. However, the investment cost of electrical heaters is several times lower [45]. For this reason, heat pumps operate as a baseload technology, reaching more than 4000 full-load hours, while electrical heaters usually serve as the peak load technology.

1.1.7 The role of district heating in future energy systems

As already mentioned, P2H technologies will have a great role in future energy systems with a high share of variable RES, such as wind and solar, to secure the balancing of a power grid [46], [47]. They can efficiently utilize the excess of electricity production and transform it into thermal energy that could be used in district heating systems. According to the microeconomic theory of power market systems [48], [49], during periods of excess electricity

production, market prices are reduced and can even reach negative values [50], as shown in Figure 2. In these periods, the operational cost of P2H technologies is relatively low or can even obtain negative values.

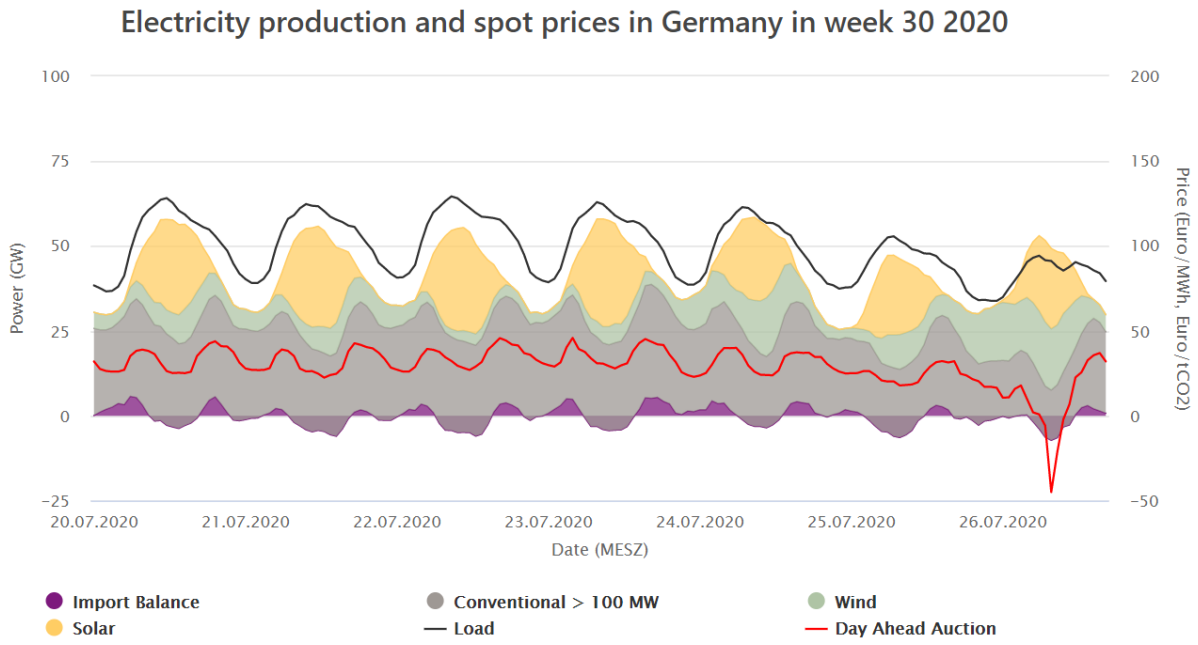

Figure 2 Power market prices and influence of RES production [51]

However, in order for the P2H technology to efficiently utilize the low power market, there has to be district heating demand, which sometimes is not the case, e.g. during nights with high wind turbine production and low heating demand. To increase the flexibility of a district heating system, P2H units are combined with thermal storage. Thermal storage can serve as an energy buffer by storing thermal energy produced via P2H units at low market prices and discharge it in the upcoming periods of high market prices. Similarly to this, thermal storage can be used in combination with CHP units. However, this time CHP will tend to operate during periods of high market prices and store the excess of heat production in thermal storage. Such systems have already been implemented, e.g. in Skagen, Denmark [52]. Currently, the Skagen DH system consists of waste heat sources, P2H and CHP units and thermal storage [53]. Its operation for a whole week is shown in Figure 3. When the power market price (green line) is below a certain threshold, the heat pumps (light yellow) are operating. In a period of relatively high power market prices, cogeneration units (dark green) are operating, and heat pumps are shut down.

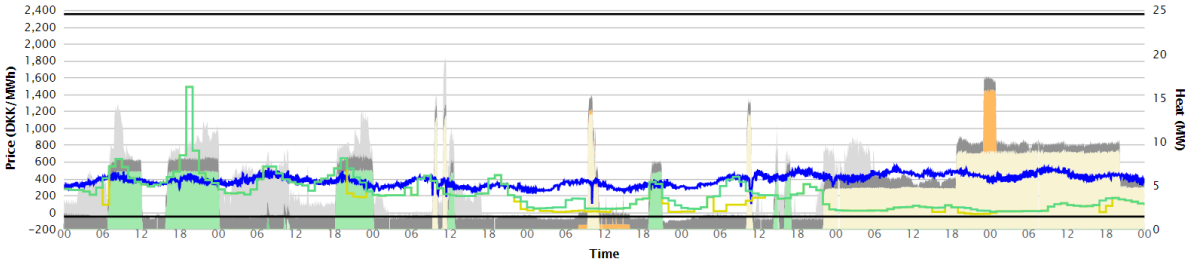

Figure 3 Skagen district heating system operation coupled with the power market [53]

When talking about power and heating sector coupling on a national energy system level, the term *Critical Excess of Electricity Production* (CEEP) should be introduced. It is defined as the excess of electrical energy production which cannot be exported, stored or transformed to other energy carriers. In other words, in order to secure the stability of the power system, such energy production, usually coming from variable RES, must be curtailed. It has been shown that large scale implementation of P2H technologies can effectively curb CEEP in energy systems with high penetration of variable RES [54].

1.1.8 District heating and cooling in urban areas

Although numerous benefits of district heating have already been mentioned, there are economical constraints that should be considered. These constraints are mostly correlated to heating demand density which is defined as the ratio of thermal energy delivered to the final customer and the corresponding area of the DH network. District heating demand mapping currently presents a crucial issue when dealing with the energy planning of district systems and is often a topic of research papers [55]. It has been shown that the increase of heating demand density drastically reduces the specific investment cost of the DH grid, thus increasing the economic feasibility of the DH implementation. Paper [56] shows that for 2,000 GJ/ha of heat demand density, the investment cost is reduced to less than 40 EUR/GJ of the annual heat demand. This means that DH is more profitable in densely populated urban areas with high heating demand density [57].

1.1.9 Future prospects for district heating systems

Although district heating is a relatively old concept, it has finally been recognized as crucial technology for heating and cooling decarbonisation in 2016 when the EU published its Strategy for Heating and Cooling [58]. According to the mentioned strategy, district heating and cooling systems will support decarbonisation, energy efficiency and the integration of renewable energy in the heating and cooling sector. Furthermore, potential for industrial waste heat integration through district systems has been identified, while cogeneration was listed as a vital technology

whose economic potential has not been fully exploited. Power-heating sector coupling was briefly mentioned, focusing on smart metering, smart grids and storage technologies. Therefore, the EU is more than aware of the importance of energy system integration. For this reason, the EU delivered the Strategy for Energy System Integration [59]. In the strategy, district heating and cooling was recognized as a useful tool for sector coupling through the utilization of P2H and thermal storage technologies.

Even though the EU promotes the expansion of existing and development of new systems, DH systems have various barriers that should be tackled in order to secure its position in future energy systems. The first barrier is related to the negative perception of DH – as a technology which brings numerous technological issues and is difficult to implement and maintain. This is the consequence of the fact that large DH systems are relatively old, use outdated technology and have large distribution losses. The best example of this issue is Romania which continuously decreases the number of connected users [60]. The second issue is related to pricing, which varies greatly in the EU [61]. In old buildings, with no individual heating substations, heat allocators should be used. This sometimes presents an additional barrier since end-users must finance it by themselves, while heating bills could stay the same or could even be increased. Furthermore, from 2020, all new buildings must be nearly-zero energy buildings (nZEB) [62]. To accomplish this, certain criteria must be fulfilled. These are usually related to primary energy consumption and RES share. However, the primary energy factor of DH varies between EU member states [63]. The main issue is that in some cases, the primary energy factor of DH is relatively high, higher even than primary energy factor for fossil fuels. This is another issue that will surely impact the expansion of future DH systems. Finally, in countries where district heating zoning has not been implemented, DH systems are in direct conflict with individual heating solutions. Although this does not represent a problem in rural areas where final customers often use biomass as a fuel, this becomes an issue in densely urban areas where final customers are choosing individual heating solutions, such as natural gas boilers [64] or electrical heaters [65], rather than DH systems.

1.2 Motivation and general overview

This section provides the main motivation for writing this thesis. Firstly, the role of natural gas in energy transition is explained, followed by the overview of natural gas usage in a heating sector. Then, exergy efficiency is introduced as a parameter for the evaluation of energy

transformation quality. Finally, the role of district heating and cooling in energy system decarbonisation is proposed and the main research question is defined.

1.2.1 The role of natural gas in energy transition

Natural gas has an almost two times lower carbon factor than coal and potentially emits a much smaller amount of PM particles during combustion. As a result, natural gas is often considered as the most environmentally friendly fossil fuel. However, it has serious problems related to the emission balancing due to fugitive emissions [66] from various locations in production, transportation and distribution infrastructure. When considering that a global warming potential of a methane is more than 20 times higher than carbon dioxide's [67], the comparison with more carbon-intensive fossil fuels changes dramatically against natural gas.

Nevertheless, natural gas is widely accepted as a "bridge" fuel between coal-based and future RES systems. According to the IEA report from 2019 [68], natural gas can achieve carbon savings and improve air quality in numerous energy markets, especially USA, China and India. Gillessen et al show that natural gas can support the transformation towards sustainable energy systems and that the energy security of natural gas increases as an energy system transformation progresses [69]. Nonetheless, numerous papers are questioning the role of natural gas in the energy transition as a "bridge fuel". McGlade et al concluded that natural gas will unlikely serve in favour of a cost-effective decarbonisation of UK energy system [70]. Zhang et al suggest that the replacement of coal with natural gas power plants can delay the introduction of near-zero emission energy systems for more than 24 years [71]. Besides electricity production, natural gas is expected to provide support in the transition of other energy sectors such as transportation and industry. The solution for future sustainable transportation is still under discussion due to numerous different options available: electricity, biofuels, hydrogen or synthetic fuels [72]. Airplanes, heavy-weight and long-range vehicles are especially challenging. Ogden et al provided insights on using natural gas as a bridge to a hydrogen-based fuel cell vehicles [73]. A potential cost-effective solution appears to be a blend of renewable hydrogen and natural gas systems, while the re-purposing of existing natural gas fuelling stations for hydrogen services is not economically feasible. According to Henry and Majumdar, the high-temperature energy demand in industry processes is one of the five challenges for decarbonisation [74]. For coal-based industries, the decarbonisation of high-temperature processes could be carried out to some extent by switching to natural gas.

While the mentioned sectors have different reasons for using natural gas as a bridge fuel during the energy transition, space heating and domestic hot water preparation in households and public buildings should use different options during the energy transition.

1.2.2 Natural gas for space heating and domestic hot water preparation

According to Bertelsen and Vad Mathiesen, around 50% of the residential heat consumption in EU in 2015 was covered by natural gas [75], as shown in Figure 4. The main reason behind this is the phase-out of coal as a fuel for residential heating during the 1990s and heating oil in the 2010s. It should be mentioned that a great part of heating oil was replaced with biomass. Throughout this period, the share of district heating has been kept almost the same. Biomass is dominantly used in rural areas with relatively low heating demand density, i.e. where district heating systems generally are not an economically viable solution. Due to this, the biggest competitor for district heating in the urban areas is natural gas. This issue becomes even more alarming when natural gas prices are considered. The average natural gas price for households in the EU is around 65 EUR/MWh [9], as shown in Figure 5. The highest price is reached in Sweden, around 118 EUR/MWh, followed by Spain, Netherlands and Italy. On the other side of the price range, the lowest natural gas prices in the EU are in Romania, Hungary and Latvia, around 35 EUR/MWh. It should be noticed that one third of EU countries have natural gas prices for households lower than 45 EUR/MWh. These prices, together with the already existing natural gas infrastructure, present a major obstacle for a successful and continuous expansion of district heating systems in cities without specified heating zones.

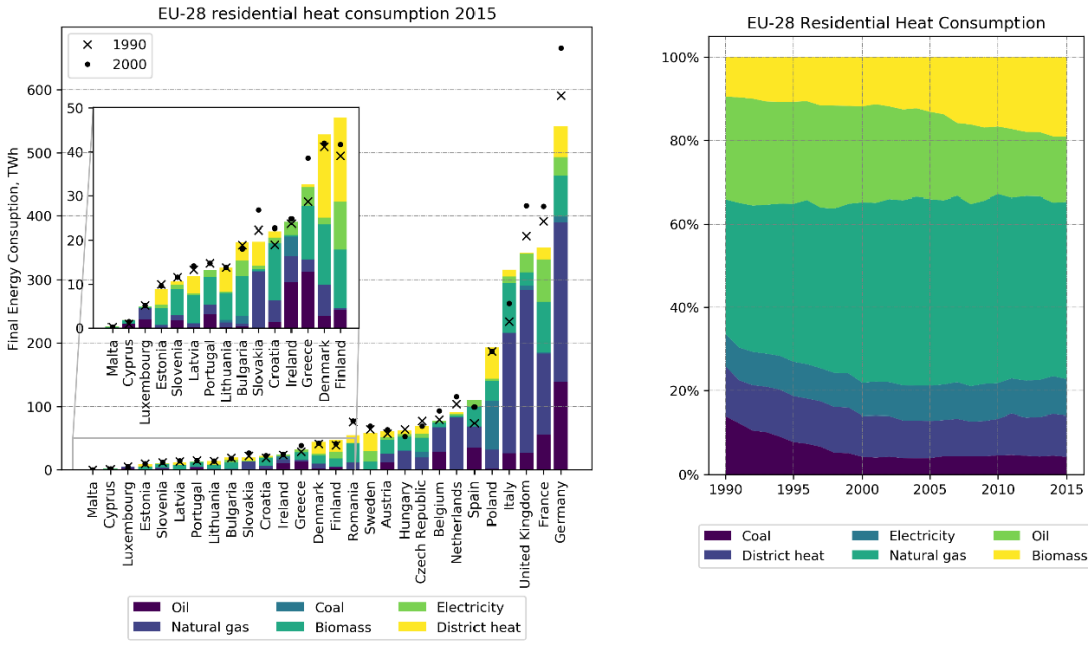

Figure 4 EU-28 Residential heat consumption [75]

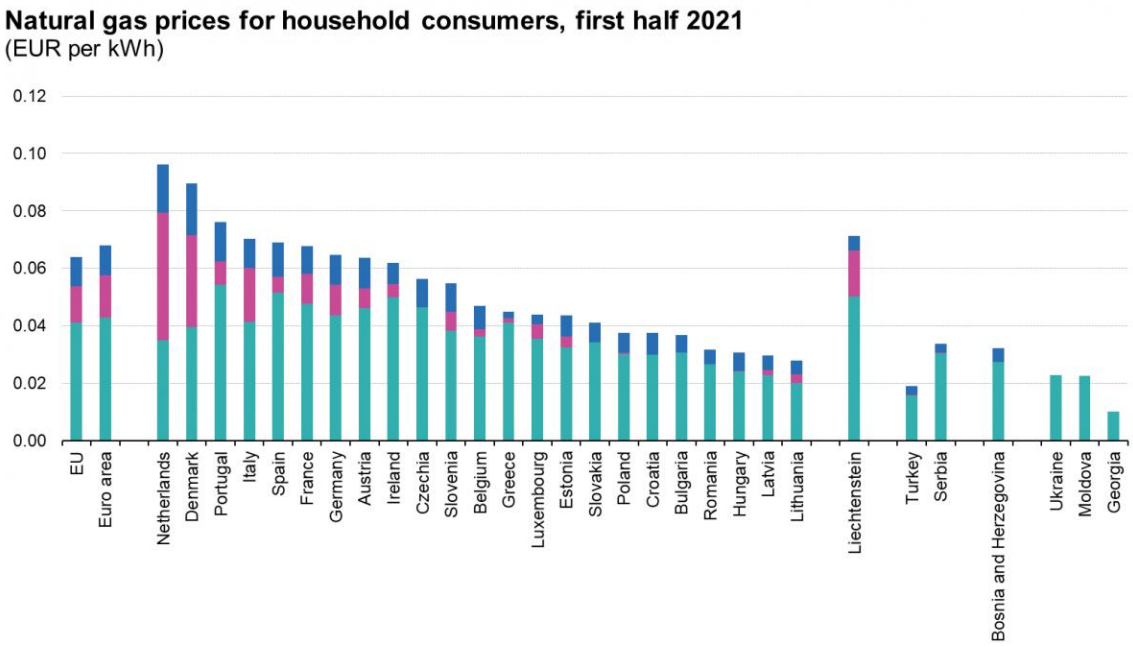

Figure 5 Natural gas prices for residential consumers [9]

1.2.3 The quality of energy transformation – exergy efficiency

When discussing natural gas utilization for space heating and domestic hot water preparation purposes, a crucial issue should be addressed. This problem is related to the quality of energy transformation, which can be described by using the exergy concept. Exergy is defined as the maximum useful work which can be extracted from a system while bringing it into the equilibrium with its environment through reversible process [76]. Thermomechanical exergy of

the system can be calculated by using temperature of the environment and the temperature at which the heat is available [77]. The higher the temperature difference is, the bigger the maximum extractable work is, i.e. exergy, and vice versa. In other words, if the heat is available at a low temperature, the exergy of such system will be lower. Exergy itself is not enough to calculate the quality of the energy transformation, thus exergy efficiency should be introduced. Exergy efficiency is defined as a ratio of exergy output and exergy input. In the case of space heating, the temperature level of output heat is relatively low, around 80°C, which corresponds to low exergy output. If such space heating demand is covered by using high temperature, i.e. high exergy, heat source as an input, exergy efficiency of such system will be low. This is exactly the case when using natural gas as a fuel for space heating purposes. Exergy efficiency of natural gas-based heat-only boiler for space heating process is relatively low. In district heating systems, exergy efficiency of a natural gas boiler is around 30% [78]. In other words, using natural gas in heat-only boilers to obtain low-temperature heat is poor and low-quality resource management and should be avoided. During the energy transition, high-quality fossil fuels, such as natural gas, should be used for high-temperature thermal demand in industrial processes or in cogeneration units.

Cogeneration technology has a relatively high exergy efficiency of around 55%. Fuel is primarily used to produce electricity, while waste heat, available at lower temperature levels, is used for covering different heating loads, e.g. space heating demand through district heating. Although natural gas-based individual boiler and CHP have equal energy efficiency, the latter one has a higher quality of energy transformation. During the energy transition, when carbon budgeting becomes a crucial issue in all energy systems, a high-quality utilization of fossil fuels will find itself at the heart of optimal resource management.

1.2.4 Heating decarbonisation through district heating

The utilization of natural gas in the heating sector during energy transition is possible, but only in cogeneration units. It is important to mention that natural gas cogeneration should not be the final solution of the heating sector decarbonisation, but only the first milestone of the energy transition. Once district heating has been acknowledged as the primary heating source in the urban areas, large-scale integration of renewable energy sources in the heating sector will be possible. The main reason for this is the fact that decarbonisation of a single source, in this case district heating supply technology, is much simpler than carrying out the decarbonisation of numerous individual heating units.

This thesis explores the issue of comparing district and individual heating systems by providing an answer to the following research question: is there a range of natural gas market prices where district systems are superior to individual heating solutions from an economic, environmental and exergetic point of view? Furthermore, can district heating be superior to individual systems even for very low households' natural gas prices?

1.3 Knowledge gap analysis

In this section, a literature review is shown, which provides knowledge gap analysis on a multi-objective optimisation of district heating and cooling systems, including exergy analysis in energy planning. Furthermore, different cost and carbon allocation methods are discussed. Finally, scientific objectives and hypothesis of this thesis are proposed, and the scientific contribution is defined.

1.3.1 Optimization of DH and DC systems

District heating and cooling systems are often analysed by using an optimization approach which seeks to obtain a minimum or a maximum value of a defined objective function. In a case of a single-objective optimization, the system cost is most often used as the objective function [45]. Modelling approaches vary but most of them are usually based on linear programming (LP), mixed-integer linear programming (MILP) [79], mixed-integer non-linear programming (MINLP) [80] problems. Genetic algorithms (GA) [81] could also be used to obtain optimal solution. The temporal level of optimization also differs between different research papers. Fang et al. did not take into account the temporal scale [82], thus accelerating the optimization procedure. A possible compromise between computation speed and accuracy is using representative days as shown in [83]. However, the most obvious approach is using an hourly level approach for a whole year period as done by Pavičević et al. in [45]. Some researchers are going even below the one-hour threshold by reaching a 15-minute level optimization as shown in [84]. The optimization of district heating systems is often used to study different parameters or processes related to district heating networks, such as an electricity price change or a heating demand reduction [85], while Pirouti et al. [86] analysed the impact of supply temperature and pressure losses. Tańczuk et al. studied the influence of fuel change, i.e. replacement of coal with a natural gas-based district heating unit [87].

1.3.2 Multi-objective optimization of district heating and district cooling systems

When one or more additional objective functions are introduced in the model, then the term multi-objective optimization is used. Besides system cost, objective functions usually include

carbon dioxide emissions, energy efficiency of the system, primary energy consumption, etc. It is important to mention that reaching the optimum for different objective solutions simultaneously is usually impossible. In that case, the final solution of a multi-objective optimization is the so-called Pareto front which presents a compromise between all objective functions. There are numerous approaches how to handle multi-objective optimization, but the most common are the weighted sum method, as used in [83] and [84], and the epsilon constraint method, as shown in [88] and [89]. The multi-objective optimization of combined heating and cooling is regularly carried out for small applications, such as in paper [90]. The system consisted of a power plant, an internal combustion engine, a biomass boiler and different chillers. A similar approach was used in [91] where the operation of a tri-generation plant was optimized for a single day. Best et al. [92] used a MILP optimization approach to model thermal and hydraulic constraints of the district heating and cooling networks. Allen et al. [93] provided an evaluation of district heating and cooling system topology optimization on an urban district level.

1.3.3 Exergy efficiency in energy planning

District heating systems are frequently studied by using exergy analysis. District heating network temperature is the topic usually considered in such papers. Gong and Werner [94] analysed Danish and Swedish district heating systems and concluded that a great share of exergy is lost in the thermal network. A similar observation was done in [95]. Li and Swendsen stated that the exergy destruction reduction potential is the highest for domestic hot water production [96]. Exergy efficiency could be used for energy planning purposes as shown by Şiir Kilkiş in [97]. Yang et al. studies solutions for DHW production by using low-temperature DH systems [98]. Baldvinsson et al. carried out a performance assessment of such systems [99]. The same group of authors developed a specific exergy cost method that could also be utilized for energy planning purposes [100]. The previously mentioned papers focused on an energy system, while the following papers discussed specific district heating technologies. Yamankaradeniz [101] studied geothermal district heating systems by using exergy analyses. Similar observations were obtained in [102] by using an artificial neural network. The exergy of other renewable technologies such as solar thermal collectors has been studied in [103], while compression heat pumps were analysed in [104]. District cooling has also been studied by using exergy analysis, as shown in [105] and [106], while exergy of cold thermal storage was evaluated in [107].

1.3.4 Economic, environmental and exergy multi-objective optimization

Although exergy is often used in optimization problems, it is usually translated to different objective functions such as the maximization of exergy efficiency or the minimization of exergy destruction or exergy loss. Furthermore, the latter could be translated into cost and minimized together with other expenditures [108]. In [109], exergy loss was used as one of indicators of the composite utility. It is important to mention that the exergy-related objective functions are rarely studied by using a single-objective optimization. Wang et al [110] optimized the configuration of an organic Rankine cycle by maximizing the exergy efficiency and minimizing the total cost of the system. In [111] a combined heating and cooling power plant was optimized by minimizing the environmental and economical objective function while maximizing exergy efficiency. Lu et al. used a similar multi-objective optimization approach to obtain a net-zero exergy district in China [112]. Di Somma developed a multi-objective optimization model of a distributed energy system which maximizes exergy efficiency and minimizes total cost. For this purpose, a MILP modelling approach combined with weighted sum method was used. In paper [113] the optimization covers only the operation of the system. This model was upgraded in [114] to be capable of additionally optimizing supply capacities. Carbon dioxide emissions have not been considered.

1.3.5 Carbon and cost allocation in CHP units

When discussing the economic and environmental optimization of cogeneration-based district heating systems, carbon and cost allocation should be introduced. This is a crucial issue since cost and carbon dioxide emissions of CHP must be separated between electricity and heat production, i.e. district heating. Noussan listed and compared numerous allocation methods which have been developed over the years [115]. Tereschenko and Nord carried out similar research focusing on the allocation of CO_2 emissions [116]. An exergy concept could be used to provide an allocation method by performing an exergoeconomic analysis [117]. Pina et al. developed a cost allocation method in trigeneration system combined with thermal storage [118].

As already mentioned, heat production in cogeneration system could be treated as waste or excess heat, i.e. it can be considered as a by-product of power production. Nevertheless, it should be mentioned that heat production reduces power production, i.e. it is a cause of power-loss. This fact was used in the development of power-loss, or sometimes called the Dresden allocation method. It is based on translating electricity lost due to heat production, into carbon

emissions. The method was mentioned in various reports [35], [36], [37] and numerous research papers [115], [119], [116], [120].

1.4 Objective and hypotheses of research

The objectives of this thesis are following. Firstly, to develop a multi-objective optimization model of a district heating and cooling system where objective functions are defined as the maximization of economic feasibility, minimization of ecological impact and maximization of exergy efficiency. Secondly, to develop a method for analysing the potential of the integration of district heating and cooling systems, which considers, besides the heating and cooling demand, the energy market conditions, supply technologies type and their capacities. Thirdly, to define the energy market price range where district heating and cooling systems have higher exergy efficiency and a lower environmental impact than individual solutions, while at the same time being economically feasible. Finally, the hypothesis of this research is that by using a method of multi-objective optimization of a district heating and cooling system the cluster of solutions where district systems are better than individual, in terms of ecological impact and exergy efficiency, while at the same time being economically feasible, could be obtained in relation to energy market prices.

1.5 Scientific contribution

This doctoral thesis has a twofold scientific contribution. Firstly, it provides the multi-objective optimization model of a district heating and cooling system which can define capacities and hourly operation of supply units, while taking into account economic feasibility, ecological impact and exergy efficiency of a system. Secondly, it defines the energy market conditions for which district heating and cooling systems are simultaneously better than individual in terms of ecological impact and exergy efficiency, while at the same being economically feasible.

2 METHODS

In this section, overall modelling approaches and methods are shown. Firstly, general overview of multi-objective optimisation and linear programming is presented. Then, district heating and cooling model is displayed in detail, followed by explanation of carbon and cost allocation methods. Finally, objective functions are defined, while programming tools and optimisation solvers are listed.

2.1 Multi-objective optimization

Optimisation is a process of obtaining an optimal value of optimization variable x_i to achieve minimum, or maximum, value of the objective function f, as shown in Equation (1). Besides objective functions, optimisation problem usually includes inequality constraints g_j and equality constraints h_k shown in Equation (2) and (3). Since this problem includes only one objective function, it represents a single-objective optimization problem.

If objective function and constraints are linear, then optimisation problem is also linear and could be written as linear programming (LP) or mixed-integer linear programming (MILP) optimisation problem.

$$\min f(x_i), \qquad i = 1, \dots, I \tag{1}$$
$$g_j(x_i) \leq 0, \quad j = 1, \dots, J \tag{2}$$
$$h_k(x_i) = 0, \qquad k = 1, \dots, K \tag{3}$$

In a case that more than one objective function is defined then the problem becomes multi-objective optimisation, as shown in Equation (4).

$$\min\left(f_1(x_i), f_2(x_i), \dots, f_n(x_i)\right), \qquad n = 1, \dots, N \tag{4}$$

In multi-objective optimisation problems, objective functions are often conflicting. This means that their minimum (or maximum) values cannot be obtained simultaneously. Usually, minimum of one objective function results in high value of other objective function and vice-versa. Multi-objective optimisation is generally linked to Pareto optimality, or Pareto efficiency, and Pareto front. The multi-objective optimisation results are Pareto optimal if there are no changes which could lead to improvement of one objective function without degrading the other objective function. The set of Pareto optimal solution is so-called Pareto front, illustrated in Figure 6. In this case, both objective functions are minimised. However, one cannot be improved without increasing the other. All feasible results, but non-Pareto optimal,

are located right of the Pareto front. Solutions located left to Pareto front are unfeasible, i.e. unreachable and represent theoretical values. The best ideal value is called Utopia point where both objective functions reach their minimum values.

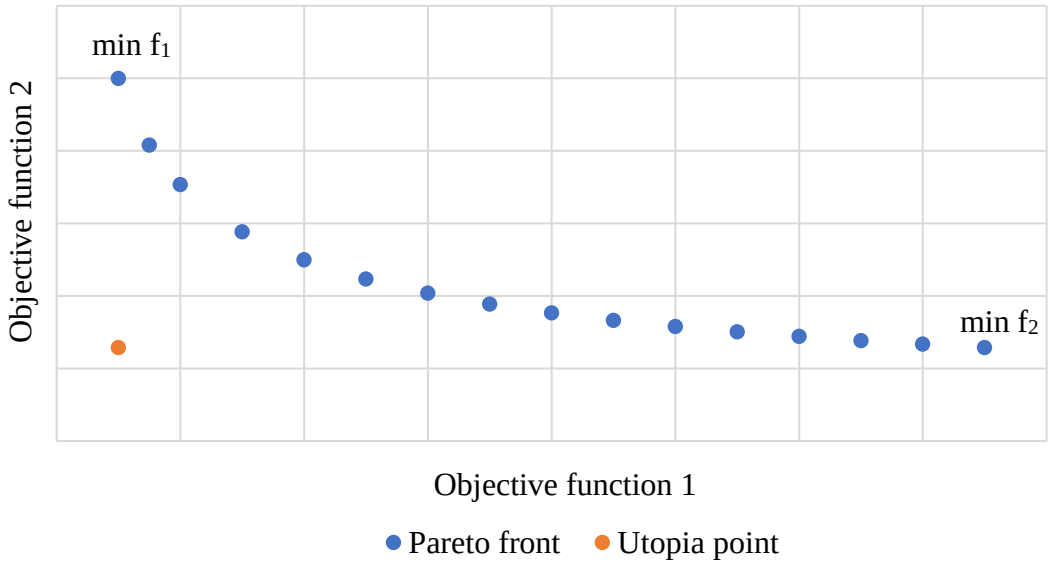

Figure 6 Illustration of Pareto front and Utopia point

Numerous approaches could be applied to solve multi-objective optimisation problem. The two most used are weighted sum and epsilon-constraint method.

Weighted sum method combines all objective functions into composite objective function F by using weighting coefficients ω_n, as shown in Equation (5) and Equation (6). By doing so, sum of weighted coefficients should always be equal to unity, as shown in Equation (7). Theoretically, a whole Pareto front could be obtained by varying weighted coefficients. However, this is not possible for non-convex Pareto fronts [88].

$$\min F(x_i) \tag{5}$$

$$F(x_i) = \omega_1 f_1(x_i) + \omega_2 f_2(x_i) + \cdots + \omega_n f_n(x_i) \tag{6}$$

$$\sum_{n}^{N} \omega_n = 1, \qquad \omega_n \geq 0 \tag{7}$$

Epsilon constraint method enables translation of multi-objective problem into single-objective optimisation by defining additional constraints. In this method, only one objective function is defined while other are treated as constraint within specific values. These constraints are usually called epsilon-constraints. Equation (8) shows multi-objective optimisation problem where only objective function f_μ is minimized, while all other are translated to constraints, as shown in Equation (9). The value of epsilon-constraint ε_n must be carefully defined, i.e. it must be in

the feasible region for the given objective function f_n. To obtain feasible region of f_n, usually optimisation procedure with respect to f_n should be carried out.

By solving single-objective optimisation problem with different epsilon constraints, the whole Pareto front could be constructed. Unlike weighted sum, epsilon-constraint method could be used for construction of non-convex Pareto fronts [88].

$$\min f_\mu(x_i) \tag{8}$$

$$f_n(x_i) \leq \varepsilon_n, \qquad n = 1,2,\dots,N \; and \; n \neq \mu \tag{9}$$

2.2 Linear programming

In a case where objective function and constraints are linear, then linear programming (LP) could be used. Objective function of the LP problem could be defined with Equation (10) where c is a so-called cost-vector. Equality and non-equality constraints could be generally written as shown in Equation (11), where a_i and b_i are problem parameters that specify given constraints.

$$\min c^T x_i \tag{10}$$

$$a_i^T x_i \leq b_i \tag{11}$$

Special type of LP is so-called mixed-integer linear programming (MILP) where some optimisation variables are non-continuous, such as integers or binary values as shown in Equations (12) and (13).

$$x_i \in \mathbb{Z}^n \tag{12}$$

$$x_i \in \mathbb{Z}^n | 0 \leq x_i \leq 1 \tag{13}$$

2.3 District heating and cooling model

District heating and cooling model is based on MILP optimisation problem. Optimisation variables are hourly operation of supply units ($Q_{i,t}$) and thermal storage ($TES_{in-out,t}$), including supply capacities (P_i) and thermal storage size (TES_{size}). Time-step of the model is one hour, while time horizon is a whole year. Visualization of the model is shown in Figure 7.

Equations (14) and (15) present essential constraint which implies that district heating ($DEM_{DH,t}$) and district cooling ($DEM_{DC,t}$) demand must be covered with thermal supply units ($Q_{i,t}$) and thermal storage $TES_{in-out,t}$.

$$DEM_{DH,t} = Q_{HOB,gas,t} + Q_{HOB,biomass,t} + Q_{EH,t} + Q_{HP,t} + Q_{CHP,gas,t} + Q_{CHP,biomass,t} - TES_{DH,1,in-out,t} - TES_{DH,2,in-out,t} \quad (14)$$

$$DEM_{DC,t} = Q_{AHP,t} + Q_{DC,HP,t} - TES_{DC\,in-out,t} \quad (15)$$

It should be mentioned that district heating and cooling are connected through absorption heat pump as shown in (16).

$$Q_{AHP} = \eta_{AHP} \cdot (Q_{HOB,gas,t} + Q_{HOB,biomass,t} + Q_{CHP,gas,t} + Q_{CHP,biomass,t}) \quad (16)$$

Maximum thermal output from supply units is bounded by installed thermal capacity of the supply unit as shown in (17).

$$0 \leq Q_{i,t} \leq P_i \quad (17)$$

Minimum possible supply capacity is defined by using binary variable b_i as shown in Equation (18).

$$b_i \cdot P_{min,i} \leq P_i \leq b_i \cdot P_{max,i},\ b_i = \{b_i \in \mathbb{Z} | 0 \leq b_i \leq 1\} \quad (18)$$

To obtain realistic operation of supply units, ramping limit is introduced as shown in Equation (19)

$$-r_{up-down,i} \cdot P_i \leq Q_{i,t} - Q_{i,t-1} \leq r_{up-down,i} \cdot P_i \quad (19)$$

Thermal storage is modelled by using following set of constraints. Hourly state-of-charge of thermal storage SOC_t in the first and the final time-step should be equal as shown in Equation (20). Consecutive SOC_t are connected by using constraint shown in Equation (21), where state-of-charge of time step t is equal to the state-of-charge of the former time-step SOC_{t-1} increased by thermal storage charge or discharge $TES_{in-out,t}$ and reduced by thermal storage losses defined with TES_{loss}. It should be mentioned that negative $TES_{in-out,t}$ presents discharge and positive $TES_{in-out,t}$ presents charging of the thermal storage. Finally, the sizing of the thermal storage is defined by using constraint shown in Equation (22) where SOC_t must be between minimum and maximum state-of-charge, i.e. TES_{size}.

$$SOC_{t=1} = SOC_{t=8760} = SOC_{start-end} \cdot TES_{size} \quad (20)$$

$$SOC_t = SOC_{t-1} + TES_{in-out,t} - SOC_t \cdot TES_{loss} \quad (21)$$

$$TES_{min} \cdot TES_{size} \leq SOC_t \leq TES_{size} \tag{22}$$

Solar thermal is modelled differently from other supply units since specific thermal production $P_{solar,specific,t}$ is defined prior to the optimisation. Operation of solar thermal $Q_{ST,t}$ is constrained because it is defined with solar thermal area A_{ST}, as shown in Equation (23). $P_{solar,specific,t}$ is defined according to the Equation (24), while collector efficiency $\eta_{c,t}$ is calculated by using Equation (25), where η_0, a_1 and a_2 are efficiency data defined for every solar thermal collector and $T_{m,t}$ is mean collector fluid temperature. Meteorological data in terms of ambient temperature $T_{ref,t}$ and solar irradiation G_t is also needed.

$$Q_{ST,t} = A_{ST} \cdot P_{solar,specific,t} \tag{23}$$

$$P_{solar,specific,t} = \eta_{c,t} \cdot G_t \tag{24}$$

$$\eta_{c,t} = \eta_0 - a_1 \frac{\left(T_{m,t} - T_{ref,t}\right)}{G_t} - a_2 \frac{\left(T_{m,t} - T_{ref,t}\right)^2}{G_t} \tag{25}$$

Besides solar thermal collector, compression heat pumps are only technology with non-constant efficiency, as shown in Equation (26), where $T_{DH,t}$ is district heating temperature and f_{Carnot} is the ratio between realistic and ideal heat pump efficiency.

$$\eta_{HP,t} = f_{Carnot} \cdot \left(\frac{T_{DH,t}}{T_{DH,t} - T_{ref,t}}\right) \tag{26}$$

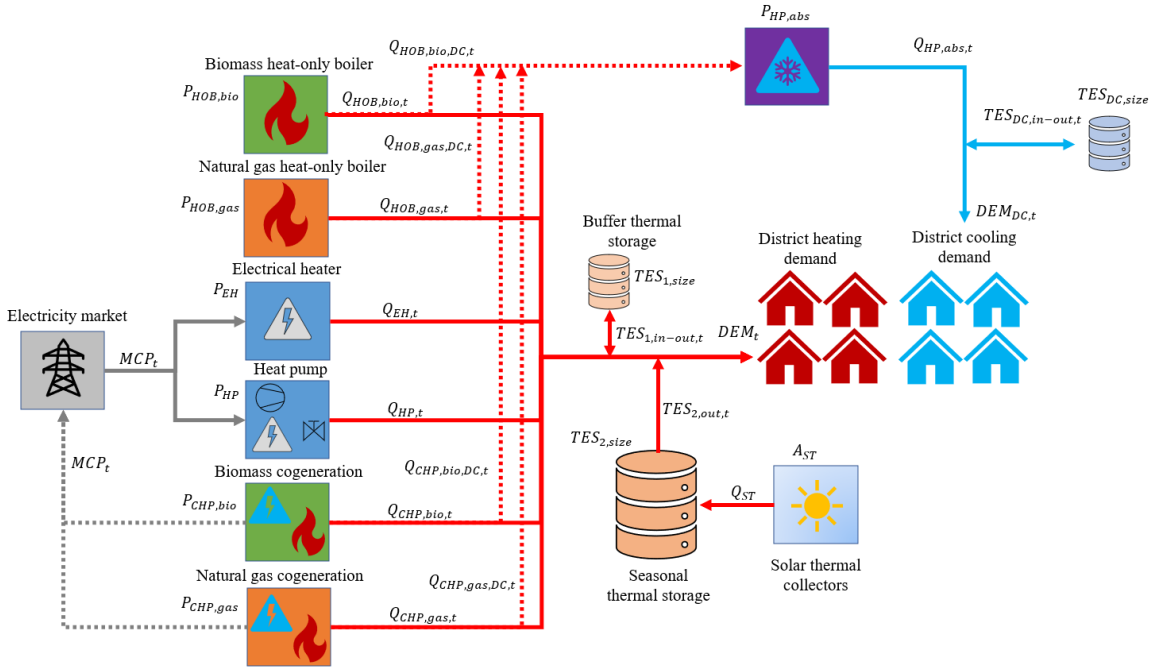

Figure 7 Visualization of district heating and cooling model, including related optimisation variables

2.4 Allocation in cogeneration units

Cogeneration is a supply unit which can produce heat $Q_{CHP_i,t}$ and electrical energy $E_{CHP_i,t}$ simultaneously. The correlation between them is usually visualized by using power-heat, or sometimes referred as P-Q, diagram as shown in Figure 8. Operating region is bounded with constraints shown in Equation (27) and (28). The first constraint correlates to back-pressure line with the slope defined with power-to-heat ratio σ_{CHP_i}. In this operating region, increase of heat production is followed with the increase of electricity production. The second boundary is so-called extraction line which has negative slope defined with a power-loss ratio β_{CHP_i}. On this line, increase of heat production causes reduction of electrical energy production. It is important to mention that fuel input across this line remains constant. The third line is parallel to the extraction line and represents technical minimum of the CHP unit. For this analysis, it was neglected to maintain linearity of the optimisation model. Finally, electrical energy production should be lower than electrical capacity of a CHP unit as shown in Equation (29).

$$E_{CHP_i,t} \geq \sigma_{CHP_i} \cdot Q_{CHP_i,t} \tag{27}$$

$$E_{CHP_i,t} \leq P_{el,CHP,i} - \beta_{CHP_i} \cdot Q_{CHP_i,t} \tag{28}$$

$$E_{CHP_i,t} \leq P_{el,CHP,i} \tag{29}$$

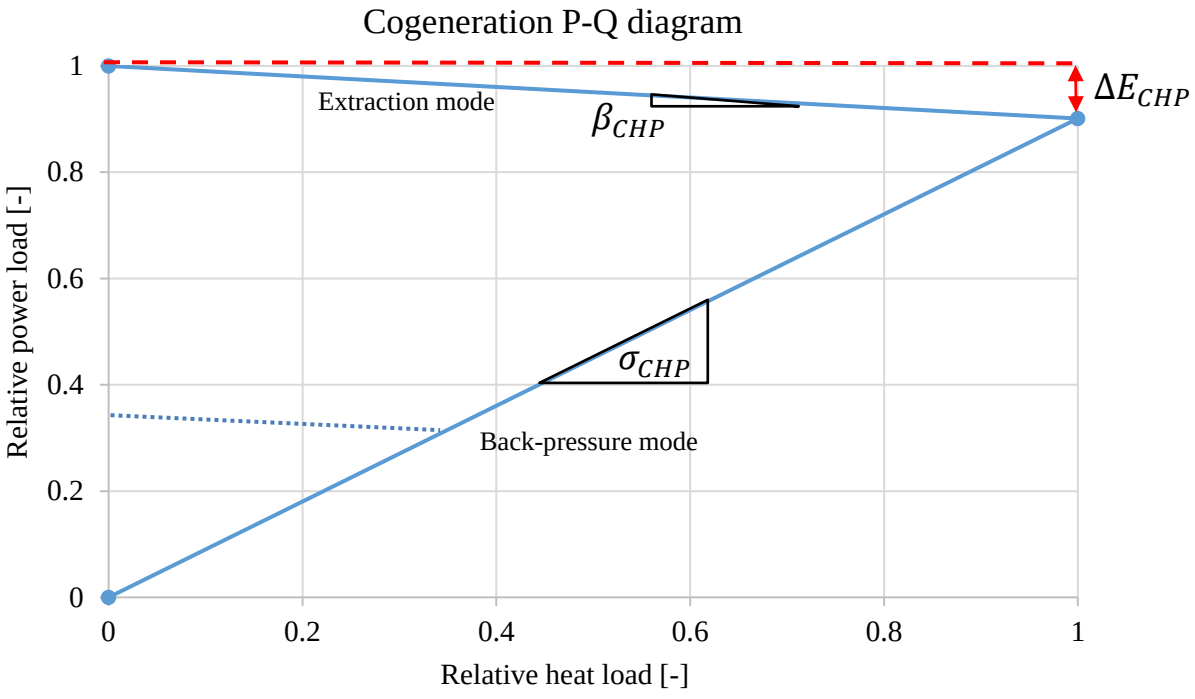

Figure 8 Illustration of P-Q diagram

It should be noticed that technical minimum and other detailed unit-commitment constraints were neglected due to the following reasons. To include them, the model would become mixed-integer non-linear problem which present great numerical challenge to solve on such long time-horizon (8760 hours). These constraints would impact hourly operation of DHC system and could affect running costs. It should be mentioned that the main objective of optimisation problem is to define DHC system capacity and share of thermal production per technology and fuel. For this purpose, hourly operation was also modelled. Since running costs are only one part of the total economic objective function, detailed unit-commitment modelling was not carried out. This present compromise between model accuracy and ability to solve optimisation problem. For the sake of illustrating the impact of technical minimum of supply units the following example is given. Most of the times, cogeneration operates above technical minimum, while only around 500 hours below (out of 8760 hours). In other words, during these 500 hours the unit should operate in other manner, thus impacting the optimal cost of the system. Since this share in the total cost is relatively small, technical minimum of CHP was neglected to maintain linearity of the problem.

Carbon and cost allocation developed for the purpose of this dissertation is based on the power-loss in cogeneration units. Power-loss due to heat production $\Delta E_{CHP_i,t}$, shown in Figure 8 can be calculated by using power-loss coefficient as shown in Equation (30). Power-loss can then be used to calculate cost and carbon emissions allocated to heat production.

$$\Delta E_{CHP_i,t} = \beta_{CHP_i} \cdot Q_{CHP_i,t} \tag{30}$$

Commonly used non-allocated cost of CHP is shown in Equation (31) which sums fuel, operation and maintenance, fixed and discounted investment costs reduced by electricity production income. On the other hand, cost of CHP allocated to heat production are shown in Equation (32). The cost of heat from CHP is equal to the cost of lost electricity production including the share of discounted investment which could be allocated to heat part of the unit.

$$Cost_{CHP_i} = \sum_{i} \sum_{t=1}^{t=8760} (E_{CHP_i,t} + \Delta E_{CHP_i,t}) \cdot \left(\frac{c_{fuel,i} + e_{CO2_i} \cdot c_{CO2}}{\eta_{el,CHP_i}} + c_{var_{CHP_i}} \right) - E_{CHP,i,t} \cdot c_{el,t} + P_{el,CHP_i} \cdot \left(c_{inv,CHP_i} \cdot CRF_{CHP_i} + c_{fix_{CHP,i}} \right) \tag{31}$$

$$Cost^{*}_{CHP} = \sum_{i} \sum_{t=1}^{t=8760} \Delta E_{CHP_i,t} \cdot c_{el,t} + P_{el,CHP_i} \cdot c_{conv,CHP_i} \cdot CRF_{CHP_i} \tag{32}$$

Carbon emissions allocated to heat production in CHP units could be calculated in similar manner. Equation (33) presents traditional approach without allocation of emissions, where all emissions produced in the CHP units are allocated to heat production. Equation (34) shows calculation of emissions from CHP allocated to heat production by using power-loss. Carbon emissions units allocated to heat are equal to CO_2 emitted from power plant with equal electricity efficiency and used fuel which needs to compensate the power-loss.

$$CO_{2_{CHP_i}} = \sum_i \sum_{t=1}^{t=8760} \frac{E_{CHP_i,t} + \Delta E_{CHP_i,t}}{\eta_{el,CHP_i}} \cdot e_{CO2_i} \tag{33}$$

$$CO^*_{2_{CHP_i}} = \sum_i \sum_{t=1}^{t=8760} \frac{\Delta E_{CHP_i,t}}{\eta_{el,CHP_i}} \cdot e_{CO2_i} \tag{34}$$

2.5 Objective functions

Since multi-objective optimisation approach has been applied, more than one objective function must be defined. For this dissertation, three objective functions have been used: minimisation of total discounted cost (f_{econ}), minimisation of carbon emissions (f_{eco}) and maximisation of exergy efficiency (f_{exe}). Allocation in CHP units is incorporated only in economical (f^*_{econ}) and environmental (f^*_{eco}) objective function.

Equation (35) and (36) show economical objective function with and without cost allocation, respectively. The cost function is constituted of overall running costs and investments. For additional details please refer to the Annex of the thesis, i.e. published papers.

$$\begin{aligned} f_{econ} = \sum_i \sum_{t=1}^{t=8760} & Q_{i,t} \cdot \left(\frac{c_{fuel,i} + e_{CO2_i} \cdot c_{CO2}}{\eta_i} + c_{var_i} \right) + P_i \cdot \left(c_{inv,i} \cdot CRF_i + c_{fix,i} \right) \\ & + TES_{size} \cdot \left(c_{inv,i} \cdot CRF_i + c_{fix,i} \right) + A_{ST} \cdot \left(c_{inv,i} \cdot CRF_i + c_{fix,i} \right) \\ & + Cost_{CHP_i} \end{aligned} \tag{35}$$

$$\begin{aligned} f^*_{econ} = \sum_i \sum_{t=1}^{t=8760} & Q_{i,t} \cdot \left(\frac{c_{fuel,i} + e_{CO2_i} \cdot c_{CO2}}{\eta_i} + c_{var_i} \right) + P_i \cdot \left(c_{inv,i} \cdot CRF_i + c_{fix,i} \right) \\ & + TES_{size} \cdot \left(c_{inv,i} \cdot CRF_i + c_{fix,i} \right) + A_{ST} \cdot \left(c_{inv,i} \cdot CRF_i + c_{fix,i} \right) \\ & + Cost^*_{CHP_i} \end{aligned} \tag{36}$$

Equation (37) and (38) present environmental objective function which includes carbon emissions with and without carbon allocation in CHP units considered.

$$f_{eco} = \sum_{i} \sum_{t=1}^{t=8760} \frac{Q_{i,t}}{\eta_i} \cdot e_{CO2_i} + CO_{2_{CHP_i}} \quad (37)$$

$$f_{eco}^{*} = \sum_{i} \sum_{t=1}^{t=8760} \frac{Q_{i,t}}{\eta_i} \cdot e_{CO2_i} + CO_{2_{CHP_i}}^{*} \quad (38)$$

Finally, exergy efficiency of the system is calculated by using Equation (39), where exergy input $Ex_{in,i,t}$ is defined by using Equation (40), while exergy $Ex_{out,i,t}$ output is defined with Equation (41).

$$f_{exe} = \frac{\sum_{t=1}^{t=8760} \sum_i Ex_{out,i,t}}{\sum_{t=1}^{t=8760} \sum_i Ex_{in,i,t}} \quad (39)$$

$$Ex_{in,i,t} = \frac{Q_{i,t}}{\eta_i} \cdot e_{Exe,i} \quad (40)$$

$$Ex_{out,i,t} = Q_{i,t} \cdot \left(1 - \frac{T_{ref_t}}{T_{DHN_t}}\right) + E_{CHP,i,t} \quad (41)$$

Epsilon-constraint approach was used to handle multi-objective optimisation, as shown in Equation (42). The problem was translated to cost-optimisation while adding constraint put on carbon emissions and exergy efficiency. By varying epsilon constraints, different Pareto fronts could be constructed. However, for each Pareto front feasible epsilon constraints should be obtained. In order to do so, extremes of Pareto front should be firstly acquired.

$$\min (f_{econ}) \text{ for } f_{ecol} \leq \varepsilon_{ecol},\ f_{exe} = \varepsilon_{exe} \quad (42)$$

2.6 Programming language and optimization solver

Optimization model was developed by using open-source and free programming language called Julia [121], i.e. Julia optimisation toolbox called JuMP [122]. Optimisation problem was solved by using academic licence for Gurobi [123], or publicly available solvers such as Cbc [124] and Clp [124].

3 SELECTED RESULTS AND DISCUSSION

This section presents the crucial results obtained for the purpose of this doctoral thesis. They are based on the published papers, available in the Annex of the thesis. Firstly, we will present the importance of coupling district heating and power systems in markets with high shares of variables RES production. Section 3.1. shows how the wind penetration in power markets affects the results of DH multi-objective optimisation, while focusing on P2H technologies. Section 3.2 shows the potential role of thermal prosumers in a district heating system and how their participation can influence the prices for the final customer. Section 3.3 presents the benefits of integrating district heating and cooling systems by using a multi-objective optimization approach. In this section, the focus will be put on the economic and environmental aspects of heating and cooling sector integration. In Section 3.4, the district heating model includes an additional objective function, defined as exergy destruction. To obtain the most suitable solution of the multi-objective optimization, the decision-making method based on the Utopia point selection, has been established. Section 3.5 presents the method which quantifies the cost of exergy destruction in heat-only boilers. Furthermore, the section provides the carbon and exergy destruction price for which a natural gas heat-only boiler is not part of the optimal solution. Finally, Section 3.6 presents the importance of carbon and cost allocation in cogeneration units and defines the energy market prices for which district solutions are better than individual.

3.1 Power and heating sector coupling

It has been shown in Section 1.1.7 that district heating will potentially have an important role in future energy systems with a high share of variable RES. During the periods of high intermittent RES production, they could provide a balancing of the power sector and simultaneously exploit low power market prices through the utilization of P2H technologies combined with thermal storage units. This section provides the results of the analysis on how wind penetration in electricity markets influences the multi-objective optimization of a district heating system. The focus is put on P2H technologies, i.e., heat pumps, and thermal storage units. The conclusions presented in this section are based on the results published in Paper 5 [125], which is available in the Annex of the thesis.

For this analysis, the correlation between power market prices and variable RES penetration had to be modelled. To avoid a detailed hourly multi-zonal dispatch and unit commitment power sector modelling for different wind penetration levels, we used a microeconomics approach illustrated in Figure 9. The power market operates as any other trade of goods, where each supplier and buyer defines the volume and corresponding price of the product, through the so-called bids. The set of all supplying bids forms the so-called "sell curve" while the set of buying bids represent the "buy curve". At their intersection, the market clearing price is achieved. In this case, the product is electrical energy. The suppliers are thermal power plants, wind turbines, cogeneration units, etc. It should be mentioned that RES technologies have lower operational cost and can offer lower bidding prices, thus shifting the supply curve to the right. This causes a reduction of the market clearing prices, as shown in Figure 9. To obtain the reference market clearing prices, we used historical hourly bidding curves for a single year, which are publicly available for the Nord Pool power market [126].

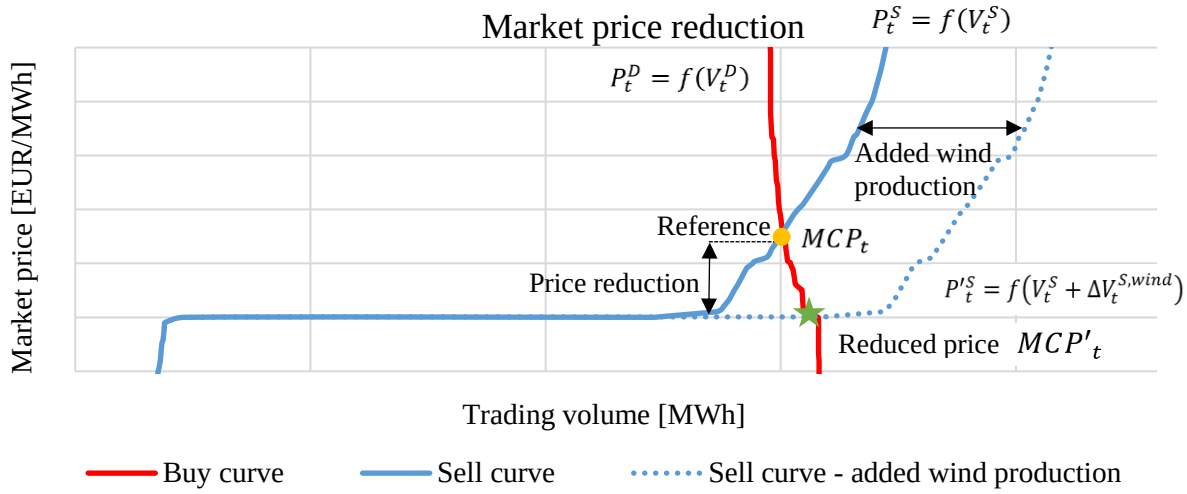

Figure 9 The impact of wind integration on the power market prices

The market clearing price reduction was obtained for different levels of wind penetration. Figure 10 shows an hourly duration curve of the market clearing prices for five different scenarios. In the reference scenario, wind production is equal to 33 TWh. Other scenarios have the same relative hourly wind production, however with higher total energy volumes equal to 45 TWh, 60 TWh, 75 TWh and 90 TWh, respectively. As expected, higher wind penetration causes a reduction of market clearing prices, a higher amount of zero and near-zero prices and generally pushes the price duration curve to the left, as shown in Figure 10.

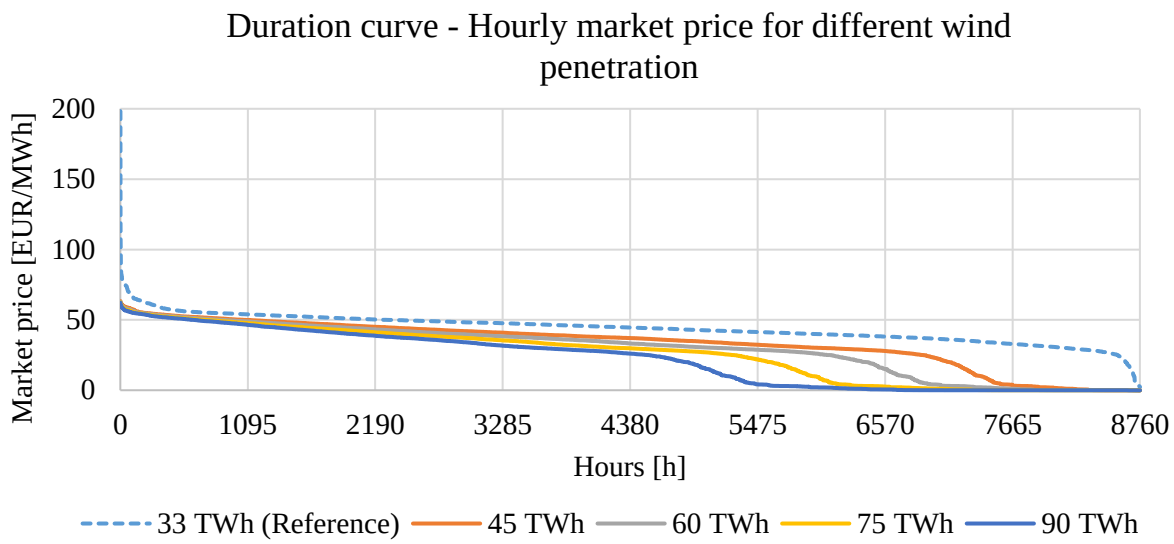

Figure 10 Power market price duration curve for different levels of wind penetration

The obtained hourly distributions were used as the input data for the district heating multi-objective optimization model. The following results will show the correlation between the energy transition of the power sector and the decarbonisation of the district heating sector, while focusing on P2H technologies.

As already explained in Section 2, the results of a multi-objective optimization are a set of solutions which lie on the so-called Pareto front. They represent a compromise between the defined objective functions. In this case, two of them have been defined: the total discounted cost (economic objective function), and the total carbon emissions (environmental objective function). The Pareto fronts for different levels of wind penetration are shown in Figure 11. Firstly, it can be noticed that Pareto fronts are shifted to the left for higher levels of wind share in the market. This indicates that district heating has lower discounted cost for the same levels of carbon dioxide emissions. For this study, we will focus on four groups of Pareto solutions: the least costly solution (with the highest CO_2 emissions), and three different levels of CO_2 equal to 6, 5 and 3 kt of CO_2 emissions.

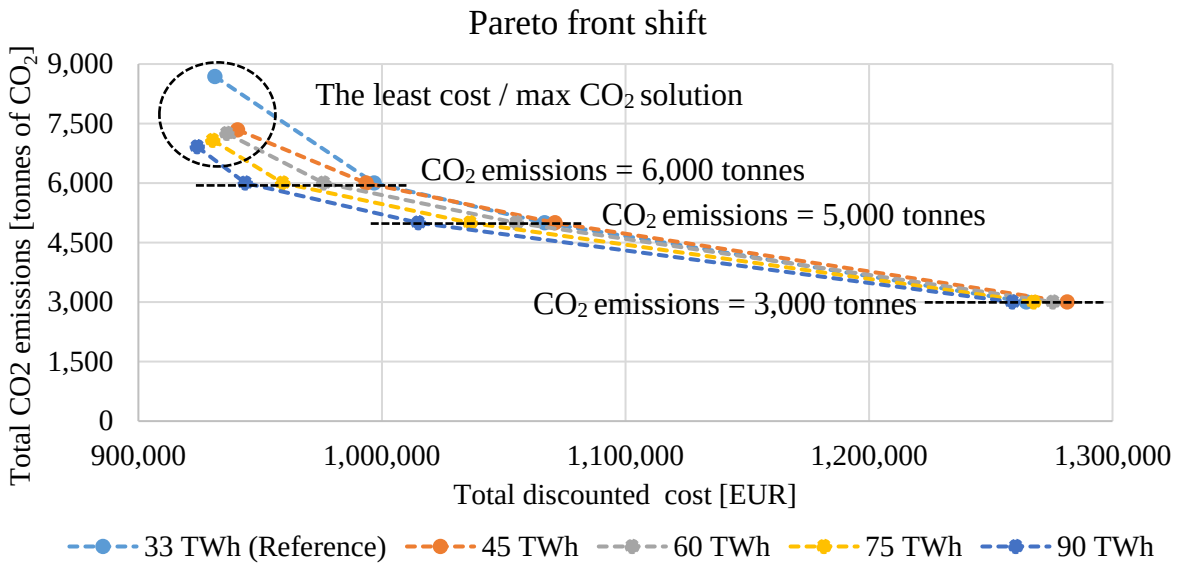

Figure 11 Pareto front shift for different levels of wind penetration

The reason behind this Pareto shift are higher heat pump capacities, enabled due the lower power market prices. It should be mentioned that in this analysis, the power sector carbon factor is equal to 0.29 kt of CO_2/MWh, while only air-source heat pumps have been considered. Figure 12 shows the optimal heat pump capacities for different wind penetration levels and four different Pareto regions. It should be noted that the optimal heat pump capacities increase follow wind penetration. In other words, the integration of variable RES in power markets supports power and heating sector coupling. The heat pump capacities are higher in the Pareto regions with lower CO_2 emissions. For example, the least costly solution does not include a heat pump for the reference level of wind penetration. However, for 60 TWh of wind penetration, the optimal capacity rises to 0.5 MW. For the Pareto solution of 5,000 tonnes of CO_2, the optimal heat pump capacity is equal to 2.35 for 60 TWh of wind penetration.

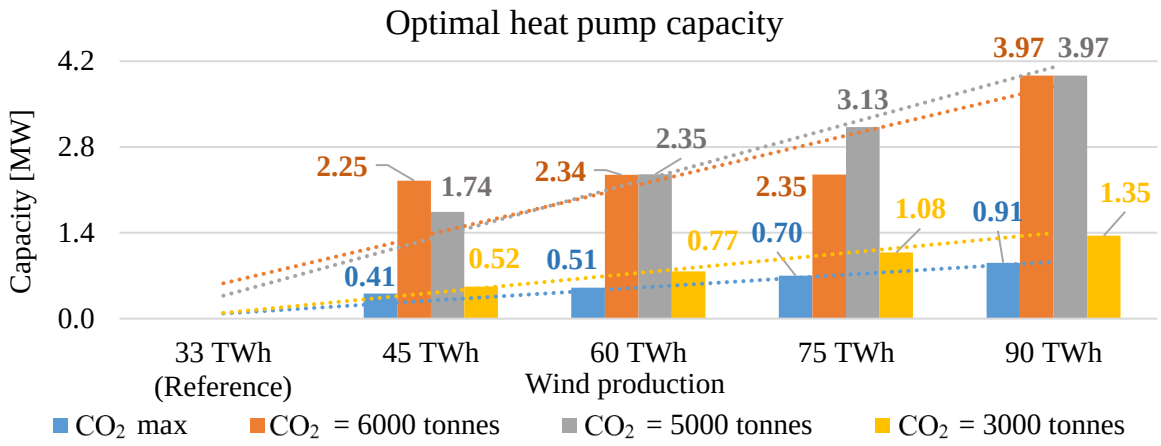

Figure 12 Optimal heat pump capacities in a district heating system for different levels of wind penetration

Similar conclusions can be drawn for optimal heat pump production, as shown in Figure 13. Heat production from heat pumps rises with wind penetration. It reaches around 20 GWh for the highest wind penetration. It can be noticed that the nominal operational hours are usually higher than 4,000 hours. However, the load factor of heat pumps is reduced for higher wind penetrations. This means that lower market clearing prices enable the investment in heat pumps even for lower amounts of nominal operation hours.

Crucial technology which enables successful power and heating sector coupling is thermal storage. This analysis proved that the optimal storage capacity is also linearly increased for higher wind penetration on the power markets. Figure 14 shows that the optimal thermal storage capacity can be increased from 12.9 MWh to 19.7 MWh for 6,000 tonnes of CO_2. Similar conclusion can be drawn for different Pareto regions, except for the least-costly solution where the thermal storage capacity is not affected by wind penetration.

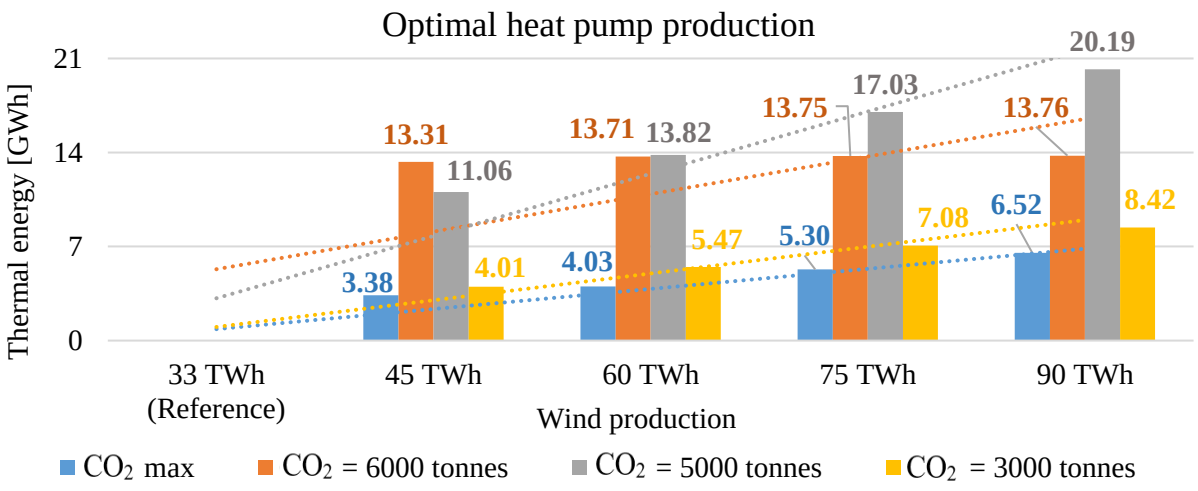

Figure 13 Optimal heat pump production in a district heating system for different levels of wind penetration

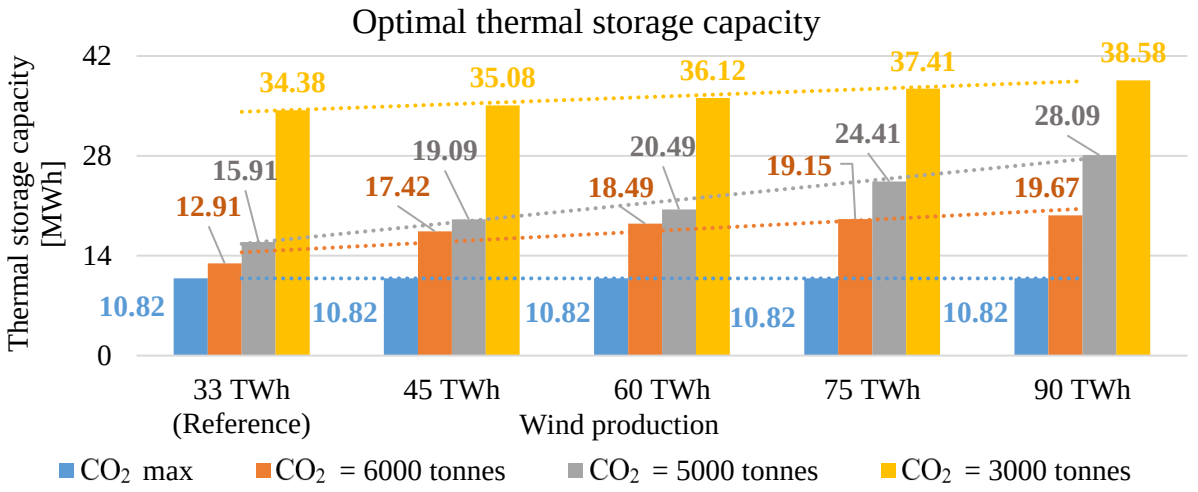

Figure 14 Optimal thermal storage capacities in a district heating system for different levels of wind penetration

This analysis suggests that there is a potential positive feedback loop between the power sector and district heating systems. The integration of variable RES in power markets causes a clearing price reduction and lower P2H running costs. This enables higher heat pump capacities in DH systems. When coupled with thermal storage, P2H units can provide a demand response thus increasing system flexibility and enabling a higher share of variable RES production on the market. Furthermore, different heat sources can enable higher COP, thus decreasing P2H operational costs even further. Finally, the future reduction of DH supply temperatures, caused by building refurbishment, can additionally improve the profitability of P2H units and secure their position in the energy transition of district heating and power systems.

3.2 The role of prosumers in district heating

Future district heating systems will be integrated in the system with other sectors such as gas, cooling, electricity and transportation networks, thus creating a so-called smart energy system. Through smart meters and numerous infrastructural digital and interconnections, suppliers and consumers will be able to communicate with each other, thus achieving the optimal operation of the system to maximise social welfare. The crucial part of the smart energy system is the prosumer, which is capable of supplying and consuming. In this section, we will present the impact of integrating various thermal prosumers in the biomass-based heat-only boiler district heating. The results are based on the analysis published in Paper 4 [127], available in the Annex of the thesis.

The developed heat market model is based on social welfare maximization of a single zone. Technology bidding prices are calculated by using the marginal operational cost. District heating constitutes of various suppliers, consumers and prosumers. The heat supply is based on two central biomass boilers that are connected to district heating network. Consumers are private and public buildings, while demand is constituted of space heating and domestic hot water demand, known for each building separately. Public buildings, such as schools, hospitals, kindergartens, etc. also have locally installed thermal supply technologies, such as solar thermal collectors or heat pumps. Due to this, they are defined as prosumers. During the periods of high demand, they can use a DH network as back-up technology. If they have an excess of thermal energy, and if the temperature levels in the network are suitable, they can export it to the thermal network. Three scenarios have been proposed, each with a different prosumer mix. In the first scenario, all prosumers have only solar thermal collectors. In the second scenario, all consumers utilize only heat pumps. Finally, the third scenario includes prosumers with both solar thermal collectors and heat pumps.

Figure 15 shows a price duration curve for different prosumer scenarios. The maximum heat market price is equal to 30 EUR/MWh, which is equal to the biomass boiler operational cost. It can be noticed that biomass boilers are the sole heat supply technology for the most part of the year, more than 4,000 hours. Scenario 1, based only on a solar thermal collector prosumer, has been shown as the one with the highest market price. The average market price for Scenario 1 is equal to 28 EUR/MWh. Nevertheless, the integration of such prosumers enables a lower heat price than in a biomass boiler-based DH system. Scenario 2, where only heat pump prosumers are enabled, achieves the lowest heat market prices, with the average price being

equal to 25 EUR/MWh. Scenario 3, which includes both solar thermal and heat pump prosumers, has an average market price equal to 27 EUR/MWh.

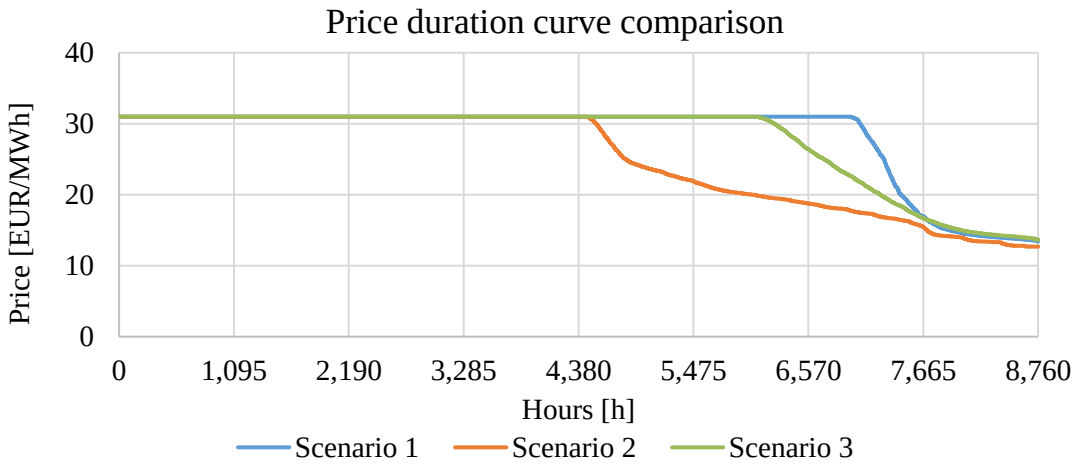

Figure 15 Heat price duration curve for different prosumer scenarios

Figure 16 shows a price comparison for a winter week, the season with the highest space heating demand, due to the lowest ambient temperatures. It can be noticed that the heat prices do not oscillate, most of the heating demand is covered by the most expensive technology, i.e. biomass heat-only boilers. The reason for this is the need for thermal energy production at the local level and high district heating network temperatures. However, there are brief periods where the prosumers are exporting energy to the thermal network, thus reducing the heat market price.

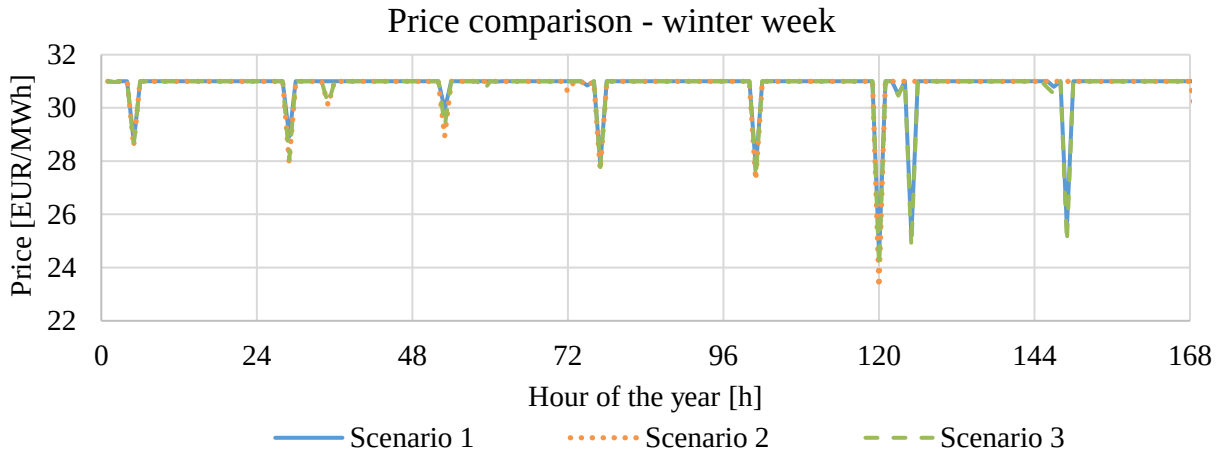

Figure 16 Heat price comparison for different prosumer scenarios – winter week

However, the summer period shows a totally different situation, as shown in Figure 17. Prosumers are heavily exporting during the summer period, due to the low space heating demand and district heating network temperatures. It can be noticed that Scenario 1 does not affect heat market prices during the night-time. Of course, this is due to the solar thermal

collectors used by the prosumers. Since Scenario 2 and Scenario 3 prosumers include heat pumps, they can reduce the heat market price even during the night-time. However, Scenario 1 and Scenario 3 can provide heat prices lower than Scenario 2 during the daytime.

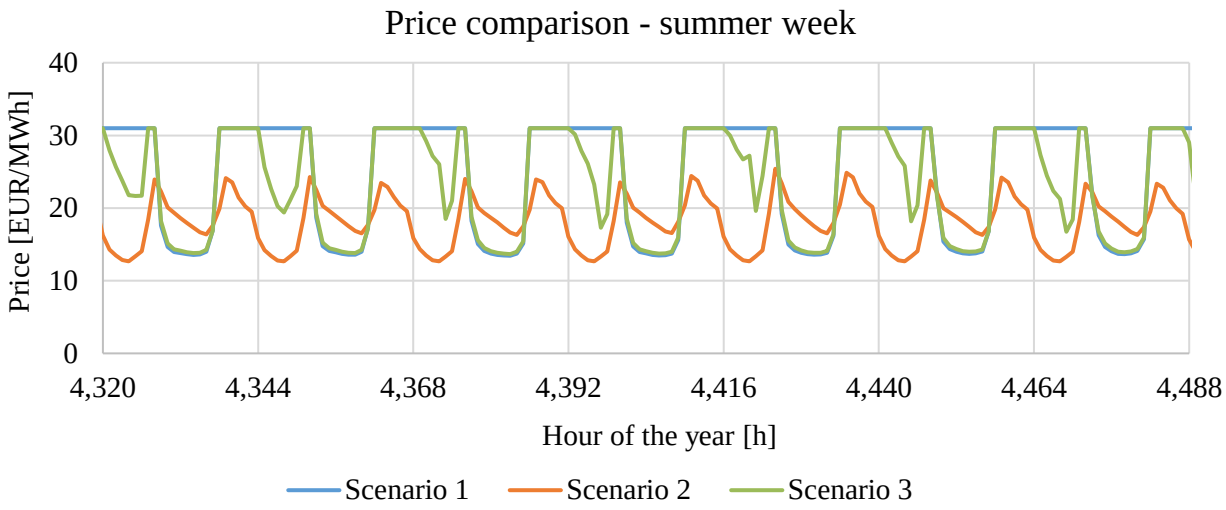

Figure 17 Heat price comparison for different prosumer scenarios – summer week

The analysis focused only on the operational costs, which are the main driver for market analysis. However, in order to fully understand the importance of prosumers, investment in locally installed technologies should be taken into account. They represent an additional cost that potentially increases the levelled cost of heat on the system level. Nevertheless, the presented results have proved that the prosumers' interaction with the thermal network has a positive impact on the heat market price reduction and provides additional flexibility for heat supply.

3.3 Benefits of integrating district heating and cooling grids

Heating and cooling sectors should be integrated in order to utilize their full economical potential. This is possible to implement by using district heating and cooling in urban areas. In this section, we will demonstrate and quantify the environmental, as well as ecological, benefits of coupling district heating and cooling systems. The results discussed below are based on the analysis published in Paper 1 [128], available in the Annex of the thesis. The district heating and cooling model used in this discussion is shown in Figure 18. District heating consists of various technologies such as heat-only boilers, electrical heater, compression heat pump, solar thermal collectors and cogeneration units. The model can choose between natural gas and biomass fuel. Cogeneration units sell electricity, while P2H technologies buy it on the power market. All supply units are connected to the district heating network and thermal storage, while covering the district heating demand. On the other hand, district cooling consists of an absorption and compression heat pump, including cold thermal storage. These technologies supply the district cooling demand. Two scenarios have been developed for the purpose of this study. In Scenario 1, district heating and cooling are operating separately from each other, with no interconnections between them. In Scenario 2, district heating and cooling are combined through an absorption heat pump which utilizes high temperature heat from a heat-only boiler and cogeneration units to produce cold output.

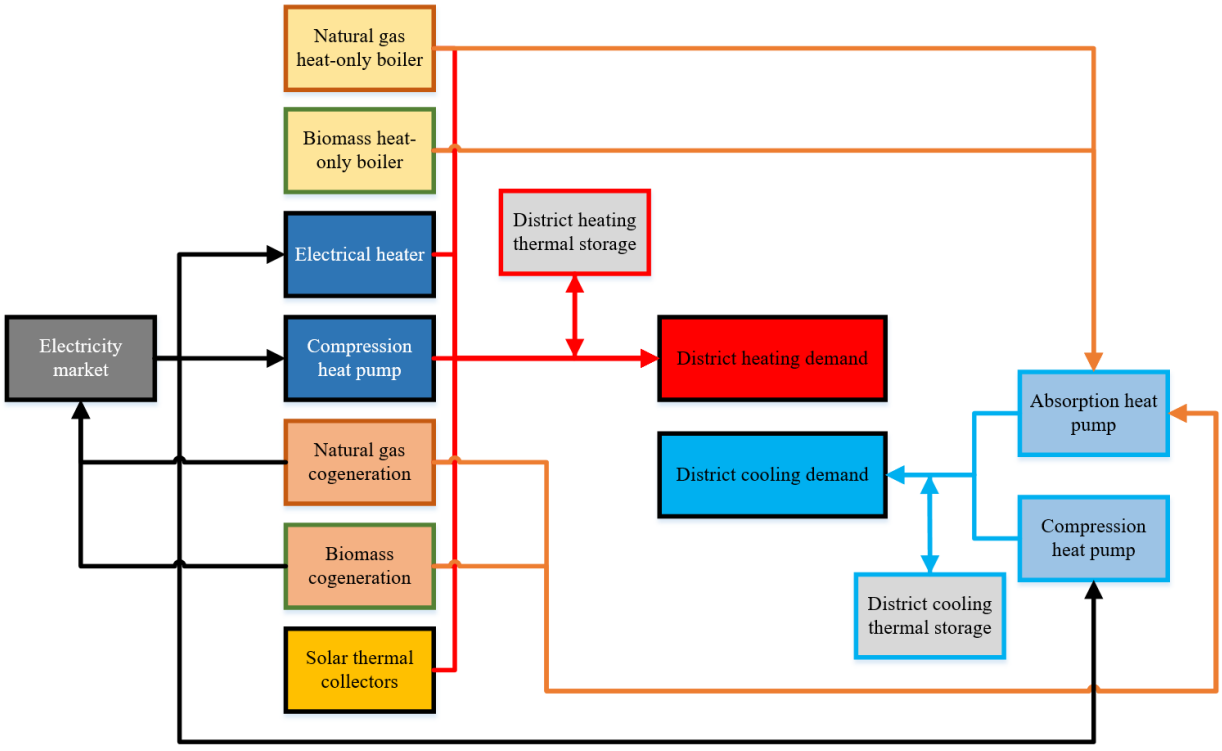

Figure 18 Combined district heating and cooling system

For this analysis, a multi-objective optimization was also used, i.e., thevresults are visualized by using a Pareto front. The results for stand-alone district heating (Scenario 1) are shown in Figure 19. The decarbonisation of the district heating is possible with the increase of the total discounted cost. Low-cost solutions have relatively high carbon emissions, reaching more than 10,000 tonnes of CO_2 emissions. These solutions are mostly based on natural gas heat-only boilers, as shown in Figure 20. Several things can be noticed. Firstly, a natural gas boiler is not part of the Pareto solution once carbon emissions drop below 2,000 tonnes. The heat supply capacity is gradually replaced with a heat pump that has a lower carbon intensity factor. It can be noticed that the heat pump capacity reaches maximum capacity around 10 MW, then it is gradually replaced with a heat-only biomass-based boiler. The most environmentally friendly solution also includes solar thermal collectors, limited to 65,000 m^2 due to assumed spatial constraints.

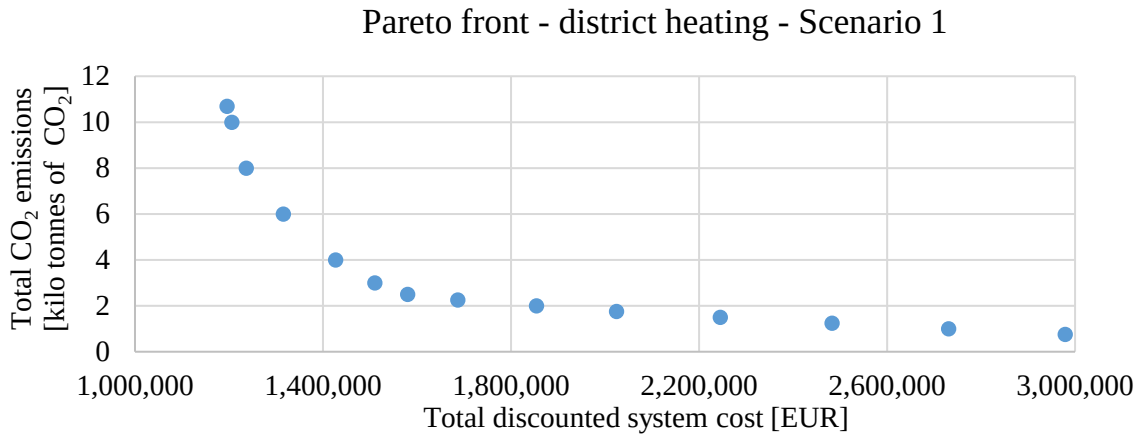

Figure 19 Pareto front for stand-alone district heating

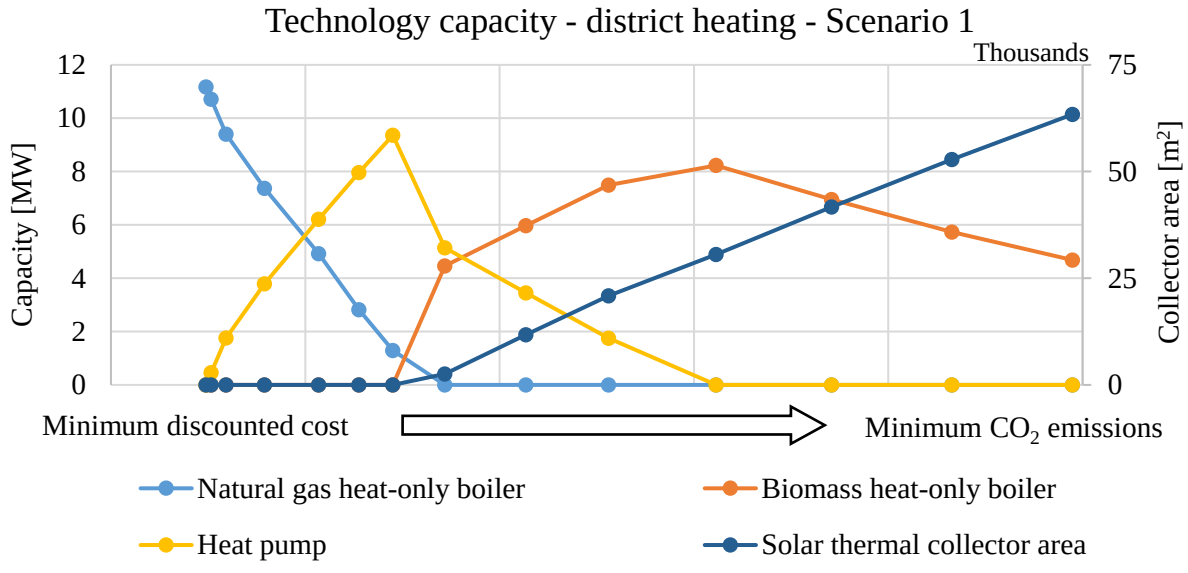

Figure 20 Optimal supply capacities for stand-alone district heating

Similar conclusion can be drawn for stand-alone district cooling (Scenario 1) as seen in Figure 21. Due to lower district cooling demand, CO_2 emissions are lower with the maximum value reaching 1,600 tonnes. Figure 22 shows optimal capacities for stand-alone district cooling. A compression heat pump once again reaches peak capacity, at 3.7 MW, and gradually reduces when approaching the most environmentally friendly solution. For the least-costly solutions, the optimal technology is an absorption heat pump combined with a natural gas heat-only boiler, while for the most environmentally friendly solution is an absorption heat pump combined with a biomass heat-only boiler.

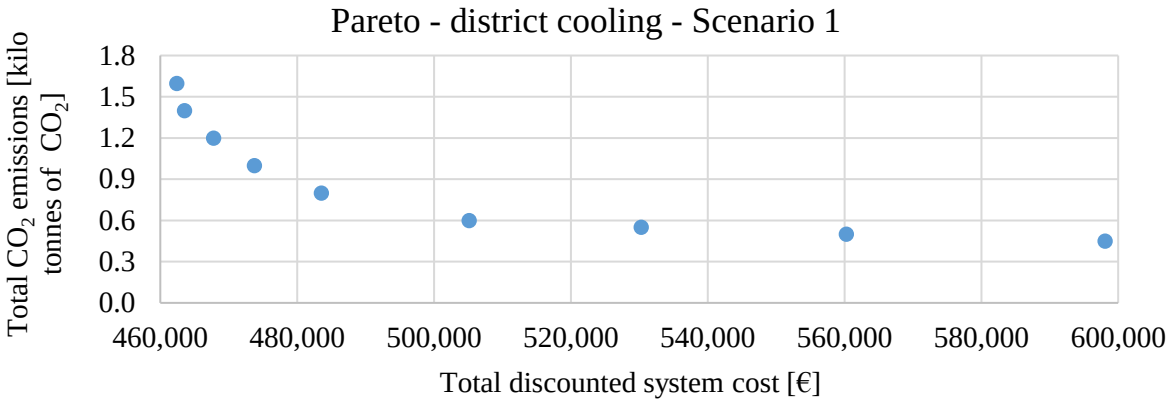

Figure 21 Pareto front for stand-alone district cooling

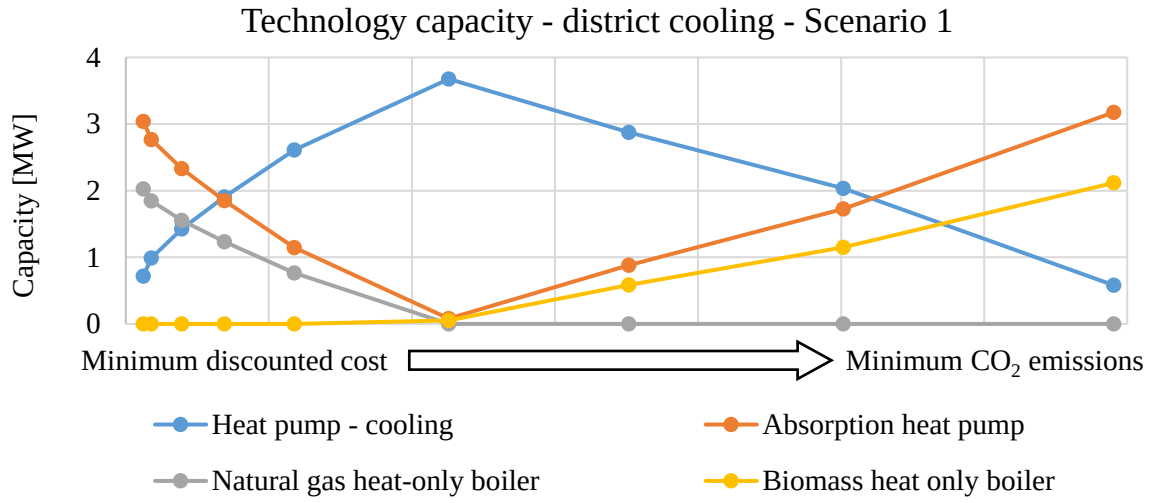

Figure 22 Optimal supply capacities for stand-alone district cooling

Figure 23 shows a comparison of Pareto solutions for separated DH and DC (Scenario 1) and combined DH and DC systems (Scenario 2). It is visible that Scenario 2 enables cost savings for the same level of carbon emissions. The cost reduction is relatively small for the least-costly solution. It should be mentioned that the cost savings are greatly increased when approaching

the most environmentally friendly solution. Of course, the reason behind this is thermal capacity sharing, i.e. heat-only boilers can be used both for district heating and driving absorption heat pump of district cooling. This is especially useful during the summertime when space heating is reduced, and the cooling demand is at its highest. As a result, this increases the load factor of the heat-only boilers and improves the economic feasibility of the investment.

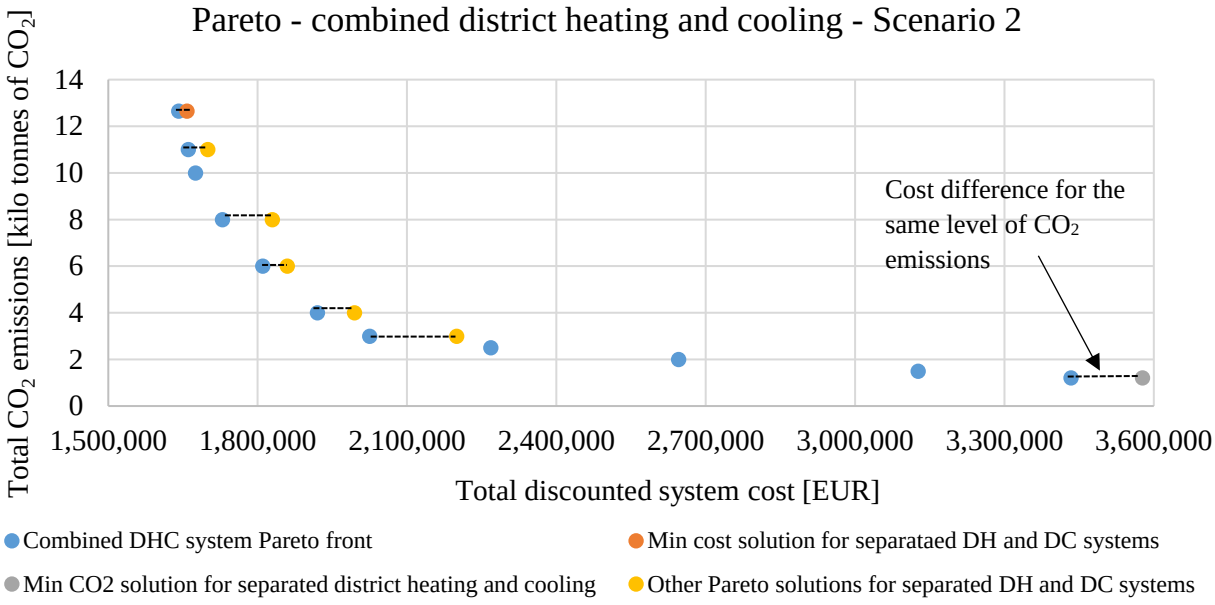

Figure 23 Pareto front comparison for combined district heating and separated district heating and cooling

Figure 24 displays the optimal capacities for combined district heating and cooling supply capacities. Firstly, it can be noticed that the left side of the Pareto front involves various technologies. The right side of the Pareto front includes only three technology types – solar thermal collectors, a biomass boiler and an absorption heat pump.

Technology which has the highest supply capacity is a natural gas boiler with 11.17 MW, which is equal to the Scenario 1 for a separated district heating system. The highest biomass boiler capacity is equal to 8.79 MW, which is 0.5 MW higher than in Scenario 1. Once again, solar thermal collectors reach a large total area equal to 63.000 m^2.

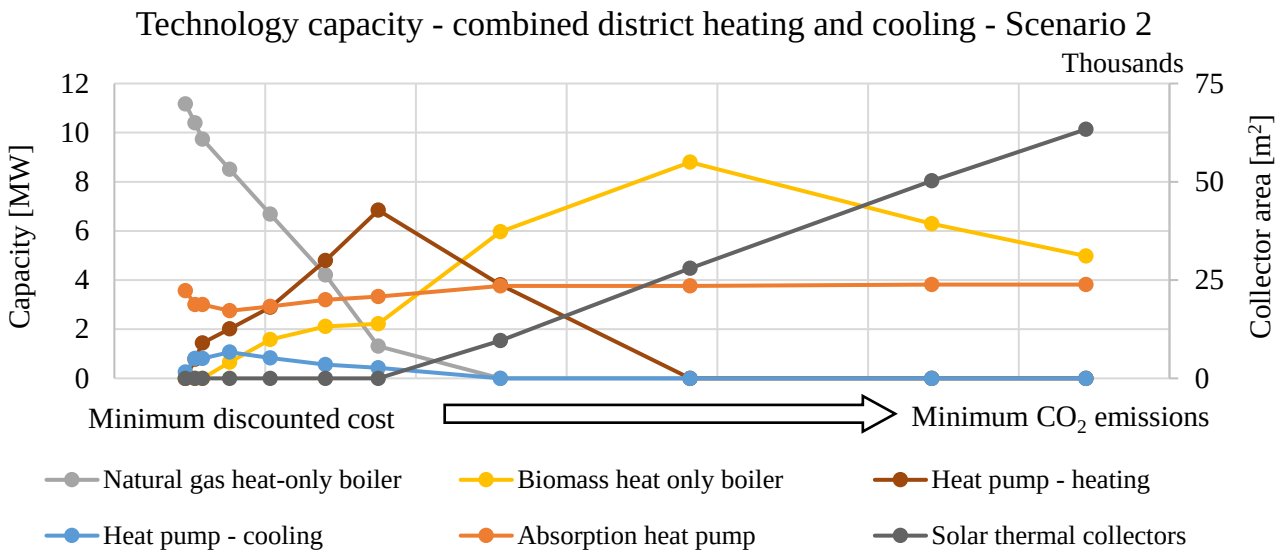

Figure 24 Optimal supply capacities for combined district heating and cooling

According to the results discussed above, it can be noticed that cogeneration units were not a part of the optimal solution, whether for separated or combined DH and DC systems. The reasons for this are as follows. Firstly, no price has been put on the carbon emissions since the maximum supply capacity is lower than 20 MW. Secondly, no carbon and cost allocation mechanisms have been assigned for CHP units. As shown in Section 3.5 and Section 3.6, they have a crucial impact on the multi-objective optimization results and the inclusion of cogeneration technologies. Finally, the exergy efficiency of the system was not considered. Since CHP has higher exergy efficiency than heat-only boiler, this aspect should be considered.

3.4 Economic, environmental and exergetic multi-objective optimization of district heating systems

Exergy analysis is often neglected in research dealing with energy system-level planning. However, exergy analysis is crucial for developing a decision-making method that will be able to compare district with individual heating solutions. For this purpose, we have upgraded the multi-objective optimization models, introduced in Section 3.1 and Section 3.3, to implement an exergy-related objective function. For this purpose, exergy destruction has been chosen as the third objective function. The results presented in this section are based on the analysis published in Paper 2 [129], available in the Annex of the thesis.

By adding a third objective function, the Pareto front becomes a Pareto surface and could be visualized in a three-dimensional Cartesian coordinate system, as shown in Figure 25. The figure presents the result of multi-objective optimization of a district heating system. The objective functions are the minimization of total discounted cost, the minimization of carbon emissions and the minimization of exergy destruction. The X-axis presents the economical objective function, the Y-axis is the exergetic objective function, while the Z-axis shows the environmental objective function. There are several specific points on the Pareto front that should be mentioned. The Pareto front is bound by three extremes. The point closet to the Y-Z plane presents the least-cost solution (marked with red). The point closest to the X-Z plane (marked with purple) is the solution with the lowest exergy destruction. In this case, it is also the solution with the highest exergy efficiency. The solution nearest to the X-Y plane (marked with green) is the most environmentally friendly, i.e. it has the lowest amount of CO_2 emissions.

The least-costly solutions have the highest environmental impact and the highest exergy destruction. However, the solutions with the lowest exergy destruction and low carbon emissions have the highest cost. The reason behind this is the non-existence of carbon and cost allocation in CHP units, which means that the whole environmental impact and economic burden is put on thermal energy production, while the electricity part is neglected.

Figure 25 displays an additional point which should be discussed. We are now referring to the so-called Utopia point. It is described as the ideal but non-reachable solution. It can be noticed it is located close to the origin of the coordinate system and out-of-reach for the Pareto solutions. Its X, Y and Z coordinates are equal to the lowest values of economical, exergetic and environmental optimal solutions, respectively.

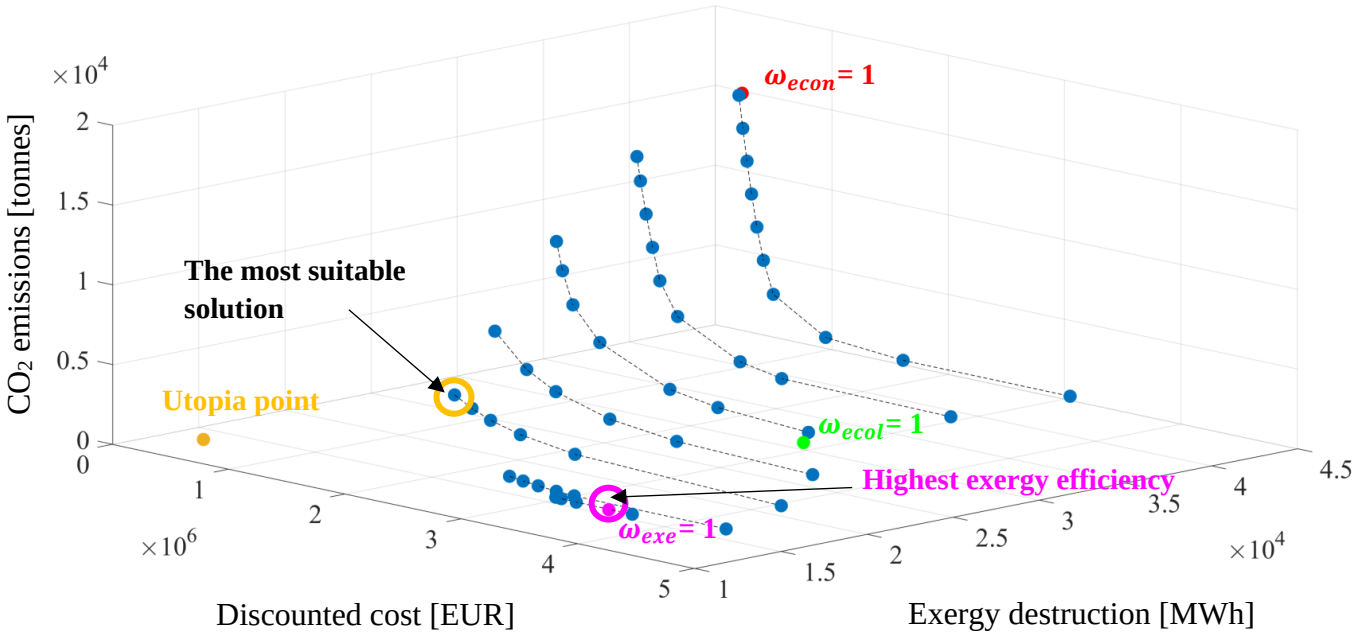

Figure 25 Pareto surface for multi-objective optimization of district heating system

Since the results of multi-objective optimization are a whole set of solutions, decision-making should be carried out. For the purpose of this analysis, the most suitable Pareto solution is the one closest to the Utopia point, marked with yellow. This solution presents the final compromise between all objective functions. It consists of a 5.5 MW heat pump which serves as a base production technology, 11 MW peak natural gas boiler and 5.000 m^2 of solar thermal collectors that operate during the summertime for domestic hot water production. It should be mentioned that exergy destruction in solar thermal collectors was assumed to be zero, since solar radiation was considered as an inexhaustible energy source. Exergy destruction was calculated only for technologies that utilize fuel with an finite utilisation potential.

Figure 26 shows the hourly heat supply, while Figure 27 displays the thermal storage operation of the most suitable solution during a winter week. It can be noticed that a natural gas boiler operates as the peak technology, while a heat pump operates as the base load, even during the nights when the heat load is reduced. The excess of thermal production is stored in the thermal storage and discharged the next morning during the morning peak demand.

It should be noticed that CHP, as the technology with a relatively high exergy efficiency is not a part of the most suitable solution. The reason for this is as follows. Exergy destruction is not the most suitable exergy-related objective function since it is not a relative parameter. Its absolute value changes with the size of the system. In other words, cogeneration units have both high exergy efficiency and high exergy destruction. Because of this, Section 3.5 and Section

3.6 will include exergy efficiency analysis. Furthermore, there is no carbon and cost allocation in CHP units.

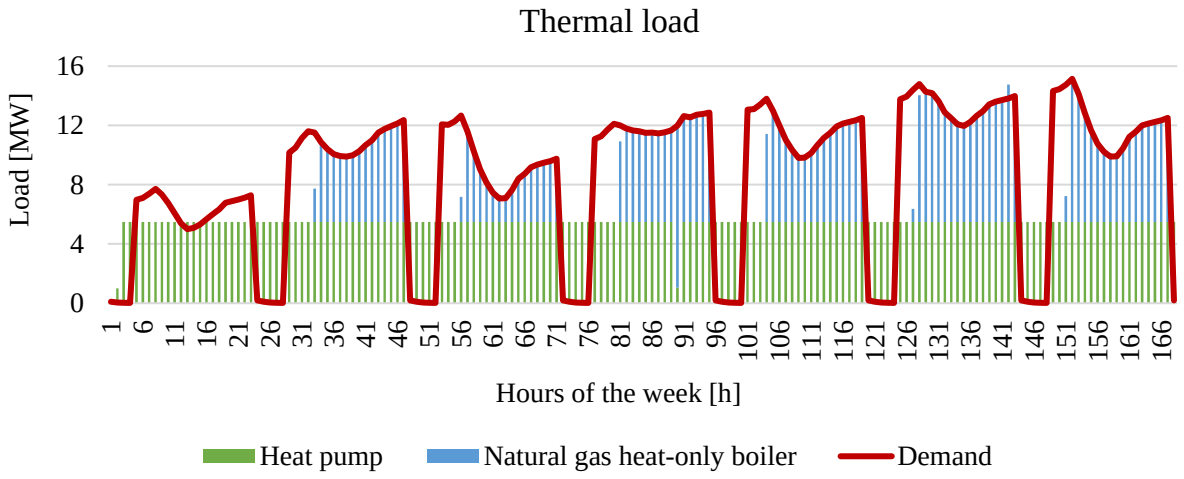

Figure 26 Hourly DH system operation for the chosen Pareto solution – winter week

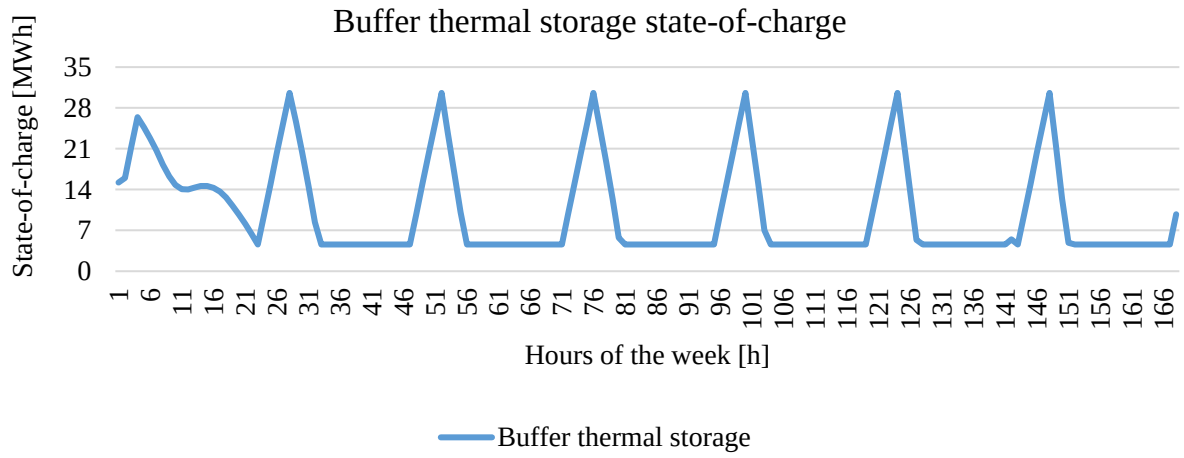

Figure 27 Hourly thermal storage operation for the chosen Pareto solution – winter week

3.5 Quantifying the cost of exergy destruction in district heating systems

Exergy destruction could be translated into cost by using numerous exergoeconomic analyses. The purpose of it is to provide total cost of the system by considering the exergy losses in the system. In this section, a novel exergy taxing approach is shown which is based on penalizing exergy destruction in heat only boilers as shown in Equation (43), where $\overline{\varepsilon_{DR,i,HOB}}$ presents a reference exergy destruction ratio for heat-only boiler technology, $\overline{\varepsilon_{DR,i,CHP}}$ is the reference exergy destruction ratio for cogeneration technology, while C_{exergy} is the specific cost of exergy destruction. Finally, Ex_{tax} is the exergy tax which should be paid since exergy destruction has occurred in heat-only boilers. It presents a theoretical system cost that could be avoided by using high-exergy quality technologies for heating purposes, such as cogeneration units. The results presented in this section are based on the conclusions of Paper 3 [130], available in the Annex of the thesis.

$$Ex_{tax} = \sum_{i} \sum_{t=1}^{t=8760} Ex_{in,t,i} \cdot \left(\overline{\varepsilon_{DR,i,HOB}} - \overline{\varepsilon_{DR,i,CHP}}\right) \cdot C_{exergy} \quad (43)$$

The proposed exergy cost approach was used to study the impact of carbon and exergy tax on displacing natural gas boilers in the cost-optimal DH system. For this purpose, two scenarios were used. In this first scenario all technologies are available, while in the second scenario CHP technologies are not allowed. Besides natural gas consumption in heat-only boilers, the focus was also put on different system characteristics such as CO_2 emissions and exergy efficiency.

Figure 28 shows the influence of carbon and exergy tax on CO_2 emissions and exergy efficiency of the system. Figure 28a and Figure 28b show that an increase of carbon tax reduces both exergy efficiency and carbon emissions for the scenario where all technologies are available. The reason behind this is the reduction of natural gas CHP that has relatively high CO_2 emissions and high exergy efficiency. For high carbon taxes, natural gas CHP is replaced with biomass CHP which has lower carbon emissions and lower exergy efficiency. On the other hand, Figure 28c and Figure 28d show a scenario that has no CHP technologies available. An increase of exergy and carbon tax provides an increase of exergy efficiency and a reduction of CO_2 emissions. However, exergy efficiency is much lower than in the first scenario. Nevertheless, it should be noticed that CO_2 emissions are lower for the second scenario when comparing solutions with carbon taxes lower than 40 EUR/tonne.

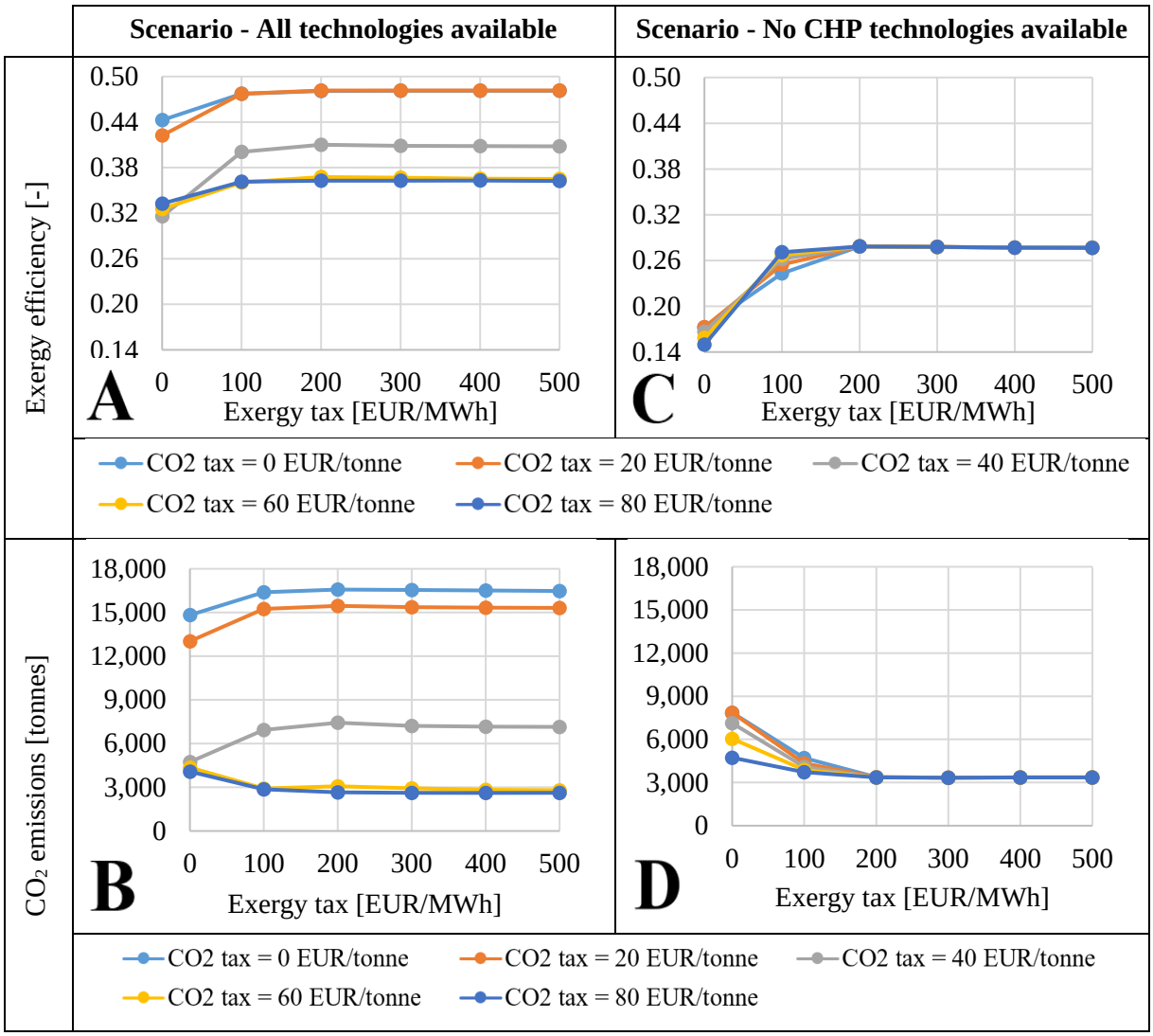

Figure 28 Influence of carbon and exergy tax on different system characteristics

Figure 29 and Figure 30 show the influence of carbon and exergy tax on natural gas reduction in heat-only boilers for the first and second scenario, respectively. For the scenario in which all technologies are available, an 80% reduction of natural gas consumption in heat-only boilers is possible already with 100 EUR/MWh of exergy tax pricing. A total phase out of heat-only natural gas boilers is challenging since most of the time they are used as peak technology. For the scenario where no CHP technologies are available, natural gas consumption in heat only boiler is higher than in the first scenario. However, it could be reduced to more than 50% for carbon tax values of 200 EUR/MWh. Nevertheless, even for exergy tax of 300 EUR/MWh, natural gas heat-only boilers are still a part of the cost-optimal DH supply system.

Although the impact of exergy tax is relatively high for the scenario, the increase of total system is relatively low, as shown in Figure 31. The share of the exergy tax cost is not higher than 10%. Carbon tax presents a much higher share, reaching more than 20% of the total system cost.

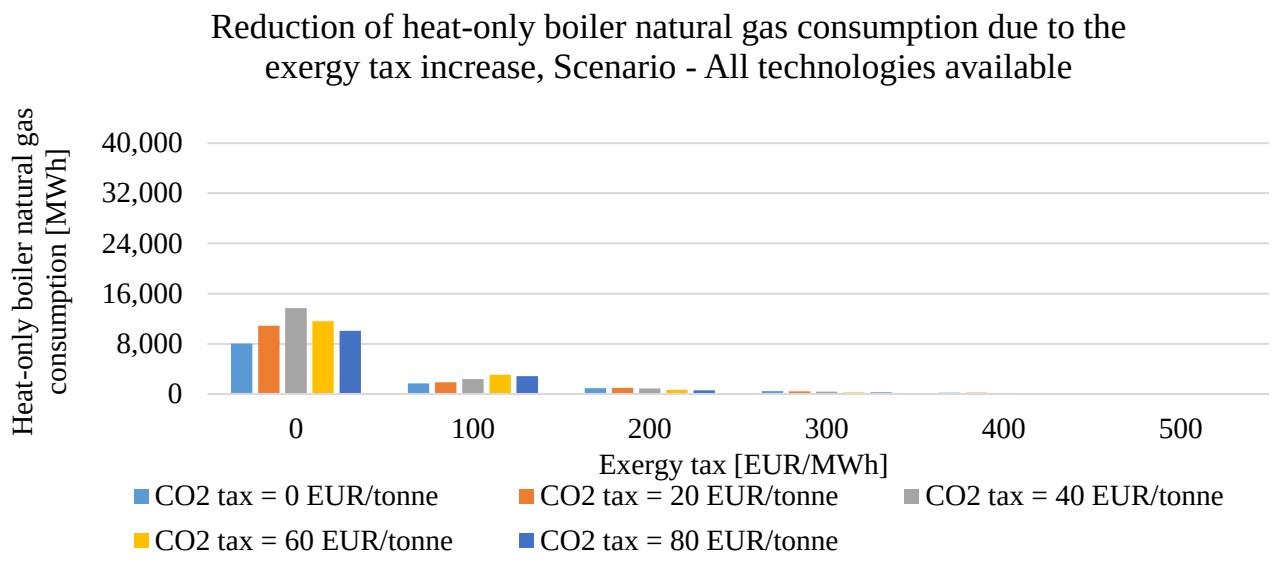

Figure 29 Influence of carbon and exergy tax on reduction of heat-only boiler natural gas consumption, Scenario - All CHP technologies available

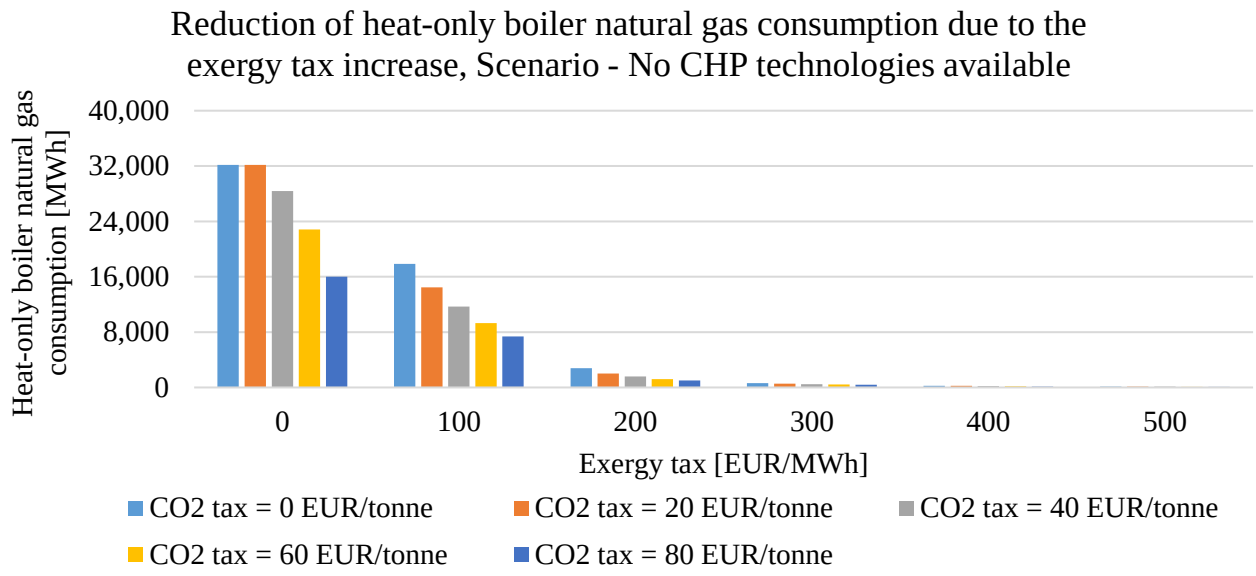

Figure 30 Influence of carbon and exergy tax on reduction of heat-only boiler natural gas consumption, Scenario - No CHP technologies available

The most important drawback of the proposed exergy taxing method is apparent from Figure 28a, where exergy efficiency is reduced with the increase of the carbon tax. The reason behind this is the allocation of CO_2 emissions, since they are fully assigned to thermal production. To address this issue, simple allocation has been introduced in CHP units which allocates 10% of the CO_2 emissions heat production, based on the power-loss method. Once carbon allocation is implemented, exergy and carbon tax have little-to-no influence on exergy efficiency and carbon emissions of the DH system, as shown in Figure 32. Furthermore, it could be noticed that carbon emissions are lower than 3,000 tonnes, even for low carbon taxes.

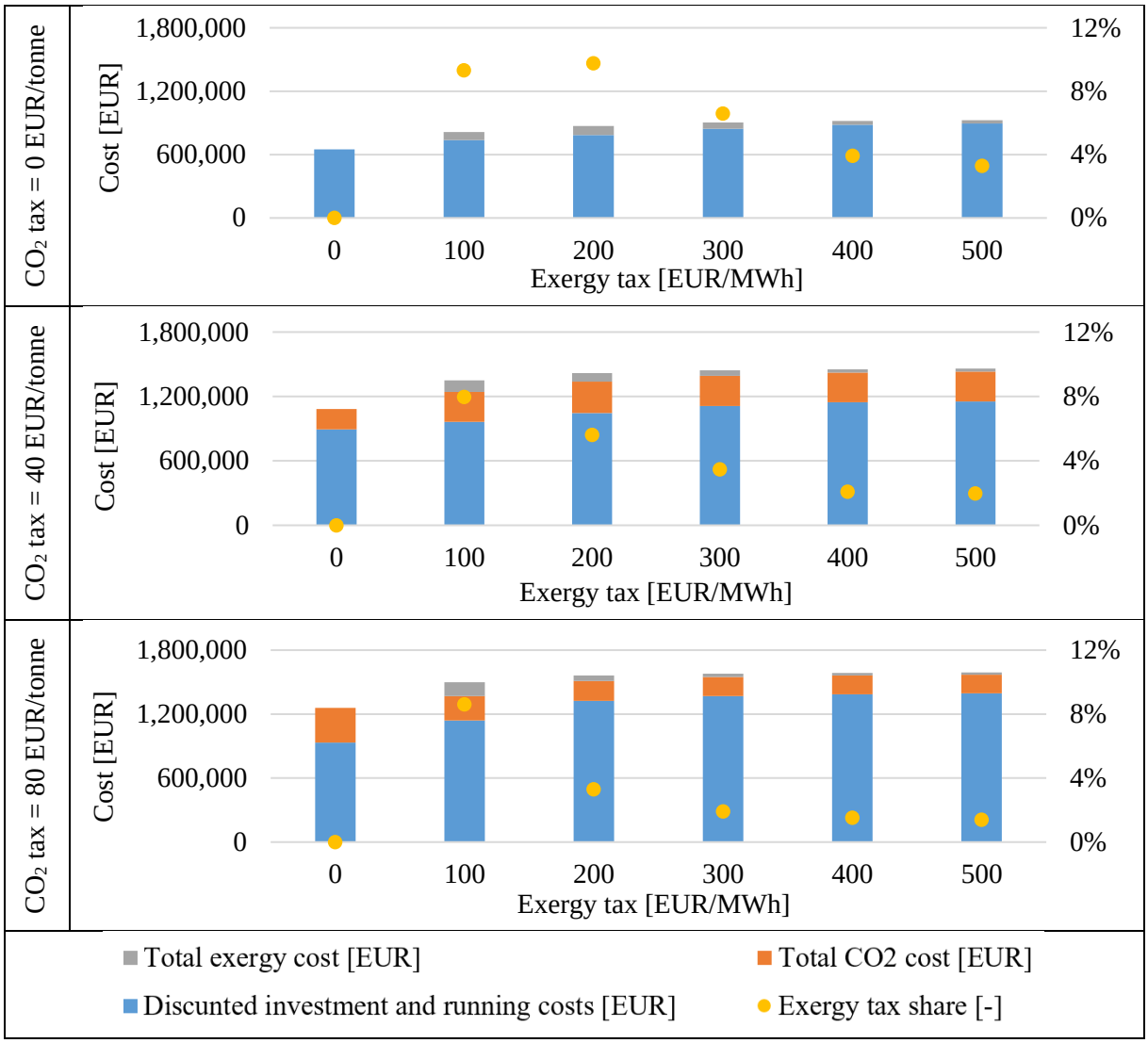

Figure 31 Cost distribution for different taxing conditions for Scenario – All technologies available

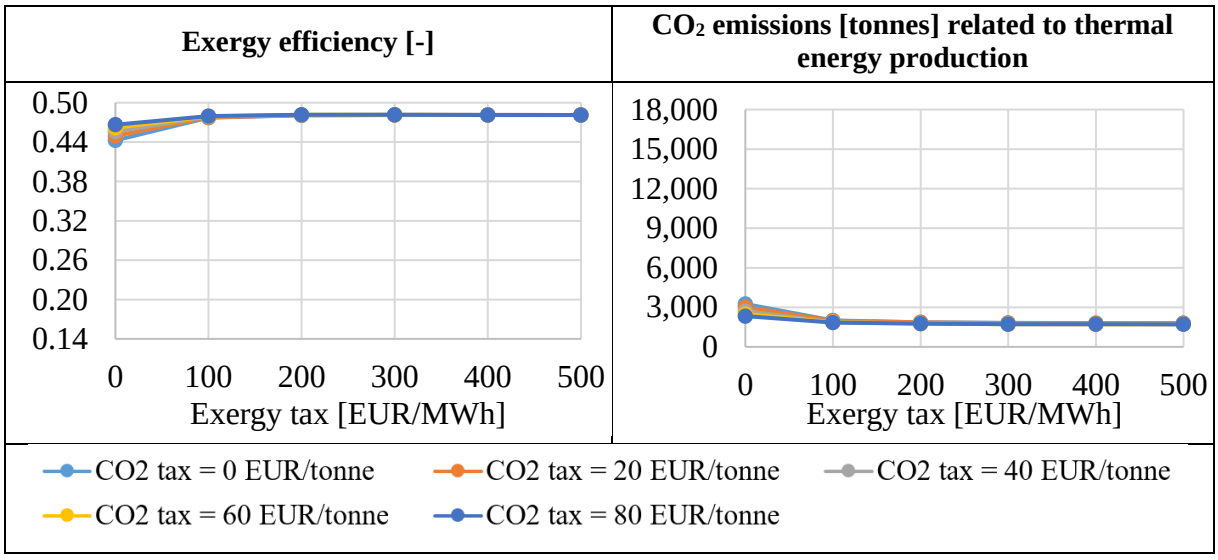

Figure 32 Exergy efficiency and CO_2 emissions of the least-cost solution for Scenario – All technologies available with CO_2 allocation in CHP units

3.6 Importance of carbon and cost allocation in cogeneration systems

The analysis presented in previous sections does not include a detailed allocation of carbon emissions and cost in cogeneration units. According to the obtained results, allocation has been shown as the crucial issue when dealing with CHP-based DH systems. For this purpose, we have developed a detailed multi-objective optimization model which considers exergy efficiency of the system together with cost and carbon emissions minimization. The carbon and cost allocation method was based on power-loss, the so-called Dresden method. The obtained Pareto solutions were compared with individual heating systems based on natural gas heat-only boilers. The conclusions presented in this section are based on the results published in Paper 6 [131], available in the Annex of the thesis.

For this evaluation, four CHP allocation scenarios were considered: no allocation, only cost allocation, only carbon allocation and finally simultaneous carbon and cost allocation. Firstly, the impact of CHP allocation on the DH Pareto solutions is shown. Figure 33 shows Pareto solutions for no CHP allocation implemented. It could be noticed that an increase of the system's exergy efficiency increases both the CO_2 emissions and the cost. In other words, the increased share of cogeneration has a negative impact on the economic and environmental objective function.

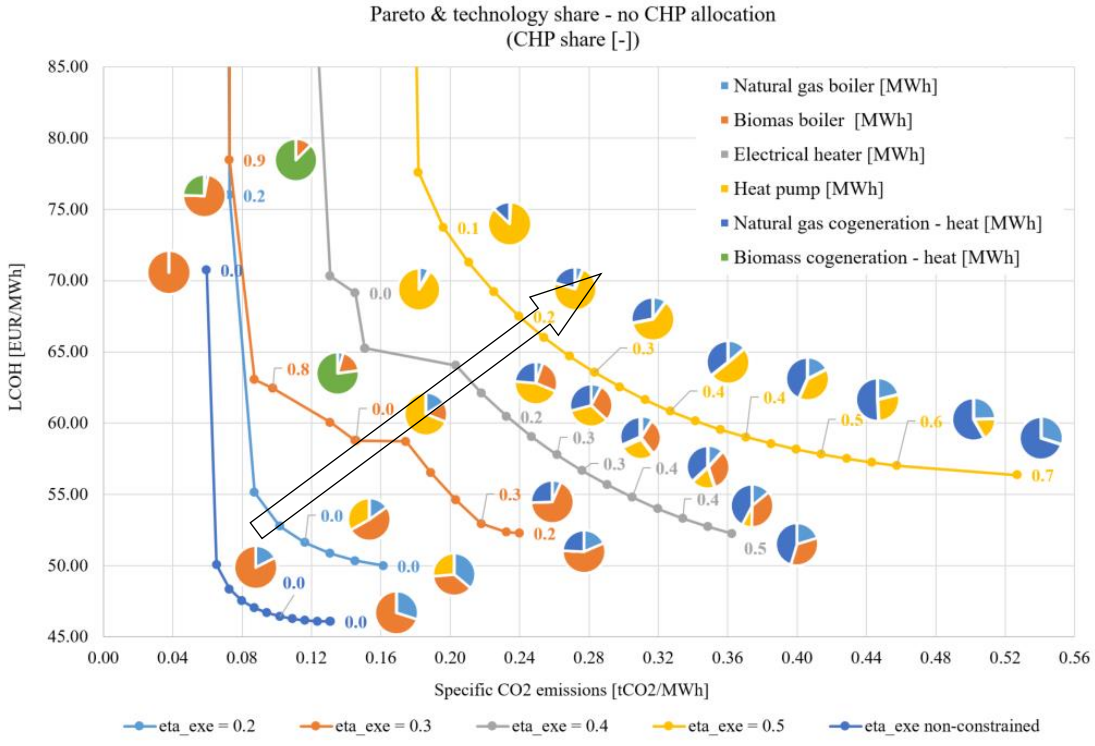

Figure 33 Pareto solutions, technologies and CHP share for no CHP allocation implemented

Figure 34 shows multi-objective optimisation solutions for cost allocation in CHP units. Cost allocation shifts the Pareto optimal solutions to the region of high carbon factors. In other words, CHP becomes relatively inexpensive but still has a high carbon impact. The least-costly solutions are CHP technologies, natural-gas based CHP for high CO_2 emissions and biomass-based CHP for low CO_2 emissions. Their cost difference is relatively low, less than 5 EUR/MWh.

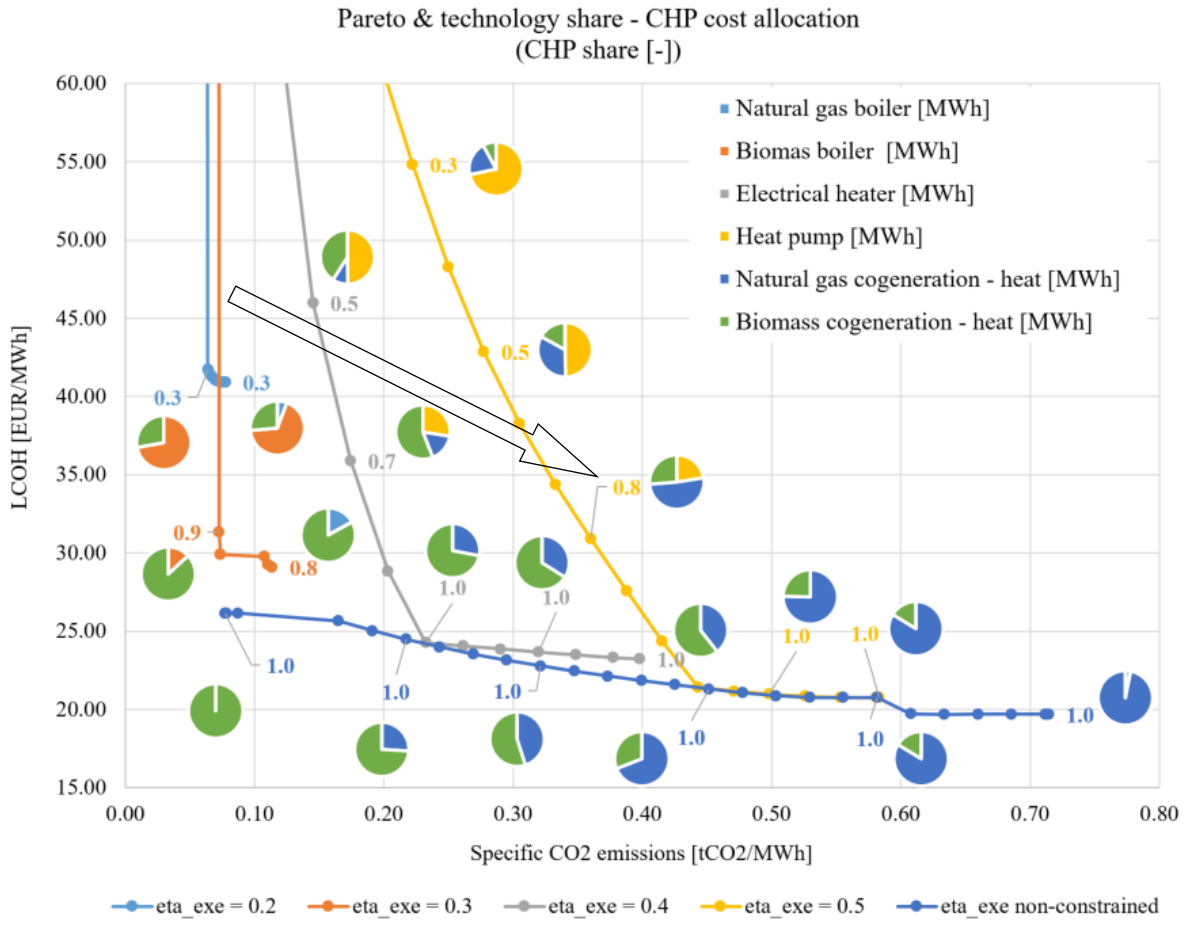

Figure 34 Pareto solutions, technologies and CHP share for cost CHP allocation implemented

On the other hand, carbon allocation reduces the carbon impact of the DH system, but the cost of the system stays relatively high, as shown in Figure 35. In this case, most of Pareto fronts are clustered together with little-to-no difference, especially around the knee-point region.

Finally, simultaneous carbon and cost allocation shows that CHP is the most suitable DH solution, as shown in Figure 36. Such CHP allocation shifts the Pareto solutions toward low carbon emissions and low system cost.

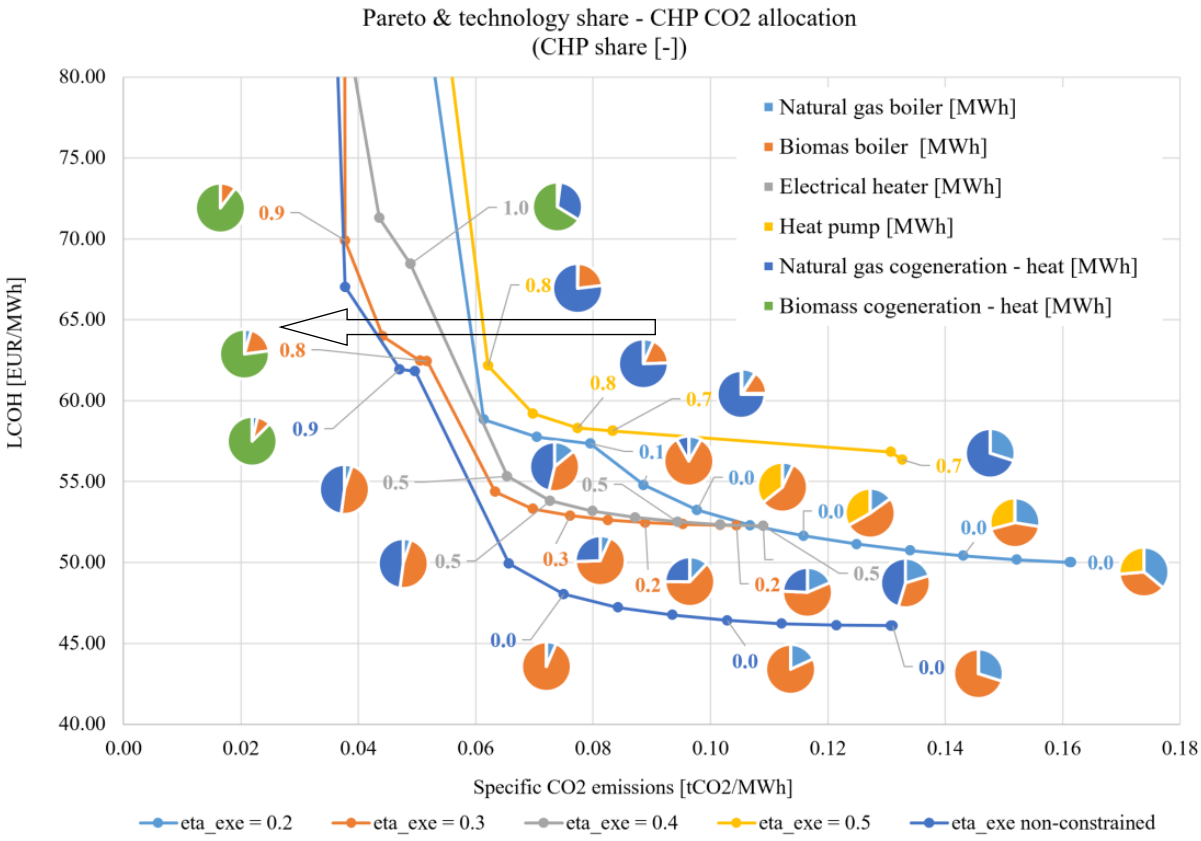

Figure 35 Pareto solutions, technologies and CHP share for carbon CHP allocation implemented

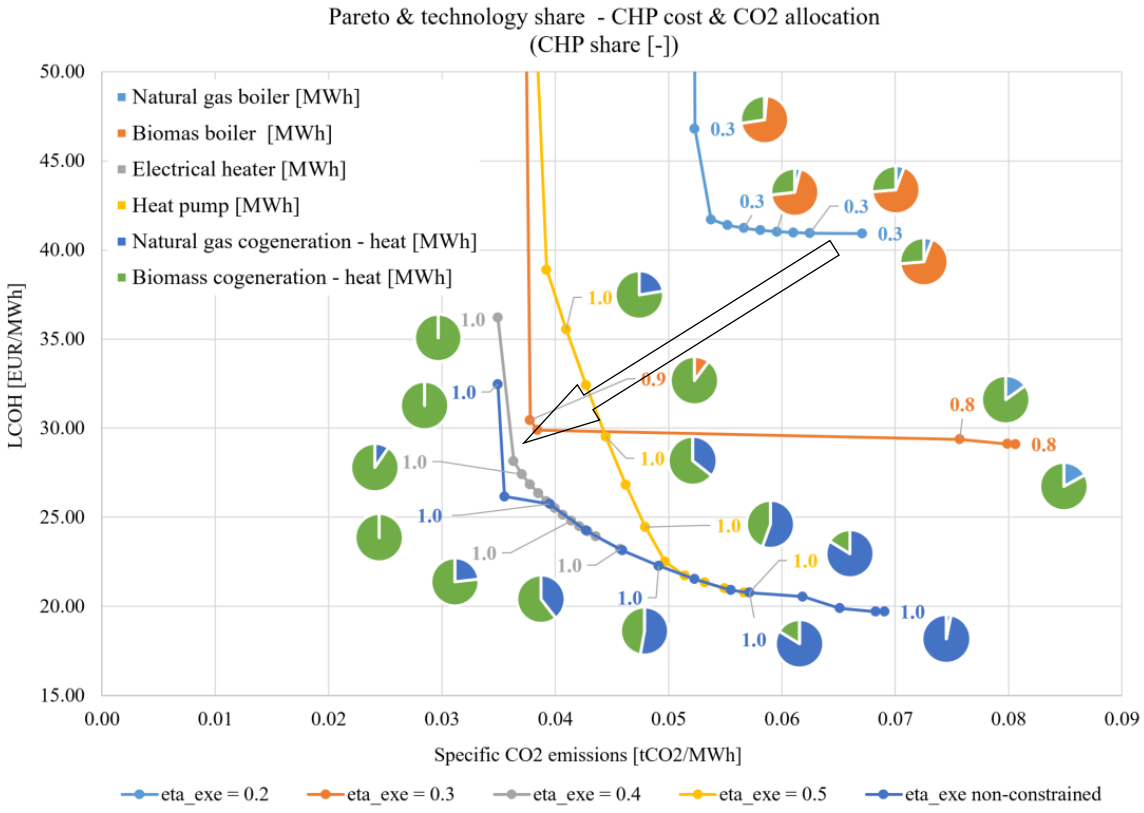

Figure 36 Pareto solutions, technologies and CHP share for cost and carbon CHP allocations implemented

Although DH supply technologies have relatively high exergy efficiency, the exergy losses of the thermal network should be considered when comparing DH and individual systems. Figure 37 shows exergy efficiency of a whole system compared to individual solutions. Exergy efficiency of individual natural gas boiler is equal to around 11 %. It can be noticed that some DH solutions have system-level exergy efficiency lower than an individual natural gas boiler. In some cases, around 50% of the exergy is lost in the network, depending on the CHP share in the technology mix. It can be concluded that DH system is better from the exergetic point of view only if the exergy efficiency of the DH supply system is higher than 20%. In other words, it should include a high-exergy efficiency technology such as CHP or a heat pump.

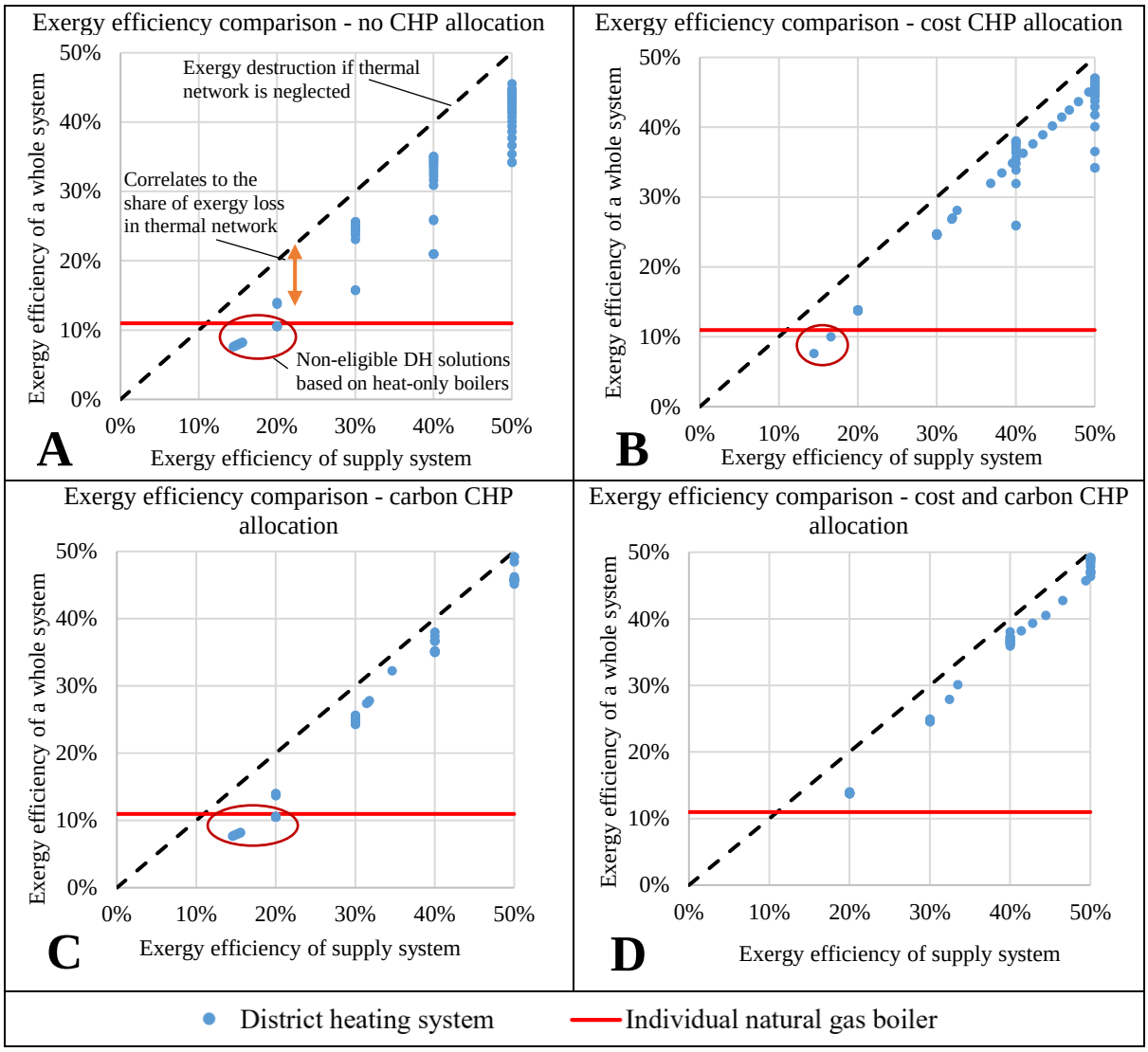

Figure 37 Exergy efficiency comparison between a district heating system and an individual natural gas-based system (exergy efficiency of the thermal network included): a) no CHP allocation, b) cost CHP allocation, c) carbon CHP allocation, d) cost and carbon allocation

The obtained district system solutions are also compared with individual heat-only boilers while focusing on system cost and carbon emissions. It should be mentioned that in this analysis the cost of the network and substations is also considered.

Figure 38 shows a comparison with individual solutions when no CHP allocation has been implemented. Without any CHP allocation, DH is more carbon-intensive than individual natural gas-based solutions. CHP-based DH is superior to individual gas only for the energy markets where natural gas prices for households are relatively high, i.e. more than 70 EUR/MWh. For countries with extremely low natural gas prices for households (such as Croatia) DH solutions are never superior to individual systems.

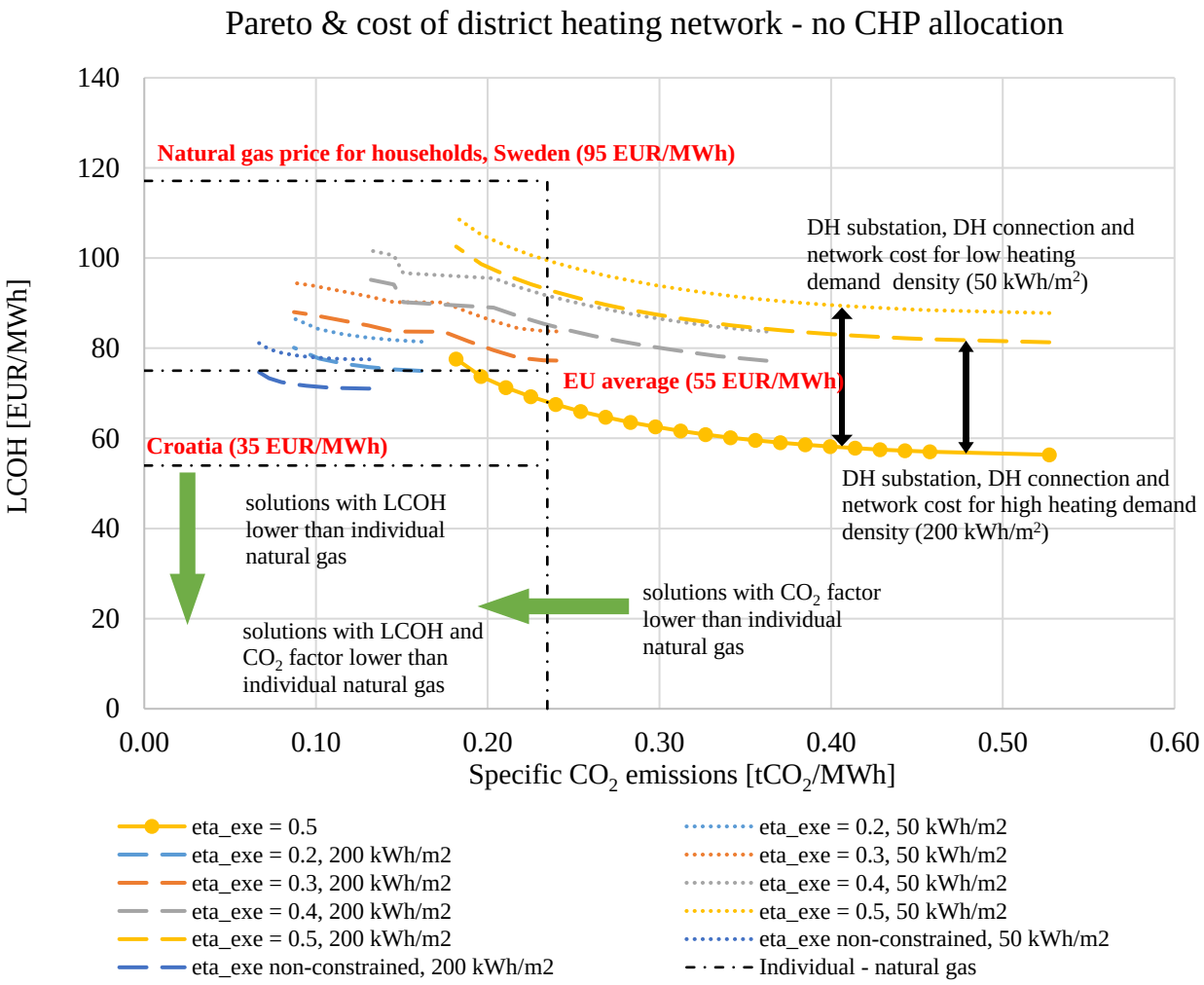

Figure 38 Pareto solutions, including network cost, and comparison with individual natural gas heating for no CHP allocation implemented

Figure 39 shows the mentioned comparison when only cost allocation is implemented in CHP units. In such a case, DH solutions are cheaper that individual ones, however most of them have a much higher carbon factor than individual natural gas boilers. District heating systems are marginally better than individual systems for extremely low natural gas market prices.

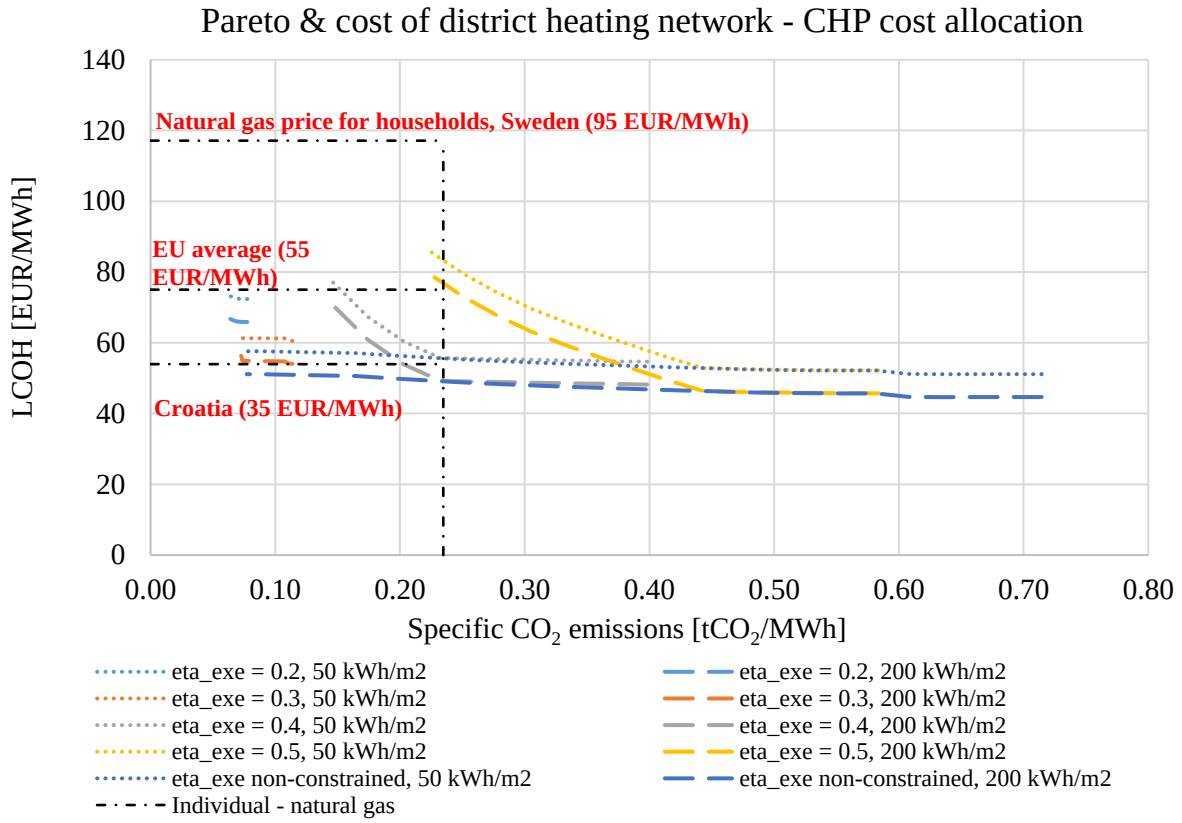

Figure 39 Pareto solutions, including network cost, and comparison with individual natural gas heating for CHP cost allocation implemented

With carbon allocation, DH always has a lower carbon factor than individual solutions, as shown in Figure 40. However, the cost of the system is kept relatively high. Furthermore, district heating is not feasible in markets with low natural gas prices. Natural gas prices for households must be at least 55 EUR/MWh to make DH economically superior to individual systems.

Once carbon and cost allocation in CHP systems is implemented, DH is economically and environmentally superior to individual systems, as shown in Figure 41. This is achievable even for Croatian natural gas prices, while the carbon factor is more than four times lower than for individual heating solutions.

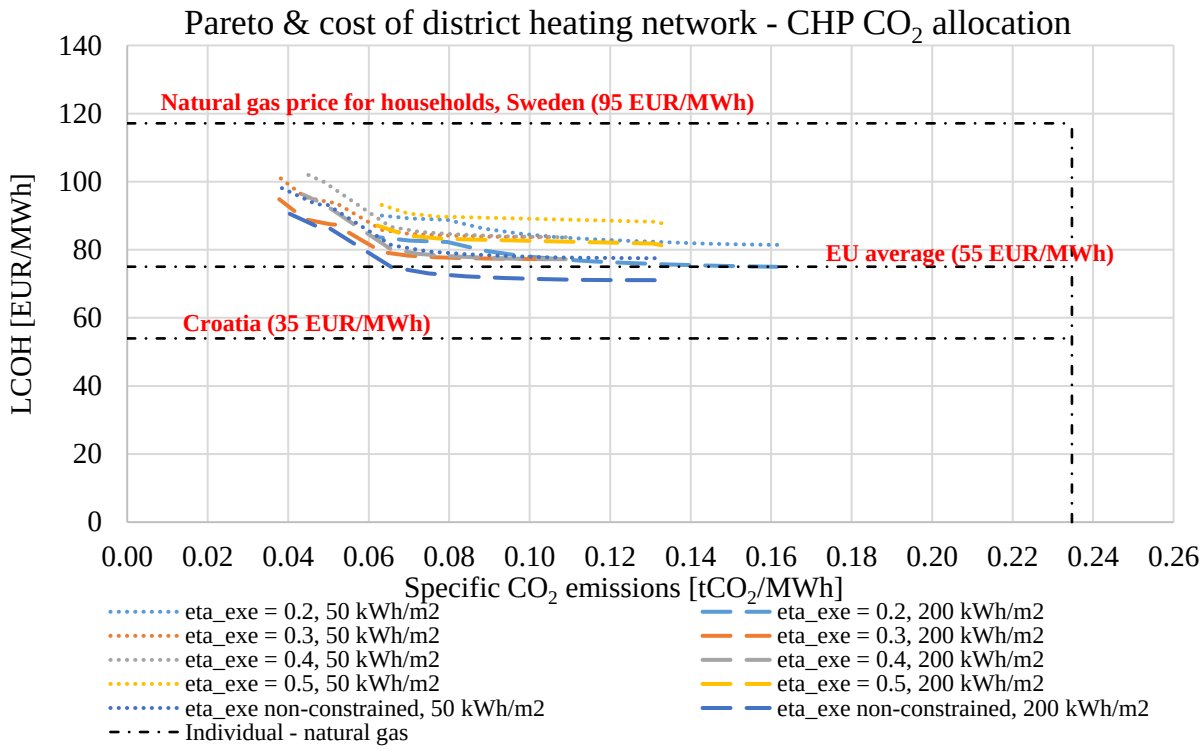

Figure 40 Pareto solutions, including network cost, and comparison with individual natural gas heating for CHP carbon allocation implemented

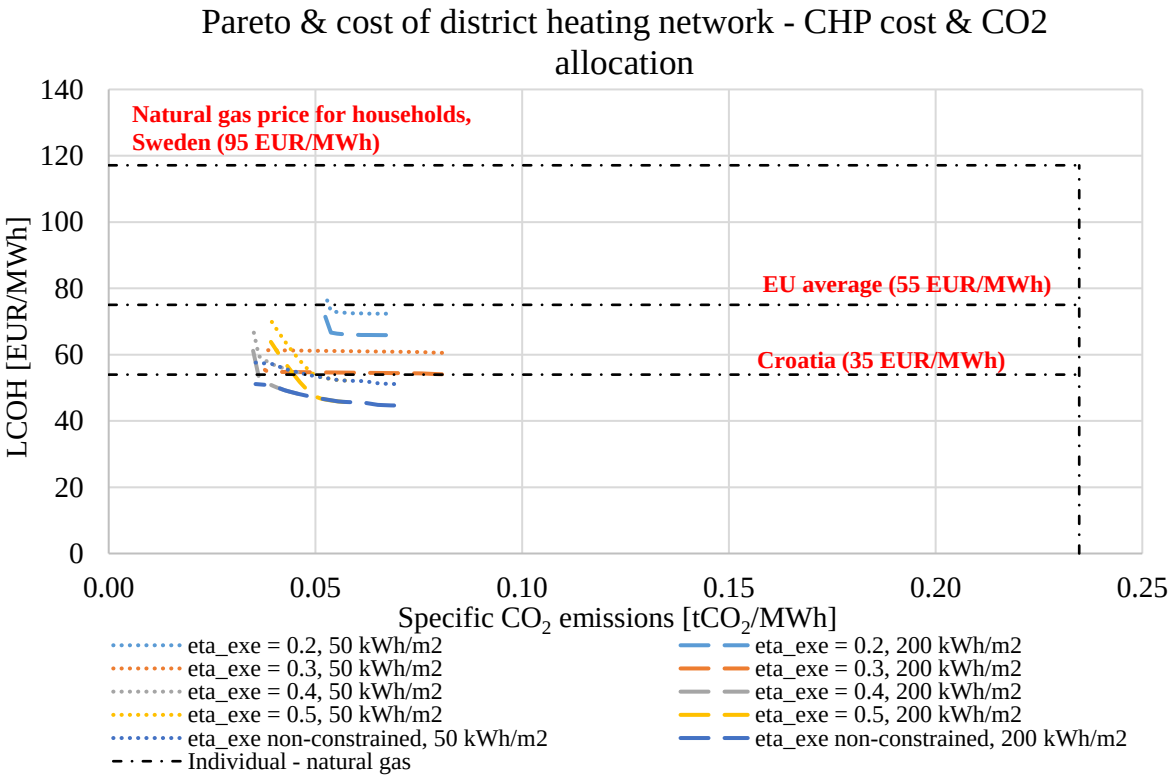

Figure 41 Pareto solutions, including network cost, and comparison with individual natural gas heating for CHP cost and carbon allocation implemented

Finally, Figure 42 and Figure 43 show the impact of district cooling and heating integration on system cost and carbon emissions. It has been shown that for additional 5 EUR/MWh of thermal energy, the heating and cooling systems can be coupled. Carbon and cost allocation in CHP units has a similar effect to the scenario when only a DH system is implemented.

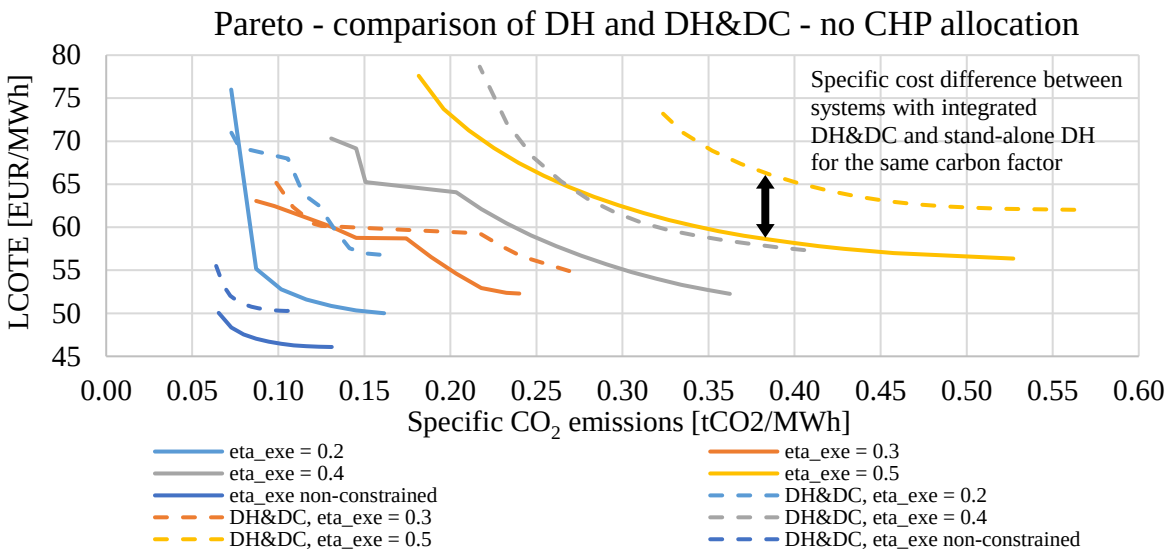

Figure 42 Pareto front comparison for systems with integrated district heating and cooling and a stand-alone district heating system – no CHP allocation implemented

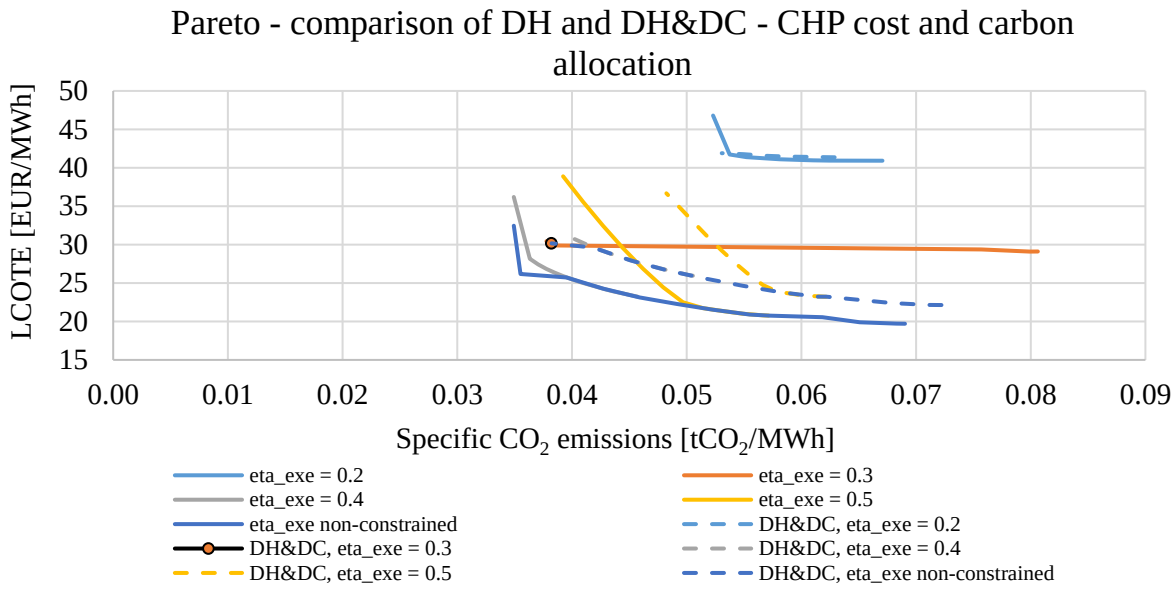

Figure 43 Pareto front comparison for systems with integrated district heating and cooling and a stand-alone district heating system – CHP cost and carbon allocation implemented

The increase of the district heating share in the upcoming decades will depend on the cogeneration allocation methods used in the various EU and country-level legislations. The allocation methods that assign the great part of CO_2 emissions emitted from CHP units to thermal energy production could negatively impact the extension of existing and future district heating grids. This is especially noticeable in the nearly-Zero Energy Building (nZEB) definition which is defined for each EU member state by using the national legislation. Numerous parameters could be used in order define the nZEB characteristics, but they are mostly based on the share of renewable energy, primary and useful energy consumption. Although CO_2 emissions are not an explicit criterion in the nZEB definition, they could be correlated to the primary energy factor of a heat source. In other words, if allocation in CHP units is carried out inappropriately, district heating could become a non-viable heating source for nZEB buildings. Strictly speaking, this implies that the newly constructed buildings have an additional challenge connecting to natural gas-based CHP district heating systems. This is for example visible in Croatian legislation, which defines the carbon factor for DH systems in Croatia in the range 0.31-0.53 tCO_2/MWh, while the average value is equal to 0.362 tCO_2/MWh [132]. For reference, the carbon factor of brown coal is 0.353 tCO_2/MWh. However, the carbon factor of the CHP based district heating system obtained in this paper, by using the power-loss based allocation method, is around three times lower. This puts CHP-based district heating systems as one of the most suitable heating options in urban areas, which could be easily integrated with renewable energy sources and power-to-heat units [31], [133], [134].

Similarly, the primary energy factors of DH systems used in the mentioned Croatian legislation are also relatively high, when compared to fossil fuels such as brown coal. They are in the range of 1.35-2.42, with the average value equal to 1.494, while the primary energy factor for brown coal is equal to 1.04 [132]. It should be mentioned that other countries have proposed lower values [63]. Interestingly, national systems with high district heating shares such as Latvia (65%), Denmark (62%), Estonia (61%) and Finland (50%), propose primary energy factors for district heating systems with relatively low values equal to 0.7, 0.8, 0.9, 0.7, respectively [63].

Natural gas-based individual boilers should not be used for space heating and domestic hot water preparation purposes in dense urban areas due to the great exergy destruction. We are proposing that natural gas should be used as a fuel only in high-temperature processes, such as industry, and cogeneration power plants. The quality of energy transformation is thus kept on a high level, and exergy destruction is greatly reduced. It should be clarified that we do not imply that natural gas-based CHP is the final goal in heating sector decarbonisation, but only

the first step. We have shown that district heating systems are economically feasible, ecologically cleaner, and exergy-wise a far better option than natural gas individual boilers. Once the dense urban areas are covered with district heating, it is much easier to decarbonise single heating source, than doing it for every building separately. Furthermore, they will be able to participate on the power market by using power-to-heat technologies and utilizing the excess of electricity coming from intermittent renewable energy sources such as wind and solar, thus contributing to the successful penetration of renewable energy in a power sector. Finally, by increasing the high quality DH share in the heating sector, a lock-in effect can be avoided. Some, countries such as the Netherlands ban new natural gas individual heating installations [135]. This decision is in line with the EU 2050 energy transition strategies [136] and the Green Deal. By promoting the natural gas phase out, additional stranded costs can be avoided since these installations will have to be replaced to reach carbon neutrality.

4 CONCLUSIONS AND FUTURE WORK

Although the EU promotes the utilisation of district heating and cooling systems, they are still not recognized as the primary heating source in densely urban areas. The main alternative is usually natural gas due to the relatively low retail prices which diminish the economic feasibility of district heating projects. Natural gas is a high quality fuel and its utilisation in the space heating sector represents high exergy destruction, i.e. waste of resources. During the energy transition, natural gas should be used for heating only in high-temperature processes that are challenging to decarbonise. On the other hand, cogeneration-based district heating represents highly efficient fuel utilisation since fuel since it is primarily used for electricity production, while the produced heat could be exploited in district heating or cooling systems.

The main objective of this doctoral thesis is to establish the multi-criteria modelling framework that will enable a systematic comparison of district and individual-based heating systems while focusing on economic, environmental and exergetic system indicators. For this purpose, we developed a multi-objective optimization model where objective functions are defined as the maximization of economic feasibility, the minimization of ecological impact and the maximization of exergy efficiency. The model considers, besides the heating and cooling demand, the energy market conditions, the supply technologies type and their capacities. The developed method was used to define the energy market price range where district heating and cooling systems have higher exergy efficiency and lower environmental impact than individual solutions, while at the same time being economically feasible.

The hypothesis of this thesis is that by using the method of multi-objective optimization of district heating and cooling systems, the cluster of solutions where district systems are better than individual, in terms of ecological impact and exergy efficiency, while at the same time being economically feasible, could be obtained in relation to energy market prices. The hypothesis of the doctoral thesis has been confirmed.

The doctoral thesis was based on six papers published in high impact journals indexed in CC database, available in the Annex of the thesis. In Paper 1 and Paper 2, a multi-objective optimisation method was developed that considers objective functions defined in the hypothesis. Furthermore, Paper 1 quantified the benefits of integrating district heating and

cooling networks in terms of carbon emissions and system cost. Paper 2 introduced the method that employs exergy destruction, the criterion that is rarely used for energy planning purposes. In Paper 3, we developed a novel taxing method based on exergy destruction in heat-only boiler units. The method was used to quantify the cost of exergy destruction and to analyse the impact of different taxing approaches on the displacement of natural gas boilers in district heating systems. Paper 4 and Paper 5 showed the importance of utilising district heating systems in future smart energy systems. In Paper 4, the integration of prosumers in district heating through a heat market was studied. It has been shown that prosumers, such as public buildings, which utilise heat pumps in combination with solar thermal could reduce the heat prices and increase the social welfare of the system. Paper 5 showed the impact of integration of variable renewable energy sources on optimal power-to-heat capacities in a local district heating. Although the impact is relatively small in the low-cost Pareto region, it has been shown that increase of the optimal heat pump size linearly follows the integration of variable renewable energy sources. Finally, in Paper 6 the comparison of district and individual-based solutions was carried out by using a multi-objective optimisation approach. Furthermore, the paper demonstrated the importance of carbon and cost allocation in CHP units, based on the power-loss method. It has been shown that for properly allocated emissions and cost, cogeneration-based district heating is economically feasible, more environmentally friendly and has higher exergy efficiency than natural-gas based district heating, even for low household prices.

District heating and cooling are topics that will bring even more attention in the upcoming years when the heating sector must be decarbonised even further. The developed method will have to be upgraded accordingly. In general, a more detailed district model is needed that considers additional system dynamics such as more detailed temperature levels, unit commitment and dispatch. Due to this, the problem is potentially becoming mixed-integer non-linear which is an additional issue that should be handled. Although this work considers heat demand density, it should be studied in more detail by considering different Geographical Information System methods. Furthermore, district heating network route optimization would be a great addition to the already developed optimization model. The cost of a substation at the building level is not studied in detail in this work, and only reference prices were used. The technical issue of connecting buildings to a DH system could be a crucial issue, and the pricing of such solutions should be considered. Furthermore, different ownership models for substations can be analysed and the most suitable should be obtained to maximize social welfare.

The refurbishment of a building stock will influence space heating temperature regimes and consequently, district heating supply temperatures. This will influence the district heating technology characteristics and shift the obtained results. Furthermore, the thermal network temperature reduction has a positive effect on the cost and carbon allocation methods since it reduces the power-loss and increases the power-to-heat factors. The impact of temperature reduction on substation design should also be considered. A lower temperature difference means a higher heat exchange area that results in higher specific costs of the substation.

Power and heating sector coupling through heat pumps should be studied in more detail, especially considering various waste heat sources with different temperature levels. The reduction of supply temperatures will open the possibility for the integration of low-temperature urban waste heat sources such as supermarkets, shopping malls and data centres. Finally, a power balancing market was not considered in this work, but it presents an additional economic benefit for cogeneration and power-to-heat units in district heating systems. With penetration of variable renewable energy sources, power system balancing will become an even more important challenge to deal with.

5 LITERATURE

[1] L. Hewage, U. Willhelm, and J. W. Mesthrige, “Global Research on Carbon Emissions: A Scientometric Review,” *Sustainability*, vol. 2, pp. 1–25, 2019.

[2] H. Huang and S. Lo, “Review and classify the GHGs-related indicators,” *Renew. Sustain. Energy Rev.*, vol. 15, no. 1, pp. 594–602, 2011, doi: 10.1016/j.rser.2010.07.023.

[3] J. B. Shukla, M. Verma, and A. K. Misra, “Effect of global warming on sea level rise : A modeling study,” *Ecol. Complex.*, vol. 32, pp. 99–110, 2017, doi: 10.1016/j.ecocom.2017.10.007.

[4] “CarbonBrief - The impacts of climate change at 1.5C, 2C and beyond.” [Online]. Available: https://interactive.carbonbrief.org/impacts-climate-change-one-point-five-degrees-two-degrees/?utm_source=web&utm_campaign=Redirect.

[5] “UNFCCC - Paris Agreement.” [Online]. Available: https://unfccc.int/process-and-meetings/the-paris-agreement/the-paris-agreement.

[6] F. Ana, M. D. Pinheiro, J. De Brito, and R. Mateus, “Decarbonizing strategies of the retail sector following the Paris Agreement,” vol. 135, no. December 2018, 2020, doi: 10.1016/j.enpol.2019.110999.

[7] E. Papadis and G. Tsatsaronis, “Challenges in the decarbonization of the energy sector,” *Energy*, p. 118025, 2020, doi: 10.1016/j.energy.2020.118025.

[8] “European Commission: EU 2020 climate & energy package.” [Online]. Available: https://ec.europa.eu/clima/policies/strategies/2020_en.

[9] “EUROSTAT.” [Online]. Available: https://ec.europa.eu/eurostat/data/database.

[10] “European Commission: EU 2030 climate & energy framework.” [Online]. Available: https://ec.europa.eu/clima/policies/strategies/2030_en.

[11] “European Commission: 2050 long-term strategy.” [Online]. Available: https://ec.europa.eu/clima/policies/strategies/2050_en.

[12] L. Reichenberg, F. Hedenus, M. Odenberger, and F. Johnsson, “The marginal system

LCOE of variable renewables – Evaluating high penetration levels of wind and solar in Europe," *Energy*, 2018, doi: 10.1016/j.energy.2018.02.061.

[13] W. Shen, X. Chen, J. Qiu, J. A. Hayward, S. Sayeef, and P. Osman, "A comprehensive review of variable renewable energy levelized cost of electricity," *Renew. Sustain. Energy Rev.*, vol. 133, 2020, doi: 10.1016/j.rser.2020.110301.

[14] S. Allard, S. Mima, V. Debusschere, T. Tran, P. Criqui, and N. Hadjsaid, "European transmission grid expansion as a fl exibility option in a scenario of large scale variable renewable energies integration," *Energy Econ.*, vol. 87, p. 104733, 2020, doi: 10.1016/j.eneco.2020.104733.

[15] M. Pavičević *et al.*, "The potential of sector coupling in future European energy systems: Soft linking between the Dispa-SET and JRC-EU-TIMES models," *Appl. Energy*, vol. 267, no. April, p. 115100, 2020, doi: 10.1016/j.apenergy.2020.115100.

[16] "European Commission: EU strategy on energy system integration." [Online]. Available: https://ec.europa.eu/energy/topics/energy-system-integration/eu-strategy-energy-system-integration_en.

[17] A. Buttler and H. Splietho, "Current status of water electrolysis for energy storage , grid balancing and sector coupling via power-to-gas and power-to-liquids : A review," no. September, 2017, doi: 10.1016/j.rser.2017.09.003.

[18] METIS, "European Commission METIS Studies Study S8 The role and potential of Power-to-X in 2050," 2018.

[19] T. Dengiz, P. Jochem, and W. Fichtner, "Demand response with heuristic control strategies for modulating heat pumps," *Appl. Energy*, vol. 238, no. September 2018, pp. 1346–1360, 2019, doi: 10.1016/j.apenergy.2018.12.008.

[20] F. L. Müller and B. Jansen, "Large-scale demonstration of precise demand response provided by residential heat pumps ☆," *Appl. Energy*, vol. 239, no. October 2018, pp. 836–845, 2019, doi: 10.1016/j.apenergy.2019.01.202.

[21] M. Hany, K. Saikia, L. F. Cabeza, D. Boer, and M. Vall, "Flexible heat pump integration to improve sustainable transition toward 4th generation district heating," *Energy Convers. Manag.*, vol. 225, no. May, 2020, doi:

10.1016/j.enconman.2020.113379.

[22] L. Kreuder and C. Spataru, “Assessing Demand Response with Heat Pumps for Efficient Grid Operation in Smart Grids,” *Sustain. Cities Soc.*, 2015, doi: 10.1016/j.scs.2015.07.011.

[23] A. Gravelsins, I. Pakere, A. Tukulis, and D. Blumberga, “Solar power in district heating. P2H flexibility concept,” *Energy*, vol. 181, pp. 1023–1035, 2019, doi: 10.1016/j.energy.2019.05.224.

[24] J. Wang, S. You, Y. Zong, C. Træholt, Z. Yang, and Y. Zhou, “Flexibility of combined heat and power plants: A review of technologies and operation strategies,” *Appl. Energy*, vol. 252, no. May, p. 113445, 2019, doi: 10.1016/j.apenergy.2019.113445.

[25] Z. Tian *et al.*, “Large-scale solar district heating plants in Danish smart thermal grid: Developments and recent trends,” *Energy Convers. Manag.*, vol. 189, no. October 2018, pp. 67–80, 2020, doi: 10.1016/j.enconman.2019.03.071.

[26] J. Pelda, F. Stelter, and S. Holler, “Potential of integrating industrial waste heat and solar thermal energy into district heating networks in Germany,” *Energy*, vol. 203, p. 117812, 2020, doi: 10.1016/j.energy.2020.117812.

[27] E. Wiechers, U. Persson, L. Grundahl, R. Søgaard, and B. Vad, “Heat Roadmap Europe: Towards EU-Wide , local heat supply strategies,” *Energy*, vol. 177, pp. 554–564, 2019, doi: 10.1016/j.energy.2019.04.098.

[28] S. Frederiksen and S. Werner, *District Heating and Cooling*. 2013.

[29] D. S. Østergaard and S. Svendsen, “Costs and benefits of preparing existing Danish buildings for low-temperature district heating,” *Energy*, vol. 176, pp. 718–727, 2019, doi: 10.1016/j.energy.2019.03.186.

[30] A. Kapil, I. Bulatov, R. Smith, and J. K. Kim, “Process integration of low grade heat in process industry with district heating networks,” *Energy*, vol. 44, no. 1, pp. 11–19, 2012, doi: 10.1016/j.energy.2011.12.015.

[31] H. Lund *et al.*, “4th Generation District Heating (4GDH). Integrating smart thermal grids into future sustainable energy systems.,” *Energy*, vol. 68, pp. 1–11, 2014, doi: 10.1016/j.energy.2014.02.089.

[32] H. Lund, N. Duic, P. A. Ostergaard, and B. V. Mathiesen, “Future District Heating Systems and Technologies : On the role of Smart Energy Systems and 4 th Generation District,” *Energy*, 2018, doi: 10.1016/j.energy.2018.09.115.

[33] S. Werner, “International review of district heating and cooling,” *Energy*, pp. 1–15, 2017, doi: 10.1016/j.energy.2017.04.045.

[34] S. Buffa, M. Cozzini, M. D’Antoni, M. Baratieri, and R. Fedrizzi, “5th generation district heating and cooling systems: A review of existing cases in Europe,” *Renew. Sustain. Energy Rev.*, vol. 104, no. June 2018, pp. 504–522, 2019, doi: 10.1016/j.rser.2018.12.059.

[35] B. Elmegaard, T. S. Ommen, M. Markussen, and J. Iversen, “Integration of space heating and hot water supply in low temperature district heating,” *Energy Build.*, vol. 124, pp. 255–264, 2016, doi: 10.1016/j.enbuild.2015.09.003.

[36] Y. Chen, J. Wang, and P. D. Lund, “Sustainability evaluation and sensitivity analysis of district heating systems coupled to geothermal and solar resources,” *Energy Convers. Manag.*, vol. 220, no. 2, p. 113084, 2020, doi: 10.1016/j.enconman.2020.113084.

[37] M. Papapetrou, G. Kosmadakis, A. Cipollina, U. La, and G. Micale, “Industrial waste heat: Estimation of the technically available resource in the EU per industrial sector, temperature level and country,” *Appl. Therm. Eng.*, vol. 138, no. February, pp. 207–216, 2018, doi: 10.1016/j.applthermaleng.2018.04.043.

[38] A. R. Christiansen *et al.*, “Analysis of possibilities to utilize excess heat of supermarkets as heat source for district heating,” *Energy Procedia*, vol. 149, pp. 276–285, 2018, doi: 10.1016/j.egypro.2018.08.192.

[39] M. Wahlroos, M. Pärssinen, S. Rinne, S. Syri, and J. Manner, “Future views on waste heat utilization – Case of data centers in Northern Europe,” *Renew. Sustain. Energy Rev.*, vol. 82, no. July 2017, pp. 1749–1764, 2018, doi: 10.1016/j.rser.2017.10.058.

[40] C. Mateu-Royo, S. Sawalha, A. Mota-Babiloni, and J. Navarro-Esbrí, “High temperature heat pump integration into district heating network,” *Energy Convers. Manag.*, vol. 210, no. December 2019, p. 112719, 2020, doi: 10.1016/j.enconman.2020.112719.

[41] P. A. Østergaard and A. N. Andersen, “Economic feasibility of booster heat pumps in heat pump-based district heating systems,” *Energy*, vol. 155, pp. 921–929, 2018, doi: 10.1016/j.energy.2018.05.076.

[42] A. S. Gaur, D. Z. Fitiwi, and J. Curtis, “Energy Research & Social Science Heat pumps and our low-carbon future: A comprehensive review,” *Energy Res. Soc. Sci.*, vol. 71, no. August 2020, p. 101764, 2021, doi: 10.1016/j.erss.2020.101764.

[43] H. Pieper, T. Ommen, J. K. Jensen, and B. Elmegaard, “Comparison of COP estimation methods for large-scale heat pumps used in energy planning,” *Energy*, vol. 205, p. 117994, 2020, doi: 10.1016/j.energy.2020.117994.

[44] P. Wang, P. Zhao, W. Xu, J. Wang, and Y. Dai, “Performance analysis of a combined heat and compressed air energy storage system with packed bed unit and electrical heater,” *Appl. Therm. Eng.*, vol. 162, no. May, p. 114321, 2019, doi: 10.1016/j.applthermaleng.2019.114321.

[45] M. Pavičević, T. Novosel, T. Pukšec, and N. Duić, “Hourly optimization and sizing of district heating systems considering building refurbishment - Case study for the city of Zagreb,” *Energy*, 2016, doi: 10.1016/j.energy.2017.06.105.

[46] O. Terreros *et al.*, “Electricity market options for heat pumps in rural district heating networks in Austria,” *Energy*, vol. 196, p. 116875, 2020, doi: 10.1016/j.energy.2019.116875.

[47] F. Levihn, “CHP and heat pumps to balance renewable power production: Lessons from the district heating network in Stockholm,” *Energy*, vol. 137, pp. 670–678, 2017, doi: 10.1016/j.energy.2017.01.118.

[48] D. Lingfors, J. Olauson, D. Lingfors, and J. Olauson, “Can electricity market prices control power-to-heat production for peak shaving of renewable power generation ? The case of Sweden,” *Energy*, vol. 176, no. 1, pp. 1–14, 2019, doi: 10.1016/j.energy.2019.03.156.

[49] M. Dillig, M. Jung, and J. Karl, “The impact of renewables on electricity prices in Germany – An estimation based on historic spot prices in the years 2011 – 2013,” *Renew. Sustain. Energy Rev.*, vol. 57, pp. 7–15, 2016, doi: 10.1016/j.rser.2015.12.003.

[50] B. Aust and A. Horsch, “Negative market prices on power exchanges : Evidence and policy implications from Germany,” *Electr. J.*, vol. 33, no. 3, p. 106716, 2020, doi: 10.1016/j.tej.2020.106716.

[51] “Fraunhofer - Energy Charts.” [Online]. Available: https://energy-charts.info/index.html?l=en&c=DE.

[52] H. Lund, A. N. Andersen, P. Alberg, B. Vad, and D. Connolly, “From electricity smart grids to smart energy systems - A market operation based approach and understanding,” *Energy*, vol. 42, pp. 96–102, 2012, doi: 10.1016/j.energy.2012.04.003.

[53] “Skagen district heating.” [Online]. Available: http://www.energyweb.dk/skagen/?english&history.

[54] D. Meha, A. Pfeifer, N. Dui, and H. Lund, “Increasing the integration of variable renewable energy in coal-based energy system using power to heat technologies: The case of Kosovo,” vol. 212, 2020, doi: 10.1016/j.energy.2020.118762.

[55] T. Novosel, T. Pukšec, N. Duić, and J. Domac, “Heat demand mapping and district heating assessment in data-pour areas,” *Renew. Sustain. Energy Rev.*, vol. 131, no. November 2019, 2020, doi: 10.1016/j.rser.2020.109987.

[56] B. Möller, E. Wiechers, U. Persson, L. Grundahl, D. Connolly, and M. Bernd, “Heat Roadmap Europe: Identifying local heat demand and supply areas with a European thermal atlas,” vol. 158, 2018, doi: https://doi.org/10.1016/j.energy.2018.06.025.

[57] U. Persson, E. Wiechers, B. Möller, and S. Werner, “Heat Roadmap Europe: Heat distribution costs,” vol. 176, pp. 604–622, 2019, doi: 10.1016/j.energy.2019.03.189.

[58] “European Commission - An EU Strategy on Heating and Cooling.” [Online]. Available: https://eur-lex.europa.eu/legal-content/EN/TXT/?qid=1575551754568&uri=CELEX:52016DC0051.

[59] “European Comission - Powering a climate-neutral economy: An EU Strategy for Energy System Integration,” 2020. .

[60] R. Büchele, L. Kranzl, and M. Hummel, “What is the impact of the policy framework on the future of district heating in Eastern European countries ? The case of Brasov,” *Energy Strateg. Rev.*, pp. 10–13, 2017, doi: 10.1016/j.esr.2017.12.003.

[61] A. Colmenar-santos, E. Rosales-asensio, D. Borge-diez, and J. Blanes-peiró, “District heating and cogeneration in the EU-28 : Current situation , potential and proposed energy strategy for its generalisation,” *Renew. Sustain. Energy Rev.*, vol. 62, pp. 621–639, 2016, doi: 10.1016/j.rser.2016.05.004.

[62] A. Magrini, G. Lentini, S. Cuman, A. Bodrato, and L. Marenco, “Developments in the Built Environment From nearly zero energy buildings (NZEB) to positive energy buildings (PEB): The next challenge - The most recent European trends with some notes on the energy analysis of a forerunner PEB example,” *Dev. Built Environ.*, vol. 3, no. March, p. 100019, 2020, doi: 10.1016/j.dibe.2020.100019.

[63] E. Latõšov, A. Volkova, A. Siirde, J. Kurnitski, and M. Thalfeldt, “Primary energy factor for district heating networks in European Union member states,” *Energy Procedia*, vol. 116, pp. 69–77, 2017, doi: 10.1016/j.egypro.2017.05.056.

[64] B. Möller and H. Lund, “Conversion of individual natural gas to district heating : Geographical studies of supply costs and consequences for the Danish energy system,” *Appl. Energy*, vol. 87, no. 6, pp. 1846–1857, 2010, doi: 10.1016/j.apenergy.2009.12.001.

[65] T. Yoon, Y. Ma, and C. Rhodes, “Individual Heating systems vs. District Heating systems : What will consumers pay for convenience ?,” *Energy Policy*, vol. 86, pp. 73–81, 2015, doi: 10.1016/j.enpol.2015.06.024.

[66] M. F. Hendrick, R. Ackley, B. Sanaie-movahed, X. Tang, and N. G. Phillips, “Fugitive methane emissions from leak-prone natural gas distribution infrastructure in urban environments,” *Environ. Pollut.*, vol. 213, pp. 710–716, 2016, doi: 10.1016/j.envpol.2016.01.094.

[67] R. G. Derwent, “Global Warming Potential (GWP) for Methane : Monte Carlo Analysis of the Uncertainties in Global Tropospheric Model Predictions,” *Atmosphere (Basel).*, pp. 1–15, 2020.

[68] “IEA - The Role of Gas in Today’s Energy Transitions,” 2019. [Online]. Available: https://www.iea.org/reports/the-role-of-gas-in-todays-energy-transitions.

[69] B. Gillessen, H. Heinrichs, J. Hake, and H. Allelein, “Natural gas as a bridge to sustainability: Infrastructure expansion regarding energy security and system

transition," *Appl. Energy*, vol. 251, no. May, p. 113377, 2019, doi: 10.1016/j.apenergy.2019.113377.

[70] C. Mcglade, S. Pye, P. Ekins, M. Bradshaw, and J. Watson, "The future role of natural gas in the UK: A bridge to nowhere ?," *Energy Policy*, vol. 113, no. November 2017, pp. 454–465, 2018, doi: 10.1016/j.enpol.2017.11.022.

[71] X. Zhang, N. P. Myhrvold, Z. Hausfather, and K. Caldeira, "Climate benefits of natural gas as a bridge fuel and potential delay of near-zero energy systems," *Appl. Energy*, vol. 167, pp. 317–322, 2016, doi: 10.1016/j.apenergy.2015.10.016.

[72] D. . Dominković, I. Bačeković, A. . Pedersen, and G. Krajačić, "The future of transportation in sustainable energy systems: Opportunities and barriers in a clean energy transition," *Renew. Sustain. Energy Rev.*, no. December 2016, 2017, doi: 10.1016/j.rser.2017.06.117.

[73] J. Ogden, A. Myers, D. Scheitrum, Z. Mcdonald, and M. Miller, "Natural gas as a bridge to hydrogen transportation fuel: Insights from the literature," vol. 115, no. December 2017, pp. 317–329, 2018, doi: 10.1016/j.enpol.2017.12.049.

[74] A. Henry, R. Prasher, and A. Majumdar, "Five thermal energy grand challenges for decarbonization," *Nat. Energy*, vol. 5, no. September, pp. 635–637, 2020, doi: 10.1038/s41560-020-0675-9.

[75] N. Bertelsen and B. V. Mathiesen, "EU-28 Residential Heat Supply and Consumption: Historical Development and Status," *Energies*, vol. 13, 2020.

[76] O. Mahian, M. Reza, A. Kasaeian, and S. Hossein, "Exergy analysis in combined heat and power systems: A review," *Energy Convers. Manag.*, vol. 226, no. September, p. 113467, 2020, doi: 10.1016/j.enconman.2020.113467.

[77] V. G. Gude, "Exergy Evaluation of Desalination Processes," *Chemengineering*, 2018, doi: 10.3390/chemengineering2020028.

[78] M. Terhan and K. Comakli, "Energy and exergy analyses of natural gas-fired boilers in a district heating system," *Appl. Therm. Eng.*, vol. 121, no. April, pp. 380–387, 2017, doi: 10.1016/j.applthermaleng.2017.04.091.

[79] A. Rieder, A. Christidis, and G. Tsatsaronis, "Multi criteria dynamic design

optimization of a small scale distributed energy system," *Energy*, vol. 74, no. C, pp. 230–239, 2014, doi: 10.1016/j.energy.2014.06.007.

[80] J. Y. Wu, J. L. Wang, and S. Li, "Multi-objective optimal operation strategy study of micro-CCHP system," *Energy*, vol. 48, no. 1, pp. 472–483, 2012, doi: 10.1016/j.energy.2012.10.013.

[81] H. S. Gholamhossein Abdollahi, "Application of the multi-objective optimization and risk analysis for the sizing of a residential small-scale CCHP system," *Energy Build.*, vol. 60, pp. 330–344, 2013, doi: 10.1016/j.enbuild.2013.01.026.

[82] T. Fang and R. Lahdelma, "Genetic optimization of multi-plant heat production in district heating networks," *Appl. Energy*, vol. 159, pp. 610–619, 2015, doi: 10.1016/j.apenergy.2015.09.027.

[83] S. Bracco, G. Dentici, and S. Siri, "Economic and environmental optimization model for the design andthe operation of a combined heat and power distributed generation system in an urban area," *Energy*, vol. 55, pp. 1014–1024, 2013, doi: 10.1016/j.energy.2013.04.004.

[84] T. Falke, S. Krengel, A.-K. Meinerzhagen, and A. Schnettler, "Multi-objective optimization and simulation model for the design of distributed energy systems," *Applied Energy*. 2016, doi: 10.1016/j.apenergy.2016.03.044.

[85] J. P. Jiménez Navarro, J. M. Cejudo López, and D. Connolly, "The effect of feed-in-tariff supporting schemes on the viability of a district heating and cooling production system," *Energy*, vol. 134, pp. 438–448, 2017, doi: 10.1016/j.energy.2017.05.174.

[86] M. Pirouti, A. Bagdanavicius, J. Ekanayake, J. Wu, and N. Jenkins, "Energy consumption and economic analyses of a district heating network," *Energy*, vol. 57, pp. 149–159, 2013, doi: 10.1016/j.energy.2013.01.065.

[87] M. Tańczuk, J. Skorek, and P. Bargiel, "Energy and economic optimization of the repowering of coal-fired municipal district heating source by a gas turbine," *Energy Convers. Manag.*, vol. 149, pp. 885–895, 2017, doi: 10.1016/j.enconman.2017.03.053.

[88] W. Jakob and C. Blume, "Pareto optimization or cascaded weighted sum: A comparison of concepts," *Algorithms*, vol. 7, no. 1, pp. 166–185, 2014, doi:

10.3390/a7010166.

[89] T. Tezer, R. Yaman, and G. Yaman, “Evaluation of approaches used for optimization of stand-alone hybrid renewable energy systems,” *Renew. Sustain. Energy Rev.*, vol. 73, no. June 2016, pp. 840–853, 2017, doi: 10.1016/j.rser.2017.01.118.

[90] D. Wei, A. Chen, B. Sun, and C. Zhang, “Multi-objective optimal operation and energy coupling analysis of combined cooling and heating system,” *Energy*, vol. 98, pp. 296–307, 2016, doi: 10.1016/j.energy.2016.01.027.

[91] A. L. Facci, L. Andreassi, and S. Ubertini, “Optimization of CHCP (combined heat power and cooling) systems operation strategy using dynamic programming,” *Energy*, vol. 66, pp. 387–400, 2014, doi: 10.1016/j.energy.2013.12.069.

[92] R. E. Best, P. Rezazadeh Kalehbasti, and M. D. Lepech, “A novel approach to district heating and cooling network design based on life cycle cost optimization,” *Energy*, vol. 194, p. 116837, 2020, doi: 10.1016/j.energy.2019.116837.

[93] A. Allen, G. Henze, K. Baker, and G. Pavlak, “Evaluation of low-exergy heating and cooling systems and topology optimization for deep energy savings at the urban district level,” *Energy Convers. Manag.*, vol. 222, no. December 2019, p. 113106, 2020, doi: 10.1016/j.enconman.2020.113106.

[94] M. Gong and S. Werner, “Exergy analysis of network temperature levels in Swedish and Danish district heating systems,” *Renew. Energy*, vol. 84, pp. 106–113, 2015, doi: 10.1016/j.renene.2015.06.001.

[95] H. Gadd and S. Werner, “Achieving low return temperatures from district heating substations,” *Appl. Energy*, vol. 136, pp. 59–67, 2014, doi: 10.1016/j.apenergy.2014.09.022.

[96] H. Li and S. Svendsen, “Energy and exergy analysis of low temperature district heating network,” *Energy*, vol. 45, no. 1, pp. 237–246, 2012, doi: 10.1016/j.energy.2012.03.056.

[97] Ş. Kilkiş, “Exergy transition planning for net-zero districts,” *Energy*, vol. 92, no. Part 3, pp. 515–531, 2015, doi: 10.1016/j.energy.2015.02.009.

[98] X. Yang, H. Li, and S. Svendsen, “Energy, economy and exergy evaluations of the

solutions for supplying domestic hot water from low-temperature district heating in Denmark," *Energy Convers. Manag.*, vol. 122, pp. 142–152, 2016, doi: 10.1016/j.enconman.2016.05.057.

[99] I. Baldvinsson and T. Nakata, "A feasibility and performance assessment of a low temperature district heating system - A North Japanese case study," *Energy*, vol. 95, pp. 155–174, 2016, doi: 10.1016/j.energy.2015.11.057.

[100] I. Baldvinsson and T. Nakata, "A comparative exergy and exergoeconomic analysis of a residential heat supply system paradigm of Japan and local source based district heating system using SPECO (specific exergy cost) method," *Energy*, vol. 74, no. C, pp. 537–554, 2014, doi: 10.1016/j.energy.2014.07.019.

[101] N. Yamankaradeniz, "Thermodynamic performance assessments of a district heating system with geothermal by using advanced exergy analysis," *Renew. Energy*, vol. 85, pp. 965–972, 2016, doi: 10.1016/j.renene.2015.07.035.

[102] A. Keçebaş, I. Yabanova, and M. Yumurtaci, "Artificial neural network modeling of geothermal district heating system thought exergy analysis," *Energy Convers. Manag.*, vol. 64, pp. 206–212, 2012, doi: 10.1016/j.enconman.2012.06.002.

[103] S. a. Kalogirou, S. Karellas, V. Badescu, and K. Braimakis, "Exergy analysis on solar thermal systems: A better understanding of their sustainability," *Renew. Energy*, pp. 1–6, 2015, doi: 10.1016/j.renene.2015.05.037.

[104] A. Rijs and T. Mróz, "Exergy evaluation of a heat supply system with vapor compression heat pumps," *Energies*, vol. 12, no. 6, 2019, doi: 10.3390/en12061028.

[105] N. Kabalina, M. Costa, W. Yang, A. Martin, and M. Santarelli, "Exergy analysis of a polygeneration-enabled district heating and cooling system based on gasification of refuse derived fuel," *J. Clean. Prod.*, vol. 141, pp. 760–773, 2017, doi: 10.1016/j.jclepro.2016.09.151.

[106] Jiangjiang Wang Ying Yang, "Energy, exergy and environmental analysis of a hybrid combined cooling heating and power system utilizing biomass and solar energy," *Energy Convers. Manag.*, vol. 124, pp. 566–577, 2016.

[107] A. Lake and B. Rezaie, "Energy and exergy efficiencies assessment for a stratified cold

thermal energy storage," *Appl. Energy*, vol. 220, no. March, pp. 605–615, 2018, doi: 10.1016/j.apenergy.2018.03.145.

[108] A. Franco and F. Bellina, "Methods for optimized design and management of CHP systems for district heating networks (DHN)," *Energy Convers. Manag.*, vol. 172, no. June, pp. 21–31, 2018, doi: 10.1016/j.enconman.2018.07.009.

[109] A. Franco and M. Versace, "Optimum sizing and operational strategy of CHP plant for district heating based on the use of composite indicators," *Energy*, vol. 124, pp. 258–271, 2017, doi: 10.1016/j.energy.2017.02.062.

[110] Y. Z. Wang, J. Zhao, Y. Wang, and Q. S. An, "Multi-objective optimization and grey relational analysis on configurations of organic Rankine cycle," *Appl. Therm. Eng.*, vol. 114, pp. 1355–1363, 2017, doi: 10.1016/j.applthermaleng.2016.10.075.

[111] F. A. Boyaghchi and M. Chavoshi, "Multi-criteria optimization of a micro solar-geothermal CCHP system applying water/CuO nanofluid based on exergy, exergoeconomic and exergoenvironmental concepts," *Appl. Therm. Eng.*, vol. 112, pp. 660–675, 2017, doi: 10.1016/j.applthermaleng.2016.10.139.

[112] H. Lu *et al.*, "Transition path towards hybrid systeLu, H., Yu, Z., Alanne, K., Zhang, L., Fan, L., Xu, X., & Martinac, I. (2014). Transition path towards hybrid systems in China: Obtaining net-zero exergy district using a multi-objective optimization method. Energy and ," *Energy Build.*, vol. 85, pp. 524–535, 2014, doi: 10.1016/j.enbuild.2014.09.074.

[113] M. Di Somma *et al.*, "Operation optimization of a distributed energy system considering energy costs and exergy efficiency," *Energy Convers. Manag.*, vol. 103, pp. 739–751, 2015, doi: 10.1016/j.enconman.2015.07.009.

[114] M. Di Somma *et al.*, "Multi-objective design optimization of distributed energy systems through cost and exergy assessments," *Appl. Energy*, vol. 204, pp. 1299–1316, 2017, doi: 10.1016/j.apenergy.2017.03.105.

[115] M. Noussan, "Allocation factors in Combined Heat and Power systems – Comparison of di ff erent methods in real applications," *Energy Convers. Manag.*, vol. 173, no. June, pp. 516–526, 2018, doi: 10.1016/j.enconman.2018.07.103.

[116] T. Tereshchenko and N. Nord, “Uncertainty of the allocation factors of heat and electricity production of combined cycle power plant,” *Appl. Therm. Eng.*, vol. 76, pp. 410–422, 2015, doi: 10.1016/j.applthermaleng.2014.11.019.

[117] J. Gao, Q. Zhang, X. Wang, D. Song, and W. Liu, “Exergy and exergoeconomic analyses with modeling for CO 2 allocation of coal- fi red CHP plants,” *Energy*, vol. 152, pp. 562–575, 2018, doi: 10.1016/j.energy.2018.03.171.

[118] E. A. Pina, M. A. Lozano, and L. M. Serra, “Thermoeconomic cost allocation in simple trigeneration systems including thermal energy storage,” *Energy*, vol. 153, pp. 170–184, 2018, doi: 10.1016/j.energy.2018.04.012.

[119] T. Tereshchenko and N. Nord, “Energy planning of district heating for future building stock based on renewable energies and increasing supply flexibility,” *Energy*, vol. 112, pp. 1227–1244, 2016, doi: 10.1016/j.energy.2016.04.114.

[120] L. Nordenstam, D. Djuric Ilic, and L. Ödlund, “Corporate greenhouse gas inventories, guarantees of origin and combined heat and power production – Analysis of impacts on total carbon dioxide emissions,” *J. Clean. Prod.*, vol. 186, pp. 203–214, 2018, doi: 10.1016/j.jclepro.2018.03.034.

[121] “Julia.” [Online]. Available: https://julialang.org/.

[122] “JuMP.” [Online]. Available: http://www.juliaopt.org/JuMP.jl/0.18/.

[123] “Gurobi.” [Online]. Available: https://www.gurobi.com.

[124] “Clp optimization solver.” [Online]. Available: https://projects.coin-or.org/Cbc.

[125] H. Dorotić, M. Ban, T. Pukšec, and N. Duić, “Impact of wind penetration in electricity markets on optimal power-to-heat capacities in a local district heating system,” *Renew. Sustain. Energy Rev.*, vol. 132, no. October, 2020, doi: 10.1016/j.rser.2020.110095.

[126] “Nord Pool.” .

[127] T. T. Sebestyén, M. Pavičević, H. Dorotić, and G. Krajačić, “The establishment of a micro-scale heat market using a biomass-fired district heating system,” *Energy. Sustain. Soc.*, vol. 10, no. 1, pp. 1–13, 2020, doi: 10.1186/s13705-020-00257-2.

[128] H. Dorotić, T. Pukšec, and N. Duić, “Multi-objective optimization of district heating

and cooling systems for a one-year time horizon," *Energy*, vol. 169, pp. 319–328, Feb. 2019, doi: 10.1016/j.energy.2018.11.149.

[129] H. Dorotić, T. Pukšec, and N. Duić, "Economical, environmental and exergetic multi-objective optimization of district heating systems on hourly level for a whole year," *Appl. Energy*, vol. 251, p. 113394, Oct. 2019, doi: 10.1016/j.apenergy.2019.113394.

[130] H. Dorotić, T. Pukšec, and N. Duić, "Analysis of displacing natural gas boiler units in district heating systems by using multi-objective optimization and different taxing approaches," *Energy Convers. Manag.*, vol. 205, no. February 2020, 2020, doi: 10.1016/j.enconman.2019.112411.

[131] H. Dorotić, T. Pukšec, D. R. Schneider, and N. Duić, "Evaluation of district heating with regard to individual systems – Importance of carbon and cost allocation in cogeneration units," *Energy*, vol. 221, 2021, doi: 10.1016/j.energy.2021.119905.

[132] "Croatian Ministry of Construction and Physical Planning - Primary energy factors and carbon factors." [Online]. Available: https://mgipu.gov.hr/UserDocsImages/dokumenti/EnergetskaUcinkovitost/meteoroloski_podaci/FAKTORI_primarne_energije.pdf.

[133] B. V. Mathiesen *et al.*, "Smart Energy Systems for coherent 100% renewable energy and transport solutions," *Appl. Energy*, vol. 145, pp. 139–154, 2015, doi: 10.1016/j.apenergy.2015.01.075.

[134] R. Lund and B. V. Mathiesen, "Large combined heat and power plants in sustainable energy systems," *Applied Energy*, vol. 142. pp. 389–395, 2015, doi: 10.1016/j.apenergy.2015.01.013.

[135] S. Walker, K. Katic, W. Maassen, and W. Zeiler, "Multi-criteria feasibility assessment of cost-optimized alternatives to comply with heating demand of existing office buildings – A case study," *Energy*, vol. 187, 2019, doi: 10.1016/j.energy.2019.115968.

[136] W. Zappa, M. Junginger, and M. van den Broek, "Is a 100% renewable European power system feasible by 2050?," *Appl. Energy*, vol. 233–234, no. November 2018, pp. 1027–1050, 2019, doi: 10.1016/j.apenergy.2018.08.109.

6 CURRICULUM VITAE

Hrvoje Dorotić was born on May 30th 1991 in Zagreb, Croatia, where he obtained a Master's Degree at the Faculty of Mechanical Engineering and Naval Architecture, at the University of Zagreb, with a specialisation in Energy and Power Engineering. During his studies he spent a period of time at TU Delft (Netherlands) as a part of the Erasmus internship program and at Unicamp (Brazil) as a guest researcher. He won a scholarship from the University of Zagreb for excellence and a scholarship of Croatian Energy Association.

In 2016 he enrolled in a PhD programme under the mentorship of prof. Neven Duić. Since 2017, he has been employed at the Department of Energy and Power Engineering, as a Research and Project Assistant. His research deals with the optimization and analysis of energy systems and the integration of renewable energy sources, with an emphasis on district heating systems. His research methods include single and multi-objective optimisation models for energy system operation (dispatch and unit-commitment) and capacity planning.

In 2021, was awarded the Marie Skłodowska-Curie Action individual fellowship for a research project dedicated to power and heating sector coupling.

He also participates in the preparation and coordination of projects within Horizon2020 (PLANHEAT, REWARDHeat, Heat Roadmap Europe), Interreg (DHswitch), EUKI (SEEETD) and other national programs such as the Croatian Science Foundation (RESFLEX). His projects deal with energy system analysis, the integration of renewable energy sources and district heating systems planning. He was part of the workgroup in several consulting projects dealing with techno-economic analysis of cogeneration, solar photovoltaics, biogas plants and industrial energy audits. He contributed to the analysis of the Zagreb post-earthquake heating sector planning and was enrolled in the consulting workgroup for the proposal of the new primary energy factors for the building sector. He participates in the organisation of SDEWES conference series as a part of the local organising committee.

He is the author or co-author of 11 scientific papers (indexed CC bases) and more than 10 conference papers. His current h-index is 5 (Web of Science). He serves as a reviewer for high-impact journals such as *Energy, Applied Energy, Renewable and Sustainable Energy Reviews, Energy Conversion and Management, Journal of Cleaner Production*, and others.

He speaks and writes in Croatian and English.

7 SUMMARY OF PAPERS

PAPER 1

H. Dorotić, T. Pukšec, and N. Duić, "Multi-objective optimization of district heating and cooling systems for a one-year time horizon," *Energy*, vol. 169, pp. 319–328, Feb. 2019, doi: 10.1016/j.energy.2018.11.149

Besides lowering supply temperatures, the concept of fourth generation of district heating (4DH) also includes integration of heating, cooling and power sector. Due to their high interconnectivity, number of involved technologies and relatively long, but at the same time detailed temporal scale, optimization of such systems presents a challenging task. So far, only hourly district heating multi-objective optimization for a whole year period has been carried out, where detailed district heating and cooling multi-objective optimization has been reserved for small scale utilization and short temporal scale, usually covering specific days or weeks. The main objective of this paper was to develop an hourly based multi-objective optimization district heating and cooling model which is capable of defining supply capacities, including thermal storage size, and their operation for a whole year period. The objective functions are minimization of a total system cost, which includes discounted investment and operational costs, and minimization of environmental impact in terms of carbon dioxide emissions. By using multi-objective optimization, this research shows that for equal level of carbon dioxide emissions, combined district heating and cooling systems have lower total discounted cost when compared to district heating and cooling systems which operate separately.

In this paper optimisation method, including district heating and cooling model were developed by Hrvoje Dorotić. Tomislav Pukšec and Neven Duić reviewed the model and the results. The paper was written by Hrvoje Dorotić and reviewed by Tomislav Pukšec and Neven Duić.

PAPER 2

H. Dorotić, T. Pukšec, and N. Duić, "Economical, environmental and exergetic multi-objective optimization of district heating systems on hourly level for a whole year," *Appl. Energy*, vol. 251, p. 113394, Oct. 2019, doi: 10.1016/j.apenergy.2019.113394

District heating systems are proven to be an effective way of increasing energy efficiency, reducing the environmental impact and achieving higher exergy efficiency than individual heating solutions. The leaders in district heating integration are Scandinavian countries with more than 50% of the covered total heating demand. Nevertheless, these systems have not reached their full potential in most European countries. The reason for this could be that energy planners often study only the economic feasibility of the system, thus neglecting other crucial aspects of the previously mentioned district heating. In research papers, district heating multi-objective optimization usually takes into account the minimization of the total discounted cost and the environmental impact. Most times, these two objectives are studied as a single objective optimization problem through the internalization of the cost related to carbon dioxide emissions. This paper presents the multi-objective optimization method which is capable of optimizing district heating technology supply capacities and their operation, including thermal storage, for a one-year time horizon in order to satisfy the optimization goals. The model was written in the open-source and free programming language called Julia, while linear programming solver named Clp was used to obtain the solution. The solver is part of Julia's optimization package called JuMP. Three separate objective functions are included in the model: the minimization of the total discounted cost, the minimization of carbon dioxide emissions and the minimization of exergy destruction. Since these three goals are often in conflict, the final result of multi-objective optimization is the so-called Pareto surface which presents the compromise between all possible results. To deal with the multi-objective optimization problem, the weighted sum method in combination with the epsilon-constraint method was used. The most suitable result has been chosen using the knee point method which is a solution the closest to the Utopia solution where all three goals reach their optimal value.

Building on Paper 1, Hrvoje Dorotić developed exergy destruction model and carried out optimisation. Tomislav Pukšec and Neven Duić the reviewed obtained results. The paper was written by Hrvoje Dorotić and reviewed by Tomislav Pukšec and Neven Duić.

PAPER 3

H. Dorotić, T. Pukšec, and N. Duić, "Analysis of displacing natural gas boiler units in district heating systems by using multi-objective optimization and different taxing approaches," *Energy Convers. Manag.*, vol. 205, no. February 2020, 2020, doi: 10.1016/j.enconman.2019.112411

District heating systems are proven to be effective way of increasing energy efficiency, reducing environmental impact and achieving higher exergy efficiency. In research papers, district heating multi-objective optimization usually takes into account minimization of the total discounted cost and environmental impact, while exergetic objective function is rarely introduced. Most of the times, economic and ecological objective functions are studied as a single objective optimization problem through internalization of the cost related to carbon dioxide emissions tax. This paper presents novel approach since additional tax, related to exergy destruction, has been introduced. The influence of these two taxing systems on a single and multi-objective optimization results of district heating system has been carried out. Two approaches have been proposed. In the first one, multi-objective optimization has been used where objective functions were defined as economic and ecological or exergetic. In the second approach, single-objective optimization has been used where cost function also includes both carbon and exergy destruction tax. It has been shown that inclusion of carbon tax causes convergence of Pareto fronts after specific exergy destruction has been reached. On the other hand, if all technologies are available, increase of exergy tax doesn't reduce carbon dioxide emissions. The most important outcome of this paper is analysis of the impact of exergy tax on natural gas consumption in heat-only boilers. Acquired results show that exergy, together with carbon tax, can effectively reduce natural gas consumption in heat-only boilers. If there are no back-pressure CHP technologies available, these taxing systems can completely push out its consumption. Finally, the analyses with carbon emissions allocation in CHP units has also been carried out. Acquired results have shown that with increase of carbon tax, exergy efficiency of the system could be increased.

Hrvoje Dorotić developed different taxing approaches and integrated them in the optimisation model. Tomislav Pukšec and Neven Duić reviewed the results. The paper was written by Hrvoje Dorotić and revised by Tomislav Pukšec and Neven Duić.

PAPER 4

T. T. Sebestyén, M. Pavičević, H. Dorotić, and G. Krajačić, "The establishment of a micro-scale heat market using a biomass-fired district heating system," *Energy. Sustain. Soc.*, vol. 10, no. 1, pp. 1–13, 2020, doi: 10.1186/s13705-020-00257-2.

Local biomass potential in South-eastern European countries is relatively high. Nevertheless, biomass residues such as wood leftovers, straw and energy crops are often not properly managed or inefficiently utilised for energy purposes in individual house heating or domestic hot water preparation. This is more relevant in rural areas, where the utilisation of biomass resources is mainly based upon traditional technologies, has low efficiency or is carried out by using individual bases without local energy supply management. Usage of biomass residues in combination with other renewable energy sources is in agreement with the targets of the EU's Energy and Climate Goals and promotes rural development and a circular economy.For this purpose, local heating and domestic hot water preparation demands, as well as the available biomass potentials, were analysed and mapped by using a geographic information system (GIS). A model for analysing the optimal operation of the district heating boiler with a relatively high share of solar energy, which is backed up by either a short- or long-term heat storage, was developed. The model takes the supply and the return temperatures from the DH network into account and decides whether the excess of solar heat produced by the prosumers can be delivered into the network. This reduces heat overproduction and enables a smooth and uninterrupted operation of the system. Such configuration would benefit both the DH Company and the prosumers. The DH Company would have the opportunity to buy cheaper excess heat from the prosumers rather than to start its own and relatively slow biomass boiler. In this paper, several scenarios are proposed for the Romanian village Ghelinta. The target village is characterised by a small-scale biomass district heating boiler with thermal storage and prosumers with either solar thermal collectors or locally installed heat pumps. Integration of seasonal thermal storage and local prosumers can smooth out the biomass district heating boiler operation and bring additional socio-economic benefits for the bioenergy village communities. This could be the first step towards the establishment of a micro-scale thermal energy market. Analysis has proven that the proposed system configuration is socio-technically feasible, even for micro-scale systems, as apparent in the Romanian target village Ghelinta. The main objective of this research is to analyse the implementation of a small-scale biomass and renewable energy-based district heating system and to prove the concept of bioenergy villages from a technical and economical perspective. Furthermore, the role of residential household

prosumers has been analysed. Based on outcomes, the transferability of the results is also discussed, while several suggestions for stakeholders who implement such projects were formulated for future research as well.

The idea and conceptualisation of the paper was carried by Hrvoje Dorotić. Tihamér Tibor Sebestyén provided input data while Matija Pavičević developed market optimisation model and carried out simulations. Tihamér Tibor Sebestyén wrote Introduction, Input data and Conclusion section, Matija Pavičević wrote Method section, while Hrvoje Dorotić wrote Results and Discussion section. Goran Krajačić provided review of the paper.

PAPER 5

H. Dorotić, M. Ban, T. Pukšec, and N. Duić, "Impact of wind penetration in electricity markets on optimal power-to-heat capacities in a local district heating system," *Renew. Sustain. Energy Rev.*, vol. 132, no. October, 2020, doi: 10.1016/j.rser.2020.110095

While the share of intermittent renewable energy sources in a power sector is constantly increasing, demand response technologies are becoming a crucial part of interconnected energy systems. The district heating sector has a great potential of offering such services if power-to-heat and thermal storage technologies are implemented. This is a well-known method of utilizing low-price electricity from the power market. However, power-to-heat optimal supply capacities are rarely studied with respect to different market conditions, especially from the point of view of multi-objective optimization. This paper shows an analysis of the impact of a wind production increase in a power market on optimal power-to-heat capacities in a local district heating system. To obtain these results, a district heating optimization model was developed by using linear programming, while the power market prices reduction is analysed by using historical bidding market data and shifting of the supply curve. The district heating model was created in the open-source and free programming language called Julia. The model was tested on a case study of the Nord Pool electricity market and a numerical example of a district heating system. The main outcome of this research is to show how district heating supply technologies operate in different market conditions and how they affect optimal power-to-heat and thermal storage capacities. Heat pump capacities linearly follow wind production increase in power markets.

In this paper, Hrvoje Dorotić developed a concept and carried out optimisation while using power market prices obtained by Marko Ban. Hrvoje Dorotić wrote the paper, while Tomislav Pukšec and Neven Duić carried out review and editing.

PAPER 6

H. Dorotić, T. Pukšec, D. R. Schneider, and N. Duić, "Evaluation of district heating with regard to individual systems – Importance of carbon and cost allocation in cogeneration units," *Energy,* vol. 221, 2021, doi: 10.1016/j.energy.2021.119905

Although, district heating has high share in the heating sector of Northern Europe, Central-Eastern European countries often do not utilize full potential for further thermal network expansion. The main reasons for this are relatively low energy market prices, such as natural gas for households, which diminish economic feasibility of the proposed projects. Even though there are numerous optimization methods which can optimize district heating system, they rarely provide cost comparison with individual heating solutions. This paper presents a novel method of evaluating district heating with respect to individual systems by using multi-objective optimization approach coupled with cost and carbon allocations in cogeneration units. Objective functions are defined as minimization of total discounted cost, including environmental impact, and maximization of exergy efficiency. To deal with multi-objective optimization, epsilon-constraint method has been used. The main outcome of this research are energy market prices for which district heating systems have lower environmental impact and exergy destruction than individual natural gas-based heating solutions, while at the same time being economically feasible. Finally, the paper demonstrates that cogeneration-based district heating systems are superior to individual heating, even for low households' natural gas prices.

Hrvoje Dorotić developed multi-objective optimisation model and incorporated cost and carbon allocation in CHP units. Daniel Rolph Schneider provided input data related to cogeneration plants. Hrvoje Dorotić wrote the paper while Tomislav Pukšec and Neven Duić carried out review and editing.

PAPER 1

Multi-objective optimization of district heating and cooling systems for a one-year time horizon

Hrvoje Dorotić*, Tomislav Pukšec, Neven Duić

University of Zagreb, Faculty of Mechanical Engineering and Naval Architecture, Department of Energy, Power Engineering and Environment, Ivana Lučića 5, 10002, Zagreb, Croatia

e-mail: hrvoje.dorotic@fsb.hr

ABSTRACT

Besides lowering supply temperatures, the concept of fourth generation of district heating (4DH) also includes integration of heating, cooling and power sector. Due to their high interconnectivity, number of involved technologies and relatively long, but at the same time detailed temporal scale, optimization of such systems presents a challenging task. So far, only hourly district heating multi-objective optimization for a whole year period has been carried out, where detailed district heating and cooling multi-objective optimization has been reserved for small scale utilization and short temporal scale, usually covering specific days or weeks. The main objective of this paper was to develop an hourly based multi-objective optimization district heating and cooling model which is capable of defining supply capacities, including thermal storage size, and their operation for a whole year period. The objective functions are minimization of a total system cost, which includes discounted investment and operational costs, and minimization of environmental impact in terms of carbon dioxide emissions. By using multi-objective optimization, this research shows that for equal level of carbon dioxide emissions, combined district heating and cooling systems have lower total discounted cost when compared to district heating and cooling systems which operate separately.

KEYWORDS

District heating and cooling; multi-objective optimization; linear programming; thermal storage; Pareto front

1. Introduction

European Union (EU) has recognized the importance of district heating and cooling (DHC) systems by including them in a proposal of the Strategy on Heating and cooling [1]. They can reduce greenhouse gasses emissions and improve energy efficiency by using waste heat and low-temperature renewable energy sources (RES). The definition of an efficient DHC system has been shown in the EU Directive on energy efficiency [2]. They will also have important role in the future energy systems with a high share of intermittent RES where the excess of electrical energy could be transformed into thermal, by using efficient technologies, such as electrical heaters or heat pumps. In the literature, future DHC systems belong to 4th generation of district heating and cooling [3]. That doesn't just mean the improvement by reduction of a supply temperatures and better building's insulation. The emphasis is placed on integration of electricity, thermal and gas grids and usage of smart energy systems. B.V. Mathiesen et al

* Corresponding author: hrvoje.dorotic@fsb.hr

shown the importance of integrating different energy sectors in order to develop smart system capable of introducing higher shares of renewable energy sources while at the same time maintaining system's operability and economical feasibility [4]. In order to increase share of district heating, European countries have to increase flexibility of energy systems and make them part of the smart city, provide additional contribution to renewable energy sources integration and enable prosumers' participation [5]. Similar conclusions have been obtained in [6], where final end-users needs have been taken into account through extensive questionnairey and interviews. There are numerous papers on how to calculate expansion potential of district heating system. In [7], comparison between results obtained by using consumer-economy and socio-economy has been presented.

District heating systems could be complex due to the great interconnection of a large number of energy and masses streams and optimizing such a system represents a challenge. Because of that, quasi-optimal solutions have been found by performing scenario analyses. Although, optimization is often used in order to choose the most suitable solution of the energy system, Lund et al. [8] provide theoretical positions for energy system modelling. In the mentioned paper, simulation and optimization approaches have been shown, including their strengths and weaknesses. In [9], scenario analysis in combination with optimization process has been carried out in order to reduce heat production costs. Work presented in [10] shows the optimal share of CHP with respect to the DHW share. In paper [11], the optimal solar share has been found. In order to start the optimization procedure, the objective function has to be defined. In most cases, it is related to a cost, such as investment or operational, or to an environmental impact of the system, such as equivalent CO_2 emissions [12]. The simplest case is a single objective optimization, which is often related to economic feasibility of a system [13]. For a multi-objective approach, at least two objective functions should be defined, which are usually total cost and environmental impact of the system [14]. In this case, a solution of optimization isn't a single value, but a whole set of them which lie at the same front, called the Pareto front. In the case of the multi-objective optimization with three objective functions, all solutions are a part of the so-called Pareto surface [15]. It is important to mention that obtained Pareto solutions are all treated equally, i.e. there is no preference among them. In order to choose the most suitable one, decision making method is needed.

There are many possible approaches on how to handle the optimization procedure. The most common one is linear programming (LP), or mixed integer linear programming (MILP), where some of the optimization parameters are continuous or in the form of integers, such as binary variables, e.g. when deciding if the power plant should work or not [16]. If there is a need for a more detailed description of the system which includes nonlinearity, mixed integer non-linear programming (MINLP) is used [17]. In some cases, even more complex approach could be used, as shown in [18], where MILP in combination with stochastic methods is proposed. When dealing with multi-objective optimization, the genetic algorithms (GA) approach is mostly used [14]. Since all Pareto solutions are considered equal, the decision making process should be carried out in order to define the most suited one. Some authors propose the system's reliability as the crucial parameter in obtaining the final solution of multi-objective optimization [19], while other propose linear programming technique for multidimensional analysis of preference (LINMAP), which is looking for ideal non dimensional objective values equal to unity [20].

One of the major issues in optimizing DH systems is the needed temporal scale. In order to capture the seasonal characteristics, the whole year should be studied on a one-hour scale to obtain the specific system's technologies dynamics. In addition to this, 4DH is a part of the

energy system that is connected to the one-hour scale electricity market. Furthermore, electricity markets are decreasing time step to a 15-minute level, which will have to be followed by even more detailed temporal scale used in energy system optimization. Sometimes, optimization doesn't have a temporal scale as shown in [21]. In order to accelerate optimization procedure, only specific days in the year could be studied, as shown in [22]. Obvious approach is a one-hour based optimization with the one-year horizon [23]. The most detailed temporal scale for single objective optimization of district heating systems found so far is 15-minute for a whole year, presented in [14]. Since 8760 hour optimization is a challenging task itself, the long term optimization of DHC systems hasn't been carried out so far. In future systems, different energy prices, heat demand and prosumers share are expected. Single objective optimization solution shift has been analysed for electricity price variations and heat demand reduction [24] while work presented in [25] shows that different heat price models could be used in the future in order to stimulate demand response. Physical model of the district heating system is rarely taken into account. Pirouti et al. [26] used optimization approach in order to minimize annual total energy consumption and costs while also considering different district heating network temperature variations and pressure losses. In [27] detailed model of cogeneration unit was studied in order to optimize repowering coal-fire district heating sources by a gas turbine.

Multi-objective optimization of combined heating and cooling system if often carried out on a micro-level scale and includes only system operation optimization. In [28], genetic algorithm was used in order to define strategy for system operation which consists of power plant, internal combustion engine, biomass boiler and electric and absorption chiller. Optimal control strategy of complex tri-generation plant was carried in [29], but for a single working day. The objective function was minimization of total energy and maintenance cost. Genetic algorithm was also applied in [15] where sizing of a small-scale combined cooling heating and power system was carried out. Stochastic methods could also be used for combined cooling heating and power system optimization as demonstrated in [19]. Mixed integer non-linear model was developed in [17] in order to optimize operation strategy under various load conditions. Optimization of the DHC systems often lacks crucial technologies proposed in the 4DH concept [30] or are investigated on the micro scale [19].

In this paper, multi-objective optimization model of combined district heating and cooling system is carried out. The time frame is a whole year with time-step equal to one hour. It is capable of optimizing supply capacity, including thermal storage size, and operation. Possible technologies include natural gas or biomass powered heat only boiler and cogeneration, absorption and compression heat pumps, electrical heater, solar thermal collectors and thermal storage. Objective function is minimization of overall operation and discounted investment cost of the system, while at the same time minimizing environmental impact of the system in terms of carbon dioxide (CO_2) emissions. Multi-objective optimization of this detailed time-scale for combined district heating and cooling systems which includes broad range of possible technologies hasn't been done so far. Furthermore, this research evaluated environmental and economic benefits of combined district heating and cooling systems in relation with separated operation. The model has been formulated with free and open-source programming language called Julia while Cbc was used as linear programming solver [31].

This paper is divided in several chapters. Chapter 2 shows methods used in order to deal with multi-objective optimization, including district heating and cooling model. Chapter 0 presents numerical case study in detail and input data used to demonstrate proposed approach. Chapter 0

displays the obtained results while Chapter 5 sums the most important outcomes of this research in the brief conclusion.

2. Method

In this paper, multi-objective optimization was used since energy planning decision making process often includes compromises. In this case, minimization of total cost and CO_2 emissions of the system. In order to deal with multi-objective optimization, district heating and cooling model was written in the LP form. The main reason for this is detailed time scale (one hour time step) and a time horizon equal to one year. In addition to this, numerous optimization runs were needed to acquire Pareto front. For these set of conditions, LP can simultaneously guarantee speed and needed precision. Furthermore, weighted sum in combination with epsilon constrained method has been used in order to reach Pareto front. Weighted sum method is appropriate if the single solution wants to be reached, such as the least-cost, the most environmentally friendly or their combination. However, if one wants to acquire the whole trend of solutions, as in this paper, epsilon constrained method is needed.

This chapter is divided in several subchapters. Firstly, multi objective optimization approach is shown in the Subchapter 2.1, Subchapter 2.2 presents district heating and cooling model, while Subchapter 0 shows programming language and tools used in this research.

2.1. Multi-objective optimization

The developed multi-objective optimization model of district heating and cooling system is defined with two objective functions: minimization of total system cost and minimization of environmental impact expressed through CO_2 emissions as shown in Equation 1.

$$\min(f_{econ}, f_{ecol}) \tag{1}$$

Since these two goals are often in contradiction, i.e. the first one could only be decreased if the second increases and vice versa, the final solution of the optimization will be set of points which will lie on the curve called Pareto front which present the compromise. Economical objective function could be calculated by using Equation 2, while environmental objective function is represented by Equation 3.

$$f_{econ} = \sum_{i} C_{investment,i} + C_{fuel,i} + C_{variable,i} + C_{other,i} - Income_i \tag{2}$$

Where $C_{investment,i}$ represents discounted investment cost of technology i, $C_{fuel,i}$ are fuel costs for each technology, $C_{variable,i}$ are variable costs, $C_{other,i}$ are other costs, and finally $Income_i$ is additional income due to the electrical energy produced in cogeneration units sold on the electricity market. Each technology has different specific investment, fuel and variable costs. In this approach, investment cost has to be discounted in order to take into account different lifetimes of used technologies. Furthermore, such approach is needed because optimization is carried out for a time horizon equal to one year where economical objective function represents yearly discounted cost. Other costs include additional expenses which exist only for some technologies. For example, additional fixed monthly cost paid to the grid operator for power capacity when using power-to-heat technologies. It is important to mention that investment and operational cost of the district heating and cooling network hasn't been taken into account since

heating and cooling demand are put as a boundary condition, i.e. treated as a constant value which could added to the final solution.

$$f_{ecol} = \sum_{t=1}^{t=8760} \sum_{i} e_{CO_2,i} \cdot Q_{i,t} / \eta_i \tag{3}$$

Total CO_2 emissions of the system can be calculated by using Equation (3), where $e_{CO_2,i}$ is specific carbon dioxide emissions for each technology, i.e. fuel, $Q_{i,t}$ is defined as thermal energy production for time step t and technology i, while η_i represents efficiency of technology i.

In this paper weighted sum coefficient method was used in order to obtain solution of the multi-objective optimization. This method enables translation of objective functions into single, weighted function by assigning weighted coefficients, as shown in Equation (4). It is important to mention that sum of weighted coefficients should be equal to unity, Equation (5).

$$F_{weighted} = \left(\frac{\omega_{econ}}{f_{econ_{\omega_{econ}=1}}}\right) \cdot f_{econ} + \left(\frac{\omega_{ecol}}{f_{ecol_{\omega_{ecol}=1}}}\right) \cdot f_{ecol} \tag{4}$$

$$\omega_{econ} + \omega_{ecol} = 1 \tag{5}$$

Since economical and environmental objective functions have different order of magnitude, normalization has to be carried out, as shown in Equation (4). Combining weighting coefficients, ω_{econ} and ω_{ecol}, all possible solutions could be obtained thus creating the Pareto front. However, due to the nature of this method, by using relatively high step, e.g. equal to 0.1, some solutions couldn't be obtained. In order to accelerate the process of acquiring Pareto front, epsilon constraint method was used. After acquiring the most optimal economical and the most optimal environmental solution, extremes of the Pareto front are obtained. By using epsilon constraint method, the constraint is put on one of the objective functions, while minimizing other one, thus obtaining more detailed Pareto front. Equation (6) presents epsilon constraint method used in this paper. The constraint ε was put on environmental objective function, while minimizing economical goal. By increasing the constraint, objective function is moving from one end of the Pareto front to the other. With this approach, multi-objective optimization problem has been translated to single-objective optimization with additional set of constraints.

$$\min(f_{econ}) \; for \; f_{ecol} = \varepsilon \tag{6}$$

2.2. District heating and cooling model

In this paper, in order to optimize hourly operation of the district heating and cooling system on the annual level, simplified model has been develop. It is based on system's energy balances with addition of several technology constraints. In the district heating (DH) model, several technologies' capacities, including their operation, are optimized. Possible technologies utilized in this model are following: natural gas and biomass boiler and cogeneration, electrical heater, air-source compression heat pump, solar thermal collectors and thermal storage. Their operation is defined by set of constraints shown below.

$$Q_{HOB,gas,DH,t} + Q_{HOB,biomass,DH,t} + Q_{EH,t} + Q_{HP,DH,t} + Q_{CHP,DH,gas,t} + Q_{CHP,DH,biomass,t} + Q_{ST,t} - TES_{DH,in-out,t} = DEM_{DH,t} \tag{7}$$

$$0 \leq Q_{i,t} \leq P_i \tag{8}$$

$$-r_{up-down,i} \cdot P_i \leq Q_{i,t} - Q_{i,t-1} \leq r_{up-down,i} \cdot P_i \tag{9}$$

Equation (7) indicates that district heating demand $DEM_{DH,t}$ should be satisfied with thermal energy production from optimal combination of technologies $Q_{i,t}$ including thermal storage charge and discharge $TES_{DH,in-out,t}$, in each hour. Thermal energy supply is coming from supply capacities. Technology operation $Q_{i,t}$ is optimized for each technology and every time step. From Equation (8) it can be seen that technology load, can't be larger than optimal technology capacity P_i and lower than zero. Thermal storage charge and discharge $TES_{DH,in-out,t}$ can have negative values: negative values during discharging and positive values during thermal storage charging. In order to obtain more realistic technology operation, ramp-up and ramp-down limits, $r_{up-down,i}$ are introduced for each technology, as shown in Equation (9). Thermal storage operation is defined with additional set of constraints.

$$SOC_{t=1} = SOC_{t=8760} = SOC_{start-end} \cdot TES_{size} \tag{10}$$

$$SOC_t = SOC_{t-1} + TES_{in-out,t} \tag{11}$$

Where SOC represents thermal storage state of charge in time step t, while TES_{size} represents optimal thermal storage size. Cooling and heating thermal storage are modelled by using similar set of constraints as shown in Equations (10) and (11). It could be seen from Equations (10) and (11) that thermal storage losses have been neglected. According to [32], thermal losses of seasonal thermal storage can reach up to 100% when operating in correct conditions. One of the main reasons for this is extremely low surface-to-volume ratio. Thermal losses of smaller thermal storages such as steel tanks are larger than for the seasonal one, accounting up to 5% for the storage cycle of one week [32]. Thermal losses could be reduced if additional insulation is installed. Although neglecting thermal loses doesn't cause great errors in terms of total discounted cost and environmental impact of the system, especially in case of seasonal thermal storage, future work should include losses calculation. This will make a model more complex but also more realistic in terms of storage capacity and operation optimization.

Solar thermal collectors' production have been modelled by using method described in detail in [20]. The simplified model is based on solar collector efficiency European standard EN12975 standard described in [33]. Solar collector efficiency could be obtained by using Equation (12) [33]:

$$\eta_{c,t} = \eta_0 - a_1 \frac{\left(T_m - T_{a,t}\right)}{G_t} - a_2 \frac{\left(T_m - T_{a,t}\right)^2}{G_t} \tag{12}$$

Where $\eta_{c,t}$ represents solar collector efficiency in time step t. It is dynamic variable because depends on hourly meteorological data such as global solar irradiation G_t and air temperature $T_{a,t}$. Meteorological data could be acquired by using numerous open-source databases such as PVGIS [34]. Other parameters in equation are taken as constants: maximum efficiency if there is no heat loss, also known as optical efficiency η_0, first order heat loss coefficient a_1, second order heat loss coefficient a_2 and T_m which represents mean solar thermal collector temperature. The last one is dynamic parameter, but since detailed physical model is needed to acquire correct value, this variable for purpose of this research was also taken as a constant. These parameters could be found in solar thermal collector factsheets.

Publicly available solar thermal collectors' specification database is available in [35]. For purposes of this research flat-plate collector data has been used. Specific solar thermal production $P_{solar,specific,t}$ could be calculated by using Equation (13):

$$P_{solar,specific,t} = \eta_{c,t} \cdot G_t \tag{13}$$

Optimization variable related to solar thermal collectors is the total collector area A_{ST}, while their operation is predefined by specific solar thermal production, as shown in Equation (14).

$$Q_{ST,t} = A_{ST} \cdot P_{solar,specific,t} \tag{14}$$

District cooling (DC) system is modelled with similar set of constraints, only difference is that other technologies are utilized: absorption heat pump driven by heat only boiler or cogeneration's thermal energy and compression heat pump, as shown in Equation (15).

$$Q_{HP,DC,t} + Q_{HP,abs,t} - TES_{in-out,DC,t} = DEM_{DC,t} \tag{15}$$

In this equation, again, supply units operation, $Q_{i,t}$, can have only positive values, since they represent cooling energy production, while $DEM_{DC,t}$ is cooling energy demand. As visible from Equation (15), thermal storage also exists. It is modelled in the same manner as the storage in the district heating model, as shown in Equations (10) and (11). Cooling thermal storage charge and discharge in this case can also achieve negative or positive values, depending on thermal energy flow. If storage discharges, $TES_{in-out,DC,t}$ is negative and if it is charging, than $TES_{in-out,DC,t}$ has positive values.

Energy balance of the absorption heat pump is represented by Equation (16).

$$\begin{aligned} &Q_{HP,absorption,t} \\ &= (Q_{HOB,DC,gas,t} + Q_{HOB,DC,biomass,t} + Q_{CHP,DC,gas,t} \\ &+ Q_{CHP,DC,biomass,t}) \cdot \eta_{HP,abs} \end{aligned} \tag{16}$$

Thermal energy from heat supply units is used to generate cooling energy through absorption heat pump which efficiency is defined with $\eta_{HP,abs}$. According to [36], absorption heat pumps' efficiency mainly depends on a temperature of a heat source. Because of this, only high temperature technologies, such as heat-only boiler and cogeneration are chosen to operate in combination with an absorption heat pump.

District heating and cooling systems could be connected through absorption heat pump which has possibility of utilizing excess of thermal energy during summer season from heat-only boilers and cogeneration units. In that case thermal energy produced in heat-only boilers and cogeneration units could be simultaneously used in district cooling and district heating as shown in Equations (17-20).

$$Q_{HOB,biomass,t} = Q_{HOB,DH,biomass,t} + Q_{HOB,DC,biomass,t} \tag{17}$$

$$Q_{HOB,gas,t} = Q_{HOB,DH,gas,t} + Q_{HOB,DC,gas,t} \tag{18}$$

$$Q_{CHP,biomass,t} = Q_{CHP,DH,biomass,t} + Q_{CHP,DC,biomass,t} \tag{19}$$

$$Q_{CHP,gas,t} = Q_{CHP,DH,gas,t} + Q_{CHP,DC,gas,t} \tag{20}$$

Where $Q_{i,DH,t}$ represents thermal energy coming from technology i to be used in district heating in a time step t. In a same manner, $Q_{i,DC,t}$ is thermal energy to be used in district cooling through absorption heat pump. These optimization variables exist only in the model where district heating and cooling systems are operating as a part of a single system.

2.3. Programming language and tools

Since all optimization variables are continuous, the optimization problem has been modelled by using linear programming. The model was written by using Julia programming language [31]. It is free and open-source language developed in order to achieve better performance in terms of speed of solving and building the model. In order to easily built the optimization model, JuMP package has been used [37]. It is Julia add-on used for mathematical programming. Furthermore, it also has built-in various free and open source optimization solvers. For the purposes of this research coin-or branch-and-cut linear programming solver has been used, called Cbc [38].

3. Case study

In order to validate the model, numerical test case has been performed, where Croatian city of Velika Gorica has been chosen as the case study. Useful heating and cooling demand on yearly level has been mapped. In order to obtain hourly distribution of heating and cooling demand, heating and cooling degree-hour method has been used. District heating demand also includes thermal energy for domestic hot water production. Velika Gorica currently has several smaller district heating systems which connect small number of building blocks, while no district cooling has been implemented so far.

In this paper two scenarios have been developed. In the first scenario district heating and cooling systems operate separately, i.e. there is no interconnection between them. In the second scenario connection between them has been introduced. In the first scenario, i.e. during separate operation, there is no connection between district heating and cooling networks, which means that thermal energy produced in heating network can't be used in district cooling and vice versa. Interconnection between district heating and cooling systems means linking of thermal supply capacities, which implies that heat could be simultaneously used in district heating and cooling network. Connection between all possible technologies in Scenario 2 can be seen in Figure 1. It could be noticed that thermal energy from biomass and natural gas heat-only boilers and cogeneration units could be directly used for heating (red line in the figure) or for cooling energy production through absorption heat pump unit (orange line in the figure). This interconnection should increase overall flexibility of the system thus having great impact on the solution of the multi-objective optimization in comparison with the first scenario.

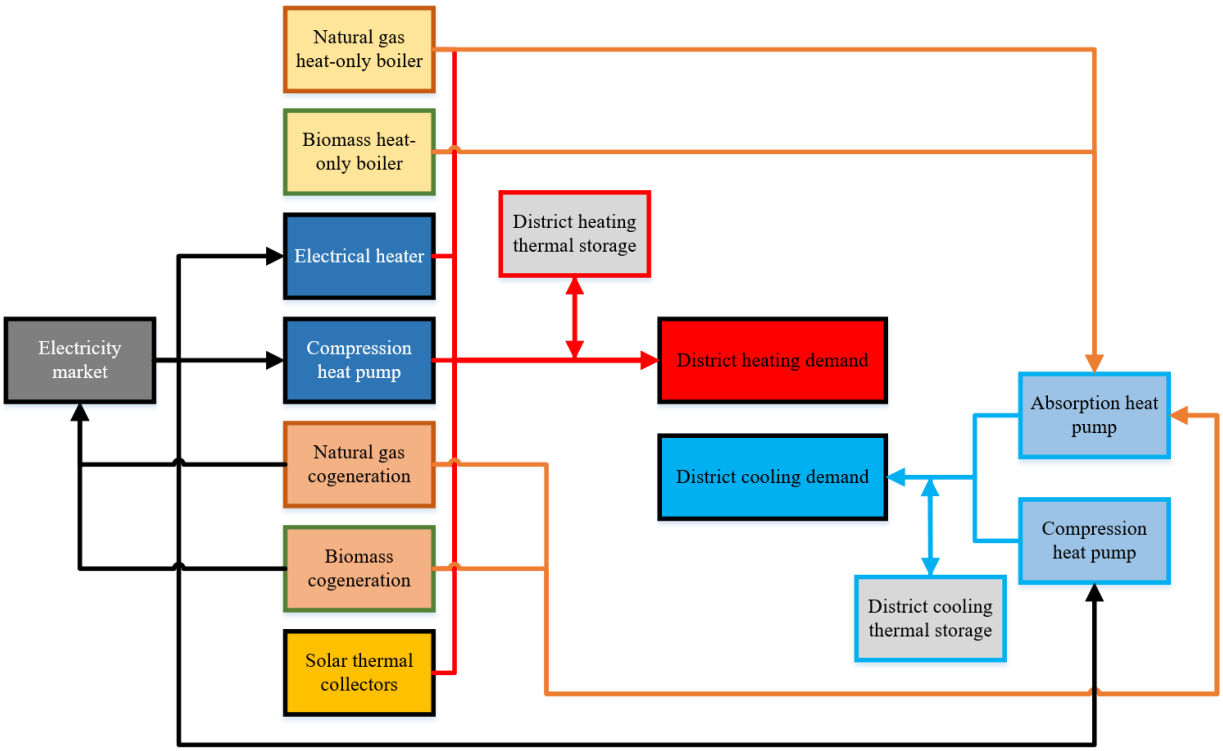

Figure 1 Scheme of interconnection between district heating and cooling in Scenario 2

Table 1 shows technology input data used for multi-objective optimization. Most of the data is publicly available through various technology databases, such as [32]. Characteristics of district heating and cooling demand, in terms of total and peak demand, are shown in

Table 2.

Table 1 Input data for multi-objective optimization

Technology	**Investment cost [€/MW] / [€/m²] /[€/MWh]**	**Fuel cost [€/MWh]**	**Variable cost [€/MWh]**	**Emission factor [TCO_2/MWh]**
Natural gas boiler	100.000	20	3	0,22
Biomass boiler	800.000	15	5,4	0,04
Electrical heater	107.500	Electricity market	0,5	0,137
Heat pump, heating	680.000	Electricity market	0,5	0,137
Cogeneration natural gas	1.700.000	20	3,9	0,22
Cogeneration biomass	3.000.000	15	5	0,04
Solar thermal	300 €/m²	0	0,5	0
Thermal storage district heating	500 €/MWh	0	0	0
Heat pump cooling	680.000	Electricity market	0,5	0,137
Absorption heat pump	400.000	0	3,5	0
Thermal storage district cooling	3.000	0	0	0

Table 2 District heating and cooling demand

System	**Total demand [MWh]**	**Peak demand [MW]**
District heating	43.767	14,98
District cooling	13.262	8,1

4. Results and discussion

Multi-objective optimization results for district heating system in Scenario 1 is shown in Figure 2. Figure 2a shows Pareto front putting into correlation economical and environmental objective function. Figure 2b shows optimal configurations which was obtained for specific points on the Pareto front. The capacities on the left side of the diagram represent solutions where economical objective function has advantage compared to environmental objective minimization, i.e. natural gas is frequently used. Right side of the diagram involves technologies for which environmental impact is minimized, such as solar thermal collectors and biomass heat-only boiler. It is important to notice that usage of heat pumps also emits carbon dioxide emissions due to the electricity sector emission factor defined on the national level. This is major drawback of the proposed model, since it doesn't take into account future decarbonisation of the power sector. The model proposes optimal configuration of the supply system for a given set of starting condition: heat demand, system prices, emission factors, etc. Although used Croatian power sector emission factor is lower than European average, heat pump couldn't be found in the most environmentally friendly solutions in Figure 2a. Figure 2c shows respective optimized thermal storage capacity for capacity solutions determined by optimization. It can be noticed that economically optimal solution has total discounted cost equal to 1.200.000 € and emissions equal to 10.600 tonnes of CO_2 per year. Total heat demand is covered with 11,17 MW natural gas heat-only boiler and thermal storage with capacity equal to 145 MWh. Reduction of environmental impact gradually increases total discounted cost of the system up to the 1.687.000 € where heat demand is covered with more environmentally friendly technologies such as biomass boiler, heat pump and solar thermal. District heating system emits around 2.250 tonnes of CO_2 per year for this configuration. After this point, further CO_2 reduction is possible only with large addition of solar thermal collectors in the system. The environmental impact slightly decreases at the expense of large increase of total discounted cost of the system. Linear addition of the solar thermal collectors in Figure 2b is followed by linear increase of seasonal thermal storage, as shown in Figure 2c, which is the cause of the high investment cost. The system could operate with almost zero emissions, but it would require unrealistic seasonal thermal storage capacity. Cogeneration and electrical heater aren't part of any optimal configuration, as seen in Figure 2b. Main reason why cogeneration units aren't part of any Pareto solution are low electricity market prices and inexistence of feed-in tariff or premiums. Electrical heaters aren't used due to low efficiency when compared to heat pumps, and high fixed cost related to power capacity which is payed monthly to the grid operator. Lower efficiency also implies higher CO_2 emissions in relation to heat pumps.

Figure 3 shows optimization results for district cooling system in Scenario 1 in the similar manner. Figure 3a shows Pareto front for district cooling optimization. Optimal capacities which satisfy objective functions are shown in Figure 3b. The least-cost solution has configuration: 3 MW absorption heat pump, 2 MW natural gas heat-only boiler and 0,7 MW compression heat pump. Interesting solution is obtained with 600 tonnes of CO_2 emissions per year where compression heat pump reaches peak equal to 3,7 MW. Again, cogeneration has never been chosen for optimal configuration due to low electricity market prices. Furthermore, they don't receive any additional subsidies such as feed-in premium of feed-in tariffs.

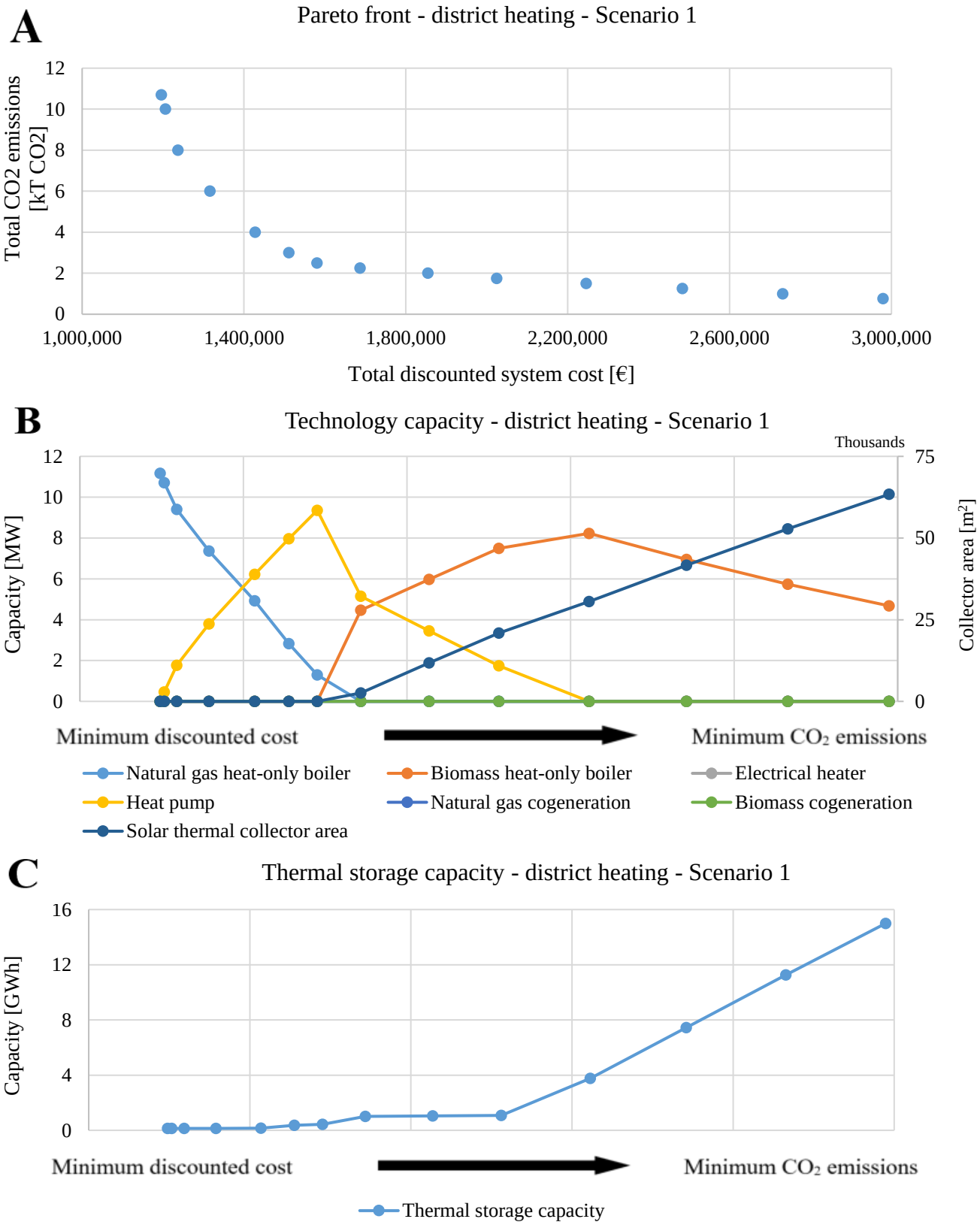

Figure 2 Multi-objective optimization results of district heating system: Pareto front (a), supply capacities (b), thermal storage size (c)

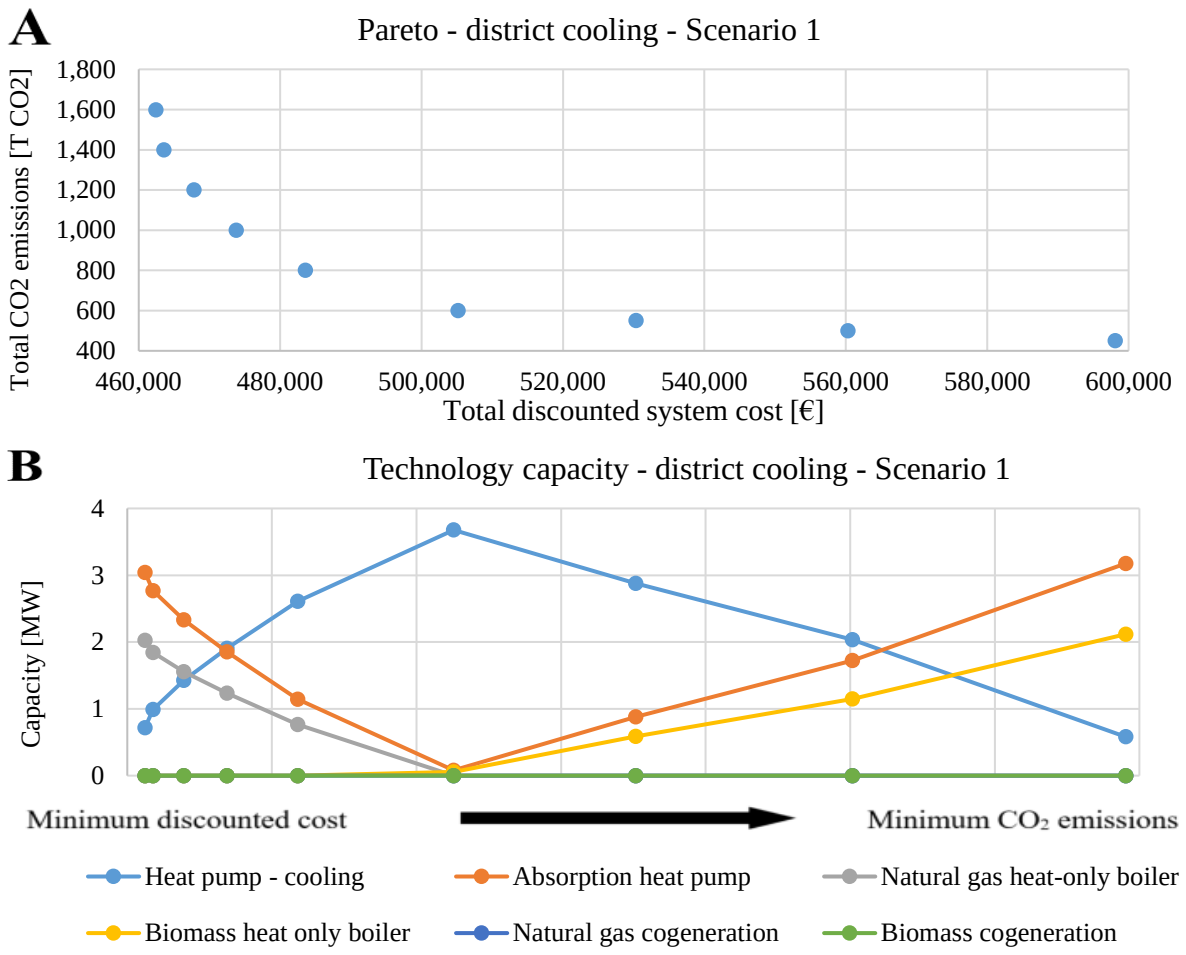

Figure 3 Multi-objective optimization results of district heating system: Pareto front (a), supply capacities with relation to optimal cost (b)

Results of the Scenario 2, where district heating and cooling systems are combined, are shown in
Figure 4. Besides presenting the results of the Scenario 2,
Figure 4a shows comparison between Pareto front where district heating and cooling systems are combined and specific Pareto points for Scenario 1 where district heating and cooling systems are operating separately. Firstly, solutions with least-cost and lowest environmental impact are explained in detail. It can be seen that least-cost solutions are almost equal total with value of 1.600.000 €. Nevertheless it is worth mentioning that Scenario 2 can provide configuration with lower discounted cost for the same level of carbon dioxide emissions. The solution with lowest environmental impact is again in favour of Scenario 2, where 200.000 € of discounted cost could be saved by configuration which combines district heating and cooling systems. If other Pareto solutions are observed in the assumed economically feasible region, i.e. up to the total discount cost approximately equal to 2.000.000 €, it can be seen that combined district heating and cooling systems have smaller discounted total cost for the same total yearly CO_2 emissions due to the interconnection through absorption heat pump which utilizes heat from heat-only boilers. Optimal supply capacities are shown in
Figure 4b. Again, cogeneration units haven't been chosen as a part of optimal system's configuration. The reason for this is relatively low electricity market price and no subsidies available for biomass cogeneration. Reason why electrical heaters aren't part of the solution,

although they have lowest specific investment price, is extra cost related to the electrical power capacity which is payed annually.

As already mentioned, developed model is capable of simultaneously optimizing capacity and operation of supply capacities. In Figure 5, hourly operation of heating and cooling technologies is shown for Scenario 2 and configuration marked with red square in Figure 4. Figure 5a, shows operation of heating supply technologies. Total heat demand is covered with 4,2 MW natural gas heat-only boiler, 4,8 MW compression heat pump, 2,11 MW biomass heat-only boiler integrated with 175 MWh thermal storage. Operation of district heating thermal storage is shown in Figure 5b. Natural gas operates only during winter season as the peak boiler, while the heat pump operates through the whole year covering base load in the combination with thermal storage. Biomass boiler also operates through the whole year, but during summer period share of the heat is used in the absorption heat pumps to cover part of the cooling load. Figure 5c shows optimal operation of district cooling system. Cooling compression heat pumps cover the base cooling demand which consists of tertiary sector buildings and other facilities which have constant cooling load. Figure 5d displays optimal operation of district cooling thermal storage.

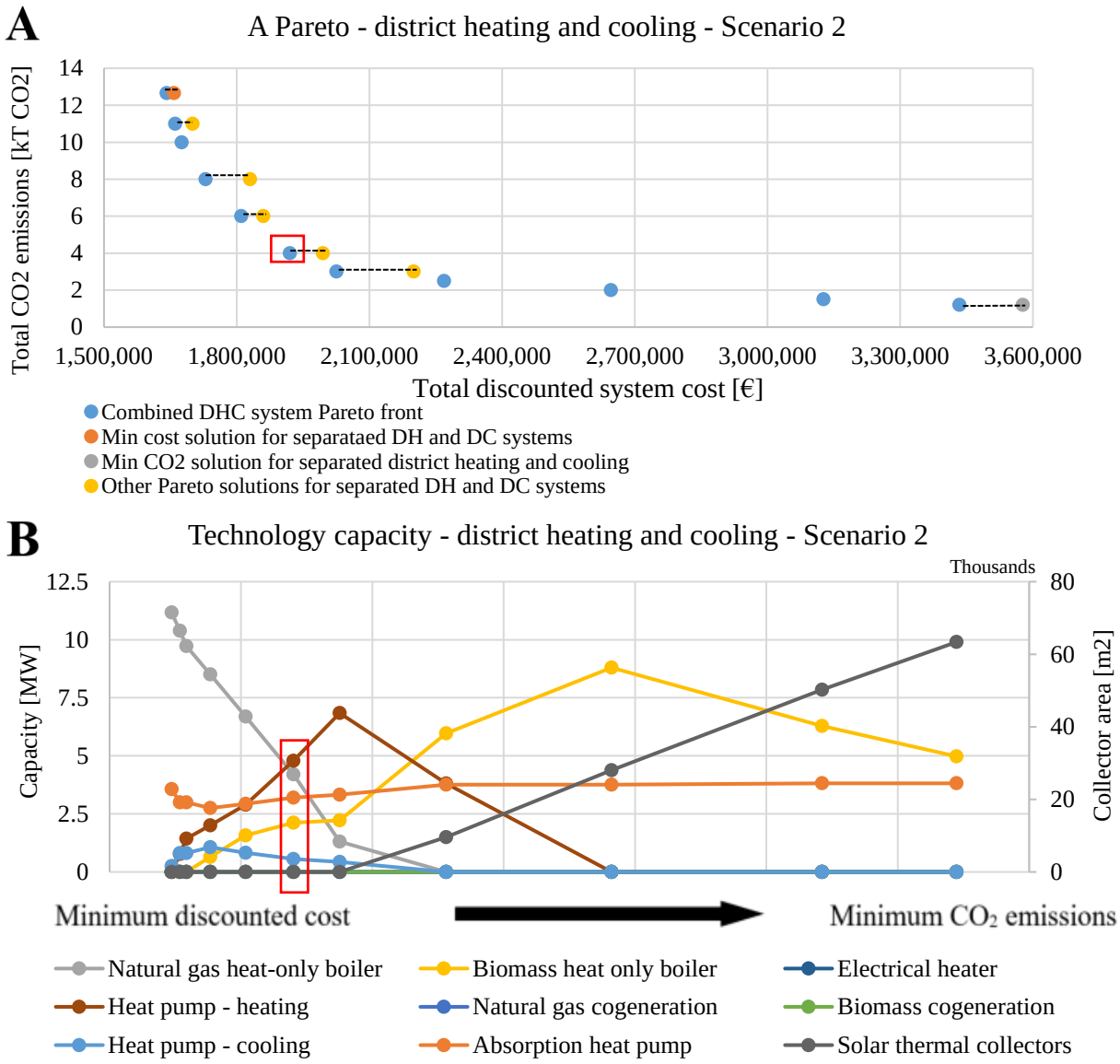

Figure 4. Multi-objective optimization results of district heating system: Pareto front comparison for separated and combined DHC systems (a), supply capacities (b),

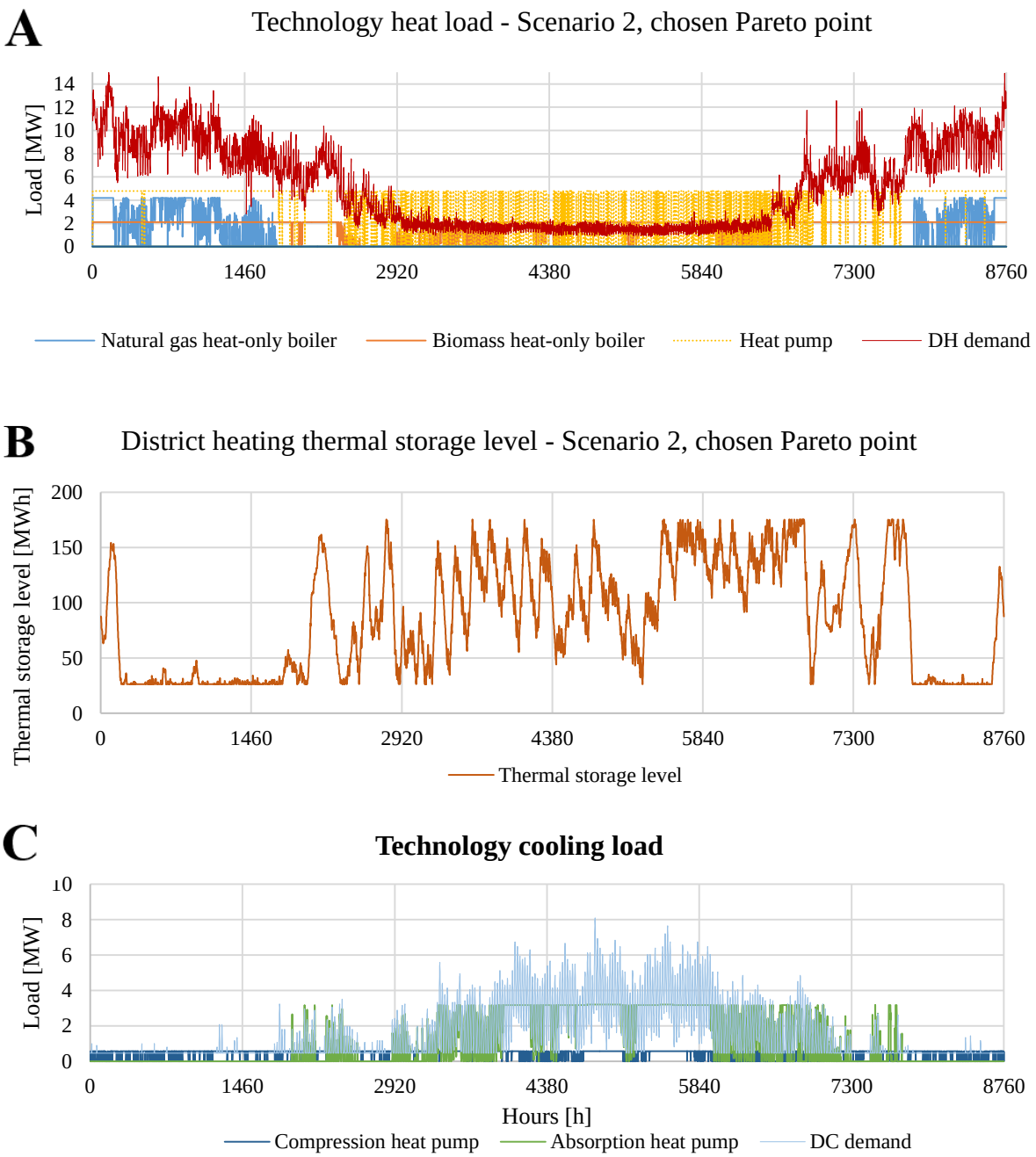

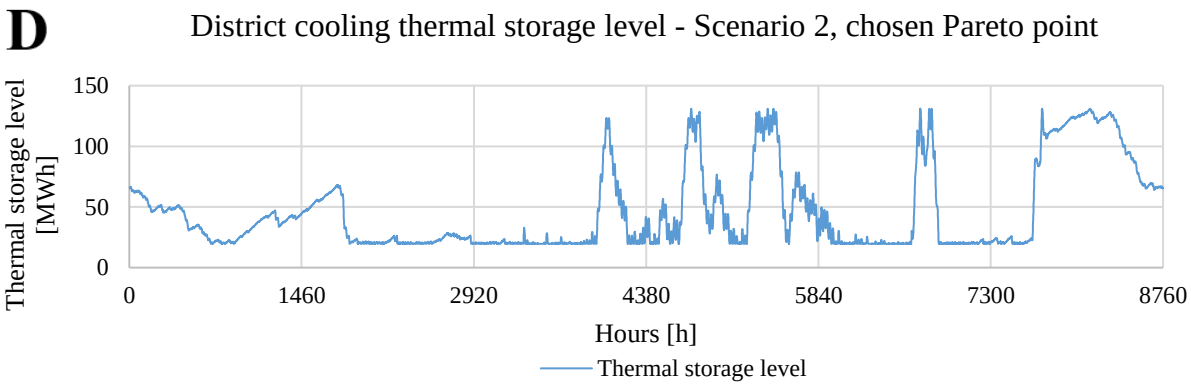

Figure 5 Optimized hourly operation combined systems: district heating (a), heating thermal storage (b), district cooling (c) and cooling thermal storage (d)

5. Conclusion

In this paper, multi-objective optimization model of district heating and cooling system has been developed in order to analyse benefits of integrated district heating and cooling systems. In order to obtain Pareto front, weighted sum and epsilon constrain methods were used. The model is able to define the compromise between total discounted cost and environmental impact of the system in terms of tonnes of CO_2 emissions. Since the model is hourly based for a whole year period, it is capable of optimizing supply capacities and hourly operation of optimal technology configuration, including thermal storage. This is novel approach of analysing district heating and cooling systems since multi-objective optimization on this level of temporal resolution and with this broad scope of possible technologies to be utilized hasn't been done so far, according to the authors' knowledge. The model was written in free and open-source programming language called Julia, while Cbc was used as the linear programming solver. The model was tested on the case study of Velika Gorica, where mapped yearly heating and cooling demands were combined with degree-hour method in order to create hourly demand distributions. Two scenarios were analysed: the first one where district heating and cooling systems operate separately and the second one where mentioned two systems operate simultaneously through utilization of absorption heat pumps. The obtained results of multi-objective optimization show that combined district heating and cooling systems can operate with the same yearly CO_2 emissions as when they operate separately, but with lower total discounted cost. In addition to this, the hourly multi-objective optimization model developed in this paper defined of technology configurations trends, including their operation, should be used in order to satisfy economical and environmental goals of the district heating and cooling system. Developed model and provided results shown in this paper could be utilized for energy policy making decisions when considering district heating and cooling systems. However, provided model can be used in order to define supply capacities and thermal storage size for more detailed technical and economic feasibility study. Furthermore, model includes real-life constraints, such as ramp-up and ramp-down speed in order to bring the model closer to real-life engineering applications.

References

[1] European Commission, "Communication from the Commission to the European Parliament, the Council, the European Economic and Social Committee and the Committee of the Regions, An EU Strategy on Heating and Cooling." .

[2] EU Commission, “Directive 2012/27/EU of the European Parliament and of the Council of 25 October 2012 on energy efficiency, amending Directives 2009/125/EC and 2010/30/EU and repealing Directives 2004/8/EC and 2006/32/EC,” no. October, pp. 1–56, 2012.
[3] H. Lund *et al.*, “4th Generation District Heating (4GDH). Integrating smart thermal grids into future sustainable energy systems.,” *Energy*, vol. 68, pp. 1–11, 2014.
[4] B. V. Mathiesen *et al.*, “Smart Energy Systems for coherent 100% renewable energy and transport solutions,” *Appl. Energy*, vol. 145, pp. 139–154, 2015.
[5] M. A. Sayegh *et al.*, “Trends of European research and development in district heating technologies,” *Renew. Sustain. Energy Rev.*, pp. 1–10, 2016.
[6] H. Ahvenniemi and K. Klobut, “Future Services for District Heating Solutions in Residential Districts,” *J. Sustain. Dev. Energy, Water Environ. Syst.*, vol. 2, no. 2, pp. 127–138, 2014.
[7] L. Grundahl, S. Nielsen, H. Lund, and M. Bernd, “Comparison of district heating expansion potential based on consumer-economy or socio-economy,” pp. 1–8, 2016.
[8] H. Lund *et al.*, “Simulation versus Optimisation : Theoretical Positions in Energy System Modelling,” pp. 1–17, 2017.
[9] R. Mikulandrić *et al.*, “Performance Analysis of a Hybrid District Heating System : A Case Study of a Small Town in Croatia,” *J. Sustain. Dev. Energy, Water Environ. Syst.*, vol. 3, no. 3, pp. 282–302, 2015.
[10] A. Ziebik and P. Gładysz, “Optimal coefficient of the share of cogeneration in district heating systems,” *Energy*, vol. 45, no. 1, pp. 220–227, 2012.
[11] E. Carpaneto, P. Lazzeroni, and M. Repetto, “Optimal integration of solar energy in a district heating network,” *Renewable Energy*, vol. 75. pp. 714–721, 2015.
[12] T. Tezer, R. Yaman, and G. Yaman, “Evaluation of approaches used for optimization of stand-alone hybrid renewable energy systems,” *Renew. Sustain. Energy Rev.*, vol. 73, no. June 2016, pp. 840–853, 2017.
[13] A. Sheikhi, A. M. Ranjbar, and H. Oraee, “Financial analysis and optimal size and operation for a multicarrier energy system,” *Energy Build.*, vol. 48, pp. 71–78, 2012.
[14] T. Falke, S. Krengel, A.-K. Meinerzhagen, and A. Schnettler, “Multi-objective optimization and simulation model for the design of distributed energy systems,” *Appl. Energy*, 2016.
[15] H. S. Gholamhossein Abdollahi, “Application of the multi-objective optimization and risk analysis for the sizing of a residential small-scale CCHP system,” *Energy Build.*, vol. 60, pp. 330–344, 2013.
[16] A. Rieder, A. Christidis, and G. Tsatsaronis, “Multi criteria dynamic design optimization of a small scale distributed energy system,” *Energy*, vol. 74, no. C, pp. 230–239, 2014.
[17] J. Y. Wu, J. L. Wang, and S. Li, “Multi-objective optimal operation strategy study of micro-CCHP system,” *Energy*, vol. 48, no. 1, pp. 472–483, 2012.
[18] D. Xu, M. Qu, Y. Hang, and F. Zhao, “Multi-objective optimal design of a solar absorption cooling and heating system under life-cycle uncertainties,” *Sustain. Energy Technol. Assessments*, vol. 11, pp. 92–105, 2015.
[19] M. Hu and H. Cho, “A probability constrained multi-objective optimization model for CCHP system operation decision support,” *Appl. Energy*, vol. 116, pp. 230–242, 2014.
[20] S. Sanaye and A. Sarrafi, “Optimization of combined cooling, heating and power generation by a solar system,” *Renew. Energy*, vol. 80, pp. 699–712, 2015.
[21] T. Fang and R. Lahdelma, “Genetic optimization of multi-plant heat production in district heating networks,” *Appl. Energy*, vol. 159, pp. 610–619, 2015.
[22] S. Bracco, G. Dentici, and S. Siri, “Economic and environmental optimization model for the design andthe operation of a combined heat and power distributed generation system

in an urban area," *Energy*, vol. 55, pp. 1014–1024, 2013.
[23] M. Pavičević, T. Novosel, T. Pukšec, and N. Duić, "Hourly optimization and sizing of district heating systems considering building refurbishment - Case study for the city of Zagreb," *Energy*, 2016.
[24] J. P. Jiménez Navarro, J. M. Cejudo López, and D. Connolly, "The effect of feed-in-tariff supporting schemes on the viability of a district heating and cooling production system," *Energy*, vol. 134, pp. 438–448, 2017.
[25] J. Song, F. Wallin, and H. Li, "District heating cost fluctuation caused by price model shift," *Appl. Energy*, vol. 194, pp. 715–724, 2017.
[26] M. Pirouti, A. Bagdanavicius, J. Ekanayake, J. Wu, and N. Jenkins, "Energy consumption and economic analyses of a district heating network," *Energy*, vol. 57, pp. 149–159, 2013.
[27] J. Skorek, P. Bargiel, and M. Tan, "Energy and economic optimization of the repowering of coal-fired municipal district heating source by a gas turbine," *Energy Convers. Manag.*, 2017.
[28] D. Wei, A. Chen, B. Sun, and C. Zhang, "Multi-objective optimal operation and energy coupling analysis of combined cooling and heating system," *Energy*, vol. 98, pp. 296–307, 2016.
[29] A. L. Facci, L. Andreassi, and S. Ubertini, "Optimization of CHCP (combined heat power and cooling) systems operation strategy using dynamic programming," *Energy*, vol. 66, pp. 387–400, 2014.
[30] M. Anatone and V. Panone, "A model for the optimal management of a CCHP plant," *Energy Procedia*, vol. 81, pp. 399–411, 2015.
[31] "Julia." [Online]. Available: https://julialang.org/.
[32] D. Heating and E. C. Generation, *Technology data for energy plants*. 2012.
[33] P. A. Sørensen, J. E. Nielsen, R. Battisti, T. Schmidt, and D. Trier, "Solar district heating guidelines: Collection of fact sheets," no. August, p. 152, 2012.
[34] JRC, "PVGIS." [Online]. Available: http://re.jrc.ec.europa.eu/pvgis.html.
[35] "SPF Institut für Solartechnik." [Online]. Available: http://www.spf.ch/index.php?id=111&L=6.
[36] S. Frederiksen and S. Werner, *District Heating and Cooling*. 2013.
[37] "JuMP." [Online]. Available: http://www.juliaopt.org/JuMP.jl/0.18/.
[38] "Cbc optimization solver." [Online]. Available: https://projects.coin-or.org/Clp.

PAPER 2

Applied Energy 251 (2019) 113394

Contents lists available at ScienceDirect

Applied Energy

journal homepage: www.elsevier.com/locate/apenergy

Economical, environmental and exergetic multi-objective optimization of district heating systems on hourly level for a whole year

Hrvoje DorotiĆ*, Tomislav Pukšec, Neven Duić

University of Zagreb, Faculty of Mechanical Engineering and Naval Architecture, Department of Energy, Power Engineering and Environmental Engineering, Ivana Lučića 5, 10002 Zagreb, Croatia

HIGHLIGHTS

- Multi-objective optimization of district heating systems.
- Obtained the most suitable solution, defined as the closest to the Utopia point.
- Impact of the electricity market prices reduction has been analysed.

ARTICLE INFO

Keywords:
District heating
Exergy
Multi-objective optimization
Linear programming
Thermal storage

ABSTRACT

District heating systems are proven to be an effective way of increasing energy efficiency, reducing the environmental impact and achieving higher exergy efficiency than individual heating solutions. The leaders in district heating integration are Scandinavian countries with more than 50% of the covered total heating demand. Nevertheless, these systems haven't reached their full potential in most European countries. The reason for this could be that energy planners often study only the economic feasibility of the system, thus neglecting other crucial aspects of the previously mentioned district heating. In research papers, district heating multi-objective optimization usually takes into account the minimization of the total discounted cost and the environmental impact. Most times, these two objectives are studied as a single objective optimization problem through the internalization of the cost related to carbon dioxide emissions. This paper presents the multi-objective optimization method which is capable of optimizing district heating technology supply capacities and their operation, including thermal storage, for a one-year time horizon in order to satisfy the optimization goals. The model was written in the open-source and free programming language called Julia, while linear programming solver named Clp was used to obtain the solution. The solver is part of Julia's optimization package called JuMP. Three separate objective functions are included in the model: the minimization of the total discounted cost, the minimization of carbon dioxide emissions and the minimization of exergy destruction. Since these three goals are often in conflict, the final result of multi-objective optimization is the so-called Pareto surface which presents the compromise between all possible results. To deal with the multi-objective optimization problem, the weighted sum method in combination with the epsilon-constraint method was used. The most suitable result has been chosen using the knee point method which is a solution the closest to the Utopia solution where all three goals reach their optimal value.

1. Introduction

The fourth generation of district heating (DH) is a concept of an energy system that is capable of integrating power, heating, cooling and even the transport sector [1,2]. Furthermore, a higher interconnection with active consumers is also expected, thus making them prosumers [3,4]. Besides sectoral integration, it also implies the reduction of the district heating network supply temperature and the increase of overall system's efficiency [5]. Low-temperature district heating systems will be able to integrate low-temperature renewable energy sources (RES) and locally available low-temperature waste heat [1,6]. Current systems are still far away from the mentioned goals. Supply temperatures are often higher than 100 °C which, by definition, falls into the category of the second generation of district heating systems [7]. However, many

* Corresponding author.
E-mail address: hrvoje.dorotic@fsb.hr (H. DorotiĆ).

https://doi.org/10.1016/j.apenergy.2019.113394
Received 24 December 2018; Received in revised form 6 May 2019; Accepted 20 May 2019
Available online 28 May 2019

researchers are discussing concepts that are even more advanced and put emphasis on exergy analysis. While energy efficiency indicates the effectiveness resource usage, exergy analysis provides the answer on the quality of energy transformation. Space heating temperatures are relatively low when compared to combustion flames in cogeneration plants or boiler units, so from an exergetic point of view, heating demand should be covered by low-temperature sources or excess heat coming from different processes, while high temperature heat should be transformed to useful work, i.e. electrical energy.

The exergy analysis of different network temperatures carried out for Denmark and Swedish systems shows that almost 60% of exergy content in heat supply is dissipated in the distribution system [8]. Another paper also arrived to similar conclusions through a steady-state simulation approach. Authors provided suggestions on how to decrease supply temperature thus increasing energy and exergy efficiency. They concluded that further reduction of exergy destruction is possible for space and domestic hot water (DHW) heating purposes [9]. Gadd and Werner analysed district heating substations' temperature regimes for Danish and Swedish systems and stated that high temperature differences contribute to energy and exergy losses [10]. Exergy has become a common parameter in the analyses of district systems. In her PhD thesis, Şiir Kilkiş developed a rational exergy management model which could facilitate the curbing of carbon dioxide (CO_2) emissions [11]. In another paper, she developed a method for energy planning of near-zero exergy and near-zero compound CO_2 districts [12]. Yang et al. evaluated solutions for DHW demand from low-temperature DH systems [13], while Baldvinsson et al. performed a feasibility and performance assessment of such a system [14]. In some papers, researchers analysed the cost of exergy and integrated it into the exergoeconomic analysis, e.g. by using specific exergy cost (SPECO) method [15].

The previously mentioned papers performed exergy analysis of the system as a whole, while the following ones concentrated on a much more detailed analysis of the district heating system technologies. Yamankaradeniz has performed an advanced exergy analysis for each of the components used in the Bursa geothermal DH system [16]. A similar analysis was carried out in [17] where an artificial neural network modelling was used. Exergy analysis can also be implemented on district cooling systems, as shown in papers [18,19]. In the first one, a refuse-derived fuel was analysed, while biomass and solar energy exergy characteristics were assessed in the latter. The exergy of solar and its many applications, including heating, were studied in detail in [20]. Lake and Rezaie are even assessing exergy efficiency of cold thermal storage by means of a detailed simulation and model validation [21]. In paper [22] exergy efficiency analysis of the vapour compression heat pump for heating purposes was carried out.

While analysis and simulation of energy systems can provide detailed information, they can't answer the question: which solution is the most suitable choice? In order to explore this, optimization is needed. Single objective and multi-objective optimization of DH systems has been carried out on different temporal scales, with different possible technologies while taking into account various objective functions such as minimization of total cost [23–25], minimization of CO_2 emissions [26], minimization of primary energy supply [27] or different combination of mentioned objective functions. In a case where more than one objective function is defined, a multi-objective optimization approach has to be considered. There are numerous ways to handle this kind of optimization. The most often are genetic algorithms [28], mixed-integer linear programming (MILP) [29] or even non-linear mixed integer linear programming (MINLP) [30]. While many researchers are developing their own algorithms and models, there are also commercially available optimization tools, as the one shown in [31]. Multiple objective functions are usually summed up in a single weighted objective function by using a weighted sum method such as in [28] or [29]. Different approaches could also be used such as epsilon constraint method [32,33], which is more suited when acquiring the whole Pareto front and not only a single solution of multi-objective optimization.

Exergy-related objective functions are also often included in optimization problems. In [34], exergy isn't specified as an objective function, but exergy destruction is translated into economical loss and integrated in the function. Paper [35] used exergy loss as one of the indicators in a composite utility function. Exergy related parameters such as exergy input, exergy destruction or exergy efficiency are rarely used in single-objective optimization. They are usually part of a multi-objective optimization problem. Franco et al. used second law of thermodynamic in order to reach maximum efficiency of a CHP unit operation in a DH system [36]. Other papers, such as [37] used the maximization of energy efficiency, besides cost minimization, in order to optimize the configuration of organic Rankine cycle. In paper [38], a combined cooling, heating and power cycle was optimized where exergy efficiency, besides total product cost and environmental impact, was chosen as an objective function. Exergy efficiency was also chosen as one of the objective functions in [39], where a net-zero exergy district in China was optimized using a multi-objective optimization approach.

M. Di. Somma et al. in [40,41] have optimized a distributed energy system which includes the production of electricity and thermal energy, while taking into account the maximization of exergy efficiency and the minimization of total cost as objective functions. Mixed integer linear programming was used in combination with a weighted sum method in order to handle multi-objective optimization. In [40], only operation of the system was optimized, while in paper [41] supply capacities are also optimization variables. Both papers are considering only representative days, but not a whole year. The time step is equal to one hour. The environmental impact, in terms of CO_2 emissions, wasn't taken into account. Furthermore, the district heating network supply temperature wasn't considered during the calculation of exergy efficiency, i.e. exergy destruction.

Paper [42], published by DorotiĆ et al, deals with a multi-objective optimization of district heating and cooling systems, while taking into account the minimization of economic and ecological objective functions. The results have shown that for the same discounted cost of the energy system, combined district heating and cooling emits less CO_2 emissions than when operated separately. The model shown in this paper is based on the mentioned research.

In this paper, a multi-objective optimization of district heating systems, which takes into account the minimization of total cost, the minimization of carbon dioxide emissions and the minimization of exergy destruction, was carried out. The model is capable of optimizing the hourly operation and sizing of supply capacities, including thermal storages, for a time horizon of a whole year. Possible supply units include technologies frequently used in district heating systems: air-source heat pump, electrical heater, boiler, cogeneration unit, solar thermal collectors, including short-term and seasonal thermal storage. The model is capable of choosing between using biomass and natural gas as a fuel. The proposed approach is a novelty since such detailed optimization of district heating systems hasn't been reported according to performed literature review. An additional novelty is that exergy destruction is calculated by taking into account the supply temperatures of the district heating network, which can be put in relation with outside air temperature.

Finally, this paper answers the following questions:

(1) Which supply technologies should be implemented when shifting from the least-cost solutions to more environmentally friendly and higher quality solutions exergy-wise?
(2) How does the change of electricity market prices influence the aforementioned shift?

This paper is structured as follows. Section 2 presents the district heating model and the method used in order to deal with the multi-objective optimization. Section 3 shows a case study of Velika Gorica and the main input data used in this paper. Section 4 shows and

discusses the acquired results and provides a discussion. The paper finishes with a conclusion and potential ideas for future work, as shown in Section 5.

2. Method

The method used in this paper is based on the model developed in [42]. It is the multi-objective optimization model used for designing district heating and cooling systems by taking into account the minimization of the discounted cost and carbon dioxide emissions. The model is capable of optimizing supply and thermal storage capacities, including hourly operation for a whole year. The multi-objective optimization problem was handled by using a weighted sum and epsilon constraint method.

For the purposes of this paper, the mentioned model has been improved and updated as follows. First of all, the energy system used in [42] consists of district heating and cooling, while the model used in this paper focuses only on district heating. Secondly, additional thermal storage has been added which is charged only with solar thermal collectors. It could be used as a seasonal storage in a case of large scale integration of solar thermal collectors. Thirdly, the heat pump model has been updated, i.e. the efficiency of the heat pump isn't treated as a constant parameter but is modelled by taking into account the heat source (outside air) and the heat sink (DH network) temperatures. Finally, sink temperature, i.e. district heating supply temperature wasn't taken into account in [42], while its hourly variations have been considered and implemented in this paper.

The major improvement of the model is the addition of the third objective function which is related to exergy and defined as exergy destruction. In paper [42], the final result the of multi-objective optimization was a two dimensional Pareto front, while the main outcome of this paper is a three dimensional front, due to the existence of three objective functions, which shapes a Pareto surface.

Although developed method focuses on optimization of the district heating system from energetic, ecological and exergetic point of view, it is far from life cycle assessment (LCA). First of all, the optimization model covers only one, reference, year in order to optimize system's capacity and operation with a goal to minimize costs, carbon dioxide emissions and exergetic destruction. On the other hand, LCA considers a whole lifetime of each part of the system. Secondly, the method doesn't take into account neither materials nor energy consumed in order to construct the district heating system. Finally, this method doesn't take into account the processes which should be carried out once the supply capacities reach end of their lifetime and need to be decommissioned.

2.1. District heating model

The district heating model used in this paper is shown in Fig. 1. The model is capable of choosing between different supply units: heat pump, electrical heater, cogeneration, heat-only boiler, solar thermal collectors and different thermal storages. Two different fuels can be used, natural gas and biomass, while electricity bought on the market drives the power-to-heat technologies, i.e. the electrical heater and the air-water compression heat pump. Cogeneration units are selling electricity on the market, while also receiving feed-in premium in one scenario. Solar thermal collectors have separated storage which acts as a seasonal in a case of high solar fraction. Smaller, short-term thermal storage serves as a buffer for other supply technologies. The district heating network supply temperature depends on the thermal load, i.e. it is in correlation with the outside temperature, as shown in [7,43]. The yearly district heating demand is obtained by using publicly available data [44], while the hourly distribution was acquired by using modified heating-degree hour method in combination with the already known hourly distribution of domestic hot water demand [45].

2.2. Optimization variables

The optimization is carried out for the following decision variables: the size of supply technologies (P_i), including thermal storages' size (TES_{size}) and solar thermal collector area A_{ST}, and the hourly operation of each technology ($Q_{i,t}$ and $TES_{in-out,t}$) for a whole year. All decision variables are continuous which means the model could be solved by means of linear programming.

2.3. Objective functions

The model falls into the domain of a multi-objective optimization problem, which means that more than one objective function should be used. In this case, three objective functions are defined: the minimization of the total system's cost (economical), the minimization of carbon dioxide emissions (ecological) and the minimization of exergy destruction (exergetic). It is important to note that all objective functions have two summation signs, one for temporal scale (t) and one for technology type (i). The temporal summation is performed in the range from 1 to 8760, i.e. between the first and the last hour of the year.

$$f_{econ} = \sum_i C_{investment,i} + \sum_{t=1}^{t=8760} \sum_i \left(C_{fuel,i,t} + C_{O\&M,i,t} - Income_{i,t}\right) \quad (1)$$

The economical objective function can be calculated by using Eq. (1).

where f_{econ} represents the total discounted cost, i.e. the economical objective function, $C_{investment,i,t}$ is the discounted investment cost of technology i, $C_{fuel,i,t}$ is the fuel cost for technology i in a time step t, $C_{O\&M,i,t}$ is the operation and maintenance (O&M) cost of technology i in a time step t, while $Income_{i,t}$ is the additional income of technology i in a time step t. The last term on the right has a negative sign because it lowers the total cost of the system. An example of income is electricity sold on the market in case of a cogeneration unit. Investment cost doesn't have a temporal summation sign since it is paid only once, while operational costs (fuel and O&M) and income are paid for every hour of the year.

The ecological objective function can be represented with Eq. (2).

$$f_{ecol} = \sum_{t=1}^{t=8760} \sum_i \left(e_{CO_2,i} \cdot Q_{i,t}/\eta_i\right) \quad (2)$$

where f_{ecol} is the total system's CO_2 emissions, $e_{CO_2,i}$ is the CO_2 emission factor for technology i, $Q_{i,t}$ is the thermal energy production of technology i for a time step t and finally η_i is the efficiency of technology i. For the purpose of this model, technology efficiency is held as a constant in order to secure the linearity of the model. The only technology with variable efficiency is a heat pump, since it is exogenous variable which depends on the heat source and heat sink temperatures, as explained in Section 2.5.

The exergetic objective function is calculated by using Eq. (3).

$$f_{exe} = \sum_{t=1}^{t=8760} \sum_i \left(Ex_{in,i,t} - Ex_{out,i,t}\right) \quad (3)$$

where f_{exe} represents the total yearly exergy destruction, $Ex_{in,i,t}$ is the exergy input of technology i in a time step t, $E_{out,i,t}$ is the exergy output of technology i in a time step t. Exergy input and output can be calculated according to the Eqs. (4) and (5).

$$Ex_{in,i,t} = \frac{Q_{i,t}}{\eta_i} \cdot e_{Exe,i} \quad (4)$$

$$Ex_{out,i,t} = Q_{i,t} \cdot \left(1 - \frac{T_{ref_t}}{T_{DHN_t}}\right) \quad (5)$$

Thermomechanical exergy depends on the thermodynamic properties, i.e. temperature and pressure, of the system and the heat reservoir.

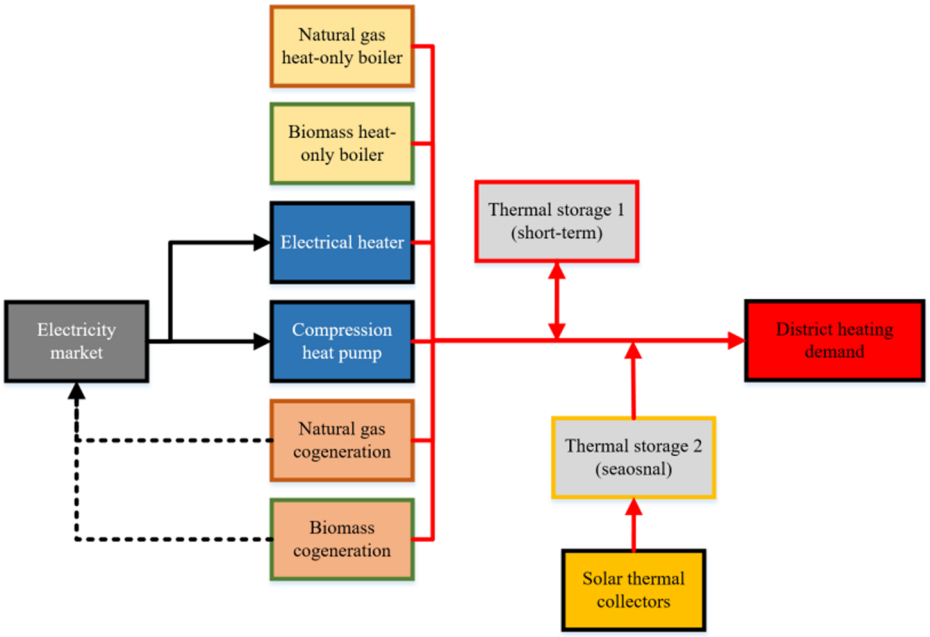

Fig. 1. District heating model.

For the processes in which there is no chemical reaction, exergy could be expressed by using the temperature of the system and the heat reservoir. However, in order to calculate the exergy of the fuel, chemical exergy shouldn't be neglected. Combustion presents a process in which new chemical species are produced. In order to obtain the total exergy of the fuel, the exergy factor $e_{Exe,i}$ could be used [40,46] which represents the ratio of exergy and energy of the fuel. It is important to mention that, in some cases, it could be higher than 1. This approach was used in order to calculate the exergy input$Ex_{in,i,t}$, as shown in Eq. (4).

In order to calculate the exergy output, only thermomechanical exergy can be taken into account, as shown in Eq. (5). Where T_{ref_t} represents temperature of the reference state (outside temperature) in a time step t, and T_{DHN_t} is the supply temperature of the district heating network in a time step t. All the mentioned temperatures are absolute temperatures, expressed in Kelvins. The term in parenthesis in Eq. (5) is known as the Carnot factor. The Carnot factor of electricity is equal to one, since it has the highest energy quality. Although exergy destruction minimization is defined as one of the objective functions, exergy efficiency is a parameter which could also be obtained by using Eq. (6).

$$\eta_{exe} = \frac{\sum_{t=1}^{t=8760} \sum_i Ex_{out,i,t}}{\sum_{t=1}^{t=8760} \sum_i Ex_{in,i,t}} \tag{6}$$

It is important to mention that exergy efficiency of solar thermal collectors is set to 100%. Although some papers calculate exergy efficiency of solar thermal collectors [20,40], the authors of this research have decided to assume it is equal to 100%, i.e. there is no exergy destruction in solar thermal collectors. The reason for this is following. Exergy analysis is used in order to evaluate the quality of energy transformation. It is crucial for energy sources which don't have infinite availability such as fossil fuels or biomass. Exergy of these fuels should be utilized as much as possible since they can't be used again once they undergo combustion process. On the other hand, solar energy has unlimited potential. If solar thermal collectors are installed in one energy system, this doesn't limit solar energy utilization in the other energy system. By taking into account exergy destruction of solar thermal collectors, renewable energy sources would be additionally penalized and their successful integration to energy system would have additional obstacle, besides investment cost, to deal with.

2.4. Optimization constraints

District heating system operation must satisfy the thermal demand which is the sum of space heating and domestic hot water (DHW) demand. This constraint could be written as follows:

$$DEM_t = Q_{HOB,gas,t} + Q_{HOB,biomass,t} + Q_{EH,t} + Q_{HP,t} + Q_{CHP,gas,t} + Q_{CHP,biomass,t} - TES_{1,in-out,t} - TES_{2,in-out,t} \tag{7}$$

Eq. (7) says that in every hour of the year, the demandDEM_t has to be satisfied with supply technologies ($Q_{i,t}$) and the charge or discharge of thermal storages $TES_{1,in-out,t}$ and $TES_{2,in-out,t}$. As explained in the Section 2.1., two thermal storages are available in the district heating system. Thermal energy of supply capacities can't be larger than its peak power. This can be expressed with Eq. (8).

$$0 \le Q_{i,t} \le P_i \tag{8}$$

In order to acquire the hourly dynamics of each technology, ramp-up and ramp-down speed constraint is also integrated in the model. This could be written as follows:

$$-r_{up-down,i} \cdot P_i \le Q_{i,t} - Q_{i,t-1} \le r_{up-down,i} \cdot P_i \tag{9}$$

where $r_{up-down,i}$ is ramp-up and ramp-down speed for technology$i$.

Thermal storage operation is defined with the following set of equations. It is important to mention that these equations could be written for both thermal storages in the same manner.

$$SOC_{t=1} = SOC_{t=8760} = SOC_{start-end} \cdot TES_{size} \tag{10}$$

$$SOC_t = SOC_{t-1} + TES_{in-out,t} - SOC_t \cdot TES_{loss} \tag{11}$$

where SOC_t is the state of charge of the thermal storage, $TES_{in-out,t}$ is the charge, i.e. discharge of thermal storage, $SOC_{start-end}$ is the predefined state of the charge (expressed as a share) in the first and the last hour of the year, TES_{size} is the thermal storage size, while the product on the right side of Eq. (11) represents the thermal storage loss in a time step t which is related to the self-discharge coefficient TES_{loss}. It is important to mention that $TES_{in-out,t}$ has a negative value if the storage discharges and has a positive value if the storage charges. Eq. (10) guarantees that thermal storage has the same state of charge in the last hour as in the first hour of the year. For the purpose of this research, $SOC_{start-end}$ for the buffer thermal storage is equal to 50%, while

$SOC_{start-end}$ for the seasonal thermal storage is put to 0% since it is charged during the summer season and is completely discharged during winter season. Eq. (11) actually presents the energy balance of the thermal storage: the state of charge in the current time step (t), is equal to the state of charge in the previous time step ($t-1$) increased by thermal storage charge or discharge ($TES_{in-out,t}$) and reduced by thermal storage loss ($SOC_t \cdot TES_{loss}$).

Although the model includes utilization of biomass as a fuel, it is important to notice that there are no constraints put on fuel availability. It means that fuel is always available and can be used for thermal energy production in any hour of the year. This assumption has also been used in other papers dealing with district heating system optimization [40,45,47]. However, the model could be easily upgraded in order to include fuel availability constraints.

2.5. Exogenous variables

In the proposed model, there are several exogenous variables: the supply temperature of district heating network, the efficiency of an air-source heat pump, i.e. the coefficient of performance (COP), and specific solar thermal production. Although they aren't constant, they can be acquired prior to the optimization procedure. The supply temperature of the district heating network (T_{DHN_t}) is in correlation with the thermal load, i.e. the outside temperature (T_{ref_t}) [7,30]. The outside temperature is defined as air temperature on a specific location which could be acquired by using different publicly available databases such as PVGIS [48] or Renewable Ninja [49].

The efficiency of the heat pump depends on the temperature difference between the heat sink and the heat source. For the purpose of this model, the heat pump's heat source is the outside air while the heat sink is defined as a district heating supply network. In order to acquire the efficiency of the heat pump, a modified equation for coefficient of performance is used [45]:

$$\eta_{HP,t} = f_{Lorentz} \cdot \left(\frac{T_{DH,t}}{T_{DH,t} - T_{ref,t}} \right) \tag{12}$$

where $\eta_{HP,t}$ is the coefficient of performance of the air source heat pump for time step$t$, which depends on the heat sink ($T_{DH,t}$) and the heat source ($T_{ref,t}$) temperatures, and $f_{Lorentz}$ is known as the Lorentz factor used to acquire the real-life COP from the ideal one [45].

Specific solar thermal collector production depends on solar thermal collector efficiency $\eta_{c,t}$, which could be acquired by using Eq. (13).

$$\eta_{c,t} = \eta_0 - a_1 \frac{(T_m - T_{ref,t})}{G_t} - a_2 \frac{(T_m - T_{ref,t})^2}{G_t} \tag{13}$$

where η_0 is zero-loss efficiency, also known as optical efficiency, a_1 is first order heat loss coefficient, a_2 is second order heat loss coefficient and T_m is mean solar thermal collector temperature. These parameters are related to solar thermal collector type and could be find in respected specification databases [50]. Finally, G_t is global solar irradiance for ideal azimuth and elevation angles obtained from publicly available databases [7,30]. It is important to notice that the mean solar thermal collector temperature is taken as a constant, but it is actually a dynamic variable that depends on various parameters such as the thermal load of the solar thermal collector, the mass flow of the medium, etc. This was done in order to secure the linearity of the optimization model. Once the solar thermal efficiency is acquired, the specific solar thermal collector production ($P_{solar,specific,t}$) and the total solar thermal collector output ($Q_{ST,t}$) can be obtained by using Eqs. (14) and (15).

$$P_{solar,specific,t} = \eta_{c,t} \cdot G_t \tag{14}$$

$$Q_{ST,t} = A_{ST} \cdot P_{solar,specific,t} \tag{15}$$

where A_{ST} represents the optimal solar thermal collector area, which is the optimization variable related to solar thermal collectors. As can be seen from Eq. (15), solar thermal collector operation$Q_{ST,t}$ is constrained.

2.6. Optimization method

As shown in Section 2.3, the proposed method includes three objective functions, which means that it falls into the domain of multi-objective optimization. Eq. (16) shows the multi-objective optimization goal.

$$\min(f_{econ}, f_{ecol}, f_{exe}) \tag{16}$$

In this paper, the weighted sum in combination with the epsilon constraint method is used. The weighted sum is one of the most used methods in order to assess Pareto optimal solutions, where all objective functions are merged into single weighted objective function by using weighting coefficients. On the other hand, the epsilon constraint method translates the multi-objective optimization problem into single objective optimization with an additional set of constraints put on other objective functions. Both of the methods are explained and compared in paper [33].

The weighted sum method is shown in Eq. (17).

$$F_{weighted} = \left(\frac{\omega_{econ}}{f_{econ\omega_{econ}=1}} \right) \cdot f_{econ} + \left(\frac{\omega_{ecol}}{f_{ecol\omega_{ecol}=1}} \right) \cdot f_{ecol} + \left(\frac{\omega_{exe}}{f_{exe\omega_{exe}=1}} \right) \cdot f_{exe} \tag{17}$$

$$\omega_{econ} + \omega_{ecol} + \omega_{exe} = 1 \tag{18}$$

By using the weighted sum method, the multi-objective optimization problem can be translated into a single-objective optimization by using weighting coefficients ω_i. As can be seen in Eq. (17), all three objective functions are summed up and multiplied with the related ω_i, thus composing weighted objective function $F_{weighted}$. Due to the fact that objective functions are usually different order of magnitude, they have to be scalarized by using the optimal value of associated objective function, $f_{i_{\omega_i=1}}$.

The final result of the multi-objective optimization isn't a single value, but a whole set of solutions which lie on a Pareto front. In case of three objective functions, it shapes a so-called Pareto surface. It represent a compromise between three different objective functions. In order to acquire a whole surface, i.e. a solution trend, the weighted coefficients are varied, while the satisfying constraint shown in Eq. (18), i.e. their sum has to be equal to one. A major drawback of this method is acquiring the wanted set of solutions on a Pareto surface, especially when having a relatively large step while varying them, e.g. 0,1. Furthermore, the weighted sum method can't provide solutions of the non-convex Pareto fronts, as described in [33].

Once the minimum values of each objective function are known, the boundaries of the Pareto surface are set. Since the goal of this research paper is to acquire a trend, the epsilon constrained method is used to find the other solutions of the Pareto surface. This method allows the translation of a multi-objective optimization problem into a single objective optimization problem with an additional set of constraints. This is shown on the example of a minimizing economical objective function with constraints put on exergy destruction and carbon dioxide emissions, Eq. (19). By increasing or reducing a specific constraint, additional solutions are acquired and the Pareto front can be fully visualized. In this way, the front with equally spaced points can be constructed which is then used for further analysis. A major drawback of this method is the necessity of running a large number of optimizations in order to obtain the Pareto surface with an acceptable level of detail. Furthermore, before using this method, the end-user should know the boundaries of the Pareto surface, since the epsilon constraint should be defined in the feasible region of solutions [33].

$$\min(f_{econ}) \text{for} f_{ecol} = \varepsilon_{ecol}, f_{exe} = \varepsilon_{exe} \tag{19}$$

2.7. Obtaining the most suitable solution

Finally, in order to choose the most suitable solution on the Pareto surface, decision making should be carried out. While various different approaches exist, in this paper the most suitable solution is defined as the one closest to the Utopia point. The Utopia point is an ideal, but unfeasible solution where all three objective functions achieve their optimal values. Mathematically speaking, the most suitable solution is the one with the least distance to Utopia point, as shown in Eqs. (20) and (21).

$$\min(P_{solution}) \tag{20}$$

$$P_{solution} = \sqrt{\sum_{j} (f_{j_{Utopia}} - f_j)^2} \tag{21}$$

where $P_{solution}$ is the distance to the Utopia point, $f_{j_{Utopia}}$ is the minimum possible value of normalized objective function j and f_j is the non-minimum value of normalized objective function j. This method is also known as the knee-point method and it could also be used in a multi-objective optimization problem when two objective functions are defined.

3. Case study

The method was tested on the town of Velika Gorica (45°43′11,9″N 16°04′19,3″E), located in Zagreb County, Croatia. Total area of Velika Gorica is equal to 552 km^2, while urban area is equal to 31 km^2. The town has population of 30.000 while the municipality has around 60.000 inhabitants. The town itself has 14 small district heating system with the overall capacity of 70 MW and around 50.000 MWh of thermal energy distributed to final customers with a thermal network efficiency equal to 80%. Most of the existing smaller DH systems covers both space heating and DHW demand. In the scope of this research, the analysis of replacing part of the district heating supply system was carried out. Furthermore, it is planned that new system would also cover domestic hot water demand and operate through a whole year. The total space heating demand of the final customers connected to that part of the system is equal to 23.000 MWh. According to [45], DHW share in the total household thermal energy demand in Eastern European countries is around 15%, while for highly insulated dwellings in Northern Europe it doesn't drop below 40%. For the purpose of this case study it is assumed that the DHW share for Velika Gorica is 10%, i.e. equal to Croatian's average share of DHW [51].

3.1. Input data

The hourly distribution of space heating was obtained by using the degree-hour method, while the hourly DHW demand was acquired by using the already known existing relative distributions [45]. Fig. 2 shows the district heating load obtained by using the modified heating-degree hour method and includes space heating and DHW demand, including thermal network losses. It can be seen that the load has a highly seasonal effect with the peak demand equal to 19,7 MW during winter season, while the summer load usually isn't higher than 1 MW. Furthermore, it is assumed that the DH system doesn't provide thermal energy to the network during the night, i.e. from 22:00 in the evening until 05:00 in the morning. A more detailed hourly distribution of the heating demand can be seen in the Section Results.

The meteorological data for the location of Velika Gorica [52], which is used for the calculation of exogenous variables and the hourly district heating demand distribution, is shown in Fig. 3. The maximum outside temperature is 36 °C while the minimum is equal to −10 °C. Temperature distribution data is needed for calculation of compression heat pump COP and the district heating supply temperature. The maximum global solar irradiation is equal to 1.180 W/m^2, while the average is equal to 156,3 W/m^2. This makes this location suitable for solar thermal collector integration [53].

Since the exact supply temperature of district heating systems depends on various parameters [7], it was assumed that existing infrastructure operates as third generation district heating. The reason for this is a relatively low household specific heating demand equal to 155,95 kWh/m^2 and a relatively short thermal network [44]. It is assumed that the maximum supply temperature is 100 °C, while the minimum supply temperature is set to 60 °C in order to satisfy the domestic hot water demand during the summer season. The relation between the district heating supply temperature and the outside temperature, including the equation of the slope in the diagram, is shown in Fig. 4. As explained in the section on the Method, the district heating supply temperature is used to calculate the heat pump efficiency, and the exergy destruction. Since it depends on the outside temperature, the supply temperature is also an hourly distribution.

The coefficient of the performance of the air source heat pump used in the model is shown in Fig. 5. As discussed in Section 2.5, it is a function of the district heating supply and the outside (reference) temperature. It is important to note that minimum COP values are obtained during the winter season, while the maximum efficiency is achieved during the summer season, i.e. when the district heating load is lower. The average COP is equal to 2,103. This has a great influence on the multi-objective optimization results, as explained in Section 4.

The specific solar thermal collector output is shown in Fig. 6. The maximum output is obtained during the summer season and it is equal to 600 W/m^2. Due to the low temperatures during the winter season, the output from solar thermal collectors is often equal to zero.

Cogeneration and power-to-heat units are connected to the electricity market. Power-to-heat technologies are buying electricity, while cogeneration units are selling it on the market. In Scenario 1, as explained in Section 3.2, cogeneration units are receiving a sliding feed-in premium, which means that, beside the electricity market price, they are also getting paid the difference between the reference value (RV) and the market price. If the RV is lower than the market price, then the feed-in premium is equal to zero. Since the Croatian legislation hasn't yet adopted a regulation on defining the RV, for the purpose of this research it has been assumed that the RV is equal to 80% of the currently used feed-in tariff for cogeneration plants [54]. Due to this, the proposed reference value is equal to 55 €/MWh. Since Croatia has established a day-ahead electricity market, called CROPEX [55], this data

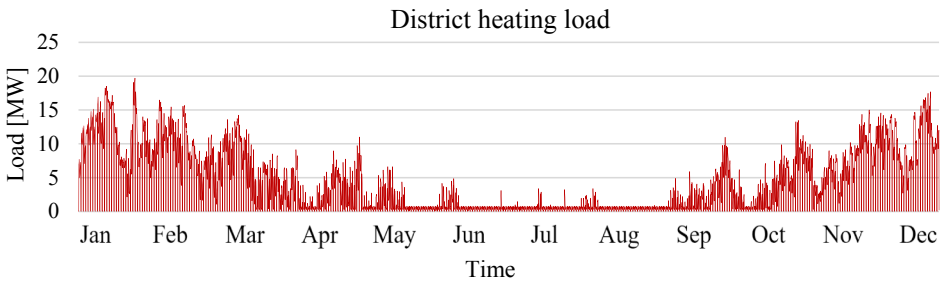

Fig. 2. District heating load.

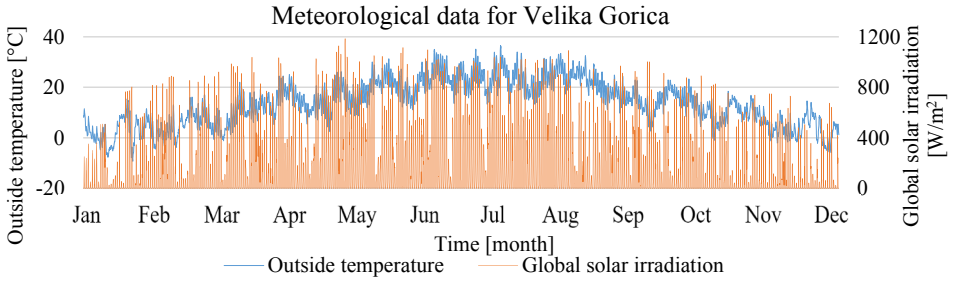

Fig. 3. Meteorological data for Velika Gorica.

has been used as an input for the optimization model. Fig. 7 shows the historical data for year 2017, which are implemented into the model. The average market price is equal to 51,9 €/MWh, which is relatively close to the feed-in premium reference value.

Table 1 shows the technology-related data, which consist of the cost (investment, variable and fuel), the emission factor, the efficiency, the ramp-up and ramp-down speed (expressed as share of the total capacity), the technical lifetime and the power-to-heat ratio needed for cogeneration units. All of the data can be found in report [56]. Besides what was previously mentioned, the assumed discount rate is the same for all technologies and is equal to 7%.

As mention in Section 2.3, the exergy factor is needed in order to calculate the exergy input of the fuels, i.e. the exergy destruction of the technology. Two possible fuels are used: natural gas and biomass. The exergy factor of the natural gas is equal to 1,04 while the exergy factor of biomass fuel is equal to 1,2 as shown in papers [35,41]. It is important to mention that the exergy factor of biomass depends on the biomass type and water content. The biomass used in this paper is woodchip with water content equal to 25%. Finally, the exergy factor of the electricity is equal to 1.

3.2. Scenario analysis

For the purpose of this research, two scenarios are proposed. In Scenario 1, i.e. the Reference Scenario, the electricity market prices are equal to those shown in Fig. 7, while cogeneration units receive a sliding feed-in premium. In Scenario 2, the electricity market prices are lowered by 30%, thus achieving an average market price equal to 36,4 €/MWh. Furthermore, in this scenario cogeneration units do not receive a feed-in premium, thus achieving lower profit.

4. Results and discussion

The proposed model was written in an open-source and free programming language called Julia [57]. Since the problem falls into the domain of linear programming, an LP solver was used, called Clp [58]. It is a free and open-source optimization coin-or branch and cut solver that is part of the JuMP package [59] used for mathematical optimization. The process of obtaining a single Pareto point lasted around 30 min. After the first few runs where weighted factors were varied, the Pareto surface was completed by using the epsilon constraint method. The optimizations were run on a laptop with Intel Core i7.

4.1. Scenario 1 – Reference electricity market prices

4.1.1. Pareto surface

The final results are shown in Fig. 8, where the blue points represent Pareto solutions forming a Pareto front. There are three points, which are the boundaries of the Pareto surface and are shown in Table 2. The point marked with red represents the least-cost solution, the green point is the most environmentally friendly solution, while the purple point represents the Pareto solution with the least exergy destruction. The lowest possible discounted cost is equal to 646.551 EUR, the lowest possible CO_2 emissions are equal to 1.111 tonnes, while the lowest exergy destruction is 10.909 MWh. Furthermore, these are the coordinates of the perfect, but unreachable, solution called the Utopia point which is marked with orange colour in Fig. 8.

The supply capacities for Pareto solutions shown in Table 2 are presented in Table 3. The least-cost solution utilizes natural gas as fuel in a 7,4 MW heat-only boiler and a 5,7 MW cogeneration unit in combination with 146 MWh of buffer thermal storage. Cogeneration operates through a whole year, since it achieves an additional income, as shown in Eq. (1), while a heat-only boiler is used during the colder winter months. The solution with the lowest CO_2 emissions utilizes the maximum available solar thermal collector area, which is set to 50.000 m^2, and a 17,5 MW biomass boiler. It is important to note that a heat-pump isn't part of this solution since it uses electricity as a fuel which also has carbon dioxide emissions due to the fuel mix in the power sector.

This is one of the major drawbacks of this method, since it optimizes the system for a reference year and could potentially cause a lock-in effect in the energy system. Lock-in effect in the energy system implies that decision has to be done without knowing which parameters will change in the future. In this case, various supply capacities have to be installed by taking into account only reference year data. However, these installed supply capacities will have to operate for next 20–30 years, while different parameters which influence their operation could change drastically. We say that the system is then "locked", i.e. it has to operate outside its optimal point. A further decrease in carbon footprint of the power sector is to be expected in the following years,

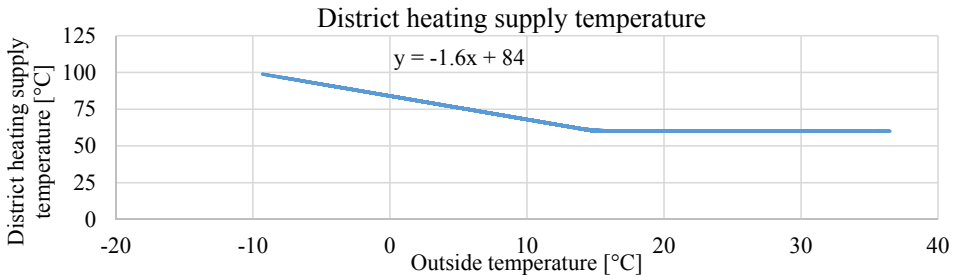

Fig. 4. District heating network supply temperature as a function of outside temperature.

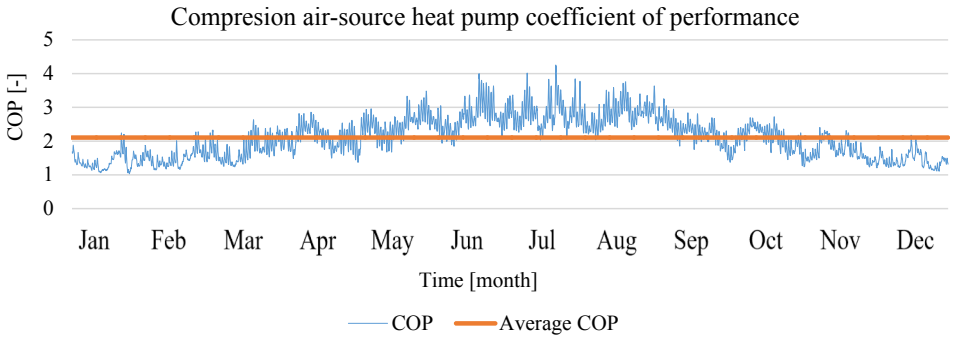

Fig. 5. Coefficient of performance of the air-source compression heat pump.

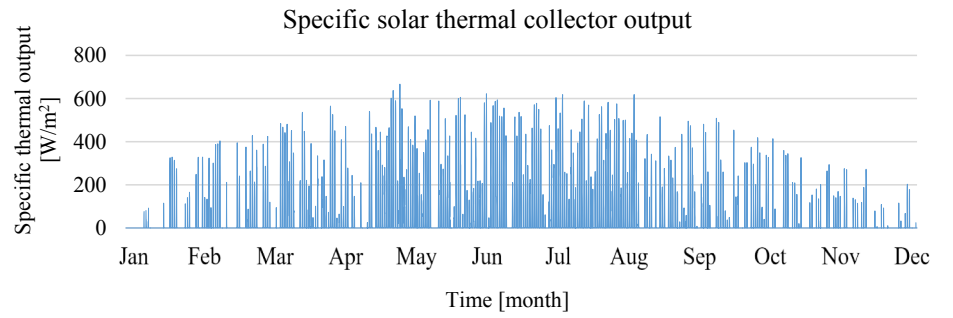

Fig. 6. Specific solar thermal collector output.

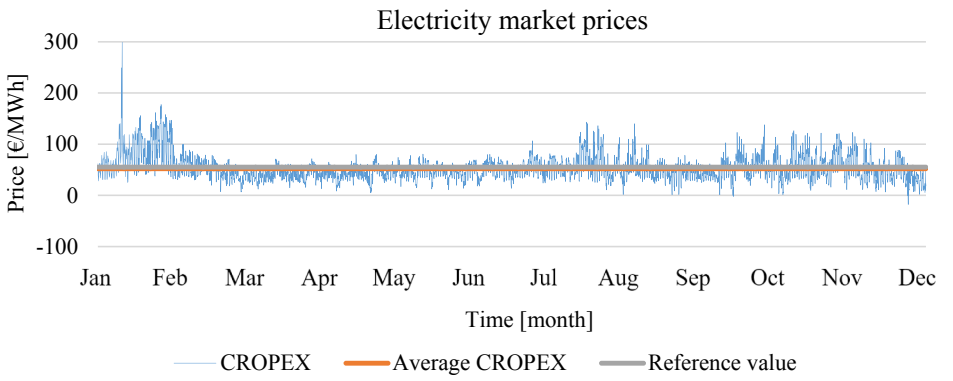

Fig. 7. Electricity market prices, CROPEX.

which will make heat pumps more environmentally friendly. Furthermore, future integration of variable renewable energy sources will also potentially lower electricity market prices thus decreasing operational cost of the heat pumps and making them more economically feasible.

Finally, the technologies utilized in the least-exergy destruction solution is a 18,7 MW heat pump and the maximum solar thermal collector area in combination with seasonal thermal storage with the capacity of 3.878 MWh. This solution also has an extremely high cost, as seen in Fig. 8. The reason for this is the necessity for installing capacities with a high investment cost in order to minimize exergy destruction.

4.1.2. Solution with the highest exergy efficiency

As mentioned in Section 2.3, exergy destruction was chosen as an objective function, while efficiency is only a calculated parameter. The solution with the highest exergy efficiency, as shown in Fig. 8 marked with a purple circle, achieves the exergy efficiency equal to 0,69. The reason for such high exergy efficiency is the utilization of the maximum amount of solar thermal collectors in combination with seasonal thermal storage and a large-scale heat pump. It is important to mention that this solution is also the one with the lowest exergy destruction.

4.1.3. The most suited solution – Supply capacities

Although all Pareto solutions are treated equally, the end-user should define which one is the most suitable, by using a decision-making method. The most suitable solution, chosen according to the method explained in Section 2.7, is also shown in Fig. 8. It is the Pareto point closest to the Utopia point and is marked with an orange circle. It achieves the total discounted cost equal to 1.755.246 EUR, 4.112 tonnes of CO_2 emissions and an exergy destruction equal to 18.000 MWh. The calculated exergy efficiency is equal to 0,31. The optimized supply capacities are shown in Table 4. It utilizes a 11 MW natural gas boiler, a 5,5 MW heat pump in combination with a 5.521 m^2 solar collectors area.

4.1.4. The most suited solution – Hourly operation

Hourly operation of a district heating system for a whole year is shown in Figs. 9 and 10. It can be seen that the heat pump operates through the whole winter period, while the natural gas boiler is used as a peak unit. During the summer season, domestic hot water demand is covered with solar thermal collectors and storage. Smaller thermal

Table 1
Technology data.

Technology	Investment cost [€/MW]/[€/m^2]/[€/MWh]	Fuel cost [€/MWh]	Variable cost [€/MWh]	Emission factor [TCO$_2$/MWh]	Efficiency/storage loss [–]	Ramp-up/down [–]	Technical lifetime [years]	Power-to-heat ratio [–]
Natural gas boiler	100.000	20	3	0,22	0,9	0,7	35	–
Biomass boiler	800.000	15	5,4	0,04	0,8	0,3	25	–
Electrical heater	107.500	Electricity market	0,5	0,234	0,98	0,95	20	–
Heat pump	680.000	Electricity market	0,5	0,234	Hourly distribution	0,95	20	–
Cogeneration natural gas	1.700.000	20	3,9	0,22	0,5 (thermal)	0,3	25	0,82
Cogeneration biomass	3.000.000	15	5	0,04	0,6 (thermal)	0,3	20	0,55
Solar thermal	300 €/m^2	0	0,5	0	Hourly distribution	–	25	–
Thermal storage, buffer	3.000 €/MWh	0	0	0	1% (loss)	–	25	–
Seasonal thermal storage	500 €/MWh	0	0	0	0,1% (loss)	–	25	–

storage serves as a buffer during the winter season and is kept on a technical minimum during the summer season. The hourly district heating load isn't shown in Fig. 9 in order to display the supply technology operation more clearly. Furthermore, a more detailed hourly operation of a district heating system for a single winter week is shown in Figs. 11 and 12. Seasonal storage does not operate during the presented winter week and because of that isn't shown in Fig. 12. The hourly operation of supply capacities (solar thermal collectors) and seasonal thermal storage during a single summer week is shown in Figs. 13 and 14, respectively. The hourly operation of buffer thermal storage isn't shown in Fig. 14 since it is kept on a technical minimum.

4.2. Scenario 2 – Lower electricity market prices

4.2.1. Pareto frontier comparison

Fig. 15a and b show Pareto frontiers obtained for Scenario 1 and Scenario 2. Due to the fact that comparison and visualization of two Pareto surface is challenging, 2D diagrams were used in order to compare two scenarios since they are easier to follow and easier to obtain the main conclusion. As explained in the section Case study, Scenario 2 considers reduction of electricity market prices for 30% and an absence of a feed-in premium for cogeneration units. Fig. 15a is actually 2D representation of Fig. 8. In Fig. 8, exergy destruction objective function is shown on additional axis (3D diagram), while in Fig. 15a, exergy destruction is a parameter treated as a constant for which Pareto fronts for other two objective functions are plotted in 2D diagram. Pareto fronts in Fig. 15a can be understood as slices of the Pareto surface shown in Fig. 8. Exergy destruction values shown in Fig. 15 are actually epsilon constraints put on exergy destruction objective function. As explained in the section Method, epsilon constraint method has been used in order to obtain equally distanced Pareto points and to visualize the Pareto surface.

First of all, it should be mentioned that the shape of Pareto fronts in a case of objective function minimization is usually similar to that shown in Fig. 15, as reported in numerous papers dealing with multi-objective optimization [28,40,42,60]. Therefore, it is to be expected that trends of Pareto fronts obtained in this paper for two different scenarios will have similar shape.

Although Pareto fronts obtained for both scenarios have similar trends, there are crucial differences between two presented scenarios. It can be noticed that Scenario 1 in the region of lower discounted cost achieves higher CO_2 emissions. The main reason for this is utilization of cogeneration units which are preferred due to the higher electricity market prices and existence of a feed-in premium. Although cogeneration units have higher exergy efficiency than heat-only boilers, they emit more CO_2 per MWh of heat produced. This is also the reason why Scenario 1 obtains lower total discounted cost, in the region where cogeneration units are used. However, in the region where exergetic objective function dominates (exergy destruction lower than 24.000 MWh), values of other two objective functions obtain similar values, both for Scenario 1 and Scenario 2. The main reason for this is utilization of similar technologies and capacities, as shown in Section 4.2.2. This means that electricity market prices have low impact on multi-objective optimization results in the region of low exergy destruction and low environmental impact of the district heating system. However some differences are evident in the region of low exergy destruction. For example, it can be noticed that Pareto fronts for exergy destruction equal to 11.000 MWh obtain different values of total discounted cost in Scenario 1 and Scenario 2. For Scenario 1 it is in range of 3.600.000 EUR up to the 4.300.000 EUR, while in Scenario 2 the range is much smaller, 3.400.000–3.550.500 EUR. As explained in Section 4.2.2, in this region, both scenarios have identical supply capacities, i.e. heat pump is dominant technology. Since Scenario 2 has lower electricity market price, total running cost of the system are also lower. However, in this region carbon dioxide emission are identical and are around 2.160 tonnes of CO_2

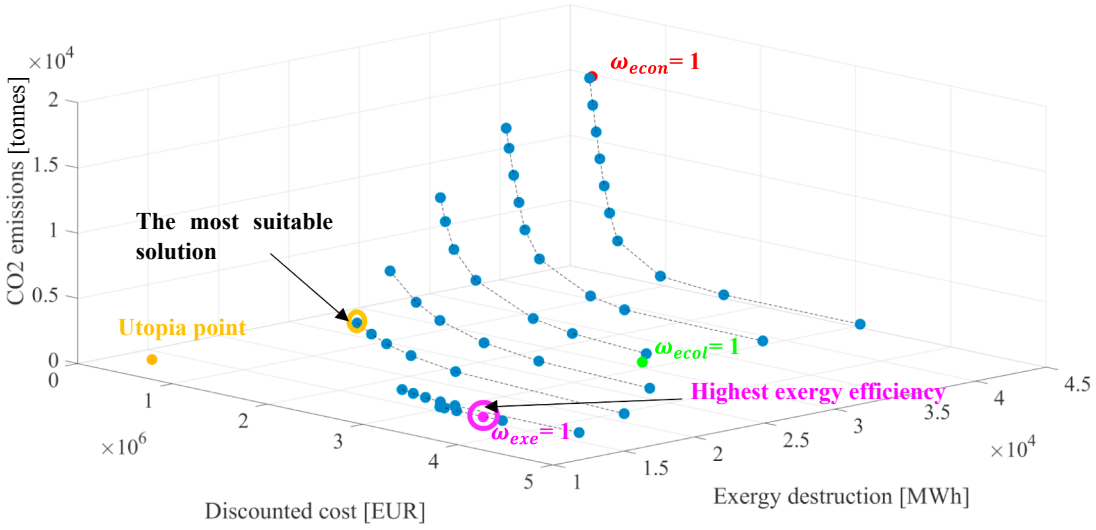

Fig. 8. Solution of multi-objective optimization.

Table 2
Optimal values of objective functions and calculated exergy efficiency.

	$f_{econ\omega_{econ}=1}$	$f_{ecol\omega_{ecol}=1}$	$f_{exe\omega_{exe}=1}$
Total discounted cost [EUR]	646.551	3.197.236	4.130.740
Total exergy destruction [MWh]	42.186	28.521	10.909
Total carbon dioxide emissions [tonnes]	16.108	1.111	2.135
Exergy efficiency [–]	0,45	0,47	0,69

Table 3
Supply capacities for solutions where objective functions reach minimum values.

Supply capacity/thermal storage capacity	$f_{econ\omega_{econ}=1}$	$f_{ecol\omega_{ecol}=1}$	$f_{exe\omega_{exe}=1}$
Natural gas heat-only boiler [MW]	7,4	0	0
Biomass heat-only boiler [MW]	0	17,5	0
Electrical heater [MW]	0	0	0
Heat pump [MW]	0	0	18,7
Natural gas CHP [MW]	5,7	0	0
Biomass CHP [MW]	0	0	20
Solar thermal collectors area [m^2]	0	50.000	50.000
Short-term thermal storage [MWh]	146	8,7	14
Seasonal thermal storage [MWh]	0	3.883	3.878

Table 4
Characteristics of the most suitable solution.

The most suitable solution Supply capacity/thermal storage capacity	
Natural gas heat-only boiler [MW]	11,0
Biomass heat-only boiler [MW]	0
Electrical heater [MW]	0
Heat pump [MW]	5,5
Natural gas CHP [MW]	0
Biomass CHP [MW]	0
Solar thermal collectors area [m^2]	5.521
Short-term thermal storage [MWh]	30,6
Solar thermal storage [MWh]	61,6
Objective functions values	
Total discounted cost [EUR]	1.755.246
Total exergy destruction [MWh]	18.000
Total carbon dioxide emissions [tonnes]	4.112
Exergy efficiency [–]	0,31

When comparing Pareto fronts obtained for Scenario 1 and Scenario 2, it can be concluded that there are three noticeable regions. The first one is region of high exergy destruction (around 30.000 MWh) and low discounted cost. In this region, Scenario 1 obtains higher carbon dioxide emissions but achieves lower exergy destruction. The main reason for this is utilization of cogeneration units due to the existence of feed-in premium incentives and higher electricity market prices. The supply capacities trends for this region are shown in Fig. 16. The second region is so called “transitional region”, where exergy destruction is around 18.000 MWh. Total cost and carbon dioxide emissions obtain similar values in both scenarios. Furthermore, the trend of supply capacities for this region are shown in Fig. 17. It can be noticed that supply capacity trend is similar but not identical. The third region is where both scenarios reach the lowest values of exergy destruction (around 11.000 MWh). In this region, both scenarios have identical supply capacities, which are mostly based on heat pump utilization. Trend of supply capacities for this region is shown in Fig. 18.

4.2.2. Supply capacities comparison

Figs. 16–18 show comparison of supply capacities of Scenario 1 and Scenario 2 for different values of exergy destruction. As explained in Section 4.2.1, there are three regions of interest which will be discussed here in more detail. The first one is region of high exergy destruction (around 30.000 MWh). The second region is so-called transitional region with exergy destruction around 18.000 MWh. The third region is where exergy destruction is almost minimal, i.e. around 11.000 MWh. Each of the mentioned regions is represented in the figures shown below. In order to understand following results, it is important to recall that each Pareto point shown in Fig. 15 contains various set of information such as: optimal supply capacities, optimal thermal storage size, optimal hourly operation of the system and calculated exergy efficiency.

In order to describe visualization of the results, supply capacities in Fig. 16 are explained in more detail. For both scenarios, three results are shown: optimal supply capacities (top diagrams), calculated exergy efficiency (diagrams in the middle) and optimal thermal storage size (diagrams at the bottom). Left side of diagrams shown in Fig. 16, represent solutions where economical objective function is dominant, while right side of the diagrams show solutions where minimization of carbon dioxide emissions is dominant objective function. For example, first supply capacities shown on the left side of the diagram in Fig. 16 represent the most left Pareto solution for exergy destruction value equal to 30.000 MWh. The most right capacities shown in Fig. 16 represents the most right Pareto solution for exergy destruction value

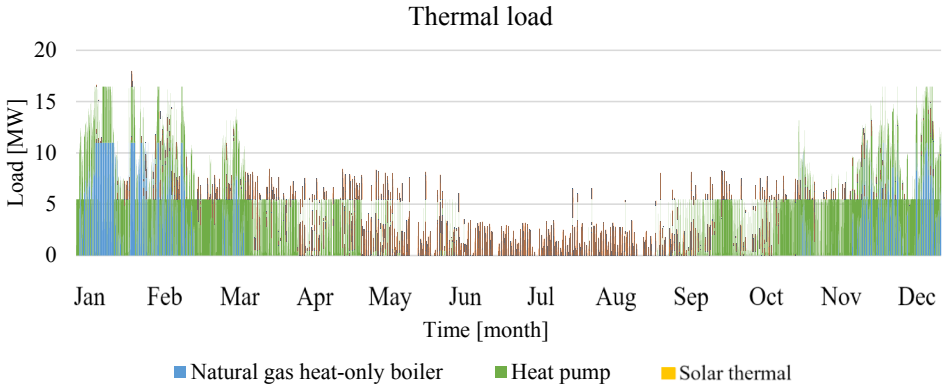

Fig. 9. Supply capacities operation of the most suitable solution for a whole year.

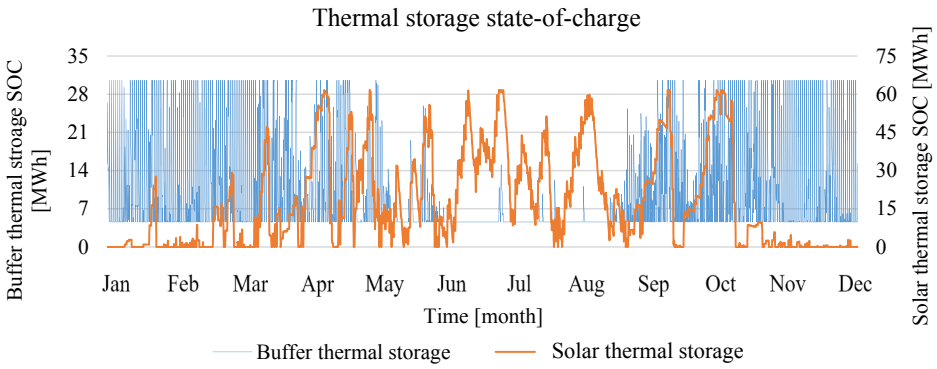

Fig. 10. Thermal storage operation of the most suitable solution for a whole year.

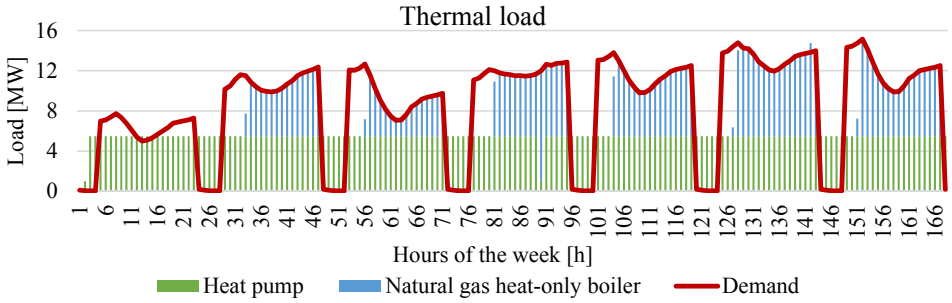

Fig. 11. Supply capacities operation of the most suitable solution for a winter week.

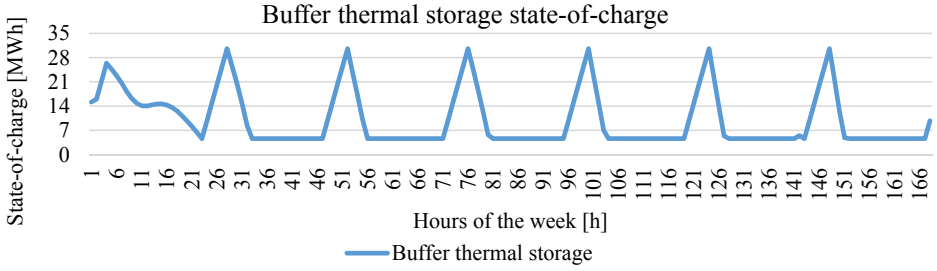

Fig. 12. Thermal storage operation of the most suitable solution for a winter week.

equal to 30.000 MWh. This has also been visualized by connecting mentioned Pareto points with respected information for both scenarios.

As said previously, Fig. 16 shows DH system information for exergy destruction equal to 30.000 MWh. Although Scenario 1 and Scenario 2 achieve the same exergy destruction values, Scenario 1, due to higher electricity market values and feed-in premium also utilizes cogeneration units. On the left side of the diagram, where economical objective function is dominant, natural gas is used. It is substituted with biomass cogeneration once approaching the right side of the diagram, where environmental objective function is dominant. In the region where cogeneration is used, Scenario 1 has higher exergy efficiency. When approaching more environmentally friendly solutions, installed capacities, are becoming similar in both scenarios. In this region, both scenarios prefer to use maximum available capacity of solar thermal

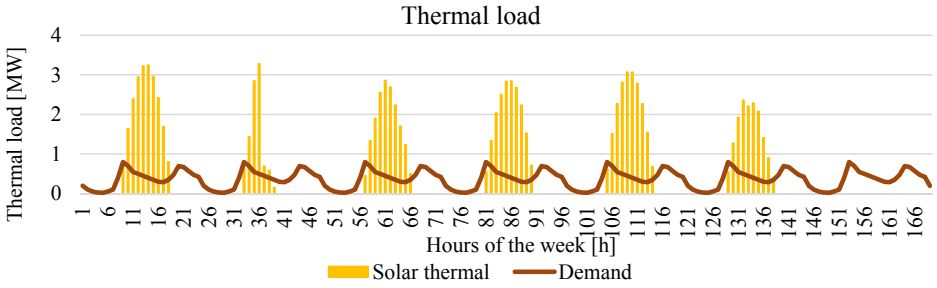

Fig. 13. Supply capacities operation of the most suitable solution for a summer week.

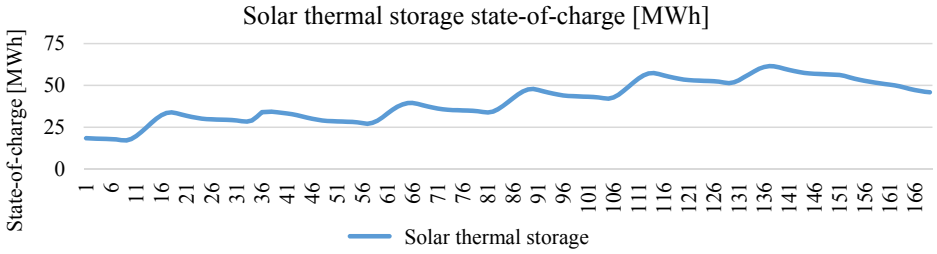

Fig. 14. Thermal storage operation of the most suitable solution for a summer week.

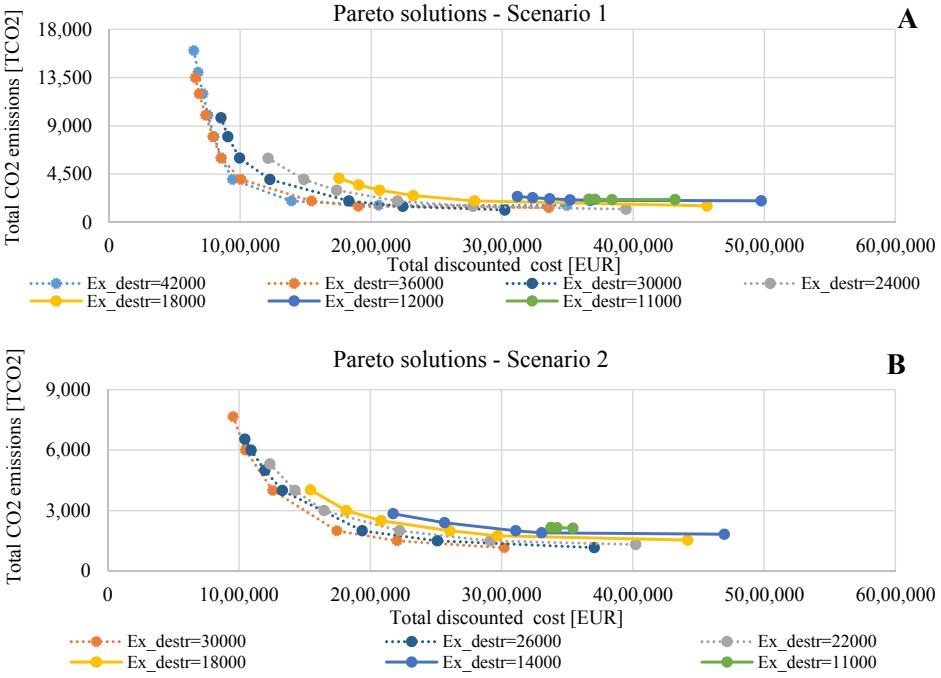

Fig. 15. Comparison of Pareto optimal solutions: a) Scenario 1, b) Scenario 2.

collectors. Buffer thermal storage is bit higher in Scenario 1 if CHP, which has lower ramp-up and ramp-down rates, is used. Exergy efficiency in Scenario 2 is gradually increasing from 0,18 up to 0,45. It can be noticed that increase of exergy efficiency follows installed solar thermal collector area. Furthermore, seasonal thermal storage size follows the solar thermal collector area.

Fig. 17 show comparison of supply capacities for two scenarios but for exergy destruction value equal to 18.000 MWh. As mentioned in the Section 4.2.1 it can be seen that both scenarios have similar optimal supply capacities. At the left side of the diagram heat pump in combination with natural gas and solar thermal collectors is used. When approaching the left side of the diagram, where environmental objective function is dominant, biomass heat-only boiler has replaced natural gas. Furthermore, solar thermal collector area has reached maximum value. It is important to notice that solar thermal collectors are not utilized only in the most environmentally friendly solution, but are gradually increased together with seasonal thermal storage size. The trend of solar thermal collector area differs between two scenarios. In Scenario 1, it increases almost exponentially, while in Scenario 2 it has saturation effect.

As already mentioned in Section 4.2.1, Pareto solutions in the region of low exergy destruction obtain identical optimal supply capacities in both scenarios. This can also be seen in Fig. 18, which shows optimal supply capacities for, relatively low exergy destruction equal to 11.000 MWh. It can be noticed that heat pump is dominant solution, while other technologies have low capacity and operate as the peak technology units. The lowest heat pump capacity is equal to 13 MW, while the highest heat pump capacity is equal to 16,9 MW.

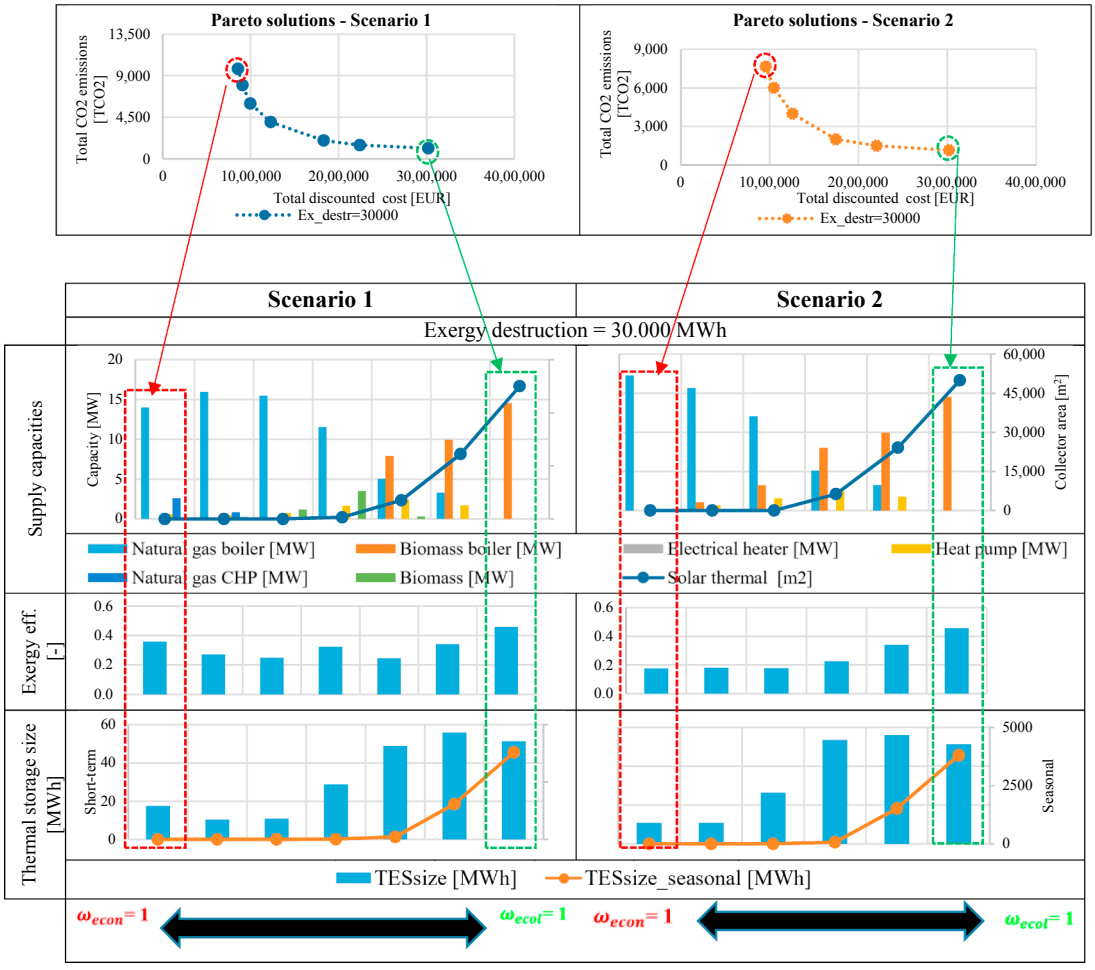

Fig. 16. Comparison of supply capacities for exergy destruction equal to 30.000 MWh.

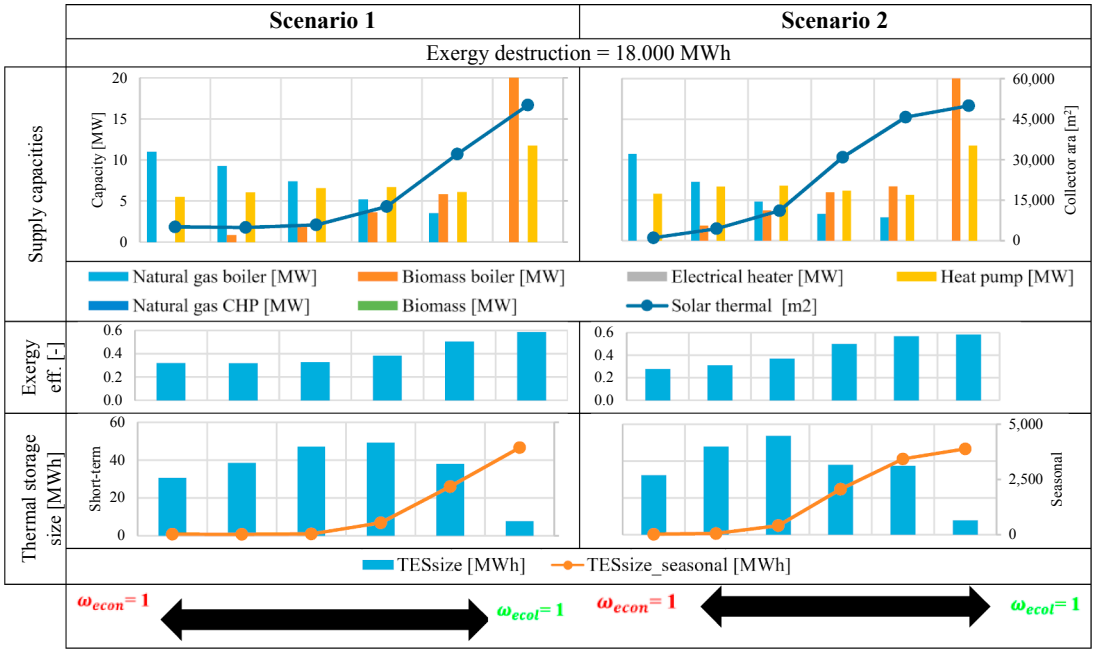

Fig. 17. Comparison of supply capacities for exergy destruction equal to 18.000 MWh.

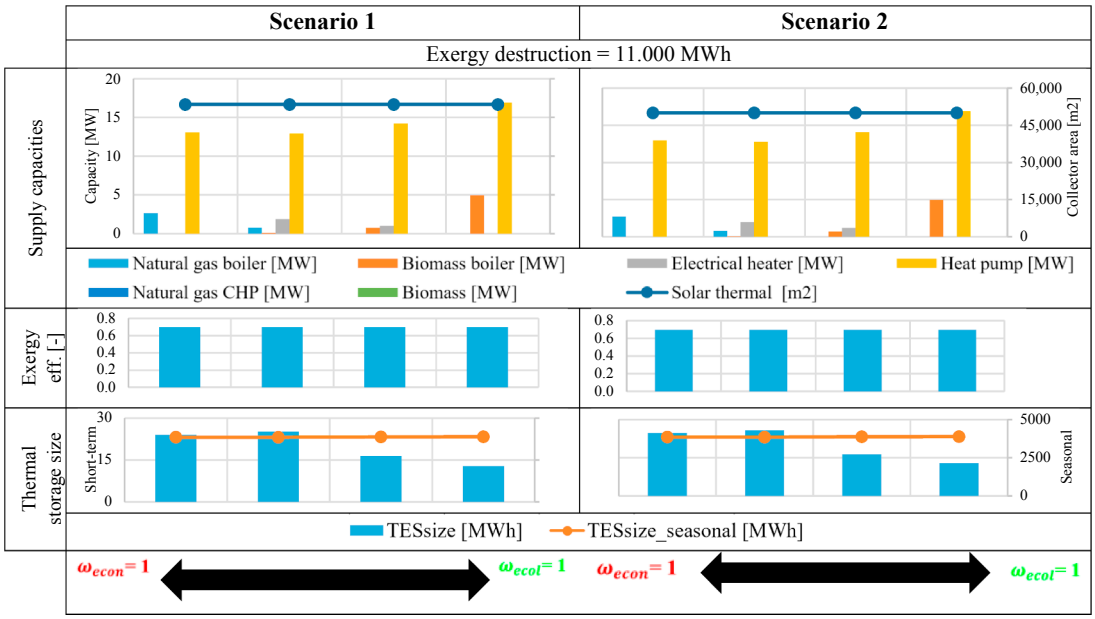

Fig. 18. Comparison of supply capacities for exergy destruction equal to 11.000 MWh.

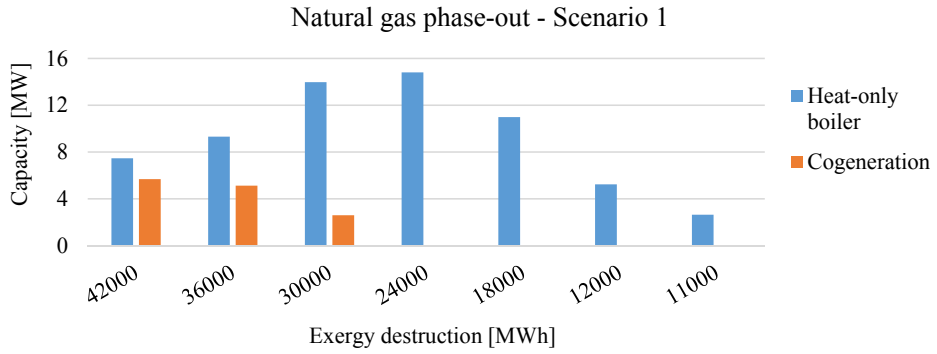

Fig. 19. Natural gas fuelled capacities as a part of the least-cost solution for different exergy destruction values, Scenario 1.

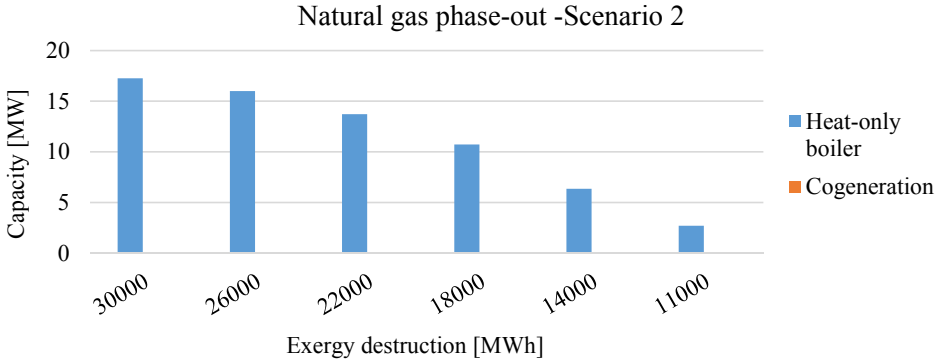

Fig. 20. Natural gas fuelled capacities as a part of the least-cost solution for different exergy destruction values, Scenario 2.

Furthermore, it can be noticed that in this region, solar thermal collectors have maximum installed area, even for the least cost solution. Exergy efficiency in this region is relatively high, around 0,65, due to the high solar thermal production. Finally, it can be noticed that electrical heater has also been included as the optimal solution in this region, operating as the peak unit.

4.3. Natural gas technologies phase-out

Natural gas as a fuel, from the exergetic point of view, shouldn't be used for thermal energy production in heat-only boiler units, due to great exergy destruction. The results acquired in this paper also lead to this conclusion. Figs. 19 and 20 show optimal natural gas fuelled capacities as a part of the least-cost solution for different exergy destruction values of Scenario 1. These capacities belong to the Pareto points in Fig. 8 with the lowest total discounted cost for different exergy destruction values, i.e. these solutions are located at the most-left side of the diagram. It can be seen that the optimal capacity of a natural gas heat-only boiler drops as exergy destruction decreases. This is especially visible in Scenario 2 where, due to the low electricity market

prices, a natural gas cogeneration unit hasn't been chosen as a part of any least-cost solutions. The phase-out of the natural gas heat-only boiler in Scenario 1 isn't that obvious, since the maximum optimal capacity isn't reached for the maximum exergy destruction value. The main reason for this is a gradual replacement of natural gas cogeneration. In the systems with low exergy destruction, natural gas operates with a relatively low load factor and acts as a peak boiler solution. For example, for an exergy destruction value equal to 18.000 MWh, the load factor of a natural gas boiler is 10%. For the lowest possible exergy destruction, natural gas isn't used as fuel. As can be seen in Figs. 16–18, the most-environmentally friendly solutions don't use natural gas a fuel. For these, thermal load is covered by biomass boiler, heat pumps and solar thermal collectors.

5. Conclusion

In this paper, a novel method for district heating multi-objective optimization has been proposed. The objective functions are defined as the minimization of total cost, the minimization of the system's carbon dioxide emissions and the minimization of exergy destruction. Two scenarios have been proposed: the first one with reference electricity market prices that also includes the feed-in premium for cogeneration units and the second one, with lower electricity market prices and without a feed-in premium. The obtained results shape the Pareto surface, which displays a compromise between the three objective functions. The most suitable solution for Scenario 1 was defined as the one closest to the Utopia point. It consist of 11 MW natural gas heat only boiler, 5,5 MW heat pump and a 5.521 m^2 of solar thermal collectors area in combination with thermal storage. The reduction of electricity market prices influences the Pareto optimal solutions, especially in the region of a low discounted cost: in Scenario 1 cogeneration units are used, while in Scenario 2 they aren't profitable due to the low electricity market prices. However, in the region where an exergetic objective function is dominant, the optimal supply capacities look identical. This research also shows the phase-out of natural gas based technologies, when approaching the solution with the lowest exergy destruction. The multi-objective optimization of district heating system developed in this paper could be used in future research in order to analyse and define an exergy tax model that could additionally penalize thermal energy production from high temperature sources.

Acknowledgement

Financial support from the PROSEU (PROSumers for the Energy Union: mainstreaming active participation of citizens in the energy transition) Horizon2020 project, grant agreement 764056, is gratefully acknowledged.

References

[1] Lund H, et al. 4th generation district heating (4GDH). Integrating smart thermal grids into future sustainable energy systems. Energy 2014;68:1–11.
[2] Lund H, Duic N, Ostergaard PA, Mathiesen BV. Future district heating systems and technologies: on the role of smart energy systems and 4th generation district. Energy 2018.
[3] Brange L, Englund J, Lauenburg P. Prosumers in district heating networks - A Swedish case study. Appl Energy 2016;164:492–500.
[4] Ahvenniemi H, Klobut K. Future services for district heating solutions in residential districts. J Sustain Dev Energy, Water Environ Syst 2014;2(2):127–38.
[5] Sayegh MA, et al. Trends of European research and development in district heating technologies. Renew Sustain Energy Rev 2016:1–10.
[6] Lake A, Rezaie B, Beyerlein S. Review of district heating and cooling systems for a sustainable future. Renew Sustain Energy Rev 2017;67:417–25.
[7] Frederiksen S, Werner S. District Heating and Cooling 2013.
[8] Gong M, Werner S. Exergy analysis of network temperature levels in Swedish and Danish district heating systems. Renew Energy 2015;84:106–13.
[9] Li H, Svendsen S. Energy and exergy analysis of low temperature district heating network. Energy 2012;45(1):237–46.
[10] Gadd H, Werner S. Achieving low return temperatures from district heating substations. Appl Energy 2014;136:59–67.
[11] Kilkiş Ş. A rational exergy management model to curb CO 2 emissions in the exergy-aware built environments of the future. Stockholm, Sweden: KTH Royal Institute of Technology; 2011.
[12] Kilkiş Ş. Exergy transition planning for net-zero districts. Energy 2015;92(Part 3):515–31.
[13] Yang X, Li H, Svendsen S. Energy, economy and exergy evaluations of the solutions for supplying domestic hot water from low-temperature district heating in Denmark. Energy Convers Manag 2016;122:142–52.
[14] Baldvinsson I, Nakata T. A feasibility and performance assessment of a low temperature district heating system e A North Japanese case study. Energy 2016;95:155–74.
[15] Baldvinsson I, Nakata T. A comparative exergy and exergoeconomic analysis of a residential heat supply system paradigm of Japan and local source based district heating system using SPECO (specific exergy cost) method. Energy 2014;74(C):537–54.
[16] Yamankaradeniz N. Thermodynamic performance assessments of a district heating system with geothermal by using advanced exergy analysis. Renew Energy 2016;85:965–72.
[17] Keçebaş A, Yabanova I, Yumurtaci M. Artificial neural network modeling of geothermal district heating system thought exergy analysis. Energy Convers Manag 2012;64:206–12.
[18] Kabalina N, Costa M, Yang W, Martin A, Santarelli M. Exergy analysis of a poly-generation-enabled district heating and cooling system based on gasification of refuse derived fuel. J Clean Prod 2017;141:760–73.
[19] Yang Jiangjiang Wang Ying. Energy, exergy and environmental analysis of a hybrid combined cooling heating and power system utilizing biomass and solar energy. Energy Convers Manag 2016;124:566–77.
[20] Kalogirou SA, Karellas S, Badescu V, Braimakis K. Exergy analysis on solar thermal systems: A better understanding of their sustainability. Renew Energy 2015:1–6.
[21] Lake A, Rezaie B. Energy and exergy efficiencies assessment for a stratified cold thermal energy storage, 2018;220:605–615, April 2017.
[22] Rijs A, Mróz T. Exergy evaluation of a heat supply system with vapor compression heat pumps. Energies 2019.
[23] Tereshchenko T, Nord N. Energy planning of district heating for future building stock based on renewable energies and increasing supply flexibility. Energy 2016;112:1227–44.
[24] Mikulandrić R, et al. Performance analysis of a hybrid district heating system: A case study of a small town in Croatia. J Sustain Dev Energy, Water Environ Syst 2015;3(3):282–302.
[25] Skorek J, Bargiel P, Tan M. Energy and economic optimization of the repowering of coal-fired municipal district heating source by a gas turbine. Energy Convers Manag 2017.
[26] Anatone M, Panone V. A model for the optimal management of a CCHP plant. Energy Procedia 2015;81:399–411.
[27] Hu M, Cho H. A probability constrained multi-objective optimization model for CCHP system operation decision support. Appl Energy 2014;116:230–42.
[28] Falke T, Krengel S, Meinerzhagen A-K, Schnettler A. Multi-objective optimization and simulation model for the design of distributed energy systems. Appl Energy 2016.
[29] Bracco S, Dentici G, Siri S. Economic and environmental optimization model for the design and the operation of a combined heat and power distributed generation system in an urban area. Energy 2013;55:1014–24.
[30] Zheng X, et al. A MINLP multi-objective optimization model for operational planning of a case study CCHP system in urban China. Appl Energy 2017.
[31] Østergaard PA, Andersen AN. Booster heat pumps and central heat pumps in district heating. Appl Energy 2016.
[32] Tezer T, Yaman R, Yaman G. Evaluation of approaches used for optimization of stand-alone hybrid renewable energy systems. Renew Sustain Energy Rev 2017;73:840–53.
[33] Jakob W, Blume C. Pareto optimization or cascaded weighted sum: A comparison of concepts. Algorithms 2014;7:166–85.
[34] Franco A, Bellina F. Methods for optimized design and management of CHP systems for district heating networks (DHN). Energy Convers Manag 2018;172(January):21–31.
[35] Franco A, Versace M. Optimum sizing and operational strategy of CHP plant for district heating based on the use of composite indicators. Energy 2017;124:258–71.
[36] Franco A, Versace M. Multi-objective optimization for the maximization of the operating share of cogeneration system in District Heating Network. Energy Convers Manag 2017;139:33–44.
[37] Wang YZ, et al. Multi-objective optimization and grey relational analysis on configurations of organic Rankine cycle. Appl Therm Eng 2016.
[38] Boyaghchi FA, Chavoshi M. Multi-criteria optimization of a micro solar-geothermal CCHP system applying water/CuO nanofluid based on exergy, exergoeconomic and exergoenvironmental concepts. Appl Therm Eng 2017;112:660–75.
[39] Lu H, et al. Transition path towards hybrid systems in China: Obtaining net-zero exergy district using a multi-objective optimization method. Energy Build 2014;85:524–35.
[40] Di Somma M, et al. Operation optimization of a distributed energy system considering energy costs and exergy efficiency. Energy Convers Manag 2015;103:739–51.
[41] Di Somma M, et al. Multi-objective design optimization of distributed energy systems through cost and exergy assessments. Appl Energy 2017;204:1299–316.
[42] DorotiĆ H, Pukšec T, Duić N. Multi-objective optimization of district heating and cooling systems for a one-year time horizon. Energy 2019;169:319–28.
[43] Tereshchenko T, Nord N. Implementation of CCPP for energy supply of future building stock. Appl Energy 2015;155:753–65.

[44] Programme of exploiting heating and cooling efficiency potential for 2016-2030.
[45] Pavičević M, Novosel T, Pukšec T, Duić N. Hourly optimization and sizing of district heating systems considering building refurbishment - Case study for the city of Zagreb. Energy 2016.
[46] Nakicenovic N, Gilli PV, Kurz R. Regional and global exergy and energy efficiencies. Energy 1996;21(3):223–37.
[47] Ziebik A, Gładysz P. Optimal coefficient of the share of cogeneration in district heating systems. Energy 2012;45(1):220–7.
[48] JRC. "PVGIS." [Online]. Available: http://re.jrc.ec.europa.eu/pvgis.html.
[49] Renewable ninja. [Online]. Available: https://www.renewables.ninja/.
[50] SPF Institut für Solartechnik. [Online]. Available: http://www.spf.ch/index.php?id=111&L=6.
[51] Odyssee-MURE. [Online]. Available: http://www.indicators.odyssee-mure.eu/energy-efficiency-database.html.
[52] Meteonorm. [Online]. Available: http://www.meteonorm.com/.
[53] Sørensen PA, Nielsen JE, Battisti R, Schmidt T, Trier D. Solar district heating guidelines: Collection of fact sheets, no. August; 2012. p. 152.
[54] Croatian energy market operator (HROTE).
[55] CROPEX." [Online]. Available: https://www.cropex.hr/hr/.
[56] Heating D, Generation EC. Technology data for energy plants; 2012.
[57] Julia programming language. [Online]. Available: https://julialang.org.
[58] Clp optimization solver. [Online]. Available: https://projects.coin-or.org/Cbc.
[59] JuMP. [Online]. Available: http://www.juliaopt.org/JuMP.jl/0.18/.
[60] Xu D, Qu M, Hang Y, Zhao F. Multi-objective optimal design of a solar absorption cooling and heating system under life-cycle uncertainties. Sustain Energy Technol Assessments 2015;11:92–105.

PAPER 3

Analysis of displacing natural gas boiler units in district heating systems by using multi-objective optimization and different taxing approaches

Hrvoje Dorotić**, Tomislav Pukšec, Neven Duić

University of Zagreb, Faculty of Mechanical Engineering and Naval Architecture, Department of Energy, Power Engineering and Environmental Engineering, Ivana Lučića 5, 10002, Zagreb, Croatia

Email: hrvoje.dorotic@fsb.hr

Abstract:

District heating systems are proven to be effective way of increasing energy efficiency, reducing environmental impact and achieving higher exergy efficiency. In research papers, district heating multi-objective optimization usually takes into account minimization of the total discounted cost and environmental impact, while exergetic objective function is rarely introduced. Most of the times, economic and ecological objective functions are studied as a single objective optimization problem through internalization of the cost related to carbon dioxide emissions tax. This paper presents novel approach since additional tax, related to exergy destruction, has been introduced. The influence of these two taxing systems on a single and multi-objective optimization results of district heating system has been carried out. Two approaches have been proposed. In the first one, multi-objective optimization has been used where objective functions were defined as economic and ecological or exergetic. In the second approach, single-objective optimization has been used where cost function also includes both carbon and exergy destruction tax. It has been shown that inclusion of carbon tax causes convergence of Pareto fronts after specific exergy destruction has been reached. On the other hand, if all technologies are available, increase of exergy tax doesn't reduce carbon dioxide emissions. The most important outcome of this paper is analysis of the impact of exergy tax on natural gas consumption in heat-only boilers. Acquired results show that exergy, together with carbon tax, can effectively reduce natural gas consumption in heat-only boilers. If there are no back-pressure CHP technologies available, these taxing systems can completely push out its consumption. Finally, the analyses with carbon emissions in CHP units has also been carried out. Acquired results have shown that with increase of carbon tax, exergy efficiency of the system could be increased.

Keywords:

District heating, Exergy, Multi-objective optimization, Linear programming, Thermal storage, Internal cost, External cost

1. Introduction

District heating (DH) systems are proven to be more energy efficient and environmentally friendly than individual heating solutions [1]. Furthermore, they will have important role in future energy systems as described in [2], [3]. However, in order to reach their full potential, additional measures should be implemented in order to overcome social and legislation issues. One of the most important advantages is their capability of using low temperature renewable energy sources through heat pumps [4], waste heat [5] and simultaneous power and heat generation [6]. Due to these, DH systems potentially have higher exergy efficiency than individual heating solutions, which are often based on natural gas heat-only boilers. Lowering the thermal network supply temperature can significantly reduce exergy destruction of the system as shown by Li and Svendsen [7]. In [8], Rhein et al are even analysing topology for 5th generation of district heating systems for ambient range of 15-25°C. However, natural gas heat-only boilers are still frequently used even in district heating systems, especially when cogeneration units aren't economically feasible or are too big [9]. Terhan et al. provided detailed analysis of the natural gas fired boiler used in district heating system [10]. They have shown that exergy efficiency is more than 50% lower than energy efficiency. The main reason for this loss is exergy destruction in the combustion chamber due to the high adiabatic combustion temperatures. Natural gas is often seen as the fuel which could be utilized in the energy transition in order to phase-out coal consumption in cogeneration plants [11].

Exergy efficiency is rarely used in decision making process related to energy systems, but is often analysed in various technologies and systems. Exergy of the system could be studied through various related parameters, such as exergy efficiency, exergy destruction, exergy input of the system, etc. [12]. Bonati et al. have developed novel method for using exergy criterion for energy planning of 100% renewable energy systems [13]. They have used EnergyPLAN tool, which is based on energy system operation optimization, in combination with scenario analysis approach to obtain the final result. Siir Kilkis has developed a method based on rational exergy management model [14]. In the other paper, the method for near-zero exergy district has been developed [15]. In paper [16], authors have demonstrated how exergy efficiency based control strategy can be economically feasible and suitable for geothermal district heating systems. Obtained results show a short payback period of 3.8 years. Sciubba developed exergy-based ecological indicators and shown how exergy analysis of complex systems can be formulated in such a way to related irreversibility with unsustainability [17]. Birol and Şiir Kilkiş developed new exergy metrics for energy, environment and economy nexus used for acquiring optimum design model of nearly-zero exergy system [18]. The model has been developed for airport energy systems, while the case study was Schiphol.

Optimization of district heating systems has been carried in numerous research papers. The goal is often to minimize system's total cost [19],[20] or ecological impact in terms of carbon dioxide (CO_2) emissions [21]. In some cases, while minimizing overall costs, even pressure losses could be taken into account by studying different operational strategies [22]. Single objective optimization is the most often approach, usually handled by using linear or mixed integer linear programming [23] and genetic algorithms [24]. Opposite to single objective optimization, where final solution is single value, results of multi-objective optimization is a whole set of values lying on the so called Pareto front. In order to handle this problem, various techniques could be used, such as weighted sum method [23] or epsilon constraint method [25]. Exergy is also often included in the optimization problem as one of the objective functions, but is rarely used in the single objective optimization problems. Franco et al. [26], optimized exergy efficiency of the cogeneration plan which operates as the part of DH system. In paper [27], exergy efficiency of the organic Rankine cycle has been part of the optimization problem. M. Di Somma et al. in papers [28] and [29] have taken into account exergy efficiency during optimization of district energy system which takes into account electricity and heat production. It is important to mention that they didn't take into account carbon dioxide emissions, neither through carbon tax system or objective function.

Carbon taxing has already been successfully implemented in the legislation of the EU, under the name of Emissions Trading System (ETS) set up in 2005 [30]. It is based on the "cap and trade" principle,

where the “cap” is defined as the total amount of greenhouse gasses which could emitted by installations covered by the system. However, the cap is reduced over time, which causes emissions reduction. Verbruggen et al. provided thorough explanation of the EU ETS system [31]. In the 2018, the ETS prices have started growing rapidly, from 8.5 EU/tonne, reaching more than 25 EUR/tonne in 2019 [32]. It is expected to go as high as 60 EUR/tonne by 2030. Soliman and Nasir provided analysis of EU emission trading system and made correlation between different energy prices [33] while Dutta has carried out modelling and forecasting of the volatility of the carbon emission market [34].

Exergy related taxing, or exergy cost approach, and exergoeconomic analysis aren’t new concepts. It has already been proposed in various papers. Chaiyat et al. have developed novel levelized energy and exergy costing per life cycle assessment [35]. The method was applied to the system of combined heating and power generation in Thailand. Usón et al. carried out exergy assessment of a renewable based and hybrid trigeneration scheme for domestic water and energy supply [36]. They have used TRNSYS software combination together with exergy cost method in order to provide detailed analysis of exergy efficiency. Franco and Versace [37] proposed composite indicators’ analysis which also included exergy loss. In [38] specific exergy cost (SPECO) method has been used in order to provide exergoeconomic analysis of a residential district heating system in Japan. Arat and Arslan have carried out exergoeceonomic analysis of the district heating system which utilizes geothermal heat pump [39]. They have simulated more than 4,500 design in order to find the optimal one. On the other hand, Meesenburg et al. have performed dynamic exergoeconomic analysis of the heat pump which could be used for ancillary services in the integrated energy systems [40]. Yang et al have evaluated domestic hot water supply through low temperature district heating systems by using exergetic and exonomic analysis [41]. Finally, exergoeconomic optimization could also be used in district cooling networks as shown in paper [42]. In paper [43], exergy lost is translated as the additional cost and added to the economic objective function. Although optimization model has been used, it doesn’t take into account carbon dioxide emissions neither as the internalized cost or objective function. Exergy costing was also used in [44] in order to analyse energy savings in systems which utilize combined heating and cooling.

According to the author’s knowledge and carried out literature review, no research papers have proposed using exergy tax in combination with multi-objective optimization in order to analyse shift of a Pareto front and phase-out of natural gas in heat-only boiler units. Furthermore, exergy taxing system used in this paper is novel since it only penalizes destroyed exergy which wasn’t potentially utilized in a cogeneration unit.

The method and the model developed in this paper is based on the two previous papers published by the authors. In paper [45] multi-objective optimization model has been developed which takes into account total cost and carbon dioxide emissions. The model was upgraded in [46] and exergy destruction as the objective function has been added. The model is capable of optimizing supply capacities and thermal storage size, including hourly operation, of the district heating system. Since seasonality of the thermal demand is crucial issue, the time horizon of the optimization model is a whole year.

In this paper, novel exergy taxing system was introduced. It is based on penalizing exergy destruction in heat-only boilers which could be potentially used in cogeneration units. Together with existing, but slightly modified, carbon taxing system, analysis of impact on multi and single objective optimization of DH system has been carried out. Finally, this paper provides scientific contributions by answering following questions:

- How do exergy and carbon taxing systems shift solutions of the multi-objective optimization of a district heating system?
- How do these taxing systems influence exergy efficiency and carbon dioxide emissions of the least-cost solution of the district heating supply system?
- What is the impact of mentioned taxing systems on reduction of natural gas consumption in heat-only boiler of an optimal DH supply system?

The paper is divided in several sections. In Section 2 the method is presented. District heating model, together with multi-objective optimization approach, based on previous papers, and exergy destruction tax has been shown in detail. Section 3 displays case study which has been used as the numerical test for this paper. Input data, including hourly distributions have been briefly discussed. Section 4 shows and discuss obtained results in detail. Finally, Section 5 concludes the paper and outlines the main outcomes and findings of this research.

2. Method

The method described in this section is based on the previously published papers [45] and [46]. In the paper [45], district heating model has been established and multi-objective optimization problem has been explained in detail. Two objective functions have been defined: minimization of system's total discounted cost and minimization of system's total carbon dioxide emissions. In the paper [46], minimization of exergy destruction was introduced as the third objective function, which enables creation of 3D Pareto front. The novelty of this paper is introduction of the carbon and exergy destruction tax and analysis of their influence on the results of multi-objective and single-objective optimization problem.

2.1. District heating model

District heating system was modelled as a linear programming (LP) problem and contains various supply technologies: heat-only boiler, cogeneration, electrical heater, heat pump, solar thermal collectors and thermal storages, which include both buffer and seasonal. Two fuels could be used: fossil fuel, i.e. natural gas, and biomass, which is representative of a carbon neutral fuel. Power-to-heat technologies are using electrical energy bought at the electricity market. Cogeneration units are selling electricity on the same market but are also receiving incentives as a feed-in premium tariff. The model is capable of optimizing supply capacities, including thermal storage size, and operation of supply units on hourly level for a whole year. In order to provide more realistic operation, ramp-up and ramp-down limitations have been added. Optimization time step is equal to one hour, while the time horizon is equal to a whole year, i.e. 8760 hours. It should be mentioned how the choice of the time-step has influence on the results due to the several reasons. First of all, heating demand has recognizable hourly profile with two noticeable peak demand during the day. Increase of the time step would cause reduction of the heat demand amplitude and neglect necessity for fast ramping and usage of thermal storage. Secondly, power-to-heat and cogeneration technologies are participating on the power-market which is also on the hourly level. Nevertheless, it should be mentioned that time-step increase from one-hour to two-hour, wouldn't have pronounced effect as e.g. increase to 24-hour time step which would totally mitigate hourly variation of the heating demand on the daily level, thus influencing the optimized results. However, such analysis unfortunately hasn't been carried out in this paper.

Prior to the optimization, the model calculates efficiency of the heat pump and solar thermal collectors, including district heating network supply temperature, which are also hourly distributions. The model was written in the Julia programming language [47] by using JuMP package for mathematical optimization [48]. The model's optimization variables and constraints are explained below.

Equation (1) presents the most important constraint of the model – thermal energy demand DEM_t has to be covered in every time step t by numerous supply sources $Q_{i,t}$ or thermal storage discharge $TES_{i,t}$. Where i denotes a technology type which is used. $Q_{i,t}$ and $TES_{i,t}$ present optimal operation of the system, i.e. optimization variables.

$$DEM_t = Q_{HOB,gas,t} + Q_{HOB,biomass,t} + Q_{EH,t} + Q_{HP,t} + Q_{CHP,gas,t} + Q_{CHP,biomass,t} - TES_{1,in-out,t} - TES_{2,in-out,t} \quad (1)$$

The supply technology can operate inside defined limits, as shown in equation (2), where P_i is supply capacity of technology i. In this case it is also maximum possible power output. It is important to mention that supply capacity is also optimization variable.

$$0 \leq Q_{i,t} \leq P_i \quad (2)$$

In order to describe operation of the system in more detailed manner, ramping limits are introduced, as shown in equation (3), where $r_{up-down,i}$ represents ramping limit of technology i.

$$-r_{up-down,i} \cdot P_i \leq Q_{i,t} - Q_{i,t-1} \leq r_{up-down,i} \cdot P_i \quad (3)$$

Operation of thermal storage is described with equations (4) and (5), where SOC_t represents state-of-charge of thermal storage in a time step t and TES_{size} is thermal storage size. Together with thermal storage operation $TES_{in-out,t}$, TES_{size} is optimization variable which defines optimal thermal storage size (in MWh). In order to assure that state-of-charge is the same at the end and at the beginning of the time horizon, equation (4) is used, where $SOC_{start-end}$ represents the predefined state-of charge at the end and at the beginning of the time horizon. Equation (5) represents energy balance of the thermal storage, where TES_{loss} represents thermal losses of the thermal storage.

$$SOC_{t=1} = SOC_{t=8760} = SOC_{start-end} \cdot TES_{size} \tag{4}$$

$$SOC_t = SOC_{t-1} + TES_{in-out,t} - SOC_t \cdot TES_{loss} \tag{5}$$

Operation of solar thermal collectors, $Q_{ST,t}$ is described with equation (6), where A_{ST} is solar thermal collectors installed area and $P_{solar,specific,t}$ is specific solar thermal production calculated for which hour, explained below. It is important to notice that solar thermal supply operation is constrained, while A_{ST} is only optimization variable associated with solar thermal collectors.

$$Q_{ST,t} = A_{ST} \cdot P_{solar,specific,t} \tag{6}$$

Specific solar thermal production is described with equation (7), where $\eta_{c,t}$ is solar thermal collector thermal efficiency in a time step t, and G_t is global solar irradiation in a time step t. The last is acquired for optimal slope an azimuth angle by using publicly available databases [49].

$$P_{solar,specific,t} = \eta_{c,t} \cdot G_t \tag{7}$$

Solar thermal collector efficiency is calculated by using equation (8) [50], where η_0, a_1, a_2 and T_m, specified for each solar thermal collector by the manufacturer [51] and $T_{ref,t}$ is hourly outside air temperature for the given location obtained by using available databases [49], [52], [53].

$$\eta_{c,t} = \eta_0 - a_1 \frac{\left(T_m - T_{ref,t}\right)}{G_t} - a_2 \frac{\left(T_m - T_{ref,t}\right)^2}{G_t} \tag{8}$$

Heat pump is supply technology which has variable efficiency $\eta_{HP,t}$. It could be calculated by using equation (9), where $f_{Lorentz}$ is factor obtained from the literature [54] and $T_{DH,t}$ is hourly supply temperature of the district heating network obtained by using data from the literature [1].

$$\eta_{HP,t} = f_{Lorentz} \cdot \left(\frac{T_{DH,t}}{T_{DH,t} - T_{ref,t}}\right) \tag{9}$$

2.2. Objective functions

Multi-objective optimization model used in this paper has two objective functions: minimization of total cost and minimization of total carbon dioxide emissions or minimization of exergy destruction. Optimization variables are supply capacities and thermal storage size, including hourly operation of supply units and storage charge, i.e. discharge. Since all objective functions, including constraints, are linear and optimization variables are continuous, the problem is described with linear programming. In this paper, two approaches have been used. In the first approach multi-objective optimization has been used, while in the second approach single-objective, i.e. cost, optimization is proposed.

Equations (10) and (11) describe the first approach. Equation (10) presents multi-objective optimization problem in which economical (f_{econ}) and ecological (f_{ecol}) objective functions have to be minimized. Equation (11) also presents multi-objective optimization problem, but instead of minimizing environmental objective function, exergetic objective function is introduced. Equation (12) presents the second approach, where single-objective has been used. Since only economical objective function has to be minimized, this also represent cost optimization problem. All objective functions are explained in more detailed below.

$$\min(f_{econ}, f_{ecol}) \tag{10}$$

$$\min(f_{econ}, f_{exe}) \quad (11)$$

$$\min(f_{econ}) \quad (12)$$

Equation (13) presents economical objective function. It represents total cost of the district heating system. $C_{investment,i}$ is discounted investment cost of technology i, $C_{fuel,i,t}$ are fuel costs of technology i in a time step t, $C_{O\&M,i,t}$ are operation and maintenance cost of technology i in a time step t and $Income_{i,t}$ presents income due to the electricity sold from CHP units. The last two terms, Ex_{tax} and Eco_{tax} present exergetic and carbon tax, respectively. The exergetic tax Ex_{tax} is taken into account during multi-objective optimization problem of minimizing economical and environmental objective function. On the other hand, carbon tax Eco_{tax} is taken into account during multi-objective optimization of minimizing environmental and exergetic objective functions. Calculation of these taxes is explained in more detail in the Section 2.3.

$$f_{econ} = \sum_{i} C_{investment,i} + \sum_{t=1}^{t=8760} \sum_{i} \left(C_{fuel,i,t} + C_{O\&M,i,t} - Income_{i,t}\right) + Ex_{tax} + Eco_{tax} \quad (13)$$

Ecological objective function could be calculated by using equation (14). It represents sum of the total carbon dioxide emissions of the district heating system, where $e_{CO_2,i}$ is specific carbon emission factor of technology i, while η_i is efficiency of technology i.

$$f_{ecol} = \sum_{t=1}^{t=8760} \sum_{i} (e_{CO_2,i} \cdot Q_{i,t} / \eta_i) \quad (14)$$

Finally, exergetic objective function is defined as total exergy destruction of the district heating system. It could be calculated by using equation (15). Exergy destruction is difference between exergy input $Ex_{in,i,t}$ and exergy output $Ex_{out,i,t}$.

$$f_{exe} = \sum_{t=1}^{t=8760} \sum_{i} (Ex_{in,i,t} - Ex_{out,i,t}) \quad (15)$$

Exergy input is calculated by using exergy factor of the fuel, $e_{Exe,i}$, as shown in equation (16). Exergy output could be calculated by using Carnot factor, which is the term in the brackets shown in the equation (17).

$$Ex_{in,i,t} = \frac{Q_{i,t}}{\eta_i} \cdot e_{Exe,i} \quad (16)$$

$$Ex_{out,i,t} = Q_{i,t} \cdot \left(1 - \frac{T_{ref_t}}{T_{DHN_t}}\right) \quad (17)$$

Although, exergy efficiency isn't objective function, it could be calculated by using equation (18). It represents the ratio of exergy output and exergy input of the system

$$\eta_{exe} = \frac{\sum_{t=1}^{t=8760} \sum_i Ex_{out,i,t}}{\sum_{t=1}^{t=8760} \sum_i Ex_{in,i,t}} \quad (18)$$

2.3. Exergy destruction and carbon dioxide emission tax

As already mentioned, two approaches have been used in this paper. In the first one, exergy destruction or carbon dioxide emissions are treated as objective functions, together with the economical objective function. In the second approach, exergy destruction and carbon dioxide emissions are translated into taxes and added to the total cost, i.e. their costs have been internalized.

Carbon dioxide emissions tax system already exists and is part of the European Union Emission Trade System (EU ETS) [31], thus doesn't present novelty itself. The only difference in this paper is that units lower than 20 MW of thermal power are also part of the taxing system. Furthermore, it is important to remember that power-to-heat technologies are not part of the carbon taxing system. Carbon tax Eco_{tax} could be calculated by using equation (19), where C_{carbon} is carbon tax value expressed in currency unit per tonne of emitted CO_2.

$$Eco_{tax} = \sum_{t=1}^{t=8760} \sum_{i} (e_{CO_2,i} \cdot Q_{i,t} / \eta_i) \cdot C_{carbon} \quad (19)$$

Proposed exergy destruction tax could be calculated by using the equation (20).

$$Ex_{tax} = \sum_{i} \sum_{t=1}^{t=8760} Ex_{in,t,i} \cdot \left(\overline{\varepsilon_{DR,HOB,i}} - \overline{\varepsilon_{DR,i,CHP}}\right) \cdot C_{exergy} \quad (20)$$

Where Ex_{tax} is total exergy destruction tax of the system, expressed in a currency, $Ex_{in,t,i}$ is exergy input of technology which uses fuel i in a time step t, $\varepsilon_{DR,HOB,i}$ is a reference exergy destruction ratio for technology which uses fuel i in a time step t, while $\overline{\varepsilon_{DR,i,CHP}}$ is a reference exergy destruction ratio for fuel i which would be used in cogeneration unit, and finally C_{exergy} is specific exergy destruction cost expressed in unit of currency per unit of exergy destroyed. Exergy destruction ratio is defined as the ratio of exergy destruction and exergy input. It is important to notice that only natural gas and biomass heat-only boilers are included in the exergy taxing system, while power-to-heat technologies are not part of the exergy taxing system. Furthermore, it should be noticed only one part of the exergy destruction is being taxed, i.e. the difference between exergy destruction in a heat-only boiler and a cogeneration unit. In other words, if the model chooses to use a CHP technology instead of a heat-only boiler, the tax could be avoided. $\overline{\varepsilon_{DR,HOB,i}}$ and $\overline{\varepsilon_{DR,i,CHP}}$ are calculated prior to the optimization process for reference conditions, in order to secure linearity of the optimization model.

2.3. Multi-objective optimization

It is important to mention that the goal of this research isn't to obtain a single solution of the multi-objective optimization problem, but to acquire a whole trend of solutions, i.e. Pareto front. In order to deal with multi-objective optimization problem, epsilon constraint method has been used. The method is based on translating multi-objective optimization problem into single-objective optimization with additional set of constraints put on other objective functions [55]. These constraints are also called epsilon constraints. In order to acquire Pareto front, several optimizations should be run with different epsilon constraints, thus marching from one end of the Pareto front to the other. However, in order to successfully set epsilon constraint, the boundaries of the Pareto front should be acquired. This could be done by running single objective optimization, firstly with the first objective function, then with the other.

In this case, epsilon constraints were put on exergetic or ecological objective function while minimizing economical objective function, as shown in equations (19) and (20). It is important to notice that the level of detail of the constructed Pareto front depends on the number of optimization runs.

$$\min (f_{econ}) \text{ for } f_{ecol} = \varepsilon_{ecol} \quad (21)$$

$$\min (f_{econ}) \text{ for } f_{exe} = \varepsilon_{exe} \quad (22)$$

3. Case study

In this section input data and scenarios are presented. Input data includes various information needed in order to run the optimization model such as: meteorological and heat demand data, parameters related to district heating thermal network and finally, technology information regarding investment and O&M costs, efficiency, ramping limits, carbon emission factors, etc. It is important to mention that data are divided in: hourly data (8760 values), such as heating demand, and single value data, e.g. carbon emission or exergy factors. Furthermore, this section presents scenarios developed in detail. Three main scenarios have been proposed. Two scenarios are based on multi-objective optimization, while one scenario is single-objective optimization. Finally, for each mentioned scenarios, the authors have defined additional subscenarios in order to provide better analysis of the different taxing systems.

3.1. Input data

In order to validate the approach, numerical test has been carried out where City of Velika Gorica has been used as the case study. It is located in Zagreb County and has 14 smaller district heating systems usually connected to several buildings. The idea main idea of this paper is to connect few smaller district heating networks and replace existing supply units with the new ones. Definition of new supply capacities is carried out by using approach presented in the Section 2. Figure 1 shows all smaller district heating systems in Velika Gorica.

Figure 1 Group of smaller district heating systems

Heat demand data could be acquired by using publicly available data, such as national energy reports, Sustainable Energy Action Plans (SEAPs) or district heating service operators' data. For the purpose of this study, National Heating and Cooling Plan has been used in order to acquire heat demand of Velika Gorica district heating system [56], [57]. Heat demand is constituted of space heating and domestic hot water (DHW) demand. Since these reports usually do not make a difference between space and DHW demand, it is important to segregate it by using other public available data such as [58], which is unfortunately on the national level. For this reason it has been assumed that DHW share for the district heating system of Velika Gorica is equal to 15%. Hourly distribution of space heating demand has been created by using degree-hour method. The method is based on distributing total yearly heating demand on hourly level by using outside and inside-of-the-building temperature difference as the key input. For DHW demand, already known distribution has been used [54]. Figure 2 shows hourly distribution for a winter and a summer week. Seasonal effect related to thermal load is evident. During winter months, thermal load consists of space heating and domestic hot water demand. During summer period, only domestic hot water demand has to be covered by district heating system. Total district heating demand is equal to 32 GWh, with a peak demand equal to 19.7 MW.

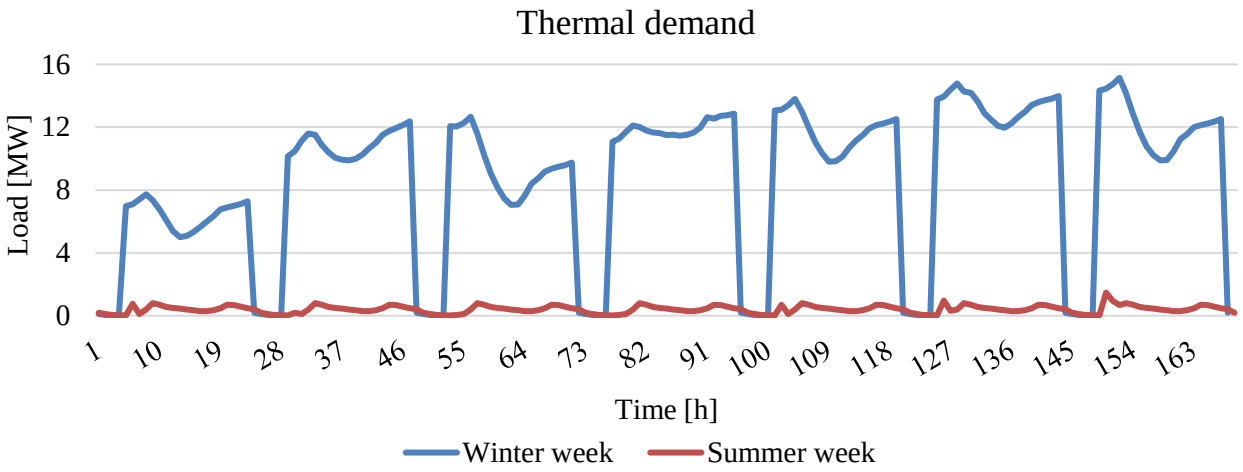

Figure 2 Thermal load for winter and summer week

Due to a relatively low specific space heating demand and a short thermal network, it has been assumed that a new district heating system operates as the third generation district system, i.e. with supply temperatures lower than 100°C [1], [57]. It is important to mention that DH supply temperature is mostly related to the outside air temperature. This correlation could be acquired by using available measurement data [1]. The exact information on district heating supply temperature could be obtained by contacting district heating system provider, but unfortunately, authors haven't received this information. Hourly distributions of meteorological data, i.e. outside temperature and global solar irradiation, which are needed inputs, were obtained by using Meteonorm [52]. Hourly power market prices are obtained from the Croatian power exchange called CROPEX [59]. Finally, all technology related data has been acquired by using publicly available databases [60] and [51]. Table 1 shows technology input data used for optimization.

In order to successfully calculate exergy destruction and exergy tax, exergy related data is needed, such as exergy factor and exergy destruction ratio. Exergy factor is defined as the ratio of exergy and energy of the fuel [28], [61]. In some cases, it can be higher than 1. As explained in the Section 2, reference exergy destruction ratio is calculated prior to the optimization in order to secure linearity of the model. Table 2 shows exergy related parameters for natural gas and biomass fuels, including exergy destruction ratio for heat-only boiler and cogeneration technologies.

Table 1 Technology data

Technology	**Investment cost [€/MW] / [€/m²] /[€/MWh]**	**Fuel cost [€/MWh]**	**Variable cost [€/MWh]**	**Emission factor [TCO_2/MWh]**	**Efficiency/ storage loss [-]**	**Ramp-up/down [-]**	**Technical lifetime [years]**	**Power-to-heat ratio [-]**
Natural gas boiler	100,000	20	3	0.22	0.9	0.7	35	-
Biomass boiler	800,000	15	5.4	0.04	0.8	0.3	25	-
Electrical heater	107,500	Electricity market	0.5	0.234	0.98	0.95	20	-
Heat pump	680,000	Electricity market	0.5	0.234	Hourly distribution	0.95	20	-
Cogeneration natural gas	1,700,000	20	3.9	0.22	0.5 (thermal)	0.3	25	0.82
Cogeneration biomass	3,000,000	15	5	0.04	0.6 (thermal)	0.3	20	0.55

Solar thermal	300 €/m^2	0	0.5	0	Hourly distribution	-	25	-
Thermal storage, buffer	3,000 €/MWh	0	0	0	1% (loss)	-	25	-
Seasonal thermal storage	500 €/MWh	0	0	0	0.1% (loss)	-	25	-

Table 2 Exergy related input data for biomass and natural gas fuels

Technology/fuel	Exergy factor	Exergy destruction ratio of heat-only boiler / CHP
Biomass	1.2	0.87 / 0.63
Natural gas	1.04	0.83 / 0.51

3.2. Scenario analyses

For the purpose of this study, several scenarios have been developed. Generally, they could be split in two groups. The first group is based on multi-objective optimization approach, i.e. Pareto solution is obtained, where one of the objective functions is always economical one, i.e. total discounted cost of the system. Other objective function is minimization of carbon dioxide emissions or minimization of exergy destruction. The second group is based on single-objective optimization, where all objective functions are translated to the total system cost by using taxing approach explained in the section Method. The details of each scenario are shown in Table 3. As previously explained, every scenario consists of several subscenarios. Scenario 1 is multi-objective optimization problem where economical and exergetic objective function is minimized, while carbon tax is implemented. In Scenario 1a, all technologies are available, in Scenario 1b biomass CHP couldn't be used, while in Scenario 1c solar thermal isn't available. Scenario 2 is also based on multi-objective optimization, but this time economic and ecological objective functions are minimized, while exergy destruction is internalized by using exergy tax. In Scenario 2a all technologies are available, while in Scenario 2b no CHP technologies are available. Finally, Scenario 3 is single-objective optimization where total cost of the system is minimized. In this scenario, both carbon and exergy taxes are used. Similarly to Scenario 2, Scenario 3a can utilize all technologies, while Scenario 3b can't use CHP technologies. In the Scenario 1 and Scenario 2, there is clear distinction between three objective functions. Each is different than the other (unique), since it takes into account different parameters of the district heating system. This is also visible from the acquired result, i.e. Pareto front – minimum can't be acquired for both at the same time. However, in the Scenario 3, ecological and exergetic objective functions are translated into the cost, by using taxing systems. In this scenario the model searches for minimum cost, while exergy efficiency and carbon emissions are only calculated parameters.

Table 3 Scenario description

Scenario name	**Tax**		**Objective function(s)**			**Technology availability**
	Carbon	Exergy destruction	Economical	Ecological	Exergetic	
Scenario 1a	✓		✓		✓	All technologies available
Scenario 1b	✓		✓		✓	No biomass CHP
Scenario 1c	✓		✓		✓	No solar thermal
Scenario 2a		✓	✓	✓		All technologies available
Scenario 2b		✓	✓	✓		No CHP technologies available
Scenario 3a	✓	✓	✓			All technologies available
Scenario 3b	✓	✓	✓			No CHP technologies available

4. Results and discussion

In this section, scenario results are presented in detail. Section 4.1. shows Scenario 1 results which include Pareto shift due to the carbon tax increase, while Section 4.2. displays Scenario 2 results which consists of Pareto shift due to the exergy tax increase. Finally, Section 4.3. shows results of the single objective optimization when both carbon and exergy tax are introduced.

Results for Scenario 1 and Scenario are shown in the form of Pareto fronts since they present multi-objective optimization problem. It is important to notice that each point on the Pareto front contains various information such as: optimal capacities, hourly operation stem and exergy efficiency of the system. However, in this paper, the emphasis is put on the analysis of the objective functions: total discounted cost, carbon dioxide emissions and exergy destruction of the system. Scenario 3 presents single-objective optimization problem, thus Pareto front couldn't be constructed. The results present chosen system characteristics (exergy efficiency and CO_2 emissions) for the least-cost solution acquired by optimization.

The optimization was run for on Intel i7 laptop with 8 GB of RAM. Every optimization run lasted for around 25 minutes. Due to this, Pareto fronts are constructed with limited number of points.

4.1. Results of Scenario 1

Scenario 1 presents multi-objective optimization scenario in which two objective functions have been studied: total discounted cost and exergy destruction of the system, while carbon dioxide emissions are translated to internal cost by using carbon taxing system which was added to the first objective function. Five Pareto fronts were obtained, each for different carbon tax price. The tax was increased from 0 EUR/tonne up to the 80 EUR/tonne with the step equal to 20 EUR/tonne. In order to provide more detailed analysis, three subscenarios have been modelled. In Scenario 1a, all technologies are available, in Scenario 1b biomass CHP isn't available, while in Scenario 1c solar thermal couldn't be used.

Figure 3 shows Pareto shift for Scenario 1, i.e. every Pareto front has been constructed for different value of a carbon tax. Two objective functions are taken into account: minimization of exergy destruction and minimization of the total system cost. It can be noticed that, for every subscenario, Pareto fronts are converging to a single front. For the first subscenario, Figure 3a, Pareto fronts are converging to equal solution, at around 14,000 MWh. The lowest possible exergy destruction is equal to around 11,000 MWh. In the region of the Pareto front where cost objective function is dominant, cogeneration technology is used. Once approaching the region with the lowest exergy destruction, solar thermal is dominantly utilised, thus achieving extremely high cost of the system. For Scenario 1a, at the carbon tax equal to 40 EUR/tonne, biomass CHP is becoming part of the least-cost solution and is present through the most of Pareto front. This is the reason why these Pareto fronts have higher exergy destruction of the least cost solutions: biomass has higher exergy content per unit of energy than natural gas.

This is the main reason why it was decided that biomass CHP isn't available in Scenario 2b, shown in Figure 1b. Again, all Pareto front are converging to a single point, at around 14,000 MWh, just as in Scenario 1a. Since solar thermal is still available in this subscenario, the lowest exergy destruction is similar to subscenario 1a, around 11,000 MWh. For carbon tax, equal to 80 EUR/tonne, biomass boiler is part of the least-cost solution. This is the reason why this Pareto front has higher exergy destruction of the least-cost solution than other Pareto fronts. Since biomass CHP couldn't' be utilized in this subscenario, heat pump is starting to be part of the optimal solution much sooner, at around 1,400,000 EUR of the total discounted cost.

Finally, Scenario 1c, shown in Figure 3c, acquires similar results as other subscenarios but, since there is no solar thermal available, minimum exergy destruction acquired is relatively higher, around 14,000 MWh. Furthermore, all Pareto fronts are converging faster than in other two scenarios. The most expensive solution has lower cost than other two scenarios, due to the unavailability of solar thermal collectors. As in Scenario 1a, biomass CHP is used part of the least-cost solution for carbon

tax higher than 20 EUR/tonne, which is the reason why these three Pareto front have higher exergy destruction in the region where cost function is dominant.

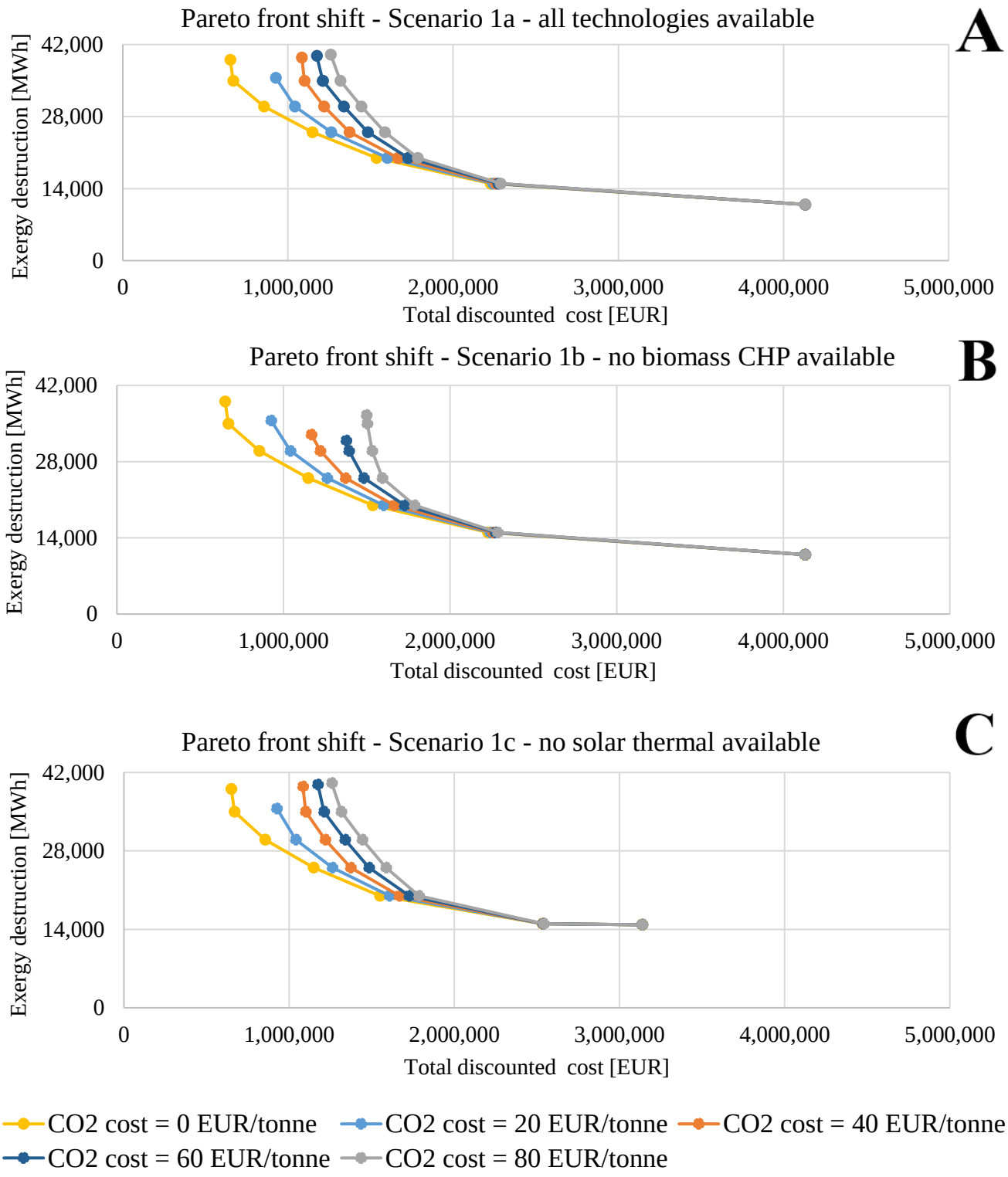

Figure 3 Pareto front shift due to the CO_2 tax increase: a) Scenario 1a - all technologies available, b) Scenario 1b - no biomass CHP available, c) Scenario 1c - no solar thermal available

4.2. Results of Scenario 2

Scenario 2 is also multi-objective optimization problem in which total discounted cost and carbon dioxide emissions are defined as objective functions. In this scenario exergy destruction is translated into the additional expense, by using previously explained exergy taxing system, and added to the cost objective function. Two subscenarios are developed. In Scenario 2a, all technologies are available, while in Scenario 2b no CHP technologies are available. For each of them, five Pareto fronts have been constructed by using epsilon constraint method. Figure 4 shows Pareto fronts for different exergy tax values, starting from zero and up to 400 EUR/MWh.

Figure 4a, shows results acquired for Scenario 2a, where all technologies are available. The least-cost solution obtains value of economical objective function around 700,000 EUR, while the CO_2 emissions reach up to 16,500 tonnes. The lowest possible CO_2 emissions is around 1,100 tonnes, obtained for every exergy tax value. It can be noticed that, when compared to Scenario 1 results, there is no convergence of Pareto fronts. They are becoming saturated with the increase of the exergy tax value. The most noticeable difference between is when the exergy tax is increased from 0 up to 100 EUR/MWh: the front is shifted to the region of higher total discounted cost and higher carbon dioxide emissions. The difference is relatively small in the region where economical objective function dominates. However, in the region where carbon dioxide emissions reach minimum values, the difference between Pareto fronts is substantial. This is due to the existence of biomass heat-only boiler with relatively high exergy destruction, i.e. high exergy tax. It is important to notice that carbon dioxide emissions of the least cost solution aren't decreasing with increase of exergy tax values. The main reason for this is following. Increase of exergy tax gives opportunity of increasing the size and load factor of CHP cogeneration units, since natural gas boiler operation is starting to be relatively expensive due to the exergy tax increase. Natural gas cogeneration has higher carbon dioxide emissions, per unit of covered heat demand, and overall carbon dioxide emissions of the system are increasing. It is important to mention that heat pump hasn't been used as the solution, since biomass cogeneration has lower carbon dioxide emission, due to the power sector emission factor. However, once exergy tax increases up to 300 EUR/MWh, electrical heaters are becoming peak demand technology, together with natural gas heat-only boiler. Biomass heat-only boiler are included only in the most expensive solutions, i.e. where carbon dioxide emissions reach minimum.

Scenario 2b, where CHP technologies aren't available, is shown in Figure 2b. When compared to Scenario 2a, obtained results differentiate to a great extent. Firstly, all Pareto front have lower values of carbon dioxide emissions. The reason of this is non-existence of CHP technologies. As explained before, CHP technologies emit more carbon dioxide per unit of thermal energy produced. Secondly, Pareto fronts are shifting to the region of lower carbon dioxide emissions with the increase of exergy tax value. Once reaching exergy tax value of 200 EUR/MWh, the least cost solutions don't differentiate much in terms of carbon dioxide emissions, i.e. saturation has been realized. However, the cost of the most environmentally friendly solution greatly depends on the exergy tax value. As in the Scenario 2a, the reason behind this is usage of biomass heat-only boiler with high exergy destruction. It is important to notice that the lowest CO_2 emissions are equal for Scenario 2a and Scenario 2b.

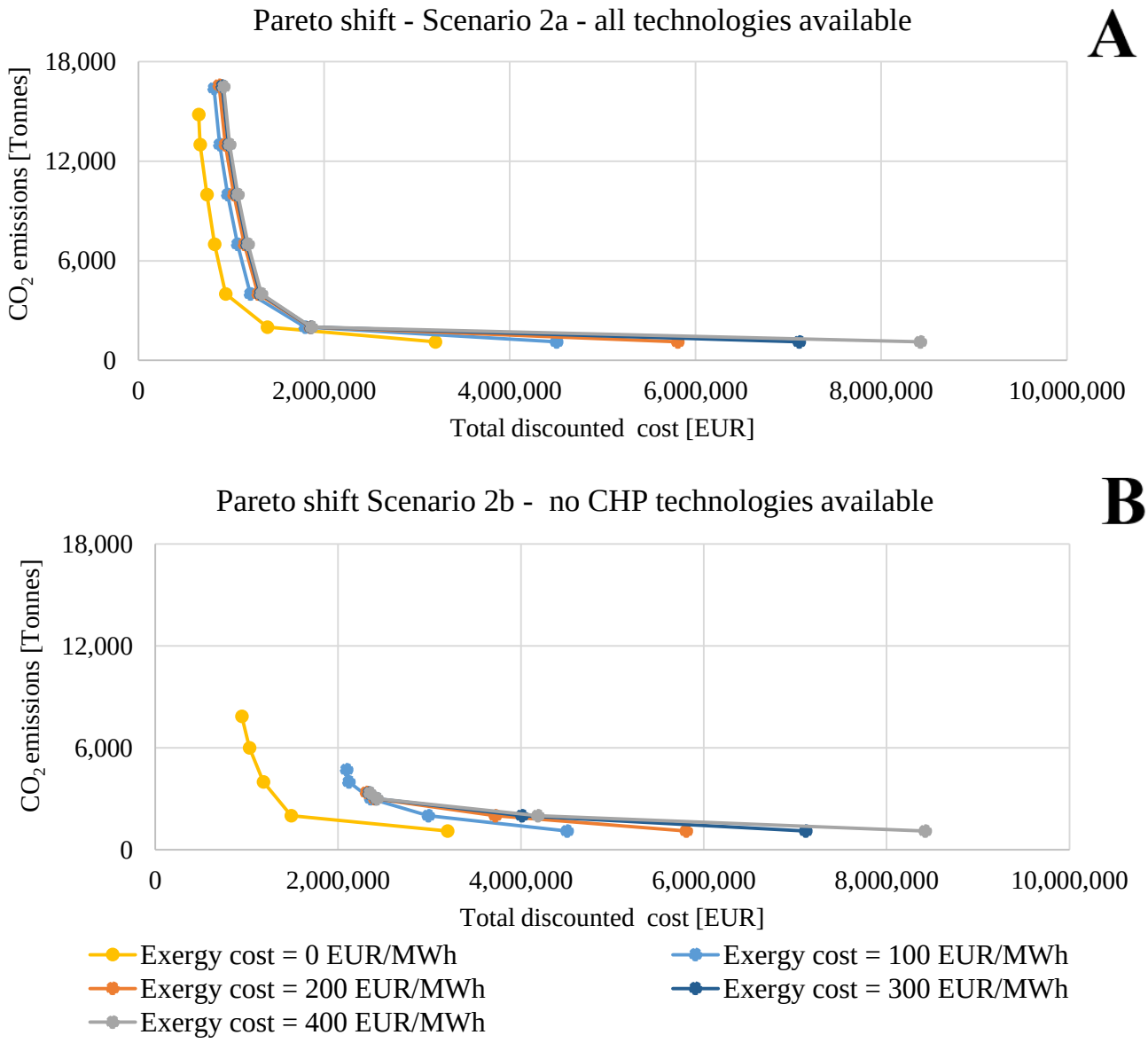

Figure 4 Pareto front shift due to the exergy tax increase: a) Scenario 2a - all technologies available, b) Scenario 2 - no CHP technologies available

4.3. Results of Scenario 3

Results of the Scenario 3 are shown in Figure 5. This scenario is based on a single-objective optimization where both exergy and carbon taxes are included in the economic objective function. Due to this, all obtained results present the least cost solution for the given taxing conditions. There are two parameters which could be followed: exergy efficiency and carbon dioxide emissions of the system. Furthermore, the sensitivity analysis of these parameters on the carbon and exergy tax value has been carried out and is explained in detail below. Two scenarios have been developed. In Scenario 3a all technologies are available, while in Scenario 3b CHP technologies aren't allowed to be utilised.

Figure 5a shows exergy efficiency of the Scenario 3a and the influence of exergy and carbon tax. In Scenario 3a, all technologies are available. It can be seen that 100 EUR/MWh of exergy tax is enough for the system to reach maximum exergy efficiency. Two groups of curves could be noticed: one has higher while the second one has lower exergy efficiency. The group with lower exergy efficiency has carbon tax. The reason for this is similar as preciously explained for Scenario 2a. Increase of carbon tax will gradually replace natural gas cogeneration with natural gas boiler and additionally introduce electrical heater as the peak demand unit, which additionally lowers exergy efficiency of the system.

It is important to remember that only boilers are included in the exergy tax system. Furthermore, it is worth mentioning that biomass heat-only boiler, heat pump and solar thermal weren't part of any solution. Biomass heat-only boiler has too high exergy destruction, thus biomass cogeneration is used, while heat pump and solar thermal have too high investment cost. Once carbon tax reaches 40 EUR/tonne, biomass cogeneration becomes part of every least-cost solution, regardless exergy tax value.

Figure 5b shows carbon dioxide emissions for Scenario 3a and the given tax system conditions. It can be noticed that exergy tax value has small influence on carbon dioxide emissions. However, the trend could be observed. If the carbon tax is lower or equal to 40 EUR/tonne, rise of exergy tax increases CO_2 emissions, while for carbon tax higher than 40 EUR/tonne, exergy tax increase reduces them. Furthermore, increase of the carbon tax to more than 20 EUR/tonne significantly reduces CO_2 emissions. The main reason for this is, as previously explained, inclusion of biomass cogeneration. It is important to mention that carbon tax is able to It is important to mention that carbon tax is able to greatly reduce carbon dioxide emissions even for exergy tax value equal to zero.

Figure 5c shows exergy efficiency of Scenario 3b for different taxing conditions. As previously mentioned, this scenario doesn't include cogeneration technologies, thus the results differ from Scenario 3a. For all values of carbon tax, from zero to 80 EUR/tonne, exergy efficiency of the system reaches plateau for value around 200 EUR/MWh. It is important to notice role of carbon tax in exergy efficiency increase. Plateau of maximum exergy efficiency will be reached for lower exergy tax value, if carbon tax is higher. For example, if carbon tax is 80 EUR/tonne, plateau is reached already at 100 EUR/MWh. Once exergy tax value reaches 200 EUR/MWh, exergy efficiency stays mostly the same for all taxing conditions. However, there is slight decrease in exergy efficiency for high exergy tax values, due to the inclusion of electrical heater. It is important to mention that heat pump is present in every solution, once exergy tax value of 200 EUR/MWh is reached. As in Scenario 3a, biomass heat-only boiler is rarely included in Scenario 3b solutions. It is only present for exergy tax value of 0 EUR/MWh and carbon tax higher or equal to 20 EUR/tonne.

Figure 5d shows carbon dioxide emissions for Scenario 3b. Similarly to Figure 5c, carbon dioxide emissions also reach plateau of minimum value once carbon tax value of 200 EUR/MWh is reached. As expected, the increase of carbon tax will boost reduction of carbon dioxide emissions for any associated exergy tax. Again, as in Figure 5b, increase of carbon tax has important role since it reduces carbon dioxide emissions of the system when there is no exergy tax.

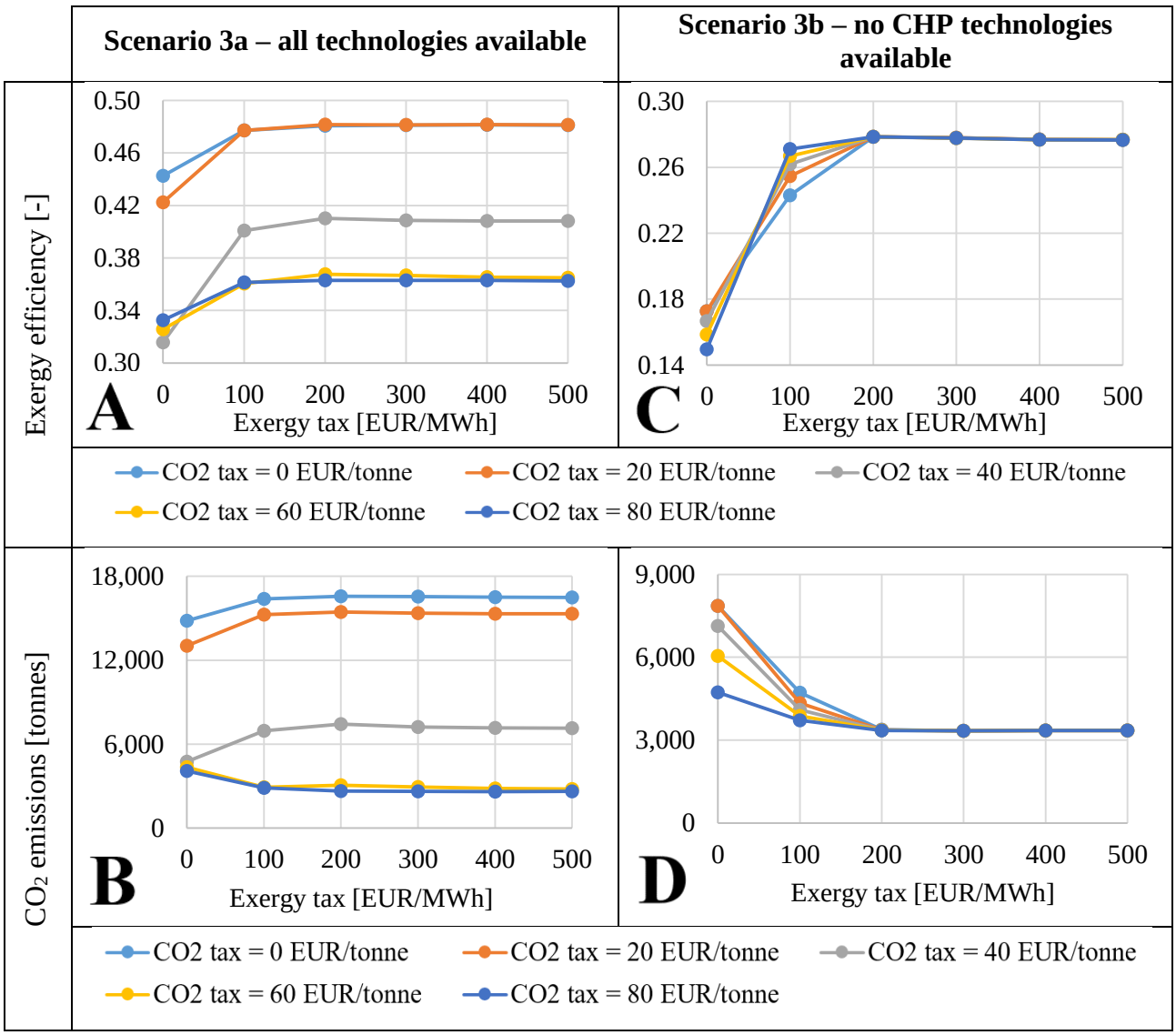

Figure 5 Exergy efficiency and CO_2 emissions of the least-cost solution for Scenario 3a and Scenario 3b

One of the important contributions of this paper is to analyse how different taxing systems can phase out natural gas consumption in heat-only boilers from the least-cost solution of the district heating system. Figure 6 shows consumption of natural gas in heat-only boilers for various taxing conditions. X-axis in Figure 6 represent different exergy tax values, while various colour bars represent different carbon tax values. First of all, it could be noticed that increase of exergy tax significantly reduces natural gas consumption in heat-only boilers, but even 500 EUR/MWh of exergy destroyed isn't enough to completely push it out. Figure 6a shows reduction of natural gas consumption in heat-only boilers for Scenario 3a. It can be noticed, similarly to Scenario 2a, that highest natural gas consumption isn't reached for carbo tax equal to zero. In this case, the highest consumption is reached for carbon tax equal to 40 EUR/MWh. Once this price is reached, biomass cogeneration becomes part of the least-cost solution. Such a trend isn't visible in Scenario 3b, as could be seen in Figure 6b. In this scenario, both exergy and carbon tax increase are resulting in natural gas consumption reduction.

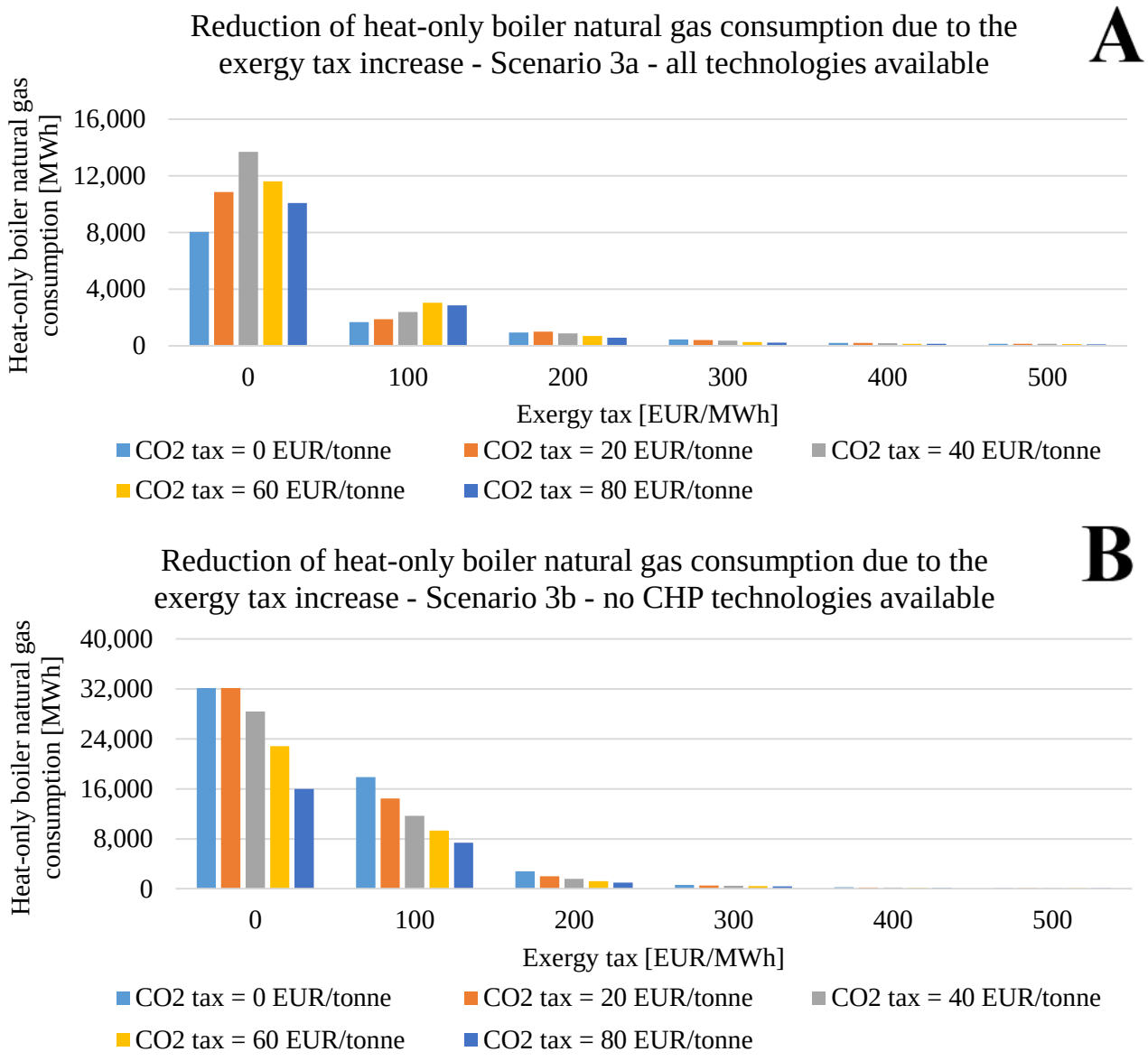

Figure 6 Influence of carbon and exergy tax cost on reduction of heat-only boiler natural gas consumption: a) Scenario 3a and b) Scenario 3b

In order to fully understand the impact of different taxing conditions on reduction of natural gas consumption in heat only boiler, it is crucial to analyse the total cost structure. Figure 7 shows cost distribution for different taxing conditions for Scenario 3a, i.e. when all technologies are available for utilization. The total cost of the system is divided into: discounted investment and running costs, total exergy tax and total carbon tax. First of all, it should be noticed that increase of carbon tax rises overall system cost from 600,000 EUR for carbon tax equal to 0 EUR/MWh up to 1,400,000 EUR for 80 EUR/tonne. Increase of exergy tax has smaller influence on the total system price. The highest impact is observed when increasing exergy tax value from 0 EUR/MWh to 100 EUR/MWh. Furthermore, the highest share of exergy tax in the overall system price is obtained for exergy tax value of 100 EUR/MWh and is around 8.5-10%. It is important to notice that this is relatively small when compared to carbon tax share which could be as high as 20% of the overall system cost. However, carbon tax itself can't push-out consumption of natural gas in the heat-only boiler unit, thus exergy tax is needed. As the conclusion, it should be noticed that exergy tax, which presents small share of the total system cost, can effectively push-out the usage of natural gas in heat-only boiler unit of the optimal least-cost solution of the district heating system.

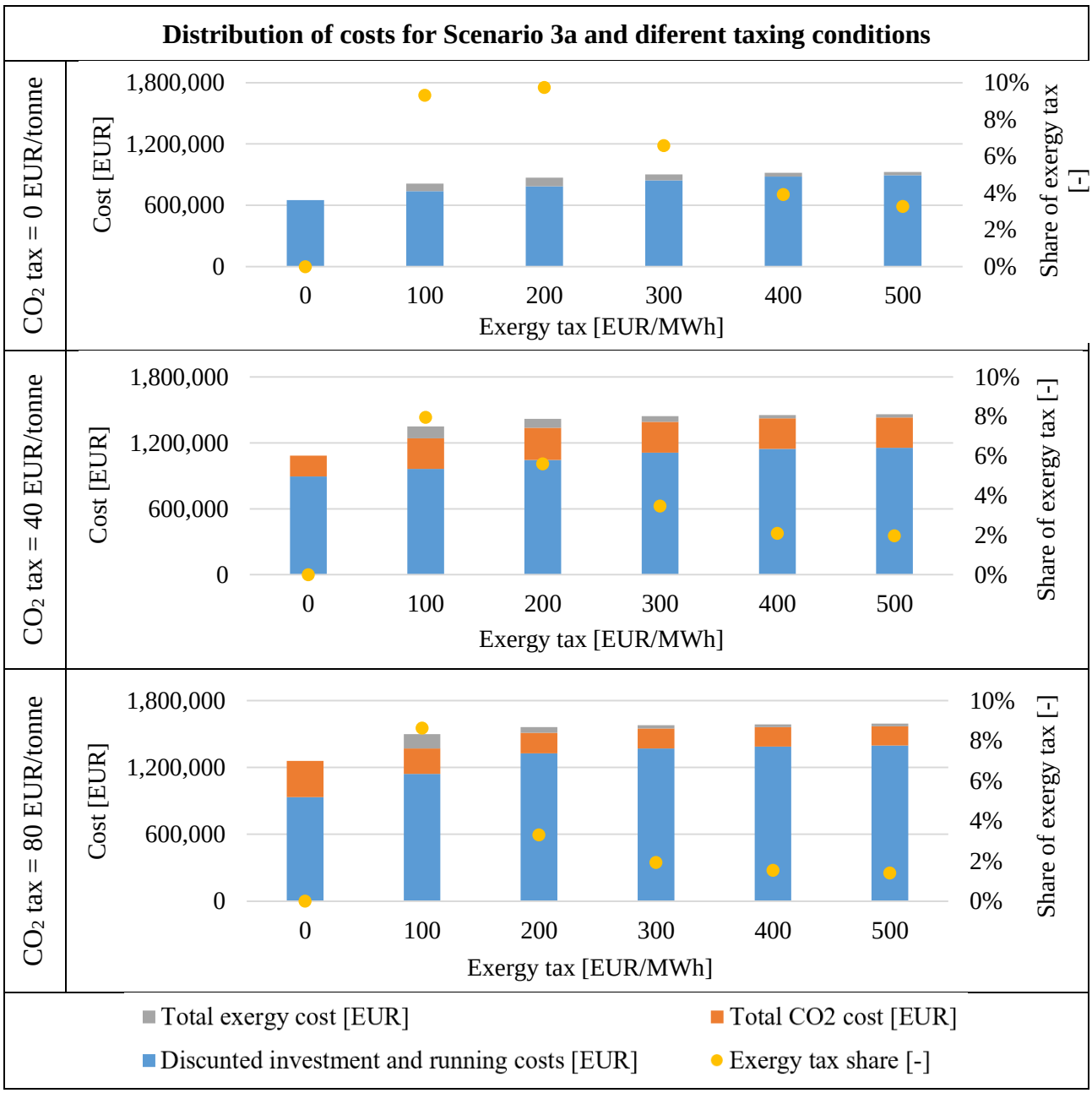

Figure 7 Cost distribution for Scenario 3a and different taxing conditions

4.4. Results of Scenario 3a with CO_2 allocation in cogeneration units

One of the major issues with the results obtained for Scenario 3a, shown in Figure 5, is following. It can be noticed that with the increase of carbon tax, exergy efficiency of the district heating is reduced. The main reason behind this is increased integration of heat-only boilers, which have higher exergy destruction rates and lower CO_2 emissions than cogeneration units. However, authors' opinion is that such approach is incomplete, since all the emissions emitted from CHP plant are allocated to district heating, i.e. thermal energy production. Heat produced in cogeneration units is mostly by-product of the electricity production process, sometimes called excess or waste heat. Due to this, CO_2 emissions from CHP units should be allocated between heat and power production. Numerous authors have already discussed the issue of CO_2 allocation in cogeneration plants. Rosen has provided overview of numerous allocation methods based on the energy output of a CHP unit [62]. One of the most noteworthy methods is the one based on power loss caused by heat recovery. In the other words, it states that CO_2 emissions linked to the district heating in CHP units should be proportional to the power loss due to the heat production. In the paper [63], it is listed as the Dresden method. According

to study [64], specific emissions for generated heat in CHP units is around 150 kg/MWh (depending on the technology), i.e. five times lower than the specific emissions for electricity production in the same CHP unit. Similar results are obtained in study [65]. Finally, paper [66] provides allocating factors for numerous technologies and compares seven different allocation methods. By using the Dresden or power-loss method, heat allocation factor is around 0.1. This means that 90% of the CO_2 emissions from CHP unit should be allocated to electricity production, while only 10% of the overall emissions should be allocated to district heating, i.e. heat production.

The authors have re-run optimization for the Scenario 3a, while taking into account findings acquired in paper [66], i.e. allocating only 10% of the overall CHP emissions to the heat production. The results of Scenario 3a with CO_2 allocation in CHP units is shown in Figure 8. It can be noticed that, if taking into account CO_2 allocation in CHP units, inclusion of carbon tax increases exergy efficiency of the least-cost district heating system, while at the same time decreases total CO_2 emissions. These findings are in contradiction with results shown in Figure 5, which shows that carbon tax increase decreases exergy efficiency of the least-cost district heating system.

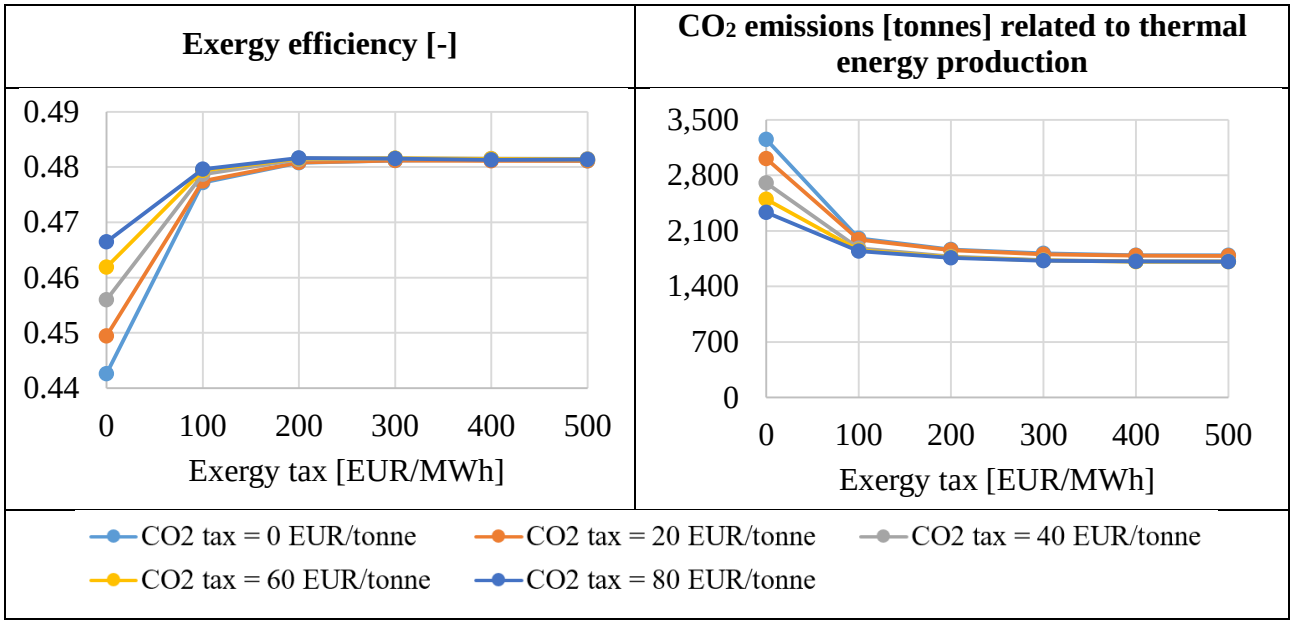

Figure 8 Exergy efficiency and CO2 emissions of the least-cost solution for Scenario 3a with CO_2 allocation in CHP units

4.5. Discussion

The method developed for the purpose of this paper is based on multi-objective optimization of district heating system's supply capacities and hourly operation. Due to this, it is challenging to verify accuracy of the model by using existing data, since the reference case doesn't exist. This issue is discussed in the text below. As explained by Lund et al in [67], there are two approaches in energy planning: simulation and optimization. Both could be used for system capacity definition and operation analysis. While simulation approach depends on the scenarios developed by the decision maker, optimization provides the solution of the problem by considering various constraints and various input data such as cost database. For this reason, supply capacities of the complex system obtained by optimization are unique solution which could be hardly obtained by using scenario analysis approach. This issue becomes even more complicated when discussing verification of multi-objective optimization since real life decisions are usually based only on economic benefits, i.e. total cost. Furthermore, this method involves exergy taxing, the approach which hasn't been introduced in real life systems, according to the authors knowledge. Nevertheless, it should be mentioned that hourly operation of the system acquired with optimization procedure could be verified. In this case, exergy taxing should be put to zero and compare obtained operation with real life data. However, it

should be mentioned that focus of this paper isn't put on the development of dispatch and unit-commitment district heating model, but on the overall system planning which includes simultaneous optimization of capacities and operation of the system.

Other papers have also tackled the issue of exergy in heating systems by using multi-objective optimization. Paper [28] uses mixed-integer linear programming in order to optimize operation of the distributed energy system with predefined technology capacities. Besides this, the crucial difference is that exergy efficiency, i.e. exergy input, has been used as one of the objective functions, while carbon tax and CO_2 emissions haven't been taken into account. The acquired points of the Pareto front are relatively undistributed since weighted sum method has been used in order to tackle multi-objective optimization. Results show that natural gas and biomass boiler isn't utilized at all when putting the weight to exergy-related objective function. This model has been upgraded in paper [29] in order to include capacity optimization and number of units per technology. Once again, Pareto front has been constructed by using weighted sum method. For the least-cost solution, the system uses natural gas cogeneration in combination with natural gas boiler and heat pump. The least cost results obtained in this paper do not utilize heat pump. The reason behind this could be constant efficiency of the heat pump (COP) assumed by authors in paper [29]. On the other hand, the optimal solution from the exegetic point of does not use natural gas boiler at all, similarly to the results obtained in this study. Finally, the natural gas phase out results from this paper could be compared with outputs from authors' previously published paper [46]. Natural gas consumption reduction strictly follows increase of exergy tax increase, while in paper [46], it is obtained with constraining exergy destruction. Around 200 EUR/MWh of exergy tax is needed in order to obtain natural gas consumption reduction achieved in paper [46]. Furthermore, the most suitable solution defined in paper [46] does not include cogeneration units, while having CO_2 emissions around 4,000 tonnes with exergy efficiency of 30%. This paper has shown that if taking into account CO_2 allocation in CHP units, exergy efficiency of the system could still be kept high at 45%, while producing lower amount of CO_2 emissions thanks to utilization of CHP units. Paper [45] dealt with multi-objective optimization of district heating systems taking into account economic and ecological objective functions, but it didn't involve any taxing methods. This paper shows how these results could be shifted by using exergy taxing methods, thus reducing CO_2 emissions.

Finally, it should be mention how this method could be used for energy planning and could present the first step in decision making. The acquired results could serve as the input for more complex analysis of the district heating system based on more realistic model of operation, i.e. unit commitment and dispatching which involves additional physical constraints. Additionally, the method could be used for policy discussion for natural gas phase-out in order to show crucial drawbacks of this fuel for heating purposes, i.e. exergy destruction.

5. Conclusion

In this paper, the influence of carbon and exergy destruction tax on the results of multi-objective optimization of district heating system has been analysed. The district heating supply model includes various technologies, such as heat-only boiler, cogeneration, solar thermal and power-to-heat units, including thermal storage. The model is capable of optimizing their capacities and hourly operation for a whole year. Objective functions are defined as minimization of total discounted cost, minimization of carbon dioxide emissions and minimization of exergy destruction. In order to carry out the analysis, two approaches has been used through three scenarios. In the first two scenarios, multi-objective optimization has been used, while in the third scenario, single-objective optimization was introduced. Scenario 1 includes economical and exergetic objective functions, while the influence of the carbon tax on the Pareto front shift was analysed. It was shown that fronts are converging to a single one no matter the carbon tax value. In Scenario 2, ecological objective function was used together with economical and the influence of exergy destruction tax was analysed. It has been shown that, if all technologies are available, introduction of exergy tax doesn't decrease carbon dioxide emissions. However, due to the additional costs, Pareto frontiers are shifting to the region of higher total cost. On the other hand, if there are no CHP technologies available, increase of exergy tax reduces carbon dioxide emissions. In Scenario 3, single objective optimizing has been carried out in order to acquire the least cost solution, while carbon and exergy tax have both been added to the cost function. It has been concluded that exergy tax of 150 EUR/MWh is enough in order to reach maximum exergy efficiency. If all technologies are available, exergy tax has small influence on the carbon dioxide emissions. On the other hand, if no CHP technologies are available, exergy tax of 200 EUR/MWh is enough to reach minimum carbon dioxide emissions. The main outcome of this paper is the analysis of exergy tax impact on natural gas consumption in heat-only boilers. It has shown that inclusion of exergy tax can significantly reduce natural gas consumption. However even for the value of 500 EUR/MWh, the least cost solution includes natural gas as one of the supply units in order to cover the peak demand if all technologies are available. The cost structure shown that share of exergy tax is relatively small, lower than 10% while carbon tax share can go up to 20% of the total system cost. However, carbon tax itself isn't enough to push out utilization of natural gas in the heat-only boiler unit.

References

[1] S. Frederiksen and S. Werner, *District Heating and Cooling*. 2013.

[2] H. Lund, N. Duic, P. A. Ostergaard, and B. V. Mathiesen, "Future District Heating Systems and Technologies : On the role of Smart Energy Systems and 4 th Generation District," *Energy*, 2018.

[3] H. Ahvenniemi and K. Klobut, "Future Services for District Heating Solutions in Residential Districts," *J. Sustain. Dev. Energy, Water Environ. Syst.*, vol. 2, no. 2, pp. 127–138, 2014.

[4] P. A. Østergaard and A. N. Andersen, "Booster heat pumps and central heat pumps in district heating," *Appl. Energy*, 2016.

[5] C. Hsu, T. Lin, J. Liang, C. Lai, and S. Chen, "Optimization analysis of waste heat recovery district cooling system on a remote island : Case study Green Island," *Energy Convers. Manag.*, vol. 183, no. 1, pp. 660–670, 2019.

[6] H. Lund *et al.*, "4th Generation District Heating (4GDH). Integrating smart thermal grids into future sustainable energy systems.," *Energy*, vol. 68, pp. 1–11, 2014.

[7] H. Li and S. Svendsen, "Energy and exergy analysis of low temperature district heating network," *Energy*, vol. 45, no. 1, pp. 237–246, 2012.

[8] J. Von Rhein, G. P. Henze, N. Long, and Y. Fu, "Development of a topology analysis tool for fi fth-generation district heating and cooling networks," *Energy Convers. Manag.*, vol. 196, no. May, pp. 705–716, 2019.

[9] M. A. Sayegh *et al.*, "Trends of European research and development in district heating technologies," *Renew. Sustain. Energy Rev.*, pp. 1–10, 2016.

[10] M. Terhan and K. Comakli, "Energy and exergy analyses of natural gas-fired boilers in a district heating system," *Appl. Therm. Eng.*, no. April, 2017.

[11] J. Skorek, P. Bargiel, and M. Tan, "Energy and economic optimization of the repowering of coal-fired municipal district heating source by a gas turbine," *Energy Convers. Manag.*, 2017.

[12] G. T. Ã, "Definitions and nomenclature in exergy analysis and exergoeconomics," vol. 32, pp. 249–253, 2007.

[13] A. Bonati, G. De Luca, S. Fabozzi, N. Massarotti, and L. Vanoli, "The integration of exergy criterion in energy planning analysis for 100% renewable system," *Energy*, 2019.

[14] Ş. Kilkiş, "A Rational Exergy Management Model to Curb CO 2 Emissions in the Exergy-Aware Built Environments of the Future," KTH Royal Institute of Technology, Stockholm, Sweden, 2011.

[15] Ş. Kilkiş, "Exergy transition planning for net-zero districts," *Energy*, vol. 92, no. Part 3, pp. 515–531, 2015.

[16] A. Keçebas, "Economic analysis of exergy efficiency based control strategy for geothermal district heating system," *Energy Convers. Manag.*, vol. 73, pp. 1–9, 2013.

[17] E. Sciubba, "Exergy-based ecological indicators : From Thermo-Economics to cumulative exergy consumption to Thermo-Ecological Cost and Extended Exergy Accounting," *Energy*, vol. 168, pp. 462–476, 2019.

[18] B. Kılkış and Ş. Kılkış, "New exergy metrics for energy, environment, and economy nexus and optimum design model for nearly-zero exergy airport (nZEXAP) systems," *Energy*, vol. 140, pp. 1329–1349, 2017.

[19] T. Tereshchenko and N. Nord, "Energy planning of district heating for future building stock based on renewable energies and increasing supply flexibility," *Energy*, vol. 112, pp. 1227–1244, 2016.

[20] R. Mikulandrić *et al.*, "Performance Analysis of a Hybrid District Heating System : A Case Study of a Small Town in Croatia," *J. Sustain. Dev. Energy, Water Environ. Syst.*, vol. 3, no. 3, pp. 282–302, 2015.

[21] M. Anatone and V. Panone, "A model for the optimal management of a CCHP plant," *Energy Procedia*, vol. 81, pp. 399–411, 2015.

[22] M. Pirouti, A. Bagdanavicius, J. Ekanayake, J. Wu, and N. Jenkins, "Energy consumption and economic analyses of a district heating network," *Energy*, vol. 57, pp. 149–159, 2013.

[23] S. Bracco, G. Dentici, and S. Siri, "Economic and environmental optimization model for the design andthe operation of a combined heat and power distributed generation system in an urban area," *Energy*, vol. 55, pp. 1014–1024, 2013.

[24] T. Falke, S. Krengel, A.-K. Meinerzhagen, and A. Schnettler, "Multi-objective optimization and simulation model for the design of distributed energy systems," *Appl. Energy*, 2016.

[25] T. Tezer, R. Yaman, and G. Yaman, "Evaluation of approaches used for optimization of stand-alone hybrid renewable energy systems," *Renew. Sustain. Energy Rev.*, vol. 73, no. June 2016, pp. 840–853, 2017.

[26] A. Franco and M. Versace, "Multi-objective optimization for the maximization of the operating share of cogeneration system in District Heating Network," *Energy Convers. Manag.*, vol. 139, pp. 33–44, 2017.

[27] Y. Z. Wang *et al.*, "Multi-objective optimization and grey relational analysis on configurations of organic Rankine cycle," *Appl. Therm. Eng.*, 2016.

[28] M. Di Somma *et al.*, "Operation optimization of a distributed energy system considering energy costs and exergy efficiency," *Energy Convers. Manag.*, vol. 103, pp. 739–751, 2015.

[29] M. Di Somma *et al.*, "Multi-objective design optimization of distributed energy systems through cost and exergy assessments," *Appl. Energy*, vol. 204, pp. 1299–1316, 2017.

[30] "EU Emissions Trading System (EU ETS)." [Online]. Available: https://ec.europa.eu/clima/policies/ets_en.

[31] A. Verbruggen, E. Laes, and E. Woerdman, "Anatomy of Emissions Trading Systems : What is the EU ETS ?," *Environ. Sci. Policy*, vol. 98, no. April, pp. 11–19, 2019.

[32] "EEX." [Online]. Available: https://www.eex.com/en/.

[33] A. M. Soliman and M. A. Nasir, "Association between the energy and emission prices : An analysis of EU emission trading system," *Resour. Policy*, no. November, pp. 0–1, 2018.

[34] A. Dutta, "Modeling and forecasting the volatility of carbon emission market: The role of outliers, time-varying jumps and oil price risk," *J. Clean. Prod.*, vol. 172, pp. 2773–2781, 2017.

[35] N. Chaiyat, S. Chaongew, P. Ondokmai, and P. Makarkard, "Levelized energy and exergy costings per life cycle assessment of a combined cooling , heating , power and tourism system of the San Kamphaeng hot spring , Thailand," *Renew. Energy*, vol. 146, pp. 828–842, 2020.

[36] S. Usón, J. Uche, A. Martínez, A. Amo, and L. Acevedo, "Exergy assessment and exergy cost analysis of a renewable-based and hybrid trigeneration scheme for domestic water and energy supply," *Energy*, vol. 168, pp. 662–683, 2018.

[37] A. Franco and M. Versace, "Optimum sizing and operational strategy of CHP plant for district heating based on the use of composite indicators," *Energy*, vol. 124, pp. 258–271, 2017.

[38] I. Baldvinsson and T. Nakata, "A comparative exergy and exergoeconomic analysis of a residential heat supply system paradigm of Japan and local source based district heating system using SPECO (specific exergy cost) method," *Energy*, vol. 74, no. C, pp. 537–554, 2014.

[39] H. Arat and O. Arslan, "Exergoeconomic analysis of district heating system boosted by the geothermal heat pump," *Energy*, 2016.

[40] W. Meesenburg, T. Ommen, and B. Elmegaard, "Dynamic exergoeconomic analysis of a heat pump system used for ancillary services in an integrated energy system," *Energy*, vol. 152, pp. 154–165, 2018.

[41] X. Yang, H. Li, and S. Svendsen, "Energy, economy and exergy evaluations of the solutions for supplying domestic hot water from low-temperature district heating in Denmark," *Energy Convers. Manag.*, vol. 122, pp. 142–152, 2016.

[42] T. Duh Čož, A. Kitanovski, and A. Poredoš, "Exergoeconomic optimization of a district cooling network," *Energy*, vol. 135, pp. 342–351, 2017.

[43] A. Franco and F. Bellina, "Methods for optimized design and management of CHP systems for district heating networks (DHN)," *Energy Convers. Manag.*, vol. 172, no. January, pp. 21–31, 2018.

[44] C. Nguyen, C. T. Veje, M. Willatzen, and P. Andersen, "Exergy costing for energy saving in combined heating and cooling applications," *Energy Convers. Manag.*, vol. 86, pp. 349–355, 2014.

[45] H. Dorotić, T. Pukšec, and N. Duić, "Multi-objective optimization of district heating and cooling systems for a one-year time horizon," *Energy*, vol. 169, pp. 319–328, 2019.

[46] H. Dorotić, T. Pukšec, and N. Duić, "Economical , environmental and exergetic multi-objective optimization of district heating systems on hourly level for a whole year," *Appl. Energy*, vol. 251, no. December 2018, p. 113394, 2019.

[47] "Julia programming language." [Online]. Available: https://julialang.org.

[48] "JuMP." [Online]. Available: http://www.juliaopt.org/JuMP.jl/0.18/.

[49] JRC, "PVGIS." [Online]. Available: http://re.jrc.ec.europa.eu/pvgis.html.

[50] P. A. Sørensen, J. E. Nielsen, R. Battisti, T. Schmidt, and D. Trier, "Solar district heating

guidelines: Collection of fact sheets," no. August, p. 152, 2012.

[51] "SPF Institut für Solartechnik." [Online]. Available: http://www.spf.ch/index.php?id=111&L=6.

[52] "Meteonorm." [Online]. Available: http://www.meteonorm.com/.

[53] "Renewable ninja." [Online]. Available: https://www.renewables.ninja/.

[54] M. Pavičević, T. Novosel, T. Pukšec, and N. Duić, "Hourly optimization and sizing of district heating systems considering building refurbishment - Case study for the city of Zagreb," *Energy*, 2016.

[55] W. Jakob and C. Blume, "Pareto Optimization or Cascaded Weighted Sum: A Comparison of Concepts," *Algorithms*, vol. 7, pp. 166–185, 2014.

[56] "Article 14.1 National Heating and Cooling Plans." [Online]. Available: https://ec.europa.eu/energy/en/topics/energy-efficiency/cogeneration-heat-and-power.

[57] "Programme of Exploiting Heating and Cooling Efficiency Potential for 2016-2030." [Online]. Available: https://ec.europa.eu/energy/sites/ener/files/documents/croatia_report_eed_art_141update_en.pdf.

[58] "Odyssee-MURE." [Online]. Available: http://www.indicators.odyssee-mure.eu/energy-efficiency-database.html.

[59] "CROPEX." [Online]. Available: https://www.cropex.hr/hr/.

[60] "Danish Energy Agency." [Online]. Available: https://ens.dk/en/our-responsibilities.

[61] N. Nakicenovic, P. V. Gilli, and R. Kurz, "Regional and Global Exergy and energy efficiencies," *Energy*, vol. 21, no. 3, pp. 223–237, 1996.

[62] M. A. Rosen, "Allocating carbon dioxide emissions from cogeneration systems : descriptions of selected output-based methods," *J. Clean. Prod.*, vol. 16, pp. 171–177, 2008.

[63] M. Noussan, "Allocation factors in Combined Heat and Power systems – Comparison of di ff erent methods in real applications," *Energy Convers. Manag.*, vol. 173, no. June, pp. 516–526, 2018.

[64] A. Dittmann, T. Sander, and S. Robbi, "Allocation of CO2-Emissions to Power and Heat from CHP-Plants." [Online]. Available: https://tu-dresden.de/ing/maschinenwesen/iet/gewv/ressourcen/dateien/veroefftlg/alloc_co2?lang=en.

[65] M. Harmelink and L. Bosselaar, "Allocating CO2 emissions to heat and electricity." [Online]. Available: http://www.harmelinkconsulting.nl/files/2015-09/harmelinkconsulting-ca8d6d8ab68a5197ace66a1969af4957-allocating-co2-emissions-to-heat-and-ele.pdf.

[66] T. Tereshchenko and N. Nord, "Uncertainty of the allocation factors of heat and electricity production of combined cycle power plant," *Appl. Therm. Eng.*, vol. 76, pp. 410–422, 2015.

[67] H. Lund *et al.*, "Simulation versus Optimisation : Theoretical Positions in Energy System Modelling," *Energies*, pp. 1–17, 2017.

PAPER 4

Energy, Sustainability and Society

ORIGINAL ARTICLE Open Access

The establishment of a micro-scale heat market using a biomass-fired district heating system

Tihamér Tibor Sebestyén[1*], Matija Pavičević[2], Hrvoje Dorotić[2] and Goran Krajačić[2]

Abstract

Background: Local biomass potential in Southeastern European countries is relatively high. Nevertheless, biomass residues such as wood leftovers, straw and energy crops are often not properly managed or inefficiently utilised for energy purposes in individual house heating or domestic hot water preparation. This is more relevant in rural areas, where the utilisation of biomass resources is mainly based upon traditional technologies, has low efficiency or is carried out by using individual bases without local energy supply management. Usage of biomass residues in combination with other renewable energy sources is in agreement with the targets of the EU's Energy and Climate Goals and promotes rural development and a circular economy.

Methods: For this purpose, local heating and domestic hot water preparation demands, as well as the available biomass potentials, were analysed and mapped by using a geographic information system (GIS). A model for analysing the optimal operation of the district heating boiler with a relatively high share of solar energy, which is backed up by either a short- or long-term heat storage, was developed. The model takes the supply and the return temperatures from the DH network into account and decides whether the excess of solar heat produced by the prosumers can be delivered into the network. This reduces heat overproduction and enables a smooth and uninterrupted operation of the system. Such configuration would benefit both the DH Company and the prosumers. The DH Company would have the opportunity to buy cheaper excess heat from the prosumers rather than to start its own and relatively slow biomass boiler.

Results: In this paper, several scenarios are proposed for the Romanian village Ghelinta. The target village is characterised by a small-scale biomass district heating boiler with thermal storage and prosumers with either solar thermal collectors or locally installed heat pumps. Integration of seasonal thermal storage and local prosumers can smooth out the biomass district heating boiler operation and bring additional socio-economic benefits for the bioenergy village communities. This could be the first step towards the establishment of a micro-scale thermal energy market.

(Continued on next page)

* Correspondence: sebesten_tiha@yahoo.com
[1]Faculty of Geography, Department of Geography in Hungarian, Babes-Bolyai University, Cluj-Napoca, Romania
Full list of author information is available at the end of the article

(Continued from previous page)
Conclusions: Analysis has proven that the proposed system configuration is socio-technically feasible, even for micro-scale systems, as apparent in the Romanian target village Ghelinta. The main objective of this research is to analyse the implementation of a small-scale biomass and renewable energy-based district heating system and to prove the concept of bioenergy villages from a technical and economical perspective. Furthermore, the role of residential household prosumers has been analysed. Based on outcomes, the transferability of the results is also discussed, while several suggestions for stakeholders who implement such projects were formulated for future research as well.

Keywords: Biomass, Solar, District heating, GIS, Optimisation, Energy market

Background

According to the EU statistics, in EU households, heating and hot water alone account for 79% of the total final energy use. In many rural areas, natural gas is one of the most common fossil fuels used [1]. Thus, a decrease of fossil fuel consumption in the heating sector offers the highest potential for achieving a more energy secure region. Although district heating (DH) is a commonly used technology, in South-Eastern Europe, it is relatively old, inefficient and rarely considered in rural areas.

In this perspective, during the last couple of years, an interest in research, development and implementation of renewable energy sources (RES) has been constantly increasing. The main triggers for this are concerns with regard to the security of local energy supply, spreading of new, low-carbon technologies and energy price increases. Another important factor is also the local population's increased awareness of on-going climate change, mainly caused by the use of fossil fuels and inefficient conventional energy systems.

In the following sections, the listed aspects are to be discussed and the importance of the present research will be argued.

Is it technically feasible?

As the utilisation of RES is becoming more accessible on both small and medium scales [1, 2], the RES-based district heating systems (DHSs) are interesting technological approaches. The RES-based DHSs can guarantee not only new environmental but also financial benefits for end consumers [3]. In the past, a centralised heating system consisted of a heating plant, a distribution grid and in-building distribution systems. Such systems have utilised fossil fuels of high energy content, such as coal and fuel oil, with significant emission levels of greenhouse gases (GHG).

One of the most important issues is the security of energy supply on a local level. In order to increase the utilisation of RES, studies on the possibilities for use were performed in different sectors and on different scales. Advanced research to investigate the application of RES for the energy supply of DHS is taking place. It has also been identified in research studies that in rural areas, local RES such as biomass, solar and geothermal energy, could be included in the local heating supply in a harmonic and sustainable way, while in urban areas the heating demand is usually higher than the available local RESs [4]. On the other hand, the utilisation of RES in rural areas can strengthen regional cohesion and mitigate the underdevelopment of rural areas [5]. The technological combination of different systems such as those based on solar energy and biomass is a viable solution for local heating supply [6]. This is especially relevant in the DHS where solar and biomass energy are integrated, sometimes also in combination with geothermal energy.

Energy mixes in DHSs for a more sustainable energy management and affordable thermal energy services were discussed by Lund, and a new generation of DHSs was implemented [2]. New technologies such as the 4th generation of DHSs [2] and the 5th generation of DHSs combined with cooling have been elaborated and are being implemented today [7]. Giuntoli et al. [6] have applied a bottom-up approach that considers virtual power plants (VPPs) as very promising instruments for the establishment of an effective integration of distributed generation (DG) and energy storage devices. The low-carbon technologies in DHSs are widely analysed in the literature and tested in various DHSs in Denmark, Germany, Sweden, etc. Rämä and Wahlroos [8] have assessed the introduction of heat pumps for a new renewable heat supply in an existing district heating system with a combination of solar collector and biomass-based CHPs. The paper that is based on an *EnergyPro* modelling tool provides optimum operation conditions of heat pumps, which have been investigated in Helsinki in a case study. Other papers have highlighted that solar heating systems in district heating networks with large CHP plants have been rarely considered in the literature [9]. To increase the feasibility of this approach, hourly based data of heat demand, solar

radiation data and efficiency factor of collectors have to be taken into consideration, while the amount of seasonal storage should also be determined. By using a Matlab code, Winterscheid et al. [10] have demonstrated that a sub-network can operate without a back-up boiler, while solar and CHP networks benefit from the interaction. Based on experimental outcomes from Sweden and Germany, solar heat helps to avoid having to start up and shut down wood-chip boilers or operate them at partial load. The combination of solar and biomass technology can even replace back-up fossil fuel systems, which provide district heating networks with energy in summer time [11]. However, examples such as Västra Götaland in Sweden mainly deal with larger biomass systems (4 MW_{th}) combined by photovoltaic plants (1000 m^2) and buffer storage (200 m^3) (SDHp2m) [12].

Is it economically feasible on a micro-scale?

Our main research focus, however, centres on how district heating systems should be realised on a micro-scale heat market, when they are based on a mix of different renewable energy sources.

In terms of energy prices, different research studies have been carried out for the optimisation of micro-grids on the electricity market. Zachar et al. [12] have explored the stochastic scheduling of power micro-grids, where energy exchange with the micro-grid must be coordinated ahead of time. In particular, a market structure is proposed in which micro-grid operators make upfront energy exchange commitments. The optimisation is used to minimise operational cost and ensure the stability of energy exchange. Using the TRNSYS 17 software, Rodrígez et al. [13, 14] have assessed the performance of several designs of hybrid systems composed of solar thermal collectors, photovoltaic panels and natural gas internal combustion engines. The main contributions to this paper are the calculations of primary energy consumption and emissions and the inclusion of a Life Cycle Cost analysis. G [6, 15]. applied Model Predictive Control (MPC) logics to minimise the energy costs, to sustain optimal environmental comfort and to optimise the renewable energy source for energy supply of residential buildings. In 2013, Giuntoli et al. [6, 16] presented a new algorithm to optimise the upfront thermal and electrical scheduling of a large-scale VPP (LSVPP). The approach includes many small-scale prosumers, energy storage and cogeneration processes. This algorithm also takes into account the actual location of each distributed energy resource in the local public network and their specific capability. On this basis, later on, Wang et al. [16] have elaborated a widely cited modelling and optimisation method for planning and operating the CHP-DH system, where the core focus is the minimisation of overall costs of net acquisition for heat and power in deregulated power markets.

In one of the studies, Jing et al. [17] have investigated the annual dynamic performance of those systems with an hourly time step. Here, the operating strategy is optimised with the aim of minimising the total system cost. In another scientific study by Marugán-Cruz et al. [13], the technical and economic feasibility of the introduction of solar energy received by heliostats of a solar tower during the summer season in a heating and cooling network has been demonstrated. Flynn and Sirén [18] have investigated a solar district heating system combined with thermal storage, which is installed in a small Canadian community. Using the TRNSYS software, the investigation analyses the performance of the DHS while taking into consideration climatic conditions. According to the results, the adoption of the 4th-generation heating systems combined with isolation leads to a successful heating system, where solar energy covered the local heat energy demand. Likewise, several authors have created a dynamic simulation model with regard to the energy economic assessment of geothermal, solar and biomass energy [19–21]. The proposed system has been modelled using the TRNSYS tool. Several applied studies have been executed in Northwestern Europe, such as in Oslo, Norway, where integrated energy systems with heat pumps and long-term thermal storage are a promising solution [20].

In many cases, the profitability of the investment in small-scale biofuel-fired DHS or CHP plants has been analysed. In those cases, the assessment of production, distribution and consumption of heat is realised. The results indicate that the economically feasible scale for biomass-based DHSs remains relatively large when a biomass boiler is among the heat production options, while the feasibility of small-scale CHP plants (under 1 MW) remains doubtful [21]. Other studies underline that the introduction of solar energy to thermal systems needs a solution to surmount the mismatch between solar energy supply and heating demand. Thus, the inclusion of thermal storage in a solar thermal system has great importance for an effective and efficient use of discontinuous solar radiation. Nowadays, there are many technical solutions for storing solar energy. From a geographical and climate point of view, the integration of long-term (seasonal) storage is a solution for northern areas because of the significant time shift between the solar radiation period and the heating demand, on a daily or seasonal basis. Kyriakis and Younger [21, 22] have studied the introduction of thermal storage into a geothermal district heating system (GDHS) whose main purpose is related to covering the peak loads in the system. Verda and Colella [22] have modelled a multi-scale thermal storage in order to analyse its operation during

the heating season and to predict their effects on primary energy consumption and cash flows within the district heating service. The results show that primary energy consumption can be reduced by 12%, while the total costs can be reduced by up to 5%. Calise et al. [23] have highlighted that in the case of Pantelleria Island, a district heating and cooling system, based on solar and geothermal sources, can cover the heating and cooling demands. In this case, a very precise control strategy has been implemented in order to avoid any heat dissipation, to match the appropriate operating temperature levels in each component, to avoid a too low temperature of geothermal fluid reinjected into the wells and to manage the priority of space heating and cooling processes [24, 25].

The energy supply of the solar-assisted residential area "Vallda Heberg, Kungsbacka" constructed between 2011 and 2016 in Sweden is characterised by a 100% renewable heating solution, a solar fraction of at least 40%, passive house standards and a reduction of heat distribution costs [http://solar-district-heating.eu/Portals/0/CasestudiesSDHplus/SE_D3.2_ValldaHeberg_EN.pdf]. A novel heating system installed in the residential area with a central wood-pellet boiler of 300-kW capacity (+ 500-kW oil back-up boiler) not only covers the head demand but also delivers heat to four substations characterised by a decentralised storage [26]. The substations are connected to a secondary distribution network, where the hot water circulation realises the space heating and domestic hot water demands. In addition, roof integrated flat plate collectors on the larger buildings deliver solar heat used for the pre-heating of domestic hot water in the substations through evacuated solar tube collectors installed at the central boiler house with steeper inclination angles for achieving optimised solar energy yields in winter time. The solar active surfaces represent 570-m^2 flat plate collectors (FPC) and 108-m^2 evacuated tube collectors (ETC). These installations are able to provide 37% of the useful thermal energy demand for the 14,000-m^2 heated floor area. These numbers are even more impressive if one considers that no seasonal storage is needed to reach this high solar fraction. The thermal storage volumes are distributed between the 13 substations and represent 75 m^3 [27].

Lindenberger et al. [28] have analysed a DHS based on solar collectors combined with seasonal storage in a small-scale pilot project of the Bavarian Research Foundation from a technical point of view. In that system, integration of condensing boilers, compression and absorption heat pumps as well as CHP have been analysed. This system is used to cover the annual total heat demand of 616 MWh from the nearby housing area [29]. An analysis compares this approach with a reference case using individual natural gas boilers and electricity taken from the public grid. Here, the most favourable scenario has a potential to achieve energy savings of between 15 and 35%. Nowadays, a few hundred solar-biomass district heating plants are in operation, where the lowest capacity has always been higher than 500 kW, and projects financed by the European Commission highlight the will to increase the interest in technical solutions based upon renewables and their adoption in the EU countries [30].

The operation of district power and heat energy supply systems was analysed by using stochastic optimisation in the case of a district of buildings on the campus of the University of Utah, USA [31]. The investigation integrates solar PVs and wind turbines for power generation along with using the existing electrical grid, while a CHP system provides power and thermal energy for heating. Electricity is used to run all of the cooling equipment. To analyse the stochastic power generation from renewable energy resources in the district, the Monte Carlo study has been applied. The optimisation of the energy supply is performed by the use of a particle swarm optimisation (PSO) algorithm based on a day-ahead model. The objective of the optimisation was to minimise the operating costs of the district. In this case, the results of the study have suggested that the proposed district power and heat energy supply might achieve 10% operating cost reductions with regard to the current system. This approach shows certain energy management solutions in different time periods that could be useful for facility managers to evaluate the operating costs of their energy supply [31].

The aim of the present research

Based on a literature review, the aim of the present research is to analyse the feasibility and socio-technical aspects of a micro-scale DHS, to optimise not only the operation of combined thermal energy services among the energy producers, prosumers and consumers, but also the storage and the costs for thermal energy supply services on a local level for the concept of a bioenergy village.

In this paper, the authors have analysed the establishment of a micro-scale heat market, having the case study from the Romanian village of Ghelinta. The proposed local market consists of a biomass-fired DH system, seasonal thermal energy storage and local prosumers that have the ability to feed excess heat produced by solar collectors or heat pumps into the network. The model takes the supply and the return temperatures from the DH network into account and decides whether the excess solar heat produced by the prosumers can be delivered into the network. This reduces heat overproduction and enables a smooth and uninterrupted operation of the system. Such configuration would benefit both the

DH Company and the prosumers. With the establishment of the market, a DH company would have the opportunity to reduce its operational costs by buying cheaper excess heat from the prosumers instead of starting its own and relatively slow biomass boilers. In order to validate the model, several scenarios have been modelled. The hypothesis of the paper is that the establishment of a micro-scale heat market would bring seasonal thermal storage together with local prosumers who could smooth out the operation of biomass district heating boilers and provide additional socio-economic benefits to the bioenergy village community. This could be the first step towards an establishment of a micro-scale thermal energy market. Analysis has proven that the proposed system configuration is socio-technically feasible, even with the proposed micro-scale systems.

The innovations within this paper are the outcomes and detailed arguments for the establishment of a thermal energy market on a local scale with a prosumer concept inspired by the electricity market and upfront energy pricing. According to the results, the new thermal energy market and supply system from a technical and economic perspective is feasible, while the price of sold thermal energy is foreseen to be significantly cheaper for the end consumer by using the below detailed approach.

From this point of view, the present novel approach could be implemented not only in the studied framework and location, but also in other regions and countries where local biomass, solar and geothermal energies are available and the local community is engaged in utilising RESs and combating climate change.

Data and methods

Mathematical model

The following model is a social welfare maximisation problem (i.e. minimisation of energy costs for the final consumer, decrease of impact on the environment, better housing conditions by using state-of-the-art energy supply systems) which is inspired by the European day-ahead electricity market clearing model developed by the Greek authors given in [32]. It is based on the following assumptions:

1. There are two homogenous and perfectly divisible inputs, quantity (kWh) and its specific price (€/kWh). They are supplied in fixed amounts.
2. The prices are also fixed and represent marginal prices of heat produced by various technologies and sources.
3. Modelling of seasonal storage is simplified in order to speed up simulation time.
4. Thermal losses in storage are given in terms of charge/discharge efficiencies.
5. The size of storage is determined retroactively.
6. Heat has to be supplied to the consumers at any price.

Objective function

The following equation represents the objective function of the analysed problem. It is a mixed integer linear programming (MILP) problem, whose aim is the maximisation of the overall social welfare w_{tot}, under a set of primal decision variables $V = \{x_{\mathrm{dn}}{}^{t}, x_{\mathrm{sn}}{}^{t}, x_{\mathrm{bo}}\}$:

$$w_{\mathrm{tot}} = c_{\mathrm{dem}} - \left(c_{\mathrm{sup}} + c_{\mathrm{bo}}\right) \tag{1}$$

where w_{tot} is the overall social welfare, c_{dem} is the total demand, c_{sup} is the supply and c_{bo} represents the block orders.

The total demand function is given as follows:

$$c_{\mathrm{dem}} = \sum_{d \in D} \sum_{n \in N} \sum_{t \in T} \left(P_{dn}^{t} \cdot Q_{dn}^{t} \cdot x_{dn}^{t}\right) \tag{2}$$

where $P_{dn}{}^{t}$ and $Q_{dn}{}^{t}$ represent the price-quantity pair of step n of the hourly priced demand bid d in trading period t, in €/MWh and MW, respectively. $x_{dn}{}^{t}$ denotes the acceptance ratio of step n of the hourly priced demand bid d in trading period t.

$$C_{sup} = \sum_{s \in D} \sum_{n \in N} \sum_{t \in T} \left(P_{sn}^{t} \cdot Q_{sn}^{t} \cdot x_{sn}^{t}\right) \tag{3}$$

where $P_{sn}{}^{t}$ and $Q_{sn}{}^{t}$ represent the price-quantity pair of step n of the hourly priced energy offer s in trading period t, in €/MWh and MW, respectively. $x_{sn}{}^{t}$ denotes the acceptance ratio of step n of the hourly priced energy offer s in trading period t.

$$C_{bo} = \sum_{bo \in BO} \sum_{t \in T} \left(P_{bo} \cdot Q_{bo}^{t} \cdot x_{bo}\right) \tag{4}$$

where P_{bo} and $Q_{\mathrm{bo}}{}^{t}$ represent a price-quantity pair of block order bo, in €/MWh and MW, respectively. In the case of a profile block order, the quantity may be different in each trading period t. x_{bo} denotes the acceptance ratio of block order bo. It is important to note that in the proposed mathematical formulation $Q_{\mathrm{bo}}{}^{t} \leq 0$ represents all demand block bids and $Q_{\mathrm{bo}}{}^{t} \geq 0$ all supply block offers.

Order clearing constraints

The objective function results in the following set of order clearing constraints that enforce that the clearing status of the profile block order is always either 0 or between its minimum and maximum acceptance ratio:

$$R_{bo}^{min} \cdot y_{bo} \le x_{bo} \le y_{bo} \forall bo \in BO \quad (5)$$

where $R_{\mathrm{bo}}^{\min}$ is the minimum acceptance ratio of block order bo, in %, and y_{bo} of the binary variable denotes the clearing status of block order bo. In the case of a maximum acceptance ratio x_{bo}, y_{bo} values are equal to 1. When the regular block orders are $R_{\mathrm{bo}}^{\min} = 1$, the respective constraint transforms into a classical "fill-or-kill" constraint offering either all or nothing. Likewise, the following constraint denotes the upper limits for the clearing of the demand bids and supply offers.

$$\begin{aligned} x_{dn}{}^{t} \le 0 \forall d \in D, n \in N, t \in T \\ x_{sn}{}^{t} \le 0 \forall s \in D, n \in N, t \in T \end{aligned} \quad (6)$$

Heat balance constraints

The objective function results in a heat balance constraint. It ensures that the market is always in an equilibrium. This is done in such a way that the sum of all the demands, supplies and block orders is equal to 0:

$$\sum_{d \in D} \sum_{n \in N} \left(Q_{dn}^{t} \cdot x_{dn}^{t}\right) - \sum_{s \in D} \sum_{n \in N} \left(Q_{sn}^{t} \cdot x_{sn}^{t}\right) - \sum_{bo \in BO} \left(Q_{bo}^{t} \cdot x_{bo}\right) \quad (7)$$
$$\forall t \in T$$

Scenarios

The case study analyses the opportunity for establishing a micro-scale biomass-fired district heating system, whose wholesale prices would be determined on the heat market. The project is in scope of the greenfield investment programme and could be implemented in the target village of Ghelința.

The village of Ghelința is a commune in Covasna County, located in the central part of Romania. It is composed of two villages, Ghelința and Harale. According to the latest census, there is a total of 4722 inhabitants living in 1710 households [33]. The total number of residential, commercial and public buildings sums up to 1895. Local people are mostly employed in the forest industry, transport, retail, manufacturing industry, public institutions and services. The heating in residential buildings is mostly based on old and inefficient wood stoves without any in-house distribution. Since the price of firewood has been increasing at a dramatic rate, central heating and DH solutions are becoming more and more popular in the region. The price of firewood has increased by more than 100% in the last 5 years in Romania because of a stricter monitoring of the logging process, enforced by a new Forest Code, and due to the limited permits for wood extraction that resulted in a raw material crisis in Romania. More than 20 SMEs are active in wood logging and the pre-processing industry.

Table 1 Heat energy demand on target public and private buildings in Ghelinta

Buildings	Heating demand (MWh)	Hot water demand (MWh)	Available rooftop area (m^2)
Medical centre	15.11	3.90	252
Local council	19.01	8.90	86
Mayoralty	2.29	11.20	120
Forest owner association no. 1.	9.31	2.40	84
Forest owner association no. 2.	11.72	5.79	110
Elementary school	21.49	7.29	304
Kindergarten	8.90	2.29	0
Bowling alley	116.20	16.11	168
Church	50.54	216.65	275
Culture centre	32.50	9.89	182
Guest no.1.	42.39	25.14	161
Guest no. 2.	82.38	33.53	140
Block of flats no. 1.	47.12	13.04	0
Block of flats no. 2.	60.17	42.56	0
Block of flats no. 3.	54	11	0
Personage	60.79	16.86	120
Store no. 1.	11	5	112
Store no. 2.	21.55	18.39	0
Store no.3.	29.05	8.73	0
Police	30.56	8.25	128
52 households	1433.97	287.21	0
Total	2160.16	754.23	2242

The local forest area is 6430 ha and offers the largest solid biomass source. According to annual statistics, wood waste and forestry residues were estimated as 3698 tons, which is equivalent to 15,409 MWh/a of heat [34]. However, the available amount of wood for energy production in Ghelința is only a few hundred tons per year, not only due to the limitation in wood extraction and the increase in raw material efficiency during wood processing in the forest-based industry, but also due to an increase in the price of logs with the result that only bigger companies can manage the supply of local or regional wood manufacturing companies.

Given the local circumstances in Ghelinta, the following assessment focuses only on the most suitable

Table 2 Technologies used in different scenarios

Scenario	Biomass boiler	Thermal storage	Heat pump	Solar thermal
Scenario 1	2	1	0	20
Scenario 2	2	1	20	0
Scenario 3	2	1	10	10

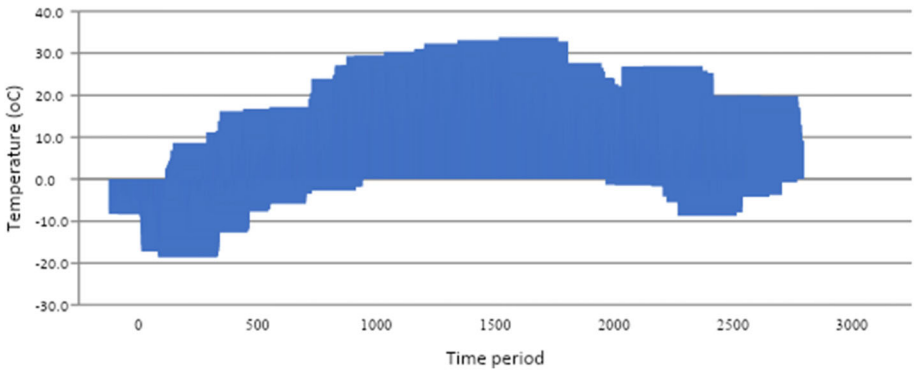

Fig. 1 Outside temperature in the target village

locations for DH systems. These are mainly public buildings and residential households located in the village centre. A list of all buildings is provided in Table 1. The data provided by the Municipality of Ghelinta, in combination with the proposed assumptions and the calculations carried out, reflects the initial status of the assessed project. The proposed project is strongly backed up by the Local Council of Ghelinta. The main issue is also, for instance, a strong trade-off between the DH price (the economic viability of the plant) and its attractiveness for potential DH consumers.

Space heating and domestic hot water demands were estimated by the degree-hour method proposed in the literature [34]. This method is based on known values of total heating demand and outside air temperature, acquired by using various publicly available databases such as PVGIS, and assumed a constant inside temperature for every hour of the year. The hourly differences between these two temperatures are called degree-hour. It is assumed that hourly heating demand is proportional to the temperature difference [7]. Based on the given heating needs, technology-specific investment costs as well as biomass and electricity prices, a levelised cost of heat was calculated for each technology. The reference price would presuppose that only biomass boilers operate and that their marginal price is equal to 0.031 EUR/kWh. However, in the present research paper, the DH consists of two boiler units and a seasonal thermal energy storage that could either store heat when the prices are low or deliver it to the network when the prices are high. All 20 public buildings represent prosumer units that can cover their own heat via solar thermal collectors or heat pumps. Their operation is configured in such a way that local heating demands are firstly covered by local sources and afterwards all excess heat can be offered on the market at marginal prices. The 52 residential buildings in Table 1 are considered as consumer units in the simulations. In order to show that such configuration is economically viable, three different scenarios were modelled. The number of all available technologies in the different scenarios is presented in Table 2.

Local climate in the studied area is a moderate continental climate influenced by the nearby mountain region. The mean daily maximum in August is 22 °C,

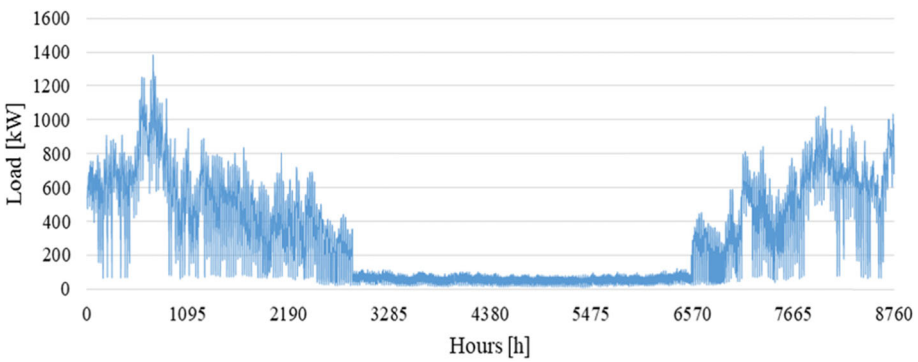

Fig. 2 Hourly heating demand

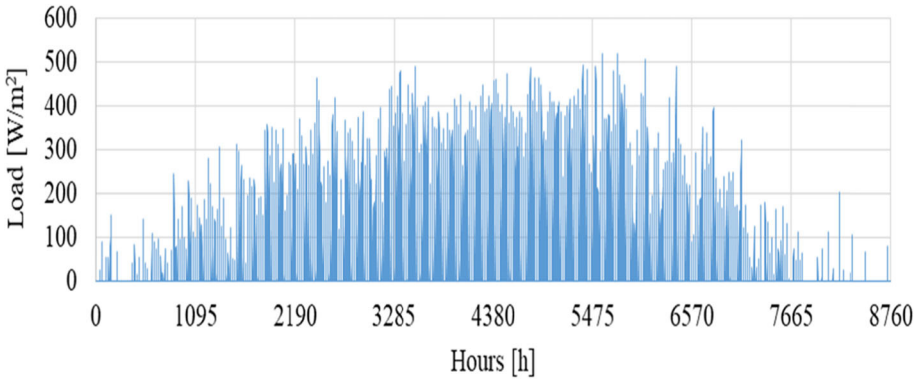

Fig. 3 Hourly solar thermal production

while in January and February, the mean daily minimum is − 6 °C. The minimum temperature accounts to − 28 °C during January, while the maximum temperature can be higher than 34 °C during July. Under normal conditions, the heating season starts on the 10th of October and, depending on the weather conditions, usually ends after the 15th of April (see Fig. 1). The hourly distribution of heating demand and the hourly solar thermal production are also shown in the following figures (Figs. 2 and 3).

Results and discussion

The simulation results of the previously defined scenarios are demonstrated in the following figures. They consist of the hourly marginal cost price, the prosumer's thermal net flow including thermal storage charging and finally the heat-only-boiler operation. Figure 4 shows scenario 1 results. The top image represents the hourly distribution of marginal prices. It can be seen that the lowest market thermal prices (0.028 EUR/kWh) are reached during the summer period due to the excess

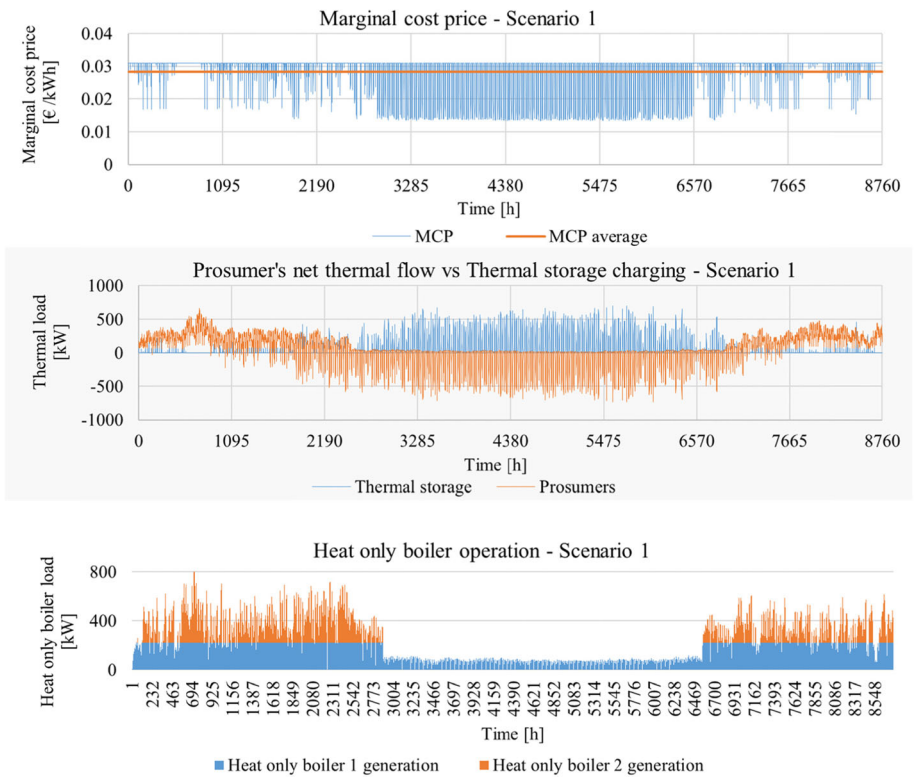

Fig. 4 Scenario 1 results: marginal cost price (top), prosumer's net thermal flow and thermal storage charging (middle) and heat-only boiler operation (bottom)

production of the solar thermal collector. This is also evident in the middle diagram which demonstrates a negative net thermal flow of the prosumer units. This means that seasonal thermal excess of heat is available and stored, as presented in Fig. 5. The bottom diagram of Fig. 4 demonstrates the operation of heat-only boilers. The larger biomass heat-only boiler operates exclusively during the winter season, while the smaller one operates throughout the year. The reason for this is the intermittent and insufficient production of the solar thermal collectors during the summer period.

Scenario 2 results are depicted in Fig. 5 and displayed in a similar manner. The marginal cost price during the summer period (0.025 EUR/kWh), including the overall average MCP, is lower when compared with the other two scenarios. The reasoning behind this is a great excess of heat from prosumer units due to the large capacity of installed heat pumps. This is happening only when the electricity costs are so low, that it makes economic sense to produce energy. Since they are located in all public buildings, such as schools and offices, they do not have a heat demand to cover the needs during long periods of time. This excess heat could be efficiently sold on the market at low market prices. When compared to scenario 1, these prosumer units have a smaller negative net thermal flow peak, but are operated at a more constant load. This is the main reason why in this scenario, the heat-only boilers do not operate in summer time.

Scenario 3 includes prosumers which have installed heat pumps or solar collectors (Fig. 6). Because of this, the marginal cost price is between the value of scenario 1 and that of scenario 2. In this scenario, excess heat peaks from the prosumers are visible during summer time. This is the reason why a larger thermal storage is needed here compared to the second scenario. Although heat pumps are installed in a number of public buildings, a smaller heat-only boiler has to be operated during the summer period which increases the overall average marginal cost price, but not at such a high level as in scenario 1 (see Table 3).

All in all, three different scenarios were determined in the results with the aim to analyse the marginal costs reached by using different technologies and combinations of renewable energy technologies. The role of the prosumers in thermal energy flow was demonstrated while the operation of boilers was also optimised.

According to the results, as expected, scenario 1 required the largest seasonal thermal storage of up to 400

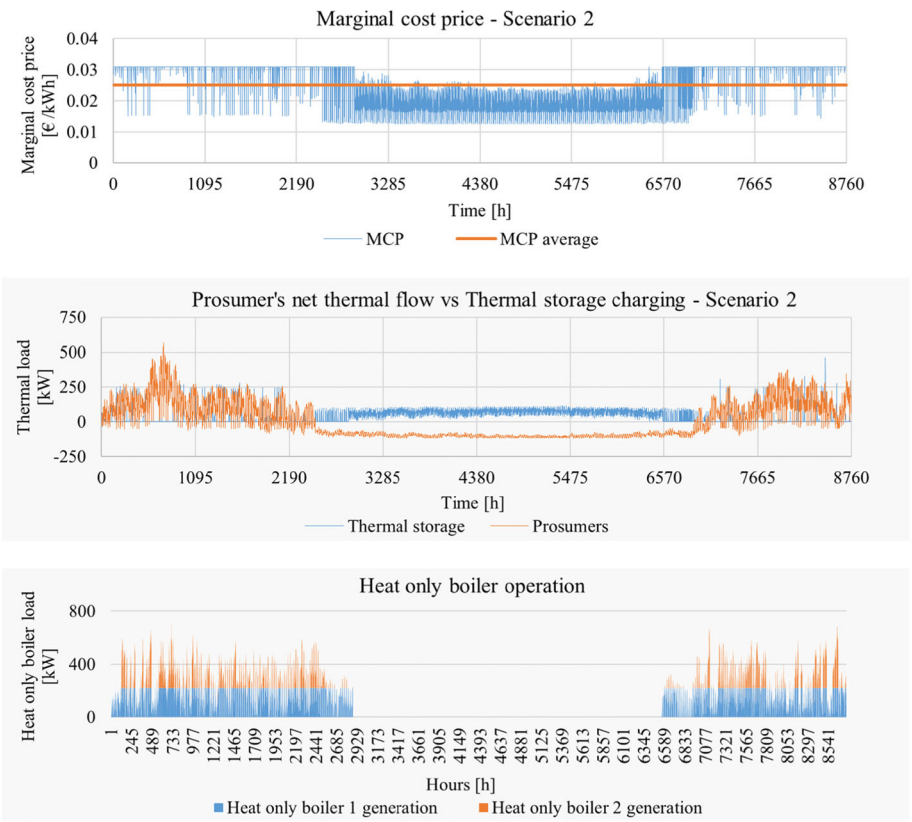

Fig. 5 Scenario 2 results: marginal cost price (top), prosumer's net thermal flow and thermal storage charging (middle) and heat-only boiler operation (bottom)

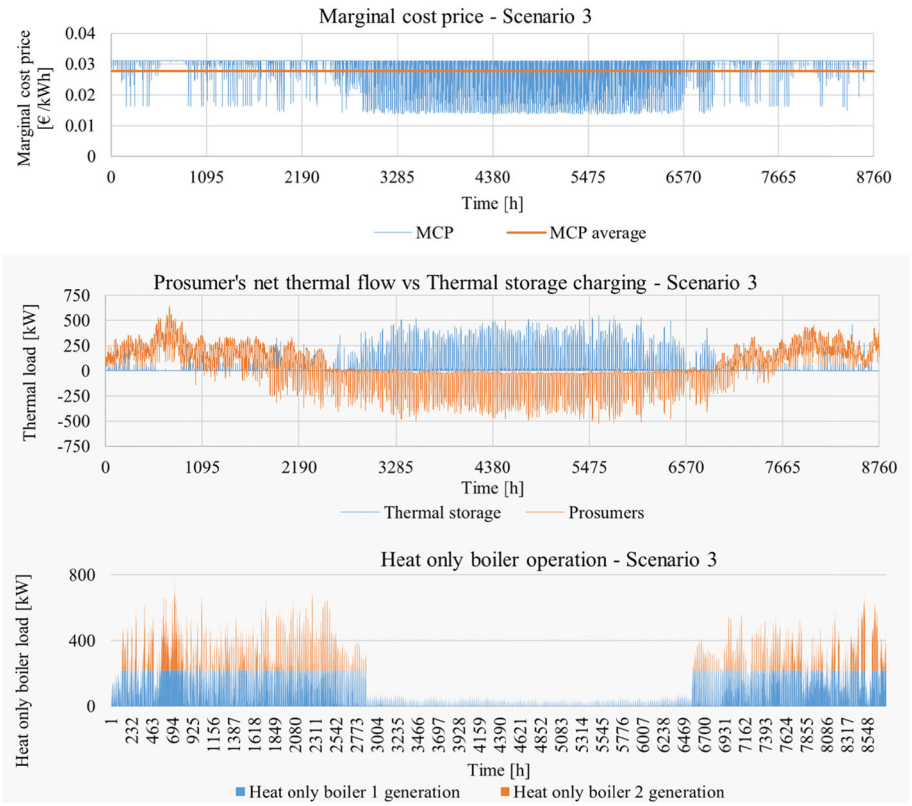

Fig. 6 Scenario 3 results: marginal cost price (top), prosumer's net thermal flow and thermal storage charging (middle) and heat-only boiler operation (bottom)

MWh due to the large amount of installed solar thermal collectors. The smallest thermal storage is needed in scenario 2 which had, as explained before, the lowest marginal cost price. Charging and discharging trends are the same in all three scenarios. Thanks to the different modelled scenarios, the optimisation of the local thermal energy market was performed. The best economic and technical approach is to install a larger number of heat pumps at public buildings to achieve an excess of heat from prosumers and sell this thermal energy efficiently on the market at low market prices, using the seasonal storage. Thermal storage level and thermal storage capacity per scenario are given in Fig. 7. The size of the thermal storage has also been simulated and indicated that the lowest level was achieved in scenario 2 with a 250-MWh storage level. If we implement a large number of solar collectors, the required capacity of thermal storage is significantly higher. It is noteworthy to mention that to construct a larger seasonal thermal storage would be the most expensive option.

Table 3 Marginal cost price and thermal storage size comparison

	Scenario 1	Scenario 2	Scenario 3
Marginal cost price [€/kWh]	0.028	0.025	0.027
Thermal storage size [kWh]	400.558	276.505	335.938

It is also demonstrated how important the role of thermal seasonal storage is. With the aim to mitigate CO_2 emission during the operation of the entire facility, the capacity of the biomass boiler and the working hours for this boiler were reduced by the introduction of a seasonal storage and dynamic energy market model. The biomass boiler was operated only when the heating and hot water demand was remarkably high, as especially during wintertime. The operator of the seasonal storage can balance the production and consumption curves. Thus, the present approach helps us to decrease the biomass consumption by 50% compared to the initial case and volume of firewood used in Ghelinta's public buildings. Actually, thermal storage reached its lowest level at nearly the same hour with all three scenarios. Figure 8 indicates the hourly block orders for larger heat-only boilers. Again, it can be noticed that there are no orders during summertime, and therefore the reason why it does not operate during the summer season. Block order distributions are almost the same in all three scenarios, but it can be observed that in scenario 1, more heat was provided compared to the least amount shown in scenario 2. This is an additional reason why the second

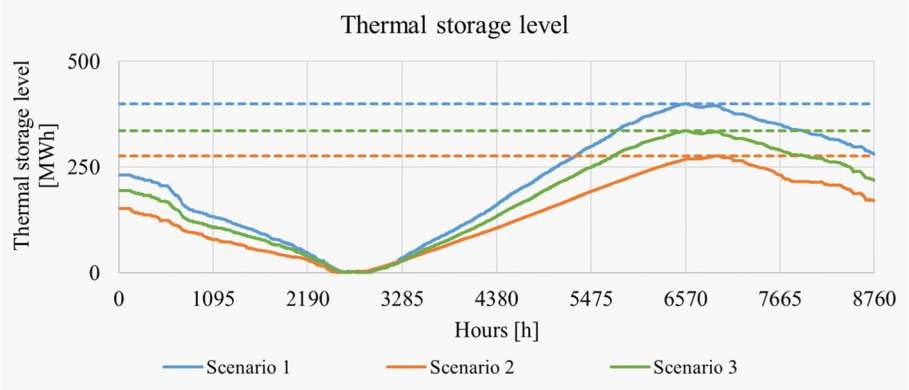

Fig. 7 Thermal storage level per scenario

scenario has the lowest marginal cost price, as is finally also evident from Fig. 9 and Table 3.

Conclusions

The first novelty of this paper is the description of the establishment and analysis of a micro-scale thermal energy market on a local level. The method described and applied in this paper represents a classical mixed integer programming model influenced by EUPHEMIA algorithm of a day-ahead market. It takes into account both continuous orders and block orders on both sides, namely the heat supply side and the heat and domestic hot water demand side. In this connection, the EUPHEMIA algorithm, which is basically used to compute the day-ahead electricity prices, is used in this paper to model the day-ahead thermal energy prices. It has to be admitted that such an approach was not applied in the simulation of thermal energy supply systems.

The main lesson learned from this paper is that the utilisation of an RES mixture in DHSs is possible, even on a micro-scale, but the optimisation in timing, the utilised energy source and the energy use for final consumers and prosumers are crucial aspects. When an algorithm of the day-ahead market is implemented, it can significantly reduce the energy price for end consumers, which is one of the most convincing factors in the decision-making process. This technical and energy management approach has to be disseminated to local communities, and long-term thinking could support the local sustainable energy management. Likewise, through optimisation of thermal energy production and appropriate utilisation of energy, a balance could be achieved so that "just enough" energy would be produced for the thermal energy supply of local final consumers.

The model was applied to the 52 residential households and 20 commercial and public buildings located in the centre of the Romanian municipality of Ghelinta. On the one hand, the residential households were modelled as consumers (consumer units) that buy heat from the local heat market. Commercial and public buildings using solar technology were modelled as prosumers (prosumer units) that are able to produce enough heat to cover their own heating needs and sell excess heat on the market. The biomass-fired district heating company, as the largest producer, can also act as a prosumer as it owns a large seasonal thermal energy storage capacity

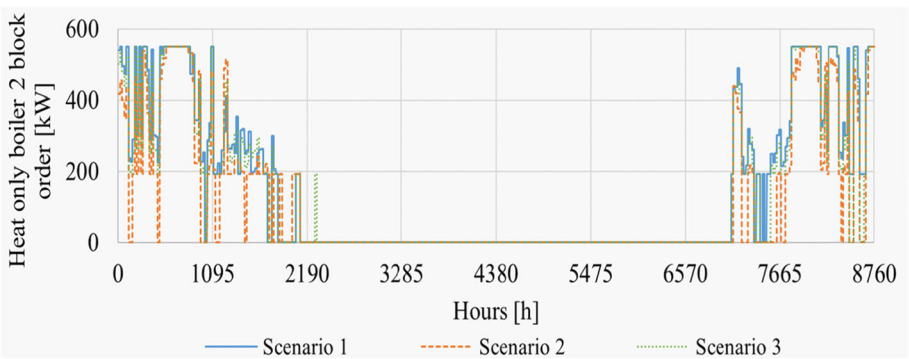

Fig. 8 Block order of heat-only boiler 2 per scenario

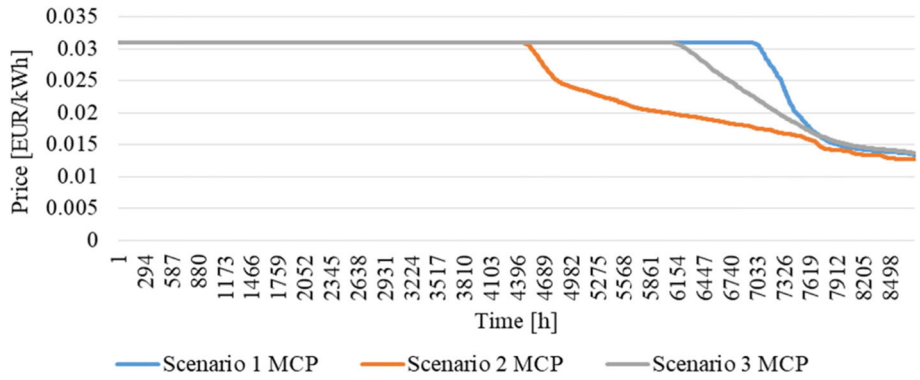

Fig. 9 MCP duration curve comparison

and can buy heat when the prices are low and sell when the prices are high. Thermal energy production was modelled depending on price of production, solar irradiation, daily and seasonal energy demand, peak load and other parameters. In order to mitigate the significance and installed capacity of the biomass boiler, a seasonal storage and dynamic energy market model was introduced. The biomass boiler has to be operated when the heating and hot water demand is remarkable, during wintertime. The operator of the seasonal storage can balance the production and consumption curves.

District cooling (DC) was not analysed in this paper because of the climatic conditions in the studied target village Ghelința, where there was no expressed need for cooling.

On the other hand, scenario analysis has proven that the proposed system configuration is socio-technically feasible, even for micro-scale systems as shown by a case study for the Romanian target village Ghelinta. Scenario analysis has also proven that the establishment of a heat market can have positive impact on the heat prices as is evident in all analysed cases. In a best-case scenario, the price of heat could be reduced by up to 18% compared to the classical biomass district heating system. The outcomes of the presented paper not only encouraged the local decision-makers to study the feasibility of a micro-scaled heat market in 2018, but also to develop and submit an innovative project proposal for implementation in the POIM 6.1. National subsidy programme in Romania. This concept should be realised in 2020–2021. Since this analysis is a work in progress, an optimised technical planning and reliable cost survey have to be performed in order to make calculations as well as the end results more accurate. These are the first steps planned for the future, while the final step would involve a full socio-techno-economic analysis of the proposed case study from which more concrete conclusions could arise.

Another innovation of this paper is that the outcomes confirmed the feasibility of an establishment of a thermal energy market on a local level, while the introduction of the prosumer concept supported the decrease of the final price of thermal energy for the final consumers, by remarkably 18%.

The presented village offered us a business-as-usual case from South-Eastern Europe where several public and commercial buildings are located in the village centre, while the households are closely located to these buildings. In our consideration of the climatic, architectural, economic and social framework, a large number of rural settlements exist for which by using a similar approach, the local thermal energy market can be established.

The present study offers a guideline for other research and design activities by demonstrating the most important aspects of the optimisation of biomass-based district heating systems with seasonal storage, mixing of solar and geothermal sources, smart energy management on a local micro-scale and optimisation of cost benefits.

Abbreviations

DH: District heating; DHS: District heating system; GIS: Geographic information system; RES: Renewable energy sources; GHG: Greenhouse gases; VPP: Virtual power plant; DG: Distributed generation; CHP: Combined heat and power; MPC: Model predictive control; LSVPP: Large-scale virtual power plant; GDHS: Geothermal district heating system; FPC: Flat plate collectors; ETC: Evacuated tube collectors; PSO: Particle swarm optimisation; MILP: Mixed integer linear programming; DC: District cooling

Acknowledgements

This research was supported by the "Phoenix Project - People for tHe eurOpean bio-ENergy mIX" Exchange of experience between researchers in the field of bioresources. The project is in the frame of the Horizon 2020 EU Program, Stimulating innovation by means of cross-fertilisation of knowledge, MSCA-RISE-2015 - Marie Skłodowska-Curie Research and Innovation Staff Exchange (RISE), grant agreement ID: 690925. We would like to thank our colleagues from the Faculty of Mechanical Engineering and Naval Architecture, University of Zagreb, who provided insight and expertise that greatly assisted the research.

Authors' contributions
The authors read and approved the final manuscript.

Funding
Not applicable.

Availability of data and materials
Not applicable.

Ethics approval and consent to participate
Not applicable.

Consent for publication
Not applicable.

Competing interests
Not applicable.

Author details
[1]Faculty of Geography, Department of Geography in Hungarian, Babes-Bolyai University, Cluj-Napoca, Romania. [2]Faculty of Mechanical Engineering and Naval Architecture, University of Zagreb, Zagreb, Croatia.

Received: 16 May 2019 Accepted: 4 May 2020
Published online: 10 June 2020

References

1. Izquierdo M (2014) An EU strategy on heating and cooling. European Commission 2015
2. Lund H, Werner S, Wiltshire R et al (April 2014) 4th generation district heating (4GDH): integrating smart thermal grids into future sustainable energy systems. Energy 68(15):1–11
3. Hendricks AM, Wagner JE, Volk TA, Newman DH, Tristan R (January 2016) Brown, a cost-effective evaluation of biomass district heating in rural communities. Appl Energy 162(15):561–569
4. Lund H, Möller B, Mathiesen BV, Dyrelund BV (2010) The role of district heating in future renewable energy systems. Energy 35(3):1381–1390
5. Benedek J, Sebestyen T, Bartok B (2018) Evaluation of renewable energy sources in peripheral areas and renewable energy-based rural development. Renew Sust Energ Rev 90:516–535
6. Giuntoli M, Poli D (2013) Optimized thermal and electrical scheduling of a large scale virtual power plant in the presence of energy storages. IEEE Trans Smart Grid 4(2):942–955. https://doi.org/10.1109/tsg.2012.2227513
7. PVGIS (2015) Photovoltaic geographical information system, developed by European Commission joint research center. Ispra, Italy
8. Rämä M, Wahlroos M (2018) Introduction of new decentralised renewable heat supply in an existing district heating system. Energy 154(1):68–79
9. SDH Knowledge Database, 2018, Solar district heating, https://www.solar-district-heating.eu/solar-district-heating-on-the-roof-of-the-world-3-2/
10. Winterscheid et al., Integration of solar thermal systems in existing district heating systems, Energy, Volume 137, 15 October 2017, Pages 579-585,
11. Dalenbäck J-O and Zetterbren G, Feasibility studies for SDH in region VästraGötaland, CIT Energy Management, Göteborg, Sweden, 2018
12. Zachar M, Daoutidis P (2017) Microgrid/macrogrid energy exchange: a novel market structure and stochastic scheduling. IEEE Transactions on Smart Grid 8(1):178–189. https://doi.org/10.1109/tsg.2016.2600487
13. Marugán-Cruz C, Sánchez-Delgado S, Rodríguez-Sánchez MR, Venegas M, Santana D (2015) District cooling network connected to a solar power tower. Appl Therm Eng 79:174–183
14. Rodríguez LR et al (2016) Analysis of the economic feasibility and reduction of a building's energy consumption and emissions when integrating hybrid solar thermal/PV/micro-CHP systems. Appl Energy 165(1):828–838
15. Bruni G et al (2015) A study on the energy management in domestic micro-grids based on model predictive control strategies. Energy Conv Manag 102(15):50–58
16. Wang H et al (2015) Modelling and optimization of CHP based district heating system with renewable energy production and energy storage. Appl Energy 159(1):401–421
17. Jing ZX, Jiang XS, Wua QH, Tang WH, Hua B (2014) Modelling and optimal operation of a15. Small-scale integrated energy based district heating and cooling system. Energy 73:399–415
18. Flynn C, Sirén K. Influence of location and design on the performance of a solar district heating system equipped with borehole seasonal storage. Renewable Energy. 2005;81:377–910 88.
19. Dimitris I. Chatzigiannis, Grigoris A. Dourbois, Pandelis N. Biskas, Anastasios G. Bakirtzis, European day-ahead electricity market clearing model, Electric Power Systems Research (2016), doi: https://doi.org/10.1016/j.epsr.2016.06.019
20. Alberto Carotenuto, Rafal Damian Figaj, Laura Vanoli, A novel solar-geothermal district heating, cooling and domestic how water system: dynamic simulation and energy-economic analysis, Energy (2017), doi: https://doi.org/10.1016/j.energy.2017.08.084f
21. Kyriakis SA, Younger PL (2016) Towards the increased utilisation of geothermal energy in a strict heating network through the use of a heat storage. Appl Thermal Eng 94:99–110
22. Verda V, Colella F (July 2011) Primary energy savings through thermal storage in district heating networks. Energy 36(7):4278–4286
23. Calise F, Macaluso A, Piacentino A, Vanoli L. A novel hybrid polygeneration system21. supplying energy and desalinated water by renewable sources in Pantelleria Island. Energy. 2017.
24. Kari S. et al, 2005, Small-scale biomass CHP plant and district heating, Energy Engineering and Environmental Protection, Helsinki University of Technology, ISBN 951-38-6723-4 (URL: http://www.vtt.fi/inf/pdf/)
25. http://solar-district-heating.eu., accessed on 05.03.2019,
26. Joly M. et al. A methodology to integrate solar thermal energy in district heating networks confronted with a Swedish real case study, in CISBAT 2017 International Conference - Future Buildings & Districts – Energy Efficiency from Nano to Urban Scale, CISBAT 2017, 6-8 September 2017, Lausanne, Switzerland
27. Thomas T et al (2019) Stochastic optimization for integration of renewable energy technologies in district energy systems for cost-effective use. MPDI Energies 12:533
28. Lindenberger D, Bruckner T, Groscurth H-M, Kummel R (2000) Optimization of solar district heating systems: seasonal. Energy 25:591–560
29. SDHp2m, Advanced policies and market support measures for mobilizing solar district heating investments in European target regions and countries, INEA, Project reference: 691624
30. European Commission, http://ec.europa.eu. accessed on 04.03.2019,
31. Thomas T. D. Tran and Amanda D. Smith, Energy technologies in district energy systems for cost-effective use, Energies 2019, 12(3), 533; doi:https://doi.org/10.3390/en12030533
32. Matija Pavičević, Tomislav Novosel, Tomislav Pukšec, Neven Duić, Hourly optimization and sizing of district heating systems considering building refurbishment – case study for the city of Zagreb, Energy, Volume 137, 2017, Pages 1264-1276, ISSN 0360-5442, doi: https://doi.org/10.1016/j.energy.2017.06.105.
33. INS, 2011: Suprafatafonduluiforestier pe categorii de terenurisispecii de paduri, macroregiuni, regiuni de dezvoltaresijudete, Bucuresti
34. INS (2011) Rezultate definitive ale. RecensământuluiPopulației și al Locuințelor – 2011

Publisher's Note

PAPER 5

Impact of wind penetration in electricity markets on optimal power-to-heat capacities in a local district heating system

Hrvoje Dorotić*, Marko Ban, Tomislav Pukšec, Neven Duić

University of Zagreb, Faculty of Mechanical Engineering and Naval Architecture,

Department of Energy, Power Engineering and Environmental Engineering, Ivana Lučića 5, 10002, Zagreb, Croatia

**corresponding author, contact email: hrvoje.dorotic@fsb.hr*

Abstract

While the share of intermittent renewable energy sources in a power sector is constantly increasing, demand response technologies are becoming a crucial part of interconnected energy systems. The district heating sector has a great potential of offering such services if power-to-heat and thermal storage technologies are implemented. This is a well-known method of utilizing low-price electricity from the power market. However, power-to-heat optimal supply capacities are rarely studied with respect to different market conditions, especially from the point of view of multi-objective optimization. This paper shows an analysis of the impact of a wind production increase in a power market on optimal power-to-heat capacities in a local district heating system. To obtain these results, a district heating optimization model was developed by using linear programming, while the power market prices reduction is analysed by using historical bidding market data and shifting of the supply curve. The district heating model was created in the open-source and free programming language called Julia. The model was tested on a case study of the Nord Pool electricity market and a numerical example of a district heating system. The main outcome of this research is to show how district heating supply technologies operate in different market conditions and how they affect optimal power-to-heat and thermal storage capacities. Heat pump capacities linearly follow wind production increase in power markets.

Keywords*:* district heating, energy planning, power-to-heat, power market, multi-objective optimization

Word count: 8 800

Highlights

- The impact of wind penetration in electricity markets on the optimal results of a district heating system has been studied
- The increase of optimal heat pump capacity and heat production linearly follows wind penetration in power markets
- Optimal thermal storage size and heat pump capacity can be doubled for higher shares of wind energy in a power market

Abbreviations

DH	district heating
RES	renewable energy sources
CHP	cogeneration

Chemical formulas

CO_2	carbon dioxide

Variables and parameters

A_{ST}	area of solar thermal collectors [m^2]
a_1	first order heat loss coefficient [W/K]
a_2	second order heat loss coefficient [W/K^2]
C	cost [EUR]
DEM	district heating demand [MW]
f_{ecol}	ecological objective function (tonnes of CO_2)
f_{econ}	economical objective function (EUR)
$f_{Lorentz}$	Lorentz factor of the heat pump [-]
G	global solar radiation [W/m^2]
MCP	market clearing price [EUR/MWh]
MCP'	reduced market clearing price [EUR/MWh]
P	supply capacity [mw]
P_t	hourly market price [EUR/MWh]
Q	thermal energy [MWh]
$r_{up-down}$	ramping limit of technology [h^{-1}]
SOC	state-of-charge [MWh]
T	temperature [K]
TES	thermal storage
TES_{in-out}	thermal storage charge and discharge [MW]
V	market volume [MWh]

Greek letters

η	technology efficiency [-]
η_0	optical efficiency of solar thermal collector [-]

Scripts

D	demand
i	technology type
ref	reference
S	supply
t	time

1. Introduction

This section provides an overview of district heating systems and the power market. Additionally, different market clearing price modelling approaches are shown while focusing on the wind penetration influence. Furthermore, the latest publications dealing with district heating and power sector integration have been reviewed. Finally, the scientific contribution of this paper is presented.

1.1. District heating systems

District heating (DH) is a relatively old concept but has been widely acknowledged as one of the crucial technologies for covering future heating demand [1], [2]. The reduction of specific heating demand will result in a reduction of supply temperatures in the DH system and an increase of overall efficiency of the thermal network. This will open possibilities for the integration of low temperature heat sources and waste heat [3] combined with heat pumps [4]. Lund has defined the fourth generation of DH which is now accepted as the standard for low temperature DH which is integrated with other sectors, thus creating a so called smart energy system [5]. In smart energy systems, DH will have a crucial role by integrating the power and heat sector through power-to-heat technologies such as heat pumps or electrical heaters [5], [6]. These units are able to efficiently and effectively transform electricity into thermal energy [7], [8]. The implementation of booster heat pumps has been studied in [9], while the combination of power-to-heat technologies in the hybrid district heating system is studied also in [10]. Such integration allows a higher penetration of variable renewable energy sources (RES) such as wind or solar photovoltaics into the power sector [11]. Sayegh et al have shown the trend of the research related to DH [12], while emphasizing the importance of thermal storage technologies and integration with other sectors, thus creating a smart energy system. Besides providing a demand response for the power sector, DH will potentially have other important roles, as discussed in [13]. However, some papers have already discussed the next generation of DH and the present existing cases in Europe [14]. Ultra-low temperature district heating systems can offer additional benefits for the integration of heat pumps due to the increased coefficient of performance. Arabkoohsar and Alsagri analysed the impact of integrating heat pumps in DH systems with three pipes [15]. Although researchers are exploring power and heating sector integration, there is still a great number of coal power plants in Europe which need to be refurbished or upgraded in order to reach the standard of the 3rd generation of DH [16].

1.2. Wind integration in power systems

The power market enables the purchasing of electricity through bidding – electricity producers sell electricity, while various consumers can buy it according to the market rules. When market supply and market demand are balanced, market equilibrium is achieved. It is defined with a market clearing price and market volume. Due to their production variability on an hourly level and market readiness, wind energy production and its successful integration in power markets presents a crucial topic for numerous authors. In order to evaluate a market clearing price and conventional production optimization with a high share of wind penetration, various methods have been proposed. Paper [17] studies wind profit maximization in the day-ahead power market by using a utility function which models the behaviour of electricity customers. The main goal is to utilise demand response technologies to achieve a higher profit for wind

generation. Li and Shi adopted an agent-based simulation to analyse the bidding optimisation of wind generation in a deregulated day-ahead power market. They have shown that it is possible to increase net earnings by using learning algorithms [18]. In paper [19] different aspects of wind energy system modelling have been taken into account in order to study the integration of mentioned technologies in a deregulated power market. Reddy et al [20] proposed a novel market clearing mechanism for a wind-thermal power system while taking into account different uncertainties in production. An optimal scheduling strategy has been acquired for a best-fit day-ahead schedule. Paper [21] analysed wind penetration in interconnected regional power systems while taking into account different uncertainties. The authors showed how higher economic efficiency could be achieved by enabling cross-border trading. Fogerlber and Lazarczyk have studied the impact of wind power volatility on production failures in other production units in the power market [22]. The focus was put on Nord Pool. The issue of successful wind power integration into the power market was also studied in paper [23]. The authors analysed the effect of spatial diversification of wind power on its market value. A case study of Chile was used and the obtained results showed that spatial diversification could vary up to $10/MWh. Cuervo and Botero [24] discussed wind power reliability in a hydro-dominated power system, where Colombia was used as the case study. It was shown that higher wind penetration causes higher reservoir levels for the same hydrological conditions. This also caused the reduction of electricity market prices.

1.3. District heating and power market integration

Optimization of DH systems often includes the possibility of utilizing power-to-heat technologies such as compression heat pumps with various heat sources and electrical heaters. Single objective optimization most often includes the minimization of total cost while optimizing supply capacities and the hourly operation of supply units [25]. In research [26], single objective optimization of DH was carried out, as well as an additional analysis of the effect of feed-in tariff supporting schemes. Power-to-heat technologies are also often included in multi-objective optimization problems, where more than one objective function is defined. It should be mentioned that the result of multi-objective optimization is not a single value but a whole set of values which lie on the Pareto front. Paper [27] used genetic algorithm in order to obtain optimal supply capacities and the hourly operation of the DH system. In [28] combined heating and cooling systems were studied in order to obtain optimal capacities of electric and absorption chillers. Besides these, the optimal operation of other DH components was also studied in [29]. Lamaison et al used mixed integer linear programming and the multi-objective parametric optimization method to study a district heating system that consists of a biomass generator, a heat-pump and heat storage in the French energetic context [30]. The electrification of heating systems can be a great obstacle for DH. In paper [31], authors analysed if ground source heat pumps could replace the existing DH systems in Sweden. They concluded that a complete replacement of DH with geothermal heat pumps is unrealistic. Paper [32] uses three types of systems to simulate how increasing the share of heat pump production influences DH systems when optimized for the lowest production costs. The findings of the simulations together with insights from the interviews imply that the viable amount of heat pump-based heat production in DH systems would be around 10-25% in Finland, which is much higher than the current 3%.

While many researchers explore the optimal supply capacities of power-to-heat technologies, they rarely analyse the impact of various parameters on power-to-heat supply capacities, such

as electricity market prices or power sector emission factors. These two parameters are greatly influenced by the penetration of variable renewable energy sources. Paper [33] shows the relationship between variable RES production and electricity market prices by using the EnergyPLAN tool for the modelling and simulation of energy systems. Amiri et al used a linear programming model to analyse a district heating system connected to the European power market [34]. They showed that interconnection with other heating systems can reduce the overall system cost. In [35], the electricity market in renewable energy systems was discussed and modelled. The case study was based on an energy system of Denmark with a 100% RES system for year 2050. Felten developed the model framework for the analysis of a coupled heat and power sector in large scale systems, such as the EU [36]. The model can provide a cost optimal dispatch and unit commitment of various technologies. In paper [37] the drivers of electricity prices spot markets were analysed and modelled on the example of the German power sector. Liu et al analysed marginal cost pricing for competitive district heating. In the paper, DH participates in the power market with cogeneration (CHP) and heat pump units. Dispatch, i.e. unit commitment was modelled by using the PLEXOS tool. It should be mentioned that power market prices are taken as the input data, i.e. it was assumed that the participating CHP and heat pump units do not shift the market equilibrium [38]. Hennessy et al [39] analysed the techno-economic feasibility of commercial power-to-heat technologies in DH systems by taking into account different various forecasts of spot market prices. However, the spot market prices were not modelled and only system operation was taken into account, while utilizing predefined capacities and technologies. In paper [40], authors analysed an integrated demand response while analysing the heat and electricity market price by optimizing bidding strategies, i.e. maximizing the net revenue of the supplier. Yifan et al modelled DH system connection with the power sector by analysing the operational flexibility of each local DH system through CHP and power-to-heat units. They showed how operational flexibility from multiple DH systems can effectively improve wind power integration [41]. Zhang et al proposed a two-layer optimization model to find out the optimal configurations of clean-heating improvements in a district energy system with high penetration of wind power. Their research focused on the implementation of power-to-heat technologies in combination with thermal storage units [42]. Fabian Levihn presented an empirical analysis of power and heat market integration from the DH network in Stockholm. The mentioned system utilizes CHP and power-to-heat units while at the same time participating in the stabilization of the power network by offering negative and positive power ramping [43]. Ma et al provided reviewed sources of flexibility in district heating systems. Power-to-heat technologies connected to the power market are a great source of flexibility [44]. Yifan et al developed a model capable of exploring electric flexibility coming from the district heating system, thus enabling increased wind penetration [41]. The model was validated on an integrated power and heating system consisting on numerous CHP and thermal power units and wind farms. In paper [45], a two-stage modelling approach was used to investigate the real-time flexibility of cogeneration power plants in district heating systems. In the first stage, the heat production plan of a CHP plant was derived to minimize the system heat cost in a deregulated heat market by using its flexibility; in the second stage, the CHP plant was dispatched to provide a real-time balancing service with the remaining flexibility.

Åberg et al. [46] provided a detailed analysis on how market prices influence the operation of power-to-heat technologies in the case of Sweden. They used historical price curves and added wind and solar capacities in order to analyse the shift of the supply curve, thus achieving new

electricity market prices. For the newly achieved prices they ran an analysis of power-to-heat operation units and drawn the following conclusions: the results show that power-to-heat production is significantly increased (up to 98%) when electricity prices are influenced by variable RES production. Besides spot prices, the power market also enables participation in an ancillary services market. This is excellent opportunity for power-to-heat technologies. Terreros et al provided an analysis of different electricity market options for heat pumps in rural DH networks in Austria. The optimal bidding strategy for heat pumps is buying 50% of the energy in the spot day-ahead market and offering 50% of the capacity for the negative balancing automatic frequency restoration reserve [47]. Thermal storage further increases the production of power-to-heat technologies by up to 46%. Paper [48] analysed the introduction of heat pumps with heat storage in a small district heating system while considering integration with a power market. They concluded that a thermal storage size can reduce the annual costs of a system effectively but can easily be oversized. In paper [49], authors demonstrated that electric boilers, which are part of a DH system, are capable of providing negative secondary control power in a flexible and a cost-effective manner. An analysis for the German energy system was carried out. Ito et al [50] analysed the role of DH cogeneration units for the purpose of maintaining grid stability. Particle swarm optimization was used in order to acquire the optimal operation of the DH system. In paper [51], a novel method for a heat and power dispatch model was proposed which also involved the thermal inertia of the system. The acquired results have shown how wind energy integration could be increased by utilizing the thermal inertia of a DH system. Gravelsins et al [52] used a system dynamics approach in order to investigate how solar photovoltaics could be integrated into DH systems to achieve economically feasible and flexible energy production by using power-to-heat technologies. Leitner et al [53] provided a method that enables a detailed technical assessment of the operation of coupled heat and power networks. Moser et al designed a heat market that is based on a merit order to evaluate industrial waste heat in DH systems. They showed that power market prices can drastically change merit order, especially during summer when heat loads are reduced [44]. Dominković et al developed dynamic pricing models for DH systems in Denmark and Finland [54]. It was shown that electricity prices have a high impact on carbon dioxide (CO_2) emissions and average marginal prices for both systems. Study [55] analyses how different electricity grid tariff structures will affect the flexible use of electricity in future Nordic district heating systems. Paper [56] summarises operation experiences of Swedish heat pumps to support and facilitate the planning of future power-to-heat solutions with heat pumps in DH systems. The authors showed that older heat pumps operate with lower utilisation capacity due to competing technologies such as cogeneration units in DH systems. In paper [57] authors used energyPRO to analyse three low-temperature DH schemes, where a booster heat pump was utilized with various thermal sources. An analysis of spot market prices reduction was not taken into account. Paper [58] uses EnergyPLAN to analyse how a shift from individual electric heating to DH affects the flexibility that the Norwegian energy system can provide to Europe. Paper [59] analyses how a Swedish municipality can contribute to lowering peak electricity demand by utilizing DH. It was shown that the choice of heating system is more important than reducing the heat demand itself to lower electricity peak demand in the future. Sorknæs et al [60] introduced the concept of a smart energy market. The authors illustrated and quantified how future renewable heating, green gas and liquid fuel markets will influence the electricity markets and vice versa. Mirzaei et al evaluated integrated power, heating and gas networks by developing a multi-network unit commitment model in

combination with storage technologies [61]. The goal is to minimize the operation costs of an integrated electricity, gas and DH system while satisfying the constraints of all three networks. In paper [62], the European heat demand was combined with a Dispa-SET power system model to evaluate a coupling pathway in terms of operating costs, efficiencies and associated CO_2 emissions. The results showed that the conversion of thermal into CHP plants increases efficiency and reduces both the operating costs and the environmental impact of the energy system.

1.4. Scientific contribution

Numerous papers dealing with multi-objective optimization of DH often do not optimise the system capacity regarding the power market prices change. In the majority of papers dealing with power and DH sector integration, spot market prices are rarely modelled, but considered through different scenario analyses. Due to this, most papers cannot provide the results on the impact of wind penetration on DH parameters. Nevertheless, paper [46] succeeded in displaying the impact of wind integration on district heating operation and demand response potential. However, the mentioned paper did not consider power-to-heat and thermal storage capacity optimization, but focused only on system operation acquired by using single-objective optimization.

The main scientific contribution of this paper is the analysis of an impact of a wind production increase in a power market on optimal power-to-heat and thermal storage capacities in a local DH system by using a multi-objective optimization approach. Furthermore, the power market clearing prices have been modelled by using publicly available historical bidding curves data in order to analyse the impact of wind production penetration. Finally, this paper provides a potential answer to the following questions:

How does wind penetration in a power market:

- shift the solution of the district heating multi-objective optimization, i.e. its Pareto front?
- impact optimal power-to-heat capacities in a district heating system for different Pareto optimal solutions?
- influence the optimal thermal storage size in a district heating system for different Pareto optimal solutions?
- affect the operation of the district heating system for different Pareto optimal solutions?

The paper is divided in following way. In Section 2, the method is explained. Section 3 shows the input data related to district heating optimization and the calculation of power market prices. Furthermore, Section 3 provides an overview of the proposed scenarios. Section 4 displays the main results obtained in this paper. Section 5 concludes the paper and displays the most important results obtained within this research.

2. Method

The overview of the method used in this paper is shown in Figure 1. The overall approach can be divided into two interconnected models: the district heating model and the modelling of the market clearing price under the influence of wind energy penetration. Market clearing price modelling is carried out by using known power market bidding curves and wind production data. In order to run the district heating model, several inputs are needed: district heating load, technology characteristics, such as efficiency and ramping limits, and prices (investment, fuel and operational costs). Besides these, every technology has a CO_2 emission factor that is related to the fuel. In the case of power-to-heat technologies, electricity is used as a fuel.

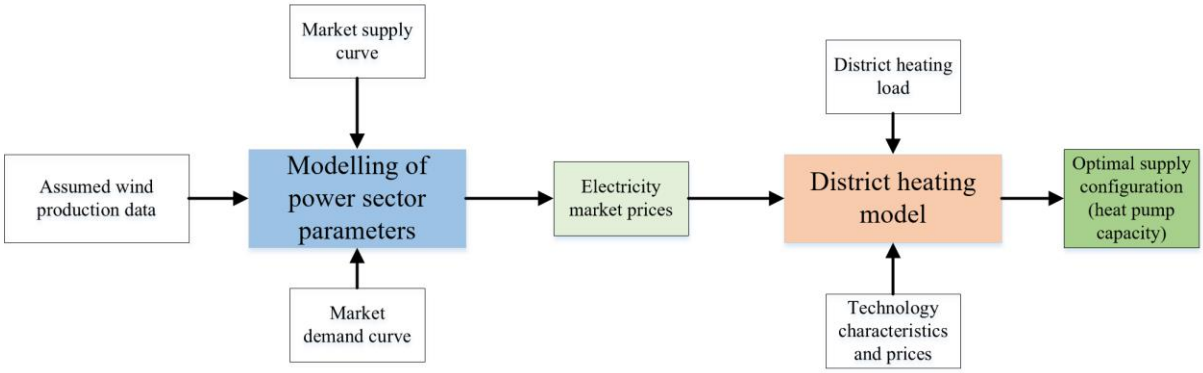

Figure 1 Overview of the method

2.1. District heating model

The district heating model used in this research is based on the model developed in the authors' previously published papers [63], [64]. The model is used for a multi-objective optimization of district heating systems with respect to the total costs and CO_2 emissions. It can be used to optimize supply capacities, including thermal storage size, and the hourly operation of the system for a whole year. The model can choose between various supply units, such as heat-only boilers, cogeneration, electrical heaters, heat pumps and solar thermal collectors. Two fuels can be used: natural gas or biomass. The optimization variables of the model are supply capacities P_i, thermal storage size TES_{size} and the hourly operation of each supply source $Q_{i,t}$ and thermal storage charging and discharging $TES_{in-out,t}$ where i represents the technology type and t the time step. The latter is equal to one hour, while the time horizon is equal to 8,760 hours, i.e. whole year. The model also includes various constraints, which are presented below.

Equation (1) presents the most important constraint which states that the hourly demand DEM_t should be covered with various supply technologies $Q_{i,t}$ where i represents the technology type. The operation of the thermal storage is defined with charging or discharging, i.e. $TES_{in-out,t}$. If the storage discharges, the term $TES_{in-out,t}$ is negative and if thermal storage is charging, the term $TES_{in-out,t}$ is positive. This is why in Equation (1), thermal storage terms have negative signs. Finally, it should be mentioned that this model includes two thermal storages. The first one is used as the buffer (short-term thermal storage) and the other one could act as the seasonal storage which could be charged solely by solar thermal technology. The connection between all the technologies is shown in Appendix.

$$DEM_t = Q_{HOB,gas,t} + Q_{HOB,biomass,t} + Q_{EH,t} + Q_{HP,t} + Q_{CHP,gas,t} + Q_{CHP,biomass,t} - TES_{1,in-out,t} - TES_{2,in-out,t} \quad (1)$$

Equation (2) presents the constraint that links the supply capacity P_i and the hourly operation of technology $Q_{i,t}$. The technology output on an hourly level cannot be higher than technology installed capacity.

$$0 \leq Q_{i,t} \leq P_i \quad (2)$$

In order to provide a more realistic operation of the system, ramping limits are put on each technology, as shown in Equation (2), where $r_{up-down,i}$ presents the ramping limit of technology i. It is defined as the percentage of the supply capacity that could be ramped up or down in a single hour.

$$-r_{up-down,i} \cdot P_i \leq Q_{i,t} - Q_{i,t-1} \leq r_{up-down,i} \cdot P_i \quad (3)$$

The thermal storage operation is defined with Equations (4) and (5). Equation (4) presents the constraint put on the state of charge (SOC_t) of a thermal storage in the first and the last hour of the optimization time horizon, i.e. they should be equal. Furthermore, the model allows defining the percentage of the state-of-charge by using the $SOC_{start-end}$ parameter. For the purpose of this paper, it is defined to 50% of the thermal storage size (TES_{size}). Equation (5) shows the hourly operation of the thermal storage. The state-of-charge in a time step t is equal to the state-of-charge in the previous time step ($t-1$) increased by the thermal storage charge (positive term) or discharge (negative term) and reduced by the thermal storage loss in the respective hour. The losses are defined with the loss factor TES_{loss}. Finally, the thermal storage state-of-charge SOC_t cannot be higher than the thermal storage size TES_{size}, shown in Equation (6). In other words, the optimal thermal storage capacity is equal to the highest SOC_t value.

$$SOC_{t=1} = SOC_{t=8760} = SOC_{start-end} \cdot TES_{size} \quad (4)$$

$$SOC_t = SOC_{t-1} + TES_{in-out,t} - SOC_t \cdot TES_{loss} \quad (5)$$

$$SOC_t \leq TES_{size} \quad (6)$$

While all technology capacities are defined with peak thermal power, the solar thermal capacity is defined with the total solar thermal area A_{ST}. Equation (7) shows the connection between the hourly operation of the solar thermal and its total area. It should be noted that the solar thermal operation is tightly constrained and depends on the optimized total solar area A_{ST} and the predefined hourly specific solar thermal output $P_{solar,specific,t}$.

$$Q_{ST,t} = A_{ST} \cdot P_{solar,specific,t} \quad (7)$$

The specific solar thermal output can be calculated by using Equation (8), where $\eta_{c,t}$ represents the solar thermal collector efficiency in a time step t, while G_t is global solar irradiation in a time step t. The last term also represents the hourly input data of the model which can be acquired by using publicly available data such as PV GIS [65] developed by JRC or other available databases [66].

$$P_{solar,specific,t} = \eta_{c,t} \cdot G_t \quad (8)$$

The calculation of solar thermal collector is obtained by using Equation (9) based on the European standard EN12975 [67], where η_0 represents optical efficiency (without thermal losses), a_1 is the first order heat loss coefficient and a_2 is the second order heat loss coefficient, while T_m represents the mean collector fluid temperature. The mentioned parameters depend on the collector type and can be obtained by checking the manufactures' factsheets which can be found in publicly available databases [68]. Finally, $T_{ref,t}$ is the outside air temperature for the given location which can be obtained by using the already mentioned publicly available databases [65], [66].

$$\eta_{c,t} = \eta_0 - a_1 \frac{\left(T_m - T_{ref,t}\right)}{G_t} - a_2 \frac{\left(T_m - T_{ref,t}\right)^2}{G_t} \tag{9}$$

The efficiency of the heat pump can be calculated by using Equation (10) [25]. It is based on the temperature difference between the heat source (air, $T_{ref,t}$) and the heat sink (DH supply network, $T_{DH,t}$) temperature multiplied with the Lorentz factor $f_{Lorentz}$. The district heating supply network temperature is not constant, but depends on the outside air temperature as shown in [69].

$$\eta_{HP,t} = f_{Lorentz} \cdot \left(\frac{T_{DH,t}}{T_{DH,t} - T_{ref,t}}\right) \tag{10}$$

It should be noted that solar thermal collector and heat pump technologies do not have constant efficiency as other supply sources, since they can be calculated prior to the optimization procedure. All other technology efficiencies are treated as constants in order to secure the linearity of the model. The problem is written as a linear programming (LP) model by using the Julia programming language and the linear programming solver called Clp.

An overview of the district heating model is presented in Appendix.

2.2. Objective functions

As already mentioned, this paper deals with multi-objective optimization. The goal of the optimization model is to minimize the economical, f_{econ}, and ecological, f_{ecol}, objective function, as shown in Equation (11).

$$\min\left(f_{econ}, f_{ecol}\right) \tag{11}$$

The economical objective function represents the total costs of the system that can be calculated by using Equation (12). $C_{investment,i}$ is the discounted investment costs of technology i. It should be noted that it does not have a temporal summation since it is paid only once. $C_{fuel,i,t}$ represents fuel costs, while $C_{O\&M,i,t}$ is operation and maintenance costs for technology i in a time step t. The last term on the right in the brackets $Income_{i,t}$ represents additional income due to the electricity sold on the market by using cogeneration units.

$$f_{econ} = \sum_i C_{investment,i} + \sum_{t=1}^{t=8760} \sum_i \left(C_{fuel,i,t} + C_{O\&M,i,t} - Income_{i,t}\right) \tag{12}$$

The ecological objective function is defined as the total CO_2 emissions of the district heating, which is obtained by using Equation (13). The specific emission factor, $e_{CO_2,i}$ is defined per fuel, while η_i is technology efficiency.

$$f_{ecol} = \sum_{t=1}^{t=8760} \sum_{i} (e_{CO_2,i} \cdot Q_{i,t} / \eta_i) \quad (13)$$

2.3. Multi-objective optimization

Before explaining the method used for handling multi-objective optimization, the crucial issue related to such optimization should be mentioned. It is impossible to simultaneously acquire the minimum of both objective functions. By acquiring the minimum of the first, the highest value of the second one will be reached and vice-versa. Thus, the solution of multi-objective optimization is not a single value but a whole set of them, which lie on the same front, the so called Pareto front. It could be understood as the compromise between two objective functions – approaching to the minimum of one is only possible at the expense of other objective function.

In order to deal with multi-objective optimization, and to construct the Pareto front, the epsilon constraint method has been used in this paper [70]. It is based on translating the multi-objective optimization problem into single-objective optimization by introducing an additional set of constraints put on the second objective function, as shown in Equation (14). Parameter ε_{ecol} represents (epsilon) constraint put on the ecological objective function, while the economical objective function is minimized. By changing ε_{ecol}, different solutions are achieved that lie on the Pareto front [70]. Due to this, the resolution of the Pareto front depends on the number of optimization runs. It is important to mention that ε_{ecol} should be in the feasible region. To define the feasible region, boundaries of the Pareto front should first be acquired.

$$\min (f_{econ}) \text{ for } f_{ecol} \leq \varepsilon_{ecol} \quad (14)$$

2.4. Market price modelling

In this paper, power-to-heat optimal capacities are analysed with regard to electricity market prices. These prices also represent an input for the district heating model. The market price was modelled with respect to wind energy penetration by using publicly available market bidding data, i.e. supply and demand market curves for each hour of the year, as explained below. The mentioned approach has also been implemented in this paper to avoid challenging power market modelling which involves detailed unit commitment and dispatch on a power plant level for a whole market on an hourly level for a whole year.

Market clearing price modelling by using supply and demand market curves has been previously shown in [46] and [71]. In paper [71], the focus was put on analysing the increase of demand on the market clearing price, i.e. the buy curve was shifted in order to obtain the new (modelled) market clearing price. In paper [46] the authors used a similar approach, but this time, the supply curve has been shifted in order to model the influence of the increased variable RES production. For the purpose of this paper, the method shown in [46] was used. However, only the wind production increase is studied since these capacities are the most promising in the analysed Nord Pool market. Finally, it is assumed that the marginal price of wind is equal to zero.

To fully understand the approach used, the market model should be explained. For this purpose, Figure 2 will be used. It represents the market situation for a single hour and must be constructed 8,760 times per year. The power or electricity market operates as any other market of goods. Two major parameters first have to be understood: the trading volume (x-axis, in MWh) and the market price (y-axis, in EUR/MWh). For every volume, the market price can be defined, which is called a "bid". The set of all bids creates the bidding curve. In Figure 2, two curves can be noted. The blue full curve represent the supply curve ("sell curve"). In the power market, the supply is represented with power plant operators: condensation power plants, cogeneration units, wind turbines, photovoltaics, etc. Since renewable energy sources have low operational costs, they can offer the trading volume at a lower price, even reaching zero or negative values. The red curve represents the demand curve ("buy curve"). Where these two curves intersect, the market clearing price and the respective trading volume are obtained. In Figure 2, this is marked with yellow dot. As already mentioned, variable renewable energy sources, e.g. wind, have low operational costs, thus offering bids at a lower price. If additional wind is introduced into the market, the supply curve is shifted to the right. In Figure 2, this is represented with the dotted blue line. Due to the shift of the supply curve to the right, the new market clearing price is obtained (marked with a green star), which is lower than the reference one. This represents the crucial effect of variable renewable energy sources integration, since it opens additional opportunities for demand response, power-to-heat, power-to-X, and other technologies that could participate on the market.

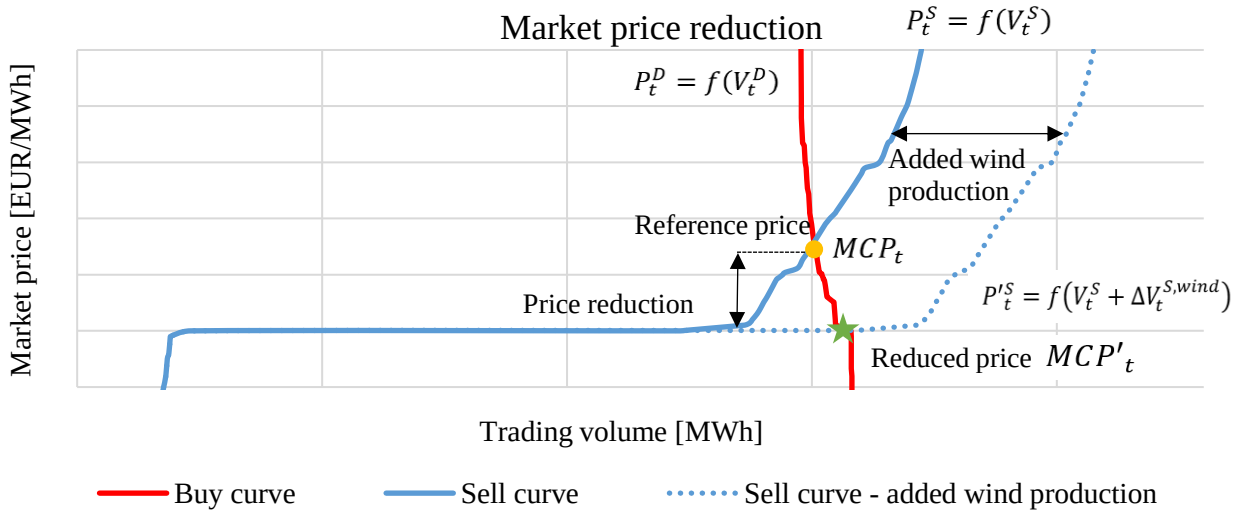

Figure 2 Illustration of the market price reduction method for a single hour

The market price modelling can also be represented with the following equations. Let us assume that price P_t in a time step t is a function of a volume participating on the market. Equation (15) shows the generic correlation between the (supply) price P_t^S and the supply volume V_t^S, while Equation (16) shows the connection between the buy (demand) price P_t^D and the demand volume (V_t^D). The market clearing price MCP_t is achieved for the market equilibrium, as shown in Equation (17). In this paper, the penetration of wind energy production into the power market is analysed, which is marked with $\Delta V_t^{S,wind}$ in Equation (18). Due to this, an updated price curve P'^S_t is acquired, as shown in Equation 17. Since the updated price curve is shifted, the new market clearing price MCP'_t is obtained as shown in Equation

(19). Since the added wind production has zero marginal costs, the new market clearing price is lower than the reference one, as shown in Equation (20).

$$P_t^S = f(V_t^S) \quad (15)$$

$$P_t^D = f(V_t^D) \quad (16)$$

$$MCP_t = P_t^S = P_t^D \quad (17)$$

$$P'^S_t = f\left(V_t^S + \Delta V_t^{S,wind}\right) \quad (18)$$

$$MCP'_t = P'^S_t = P_t^D \quad (19)$$

$$MCP'_t < MCP_t \quad (20)$$

Although this approach has been used in previously published papers [46], [71], it has some major drawbacks related to market evolution and power system dynamics:

- Buy (demand) curves are not updated, i.e. they stay the same for all levels of wind penetration.
- The acquired market clearing price represents the system price. According to [72], the system price is an unconstrained market clearing reference price. It is calculated without any congestion restrictions by setting the transfer capacities to infinity. In reality, different zones will not achieve price convergence due to the limited transfer capacities.
- Due to the lack of unit commitment and dispatch modelling, negative prices could not be obtained by using this approach.
- The impact of ramping, starting and shut-down costs cannot be obtained by using this approach since the system dynamics are not taken into account.
- The assumed running costs of wind production are equal to zero. However, there are small operation and maintenance costs.
- Since this approach does not include hourly power dispatching and unit commitment, the impact on reversible hydro storage capacities could not be taken into account.

From the drawbacks presented above, it can be concluded that the market clearing prices obtained by using this approach represent an idealized case. The major issue is the lack of dispatch and unit commitment modelling and neglecting the so-called cycling costs. These expenditures are related to starting, ramping and forced outage costs. It should be mentioned that the cycling costs mainly depend on the technology, as shown in [73]. The direct start costs can be in range from 5 EUR/MW for combined cycle natural gas turbines, up to 35 EUR/MW for nuclear power plants. Similarly, the ramping costs are equal to 0.5 EUR/MW for natural gas power supply units and 1.8 EUR/MW for coal power plants. In other words, the impact of wind and solar penetration on the cycling costs, greatly depends on the power supply technology mix. Paper [73] analysed the cycling cost for the German power system under the largescale integration of intermittent renewable energy sources, i.e. wind and solar. The cycling costs almost doubled (from 5 to 10 million EUR/week) for the wind and solar energy penetration increase from 0% to 50%. The largest contribution in the cost increase comes from the starting costs. Nevertheless, it should be noted that the total costs are reduced from 170 to 80 million EUR/week for the wind and solar share equal to 50%. The share of the cycling costs in the total generation costs is kept relatively low but increases steadily from 3% up to 15% for

a large penetration (50% share) of wind and solar. However, in this paper, the maximum wind share is much lower, equal to 21%.

Since the approach used in this paper does not include the cycling costs, it can be expected that obtained average market prices in this paper are slightly underestimated.

3. Case study

This section presents the input data needed for market price modelling. Furthermore, it includes DH system parameters needed for carrying out optimization, such as hourly distributions and technology related parameters, prices, etc. Finally, the two scenarios developed for the purpose of the analysis are also presented.

3.1. Input data

The model developed for the purpose of this paper was tested on a numerical case study of a DH system. The input data used in the analysis can be divided in hourly distributions and single-value parameters. Several hourly distributions are needed, such as: heating and domestic hot water demand, outside air temperature, global solar irradiation, specific wind power production and finally, electricity market prices, which are calculated by using the method described in Section 2.

Other district heating parameters, such as specific investment, fuel and O&M costs, the fuel emission factor, technology efficiencies, ramping limits, power-to-heat ratio for cogeneration and technical life time can be seen in Table 1 [74]. In Appendix, the hourly DH demand is shown.

Table 1 Technology data

Technology	Investment costs [€/MW] / [€/m^2] /[€/MWh]	Fuel cost [€/MWh]	Variable costs [€/MWh]	Emission factor [tonnes of CO_2/MWh]	Efficiency/ storage loss [-]	Ramp-up/down [-]	Technical lifetime [years]	Power-to-heat ratio [-]
Natural gas boiler	100,000	20	3	0.22	0.9	0.7	35	-
Biomass boiler	800,000	15	5.4	0.04	0.8	0.3	25	-
Electrical heater	107,500	Electricity market	0.5	0.293	0.98	0.95	20	-
Heat pump	680,000	Electricity market	0.5	0.293	Hourly distribution	0.95	20	-
Cogeneration natural gas	1,700,000	20	3.9	0.22	0.5 (thermal)	0.3	25	0.82
Cogeneration biomass	3,000,000	15	5	0.04	0.6 (thermal)	0.3	20	0.55
Solar thermal	300 €/m^2	0	0.5	0	Hourly distribution	-	25	-
Thermal storage, buffer	3,000 €/MWh	0	0	0	1% (loss)	-	25	-
Seasonal thermal storage	500 €/MWh	0	0	0	0.1% (loss)	-	25	-

To obtain the market clearing price, the demand and supply curves are needed for every hour of the year. They can be acquired by using publicly available Nord Pool bidding data [72]. For every hour of the year, the Nord Pool database publishes set of purchase and sell bids which enables the development of the bidding curves similar to the one shown in Figure 3. In order to acquire the market clearing price for the given hour, an intersection of the mentioned curves

has to be found. This procedure is repeated for every hour of the year, thus providing the district heating model with 8,760 values. Of course, for the reference year, the hourly market price is already available.

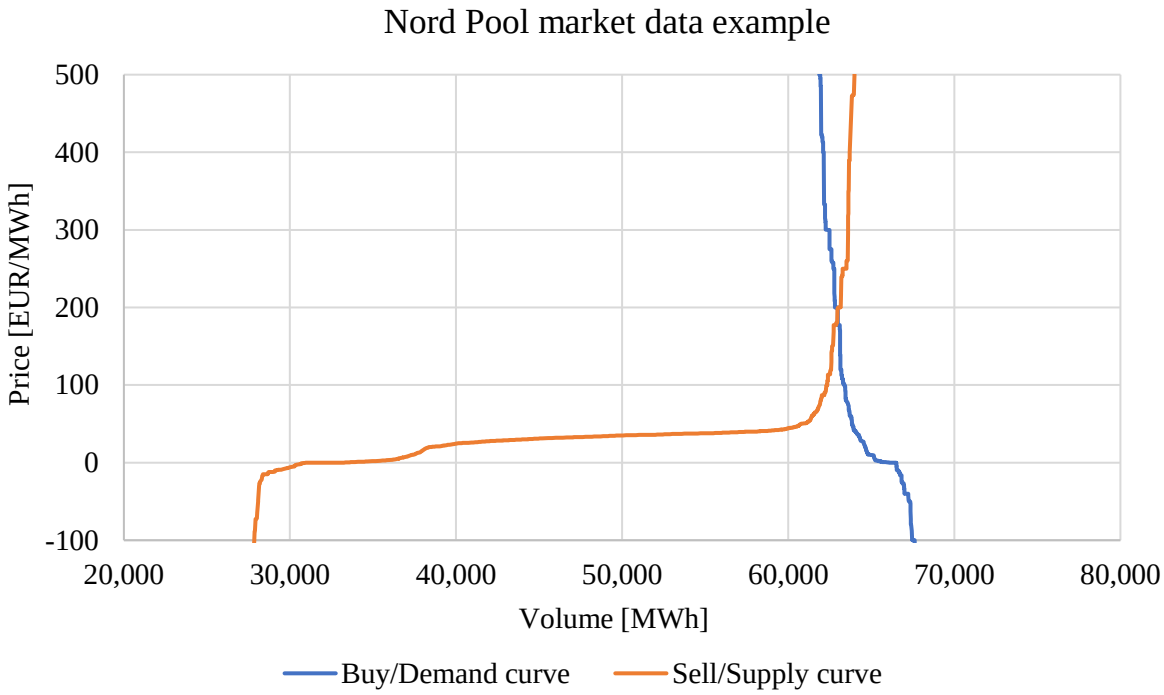

Figure 3 Nord Pool data example for a single hour [72]

One of the objectives of this paper is to analyse how increased energy production affects electricity market prices. As already explained in Section 2, the method is based on adding zero-cost volumes in the supply bid curve to obtain the new market clearing price. However, for the analysis of additional wind energy production, the hourly data for wind is also needed. In this paper, the already existing Nord Pool historical wind production data for the reference year has been used in order to acquire the predefined total yearly wind energy production [72]. Figure 4 shows the relative wind production used in this paper in order to scale the reference one and obtain the predefined total yearly wind production shown in Table 2. The relative wind power was obtained by dividing the hourly wind production, obtained for the reference year 2018 from the Nord Pool database, by the respected maximum wind production in the given year. In that case the value of 1 represents the maximum hourly wind production in that year, while the value zero represents no wind production. This hourly relative wind power distribution was used to obtain the hourly wind production for different levels of wind penetration as shown in Table 2, i.e. for 45, 60, 75 and 90 TWh of wind production. These values were then used to shift the historical Nord Pool supply curves and obtain the new (reduced) market clearing prices.

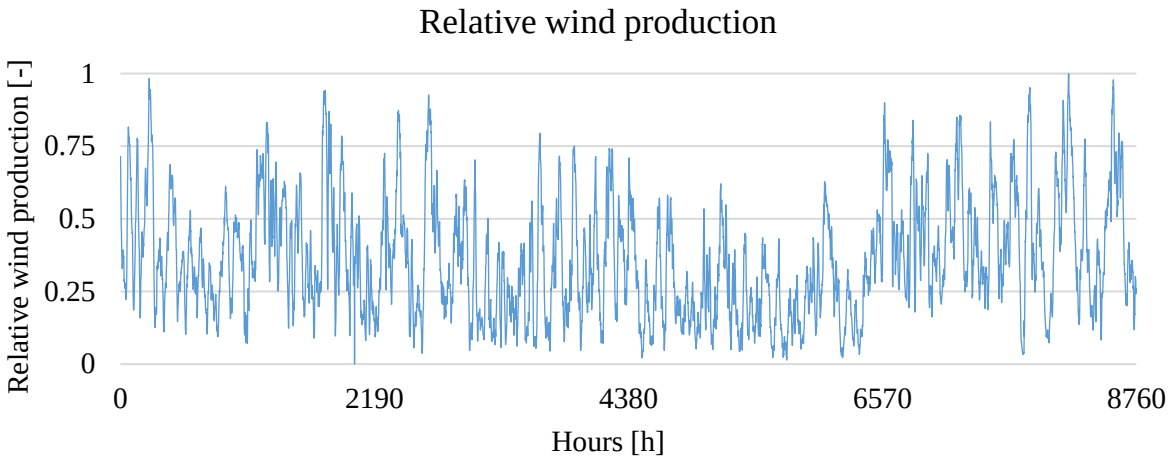

Figure 4 Relative wind production

3.2. Scenario analysis

For the purpose of this paper, two scenarios have been developed, as shown in Table 2. In Scenario 1 the power sector emission factor is taken as the historical value for Denmark, since it is assumed that it is the location of the numerical example of a new local district heating system. In the second scenario it is assumed that the power sector emission factor is equal to zero, i.e. power-to-heat units do not have CO_2 emissions. This presents an ideal case where the power sector utilizes only renewable energy sources. Furthermore, by obtaining the results with this assumption, the ideal system, which is not bounded with power sector emissions, can be analysed. For both scenarios, five levels of wind penetration have been studied. The reference case presents the historical data for the year 2018, where wind energy production was equal to 33 TWh. The electricity market prices have been recalculated for different levels of wind production penetration: 45, 60, 76, and finally, 90 TWh. The wind share is equal to 8% for the reference case and 11%, 14%, 18% and 21% for other wind penetrations, respectively. It is calculated with respect to total production for the year 2018.

Table 2 Scenario description

Scenario name	**Power sector emission factor [tonnes of CO_2/MWh]**	**Wind energy penetration**
Scenario 1	0.29	Electricity market prices are recalculated by considering penetration of wind energy production: - 33 TWh of wind penetration – Reference case (wind share of 8%) - 45 TWh of wind penetration (wind share of 11%) - 60 TWh of wind penetration (wind share of 14%) - 75 TWh of wind penetration (wind share of 18%) - 90 TWh of wind penetration (wind share of 21%)
Scenario 2	0	

4. Results and discussion

Section 4 is divided into several parts. In Section 4.1, the market price reduction results are explained and analysed in more detail. In Section 4.2 and Section 4.3, the optimal heat pump capacities and the Pareto front shift for different levels of wind penetration are discussed for both scenarios. Finally, Section 4.4 provides a comparison of district heating supply system operation for different levels of wind penetration and district heating system CO_2 emissions.

4.1. Market price reduction

As shown in Section 2, the integration of intermittent renewable energy sources reduces power market prices, due to their zero-marginal prices. This has also occurred in this study with the penetration of additional wind capacities in the Nord Pool market. The reference wind penetration was equal to 33 TWh, which presents an 8% share of the power production. Wind energy production was increased up to 90 TWh with the step equal to 15 TWh. Figure 5 shows the duration curves of hourly market prices for different levels of wind penetration. First of all, it can be noted that the peak market price drastically falls from 199 EUR/MWh for 33 TWh of wind production down to around 60 EUR/MWh for higher wind penetration levels. Furthermore, it is evident that the number of nearly-zero-price hours increases with wind penetration, as explained below.

The peak market price for the reference wind penetration of 33 TWh is relatively high, equal to 199 EUR/MWh. Such high market clearing prices are probably caused by a non-predicted external event. The bidding curves for this specific hour are shown in Figure 3. It can be seen that the demand curve intersects costly (peaking) supply technologies, resulting in a high market clearing price. It can be also noted how a small shift of the supply curve to the right (by adding a low-cost technology such as wind) drastically reduces the market clearing price. This actually happened in this paper. Unfortunately, the nature of unpredicted events is not considered in this analysis. However, those events are already integrated in the historical bidding curves and are taken into account as such.

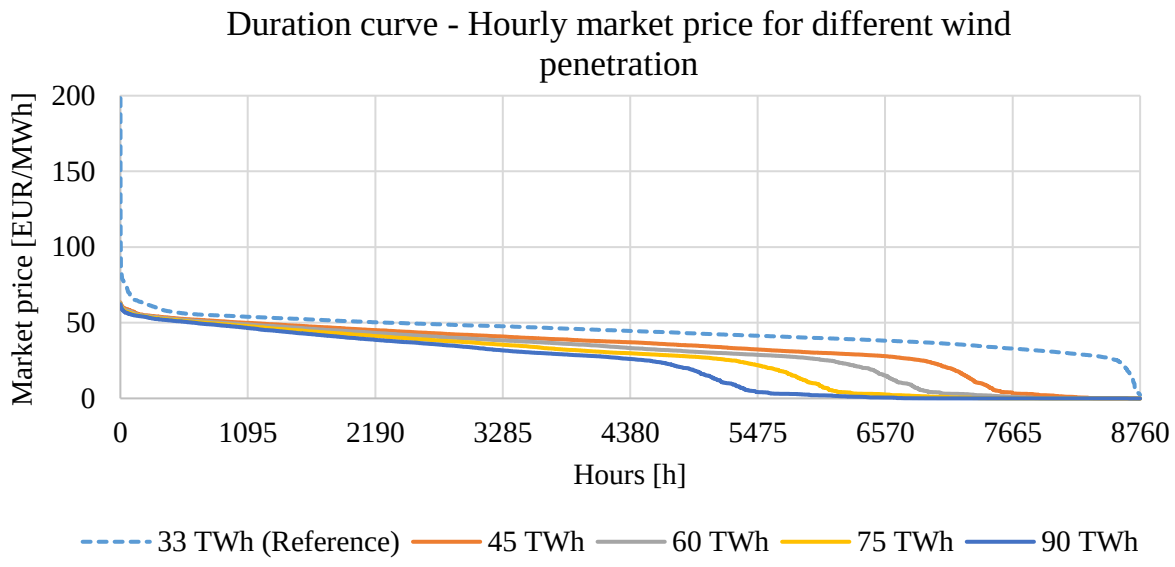

Figure 5 Duration curve of hourly market price for different values of wind penetration

Figure 6 shows the average market price and the number of zero-price-hours for different levels of wind penetration. The average market price for reference wind penetration is equal to 44 EUR/MWh. It decreases down to 22 EUR/MWh for wind penetration level of 90 TWh. It can be noted that the average market price does not fall linearly with a wind penetration increase but potentially reaches saturation. On the other hand, number of zero-price hours follows the trend of quadratic increase. The reference wind penetration has no zero-price hours, while for wind penetration of 90 TWh the number of zero-price hours reaches around 1,500. The possible reason behind this great number of zero-price hours is the following. In real markets, supply bids are not exactly 0 EUR/MWh. They are usually around this value, probably due to different operation and maintenance costs of the renewable energy source technology.

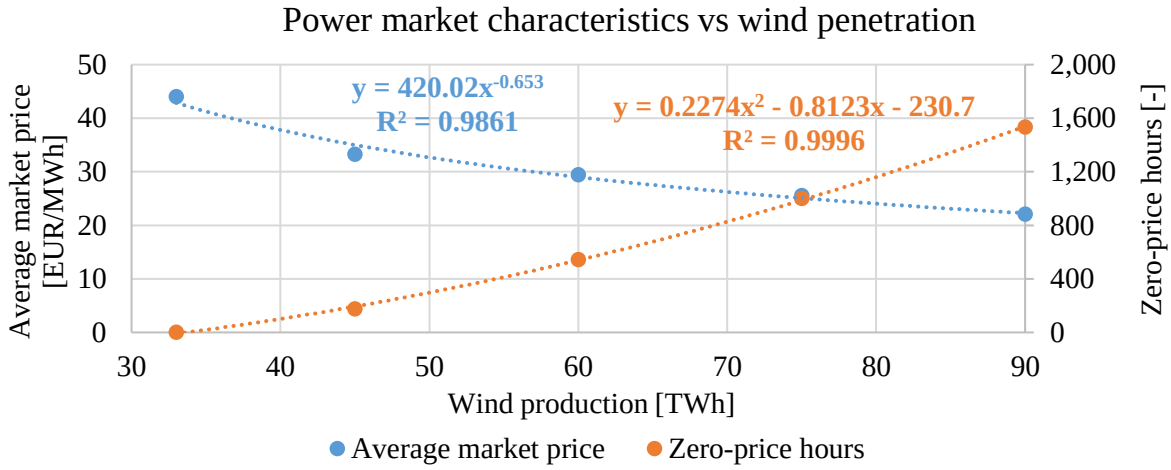

Figure 6 Average market price and zero-price hours for different wind penetration values

A more detailed comparison of power market prices is shown in Figure 7 and Figure 8. They show the hourly market price distributions for a winter and a summer week, respectively. First of all, it should be noted that the summer week obtains more zero-price hours than the winter period. The peak market prices do not differ greatly for different levels of penetration, but on the other hand the market price drops significantly in the periods of lower reference prices, i.e. when there is wind production.

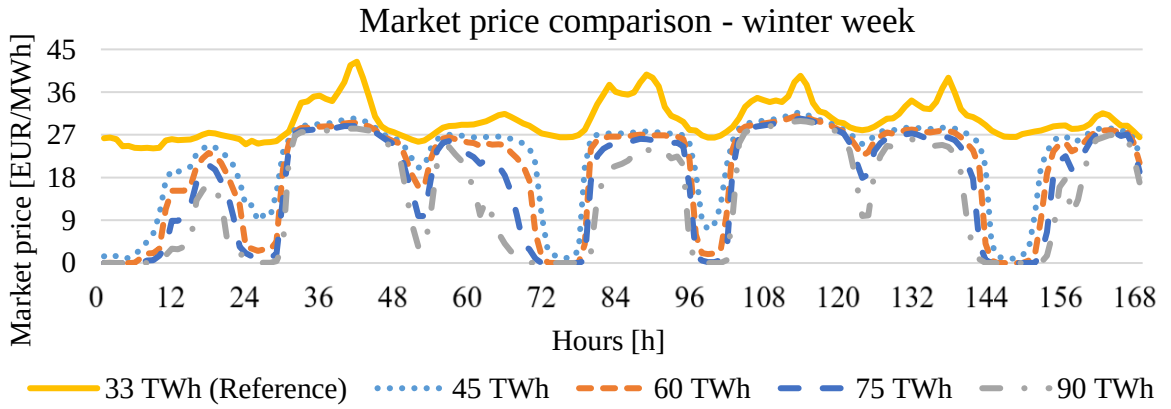

Figure 7 Market prices comparison for different wind penetration values – winter week

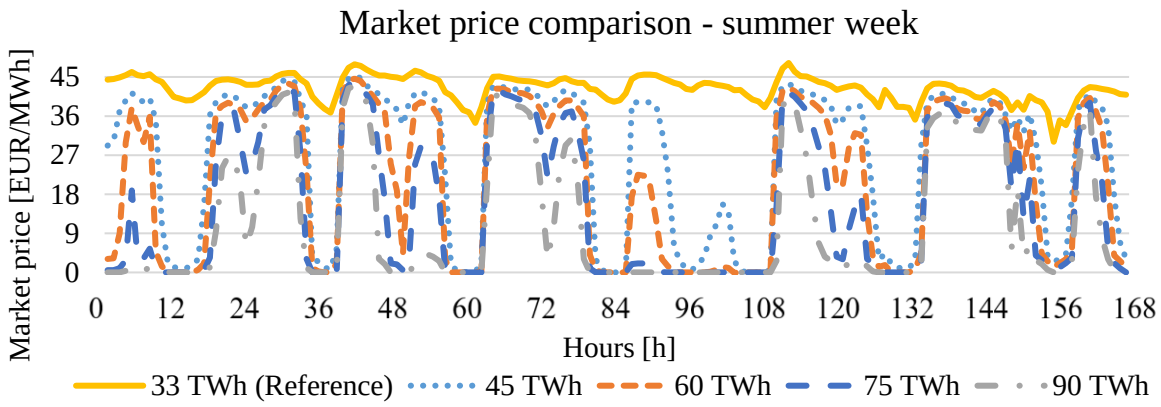

Figure 8 Market prices comparison for different wind penetration values – summer week

4.2. Optimal heat pump parameters – Scenario 1

As already mentioned in Section 2, the result of multi-objective optimization is not a single value but a whole set of them which lie on the so-called Pareto front. Figure 9 shows the Pareto front for Scenario 1, where the assumed power sector emission factor is equal to 0.29 tonnes/MWh. It is important to mention that the most environmentally friendly solution is not shown in this figure since it is off-scale, i.e. it reaches high total costs and is not of interest in this analysis. As explained in Section2, the Pareto front is constructed by using the epsilon constraint method, i.e. by obtaining a definite number of points which lie on the Pareto front. It can be seen that the epsilon constraints are equal to 6,000, 5,000 and 3,000 tonnes of CO_2 emissions. On the other hand, the most-left solutions present the most economically feasible solutions, which also emit the highest amount of CO_2. It can be noted that the penetration of wind production shifts the Pareto front to the region of lower emissions and lowers the total costs due to the increased utilization of heat pumps as can be seen in Figure 10.

Pareto fronts can also represent the savings in total costs and CO_2 emissions. The reference case includes reference power market prices with reference wind penetration. However, with additional wind production, lower market clearing prices are obtained and heat pumps become a more economically viable solution. Savings in this case refer to CO_2 emissions and system cost reductions. These savings in Scenario 1 are the most visible in Pareto front shifts in Figure 9. For the same levels of CO_2 emissions, the system cost reduction is obtained. In Scenario 1, the maximum cost reduction is around 70,000 EUR for a CO_2 emission level equal to 6,000 tonnes.

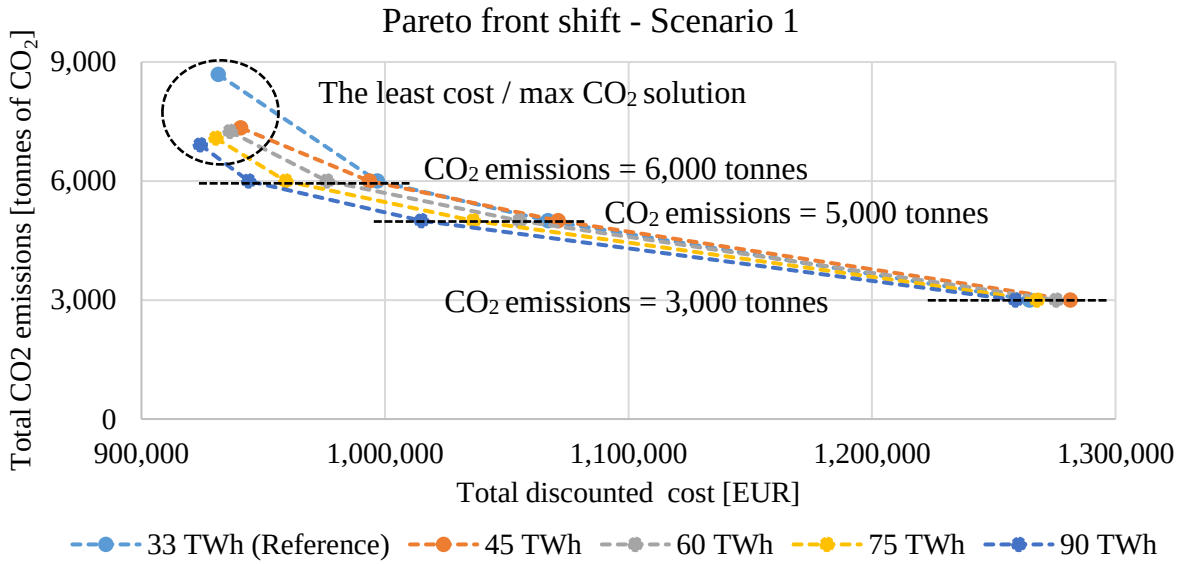

Figure 9 Pareto front shift for different wind penetration values – Scenario 1

Figure 10 shows optimal heat pump capacities for different levels of wind penetration and CO_2 emissions values. The trend is obvious: the increase of wind penetration allows larger heat pump capacities from the economical point of view. It should be noted that for reference wind penetration of 33 TWh, a heat pump is not part of the optimal solution for any CO_2 emission value. The highest heat pump capacity increase is evident for CO_2 emissions equal to 5,000 and 6,000 tonnes. For these values, the optimal heat capacity reaches around 4 MW for wind

penetration of 90 TWh. For lower CO_2 emissions, the optimal heat pump capacity is reduced due to the power sector emission factor, and more environmentally friendly technologies are used, such as solar thermal collectors or biomass boilers.

A similar trend can also be observed in Figure 11, which shows the optimal heat pump production, i.e. the thermal energy produced by using a heat pump. It can be noted that the resulting load factor is always around 0.6 as seen in Figure 12. It is to be expected that lower market prices will allow more frequent operation of power-to-heat units, especially during the night and during periods of low or even zero-price hours. In order to successfully achieve this, thermal storage is needed. In this paper, we have analysed the impact of a wind penetration increase on the optimal thermal storage size of a local district heating system. This trend is shown in Figure 13. As expected, lower power market prices cause an increase in thermal storage size used for heat pump utilization, especially during night periods, as shown in Section 4.4 in more detail.

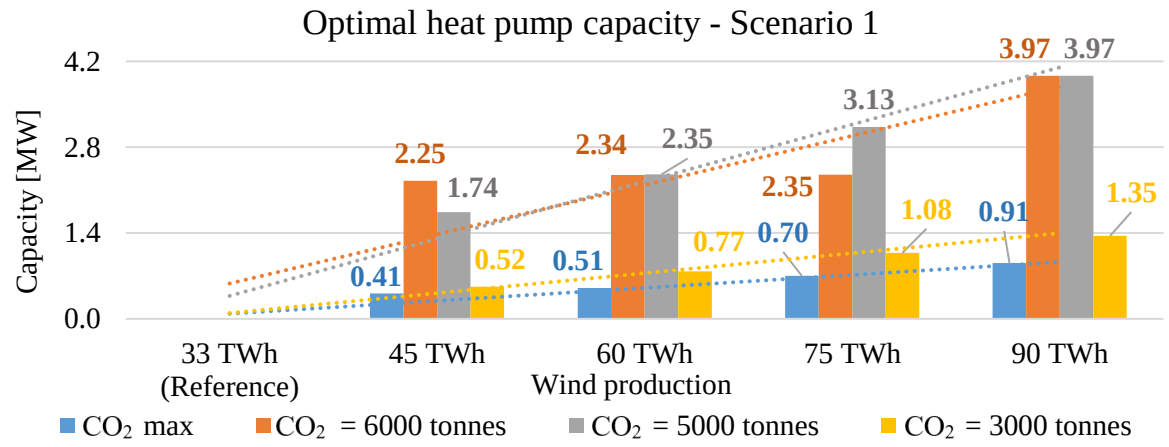

Figure 10 Optimal heat pump capacities – Scenario 1

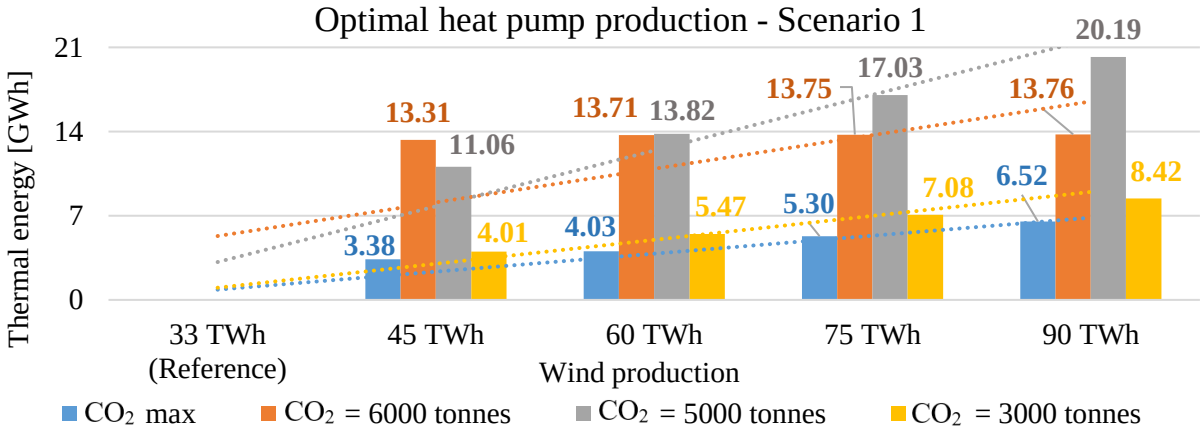

Figure 11 Optimal heat pump thermal energy production – Scenario 1

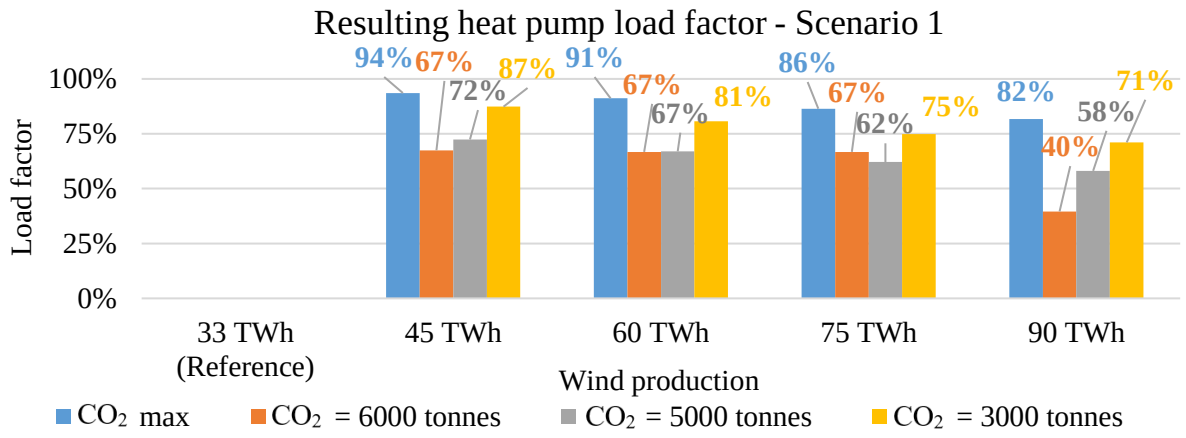

Figure 12 Resulting heat pump load factor – Scenario 1

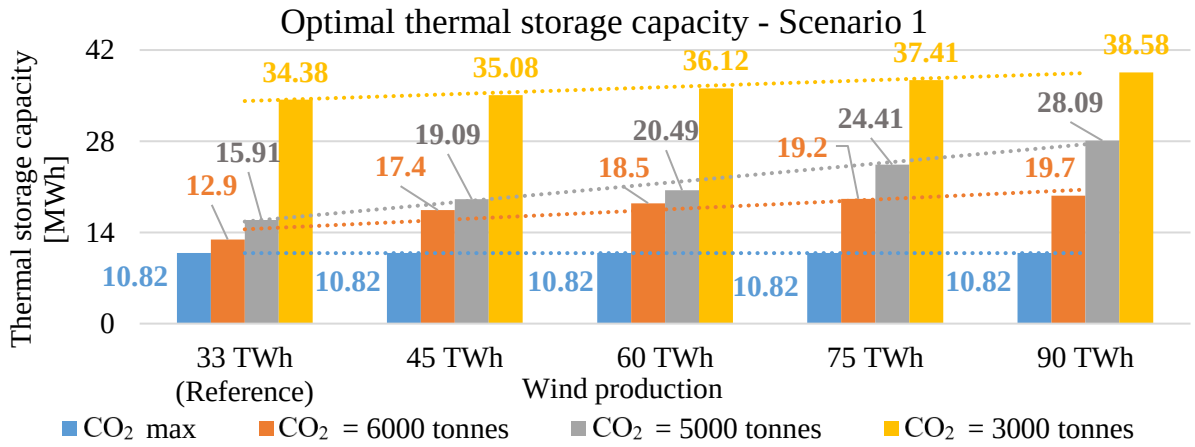

Figure 13 Optimal thermal storage capacity – Scenario 1

4.3. Optimal heat pump parameters – Scenario 2

Similarly to the analysis shown in Section 4.2 for Scenario 1, this section provides a detailed overview of the results for Scenario 2. In this scenario, the assumed power sector emission factor is equal to the ideal zero tonnes of CO_2/MWh. Figure 14 shows the Pareto front shift for Scenario 2. Similarly to Scenario 1, the Pareto fronts are also moving to the region of lower total costs and lower environmental impact. However, in this case the Pareto fronts are diverging when they approach the region of lower CO_2 emissions. The reason behind this is that the power sector emissions are equal to zero, which allows for the utilization of heat pumps, thus reducing the overall price and CO_2 emissions.

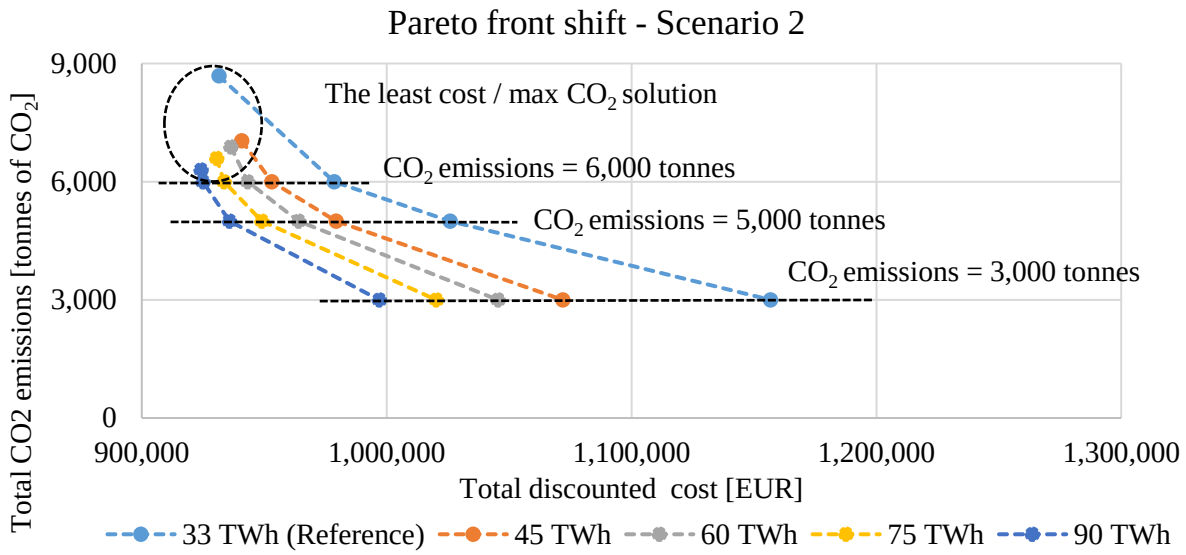

Figure 14 Pareto front shift for different wind penetration values – Scenario 2

Figure 15 shows the optimal heat pump capacities for Scenario 2. When compared with Scenario 1, this scenario also includes a heat pump as the optimal solution for the reference wind penetration of 33 TWh. Furthermore, the heat pump capacities increase as we approach the most environmentally friendly solution. The steepest trend is obtained for the least costly solution, which have the highest CO_2 emissions.

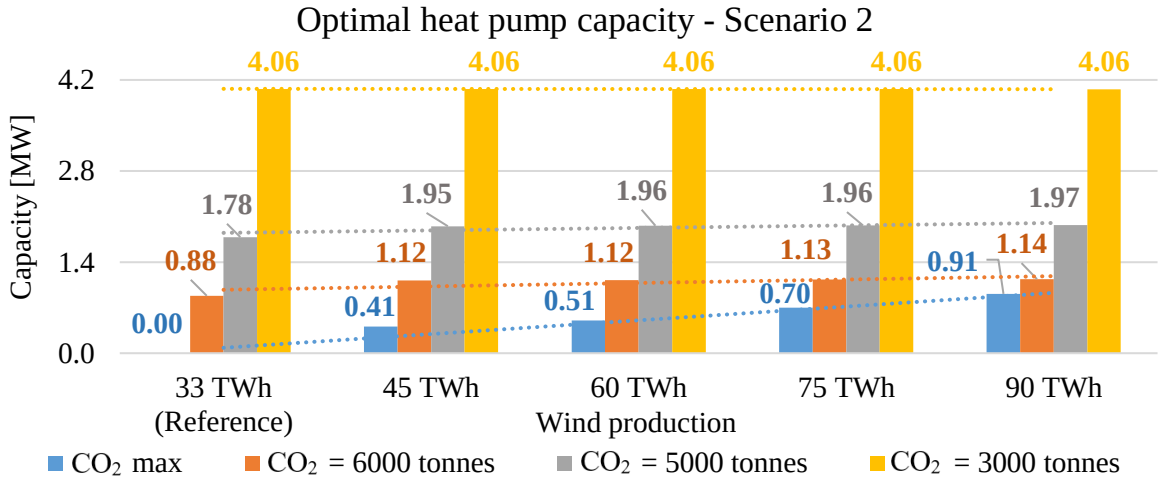

Figure 15 Optimal heat pump capacities – Scenario 2

Figure 16 shows the optimal heat pump production and has a similar trend as shown in Figure 12. As in Scenario 1, the load factor is also relatively high, around 0.6, as seen in Figure 17. Figure 18 shows the optimal thermal storage capacity for different wind energy penetration for Scenario 2. The steepest trend is acquired for the lowest observed CO_2 emissions, reaching up to 37 MWh.

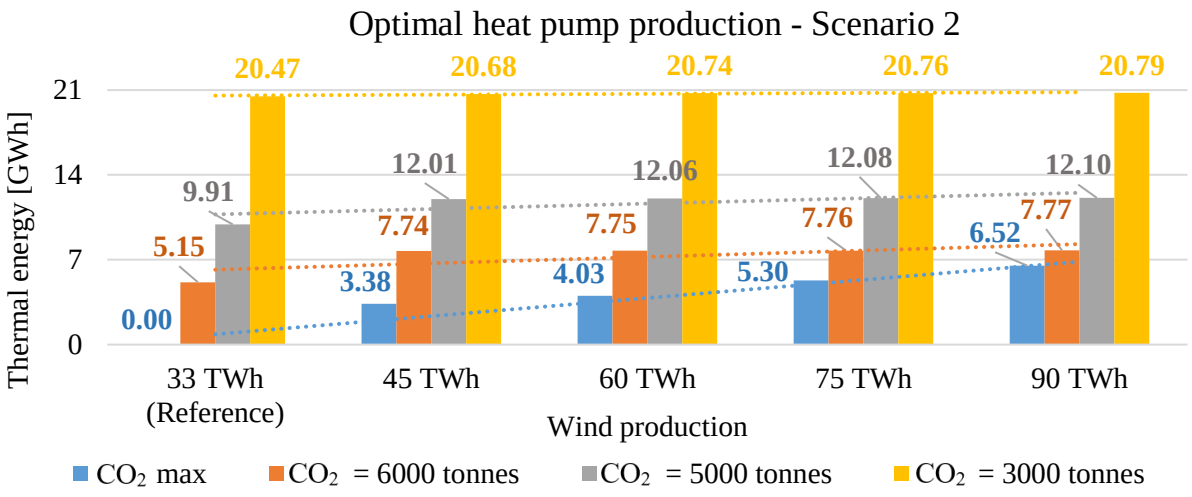

Figure 16 Optimal heat pump thermal energy production – Scenario 2

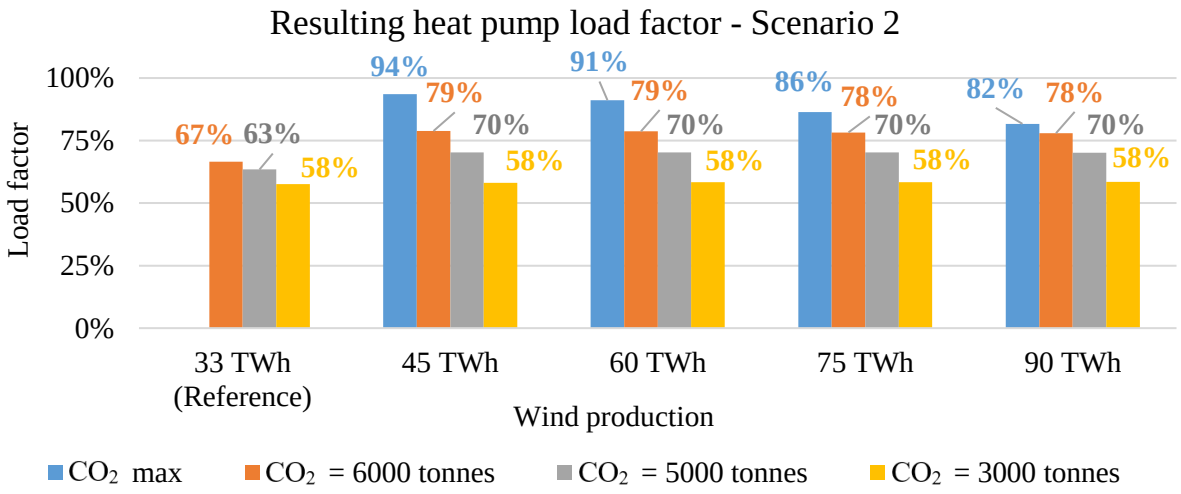

Figure 17 Resulting heat pump load factor - Scenario 2

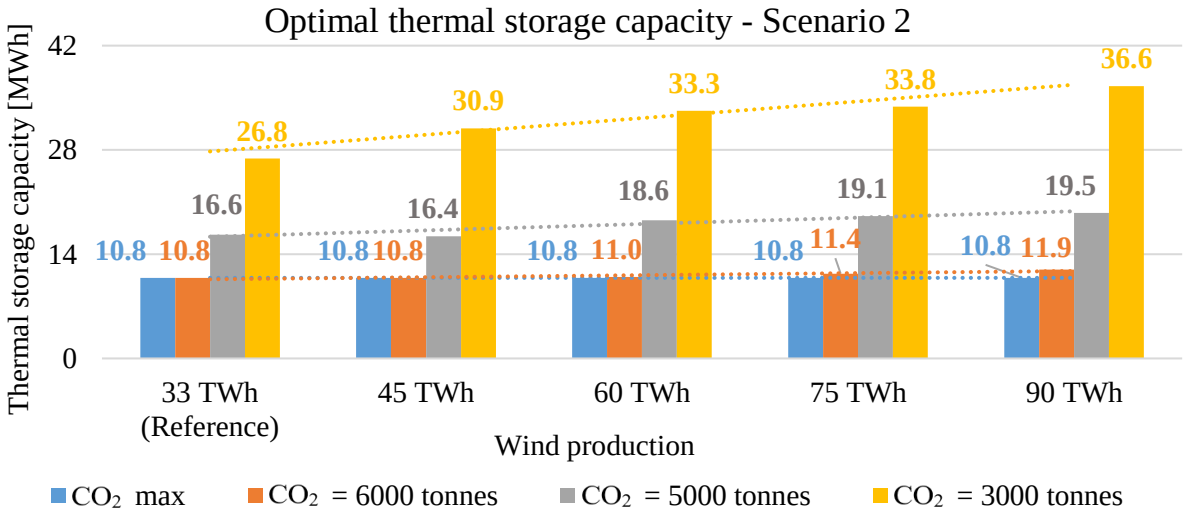

Figure 18 Optimal thermal storage capacity – Scenario 2

4.4. District heating system operation comparison

This section shows a detailed comparison of optimal district heating supply system operation for different levels of wind production penetration and CO_2 emissions. In order to analyse the impact of heating load seasonality, the hourly operation for winter and summer week is shown.

4.4.1. The least-cost/maximum CO_2 emissions solution

Figure 19 shows the DH system operation for a winter week of the least-cost solution for the wind penetration of 45 TWh and 60 TWh of wind. It can be seen that the heat pump operates in the same manner for both levels of wind energy penetration – at full load for a whole week, while charging the thermal storage during the night. The small difference can be seen when analysing the operation of the thermal storage. During night period, thermal storage is more charged for 60 TWh of wind penetration than with 45 TWh, due to the higher heat pump capacity and its utilization.

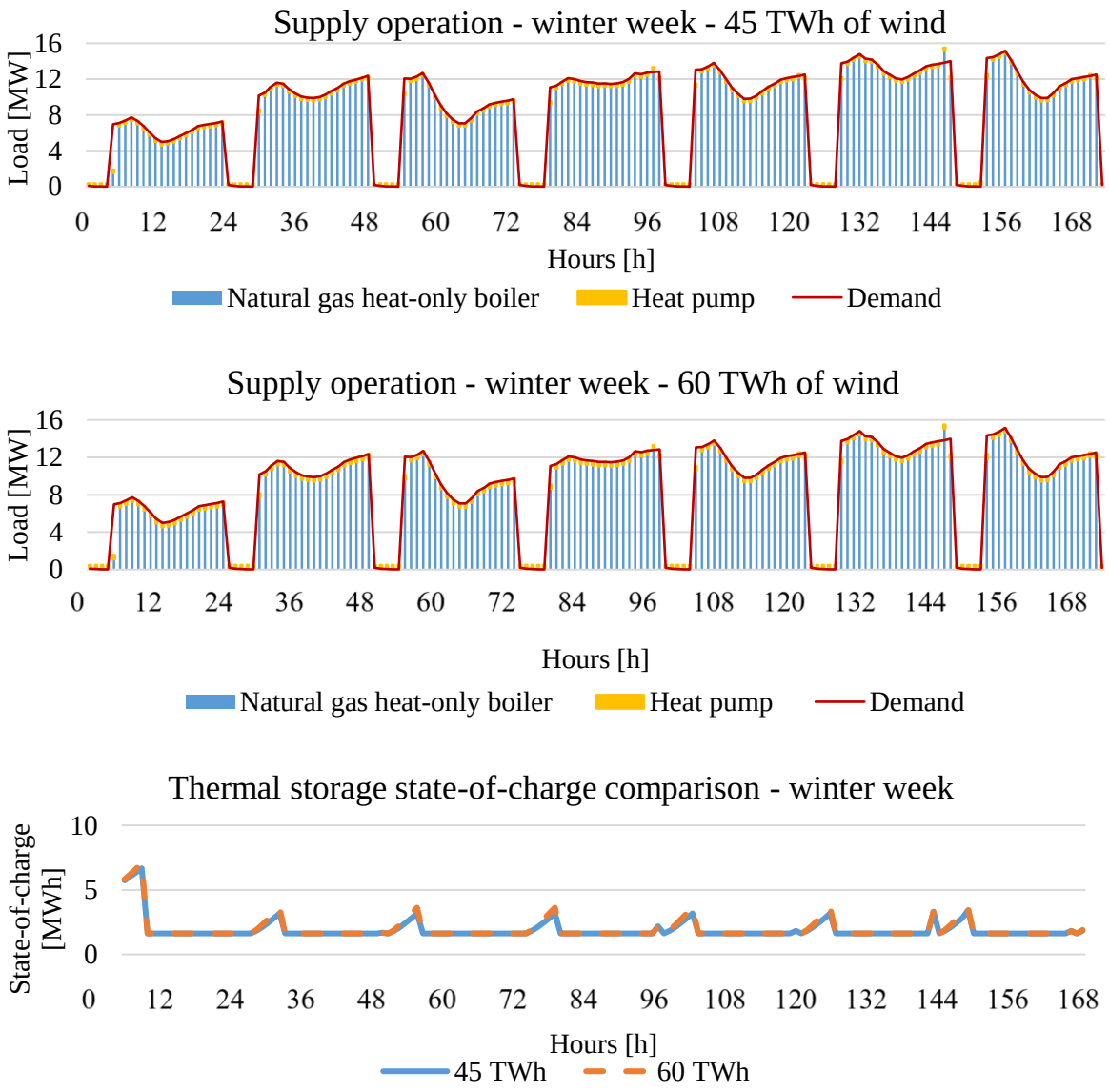

Figure 19 District heating system operation comparison for different levels of wind penetration for winter week – the least-cost solution

The difference in operation between the 45 TWh and the 60 TWh wind penetration is more obvious during summertime when the load is much smaller, only up to 1 MW. A smaller heat pump, obtained for lower wind penetration, can operate through the whole week, while a larger heat pump, obtained for higher wind penetration, will be much more dependent on the market price, i.e. during some hours, it will be able to shut down. Furthermore, the strategy of thermal storage charging is different when wind penetration is increased.

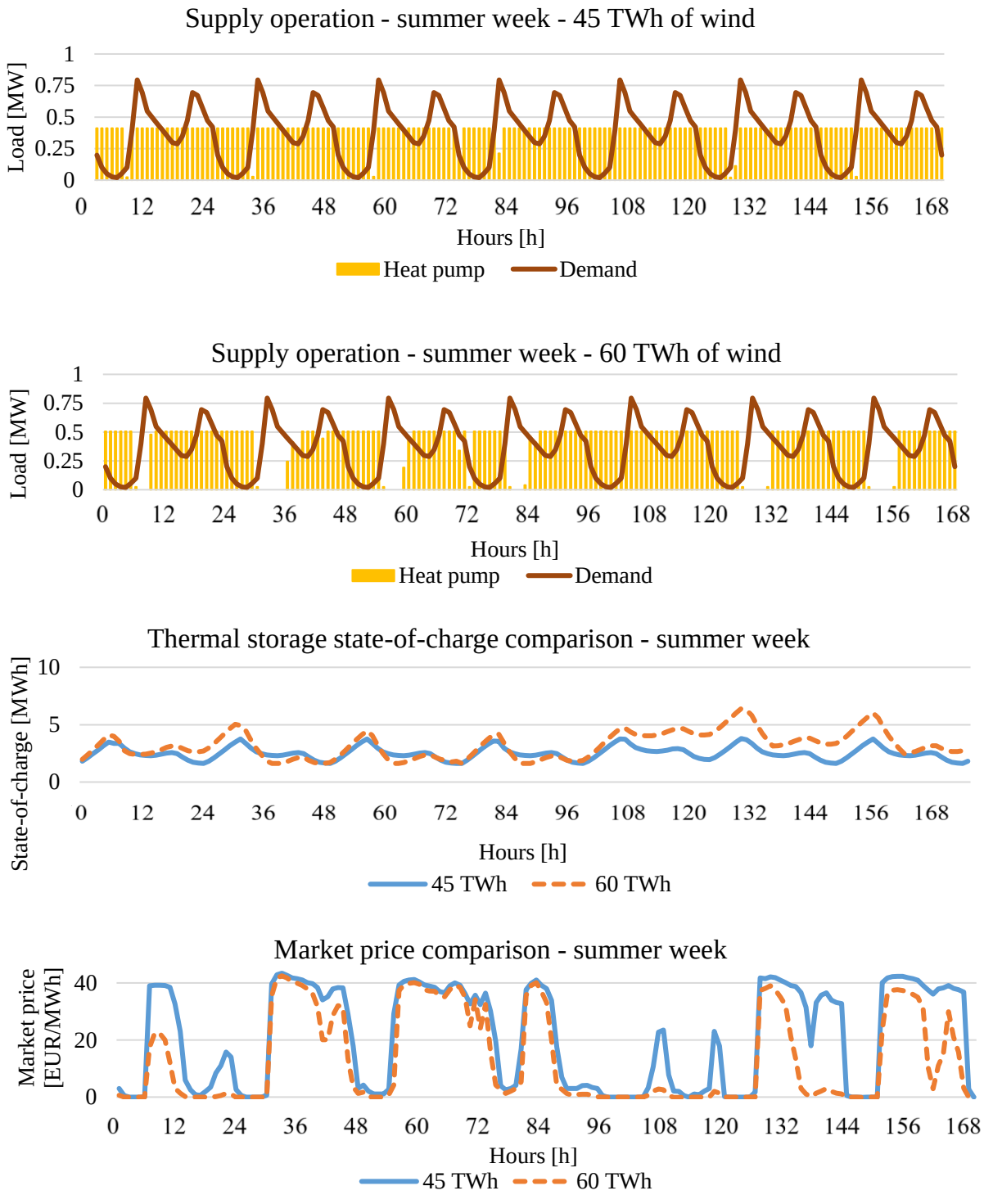

Figure 20 District heating system operation comparison for different levels of wind penetration for a summer week – the least-cost solution

4.4.2. Pareto optimal solution – 5,000 tonnes of CO_2 emissions solution

Figure 21 shows the optimal DH system operation for CO_2 emissions value of 5,000 tonnes. When compared to the least-cost solution it can be noted that a biomass boiler is also part of the optimal solution. Once again, the differences are not that obvious, but it can be seen that the state-of-charge of the thermal storage for 60 TWh of wind penetration is a little higher during the night period due to the higher optimal capacity of the heat pump.

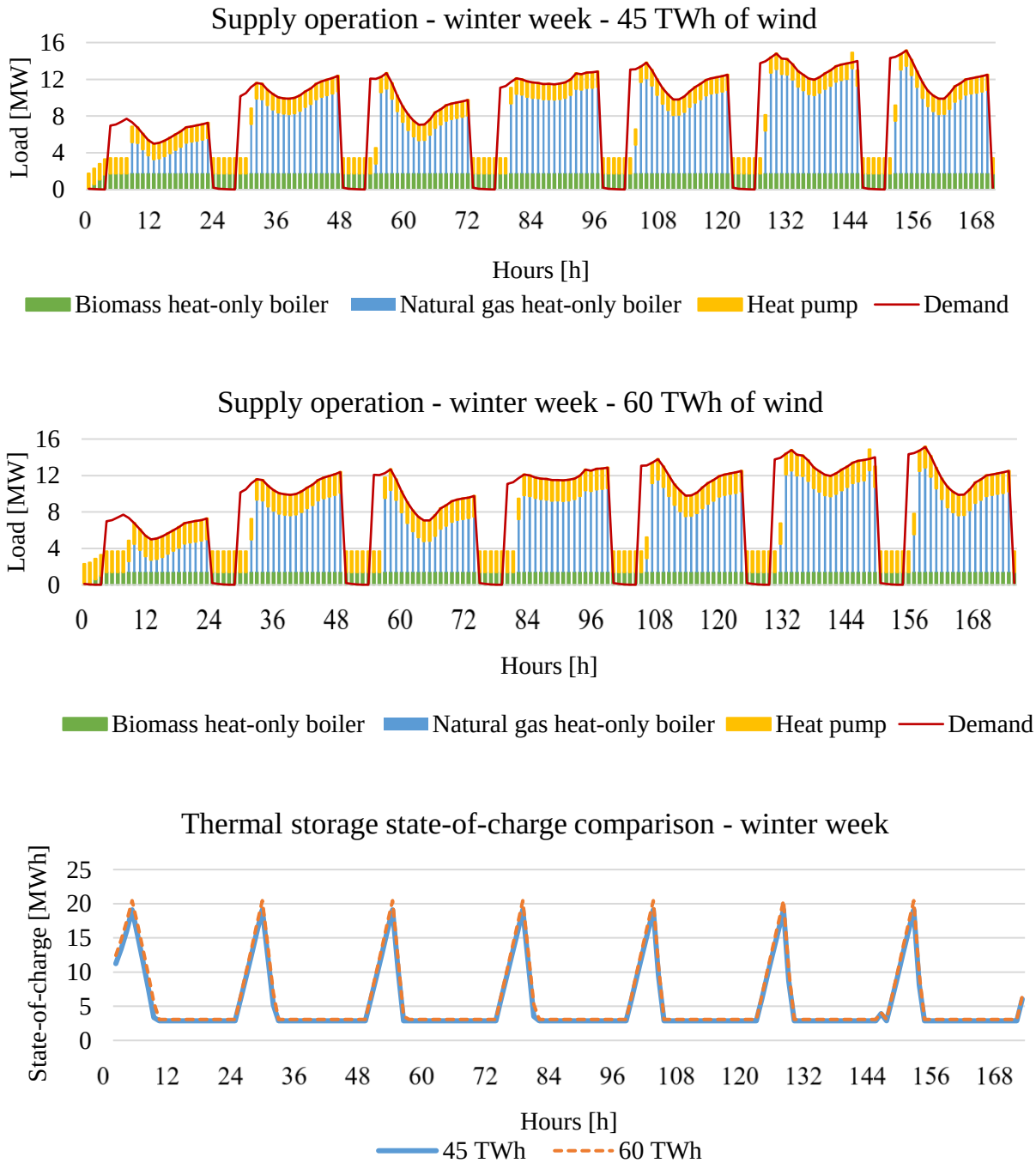

Figure 21 District heating system operation comparison for different levels of wind penetration for a winter week – the Pareto solution with 5,000 tonnes of CO_2 emissions

Figure 22 shows a comparison of DH system operation for the CO_2 emissions value of 5,000 tonnes for two different wind penetrations. The differences between operational strategies are more evident during the summertime than during a winter week. This could especially be seen in the thermal storage operation. For higher wind penetration the thermal storage is more utilized than for 45 TWh of wind production penetration.

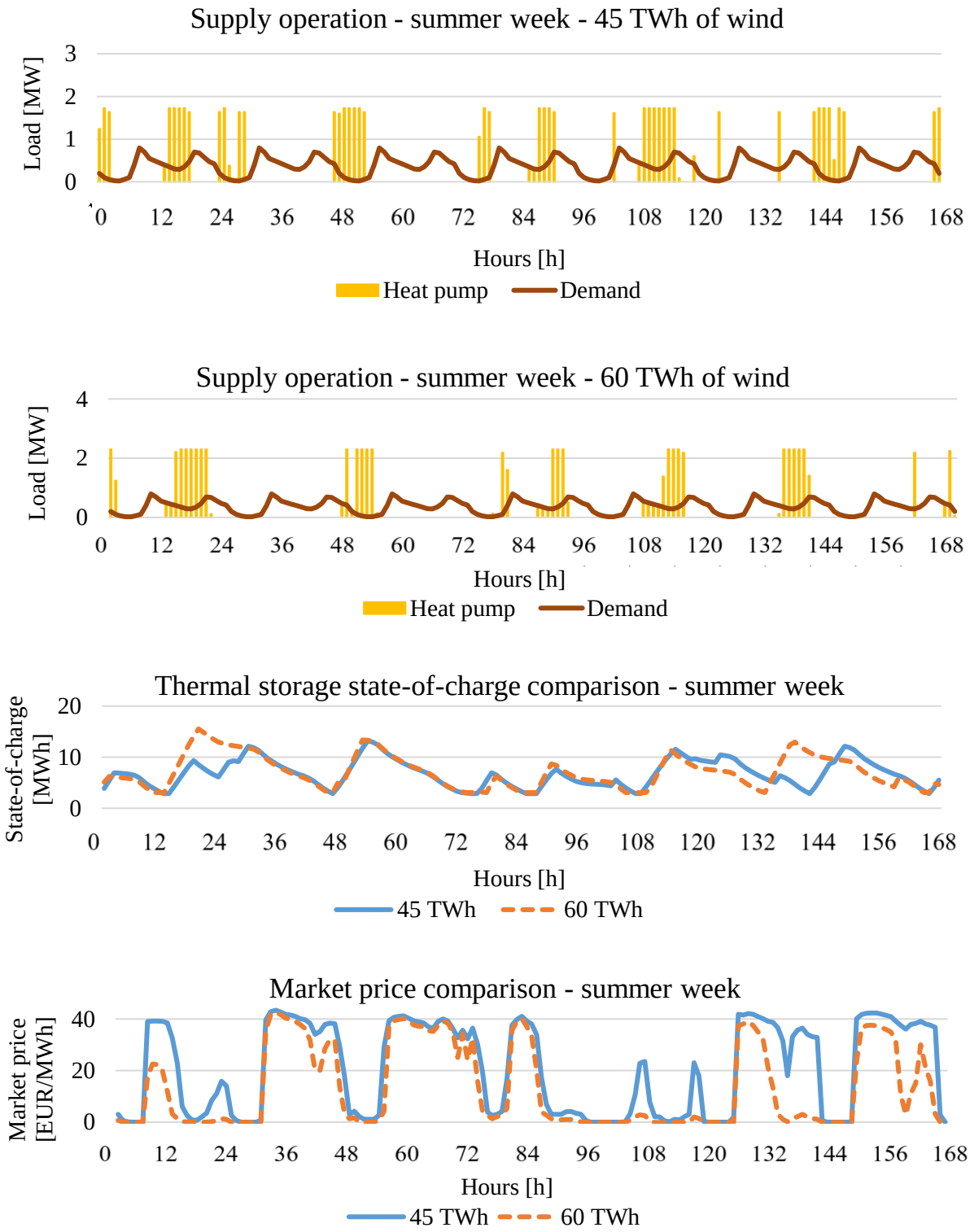

Figure 22 District heating system operation comparison for different levels of wind penetration for a summer week – the Pareto solution with 5,000 tonnes of CO_2 emissions

5. Conclusion

In this paper, an analysis of optimal heat pump capacities was performed with regard to the penetration of variable renewable energy sources. A multi-objective optimization model was used in order to acquire the optimal configuration of the district heating supply system and its operation. In order to evaluate the impact of wind production penetration on the optimal heat pump capacities, the electricity market clearing price was modelled by using publicly available Nord Pool market bidding data. The correlation between the increased wind energy production and the market price was obtained. Two scenarios were developed. In the first one, the power sector emission factor was equal to the historical one, while in the second scenario the power sector emission factor was reduced to zero. The obtained results show that increase of wind capacities enables higher capacities and thermal production of heat pumps. In Scenario 1, this was accomplished only for wind production higher than 33 TWh. However, in Scenario 2, heat pumps are part of the optimal solution for all studied electricity market prices. Furthermore, it was shown that the thermal storage capacity also increases with wind penetration.

Acknowledgements

Financial support from the RESFLEX project funded by the Programme of the Government of Republic of Croatia, Croatian Environmental Protection and Energy Efficiency Fund with the support of the Croatian Science Foundation for encouraging research and development activities in the area of Climate Change for the period from 2015 to 2016 in the amount of 1.344.100 HRK is gratefully acknowledged.

Appendix

A district heating model is shown in Figure A.1. The scheme visualizes different supply technology types and their interconnections, including short-term and long-term thermal energy storage. Furthermore, Figure A.1 displays the optimization variables: the supply capacities P_i, i.e. thermal storage size TES_{size}, and the hourly operation of the system Q_t, i.e. the thermal storage charge and discharge TES_{in-out}. All technologies must cover the district heating demand DEM_t. Finally, the connection with the hourly electricity market can be noted. Power-to-heat technologies (heat pump and electrical heater) buy electricity and cogeneration units sell it on the hourly market. The hourly electricity market clearing price is marked with MCP_t.

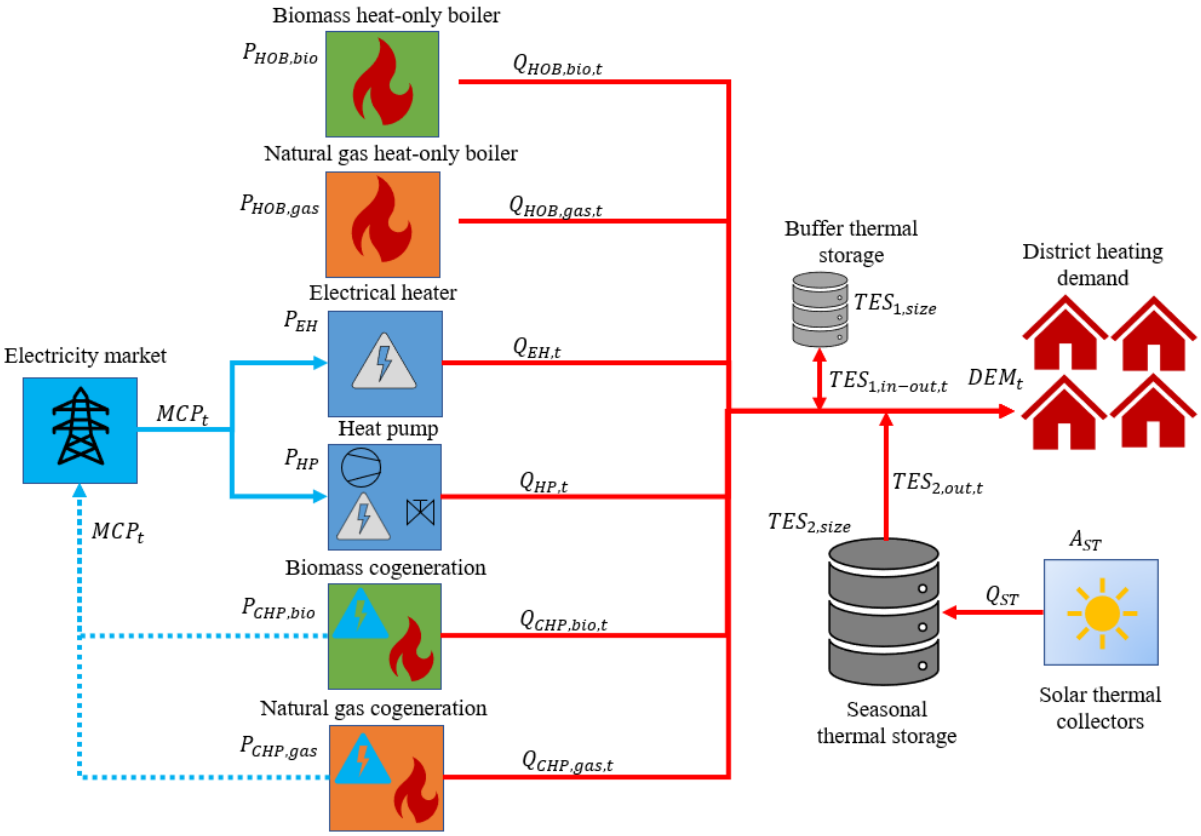

Figure A.1 District heating model

The district heating load used in this paper is shown in Figure A.1. It is constituted of the domestic hot water and space heating demand with a strong seasonal effect. The maximum demand is equal to 20 MW.

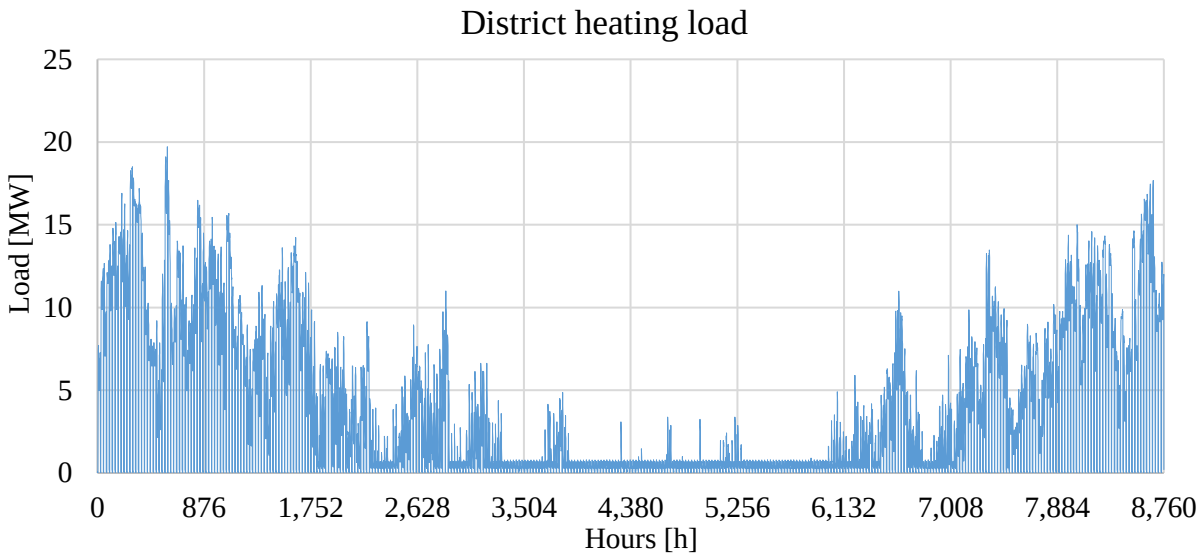

Figure A.2 District heating load

References

[1] A. R. Mazhar, S. Liu, and A. Shukla, "A state of art review on the district heating systems," *Renew. Sustain. Energy Rev.*, vol. 96, no. August, pp. 420–439, 2018, doi: 10.1016/j.rser.2018.08.005.

[2] A. Lake, B. Rezaie, and S. Beyerlein, "Review of district heating and cooling systems for a sustainable future," *Renew. Sustain. Energy Rev.*, vol. 67, pp. 417–425, 2017, doi: 10.1016/j.rser.2016.09.061.

[3] M. Wahlroos and M. Pärssinen, "Future views on waste heat utilization – Case of data centers in Northern Europe," *Renew. Sustain. Energy Rev.*, vol. 82, no. July 2017, pp. 1749–1764, 2018, doi: 10.1016/j.rser.2017.10.058.

[4] H. Lund, N. Duic, P. A. Ostergaard, and B. V. Mathiesen, "Future District Heating Systems and Technologies : On the role of Smart Energy Systems and 4 th Generation District," *Energy*, 2018, doi: 10.1016/j.energy.2018.09.115.

[5] H. Lund *et al.*, "4th Generation District Heating (4GDH). Integrating smart thermal grids into future sustainable energy systems.," *Energy*, vol. 68, pp. 1–11, 2014, doi: 10.1016/j.energy.2014.02.089.

[6] H. Lund, B. Möller, B. V. Mathiesen, and A. Dyrelund, "The role of district heating in future renewable energy systems," *Energy*, vol. 35, no. 3, pp. 1381–1390, 2010, doi: 10.1016/j.energy.2009.11.023.

[7] D. Olsthoorn, F. Haghighat, and P. A. Mirzaei, "Integration of storage and renewable energy into district heating systems: A review of modelling and optimization," *Sol. Energy*, vol. 136, pp. 49–64, 2016, doi: 10.1016/j.solener.2016.06.054.

[8] P. A. Østergaard, "Reviewing EnergyPLAN simulations and performance indicator applications in EnergyPLAN simulations," *Applied Energy*, vol. 154. pp. 921–933, 2015, doi: 10.1016/j.apenergy.2015.05.086.

[9] P. A. Østergaard and A. N. Andersen, "Booster heat pumps and central heat pumps in district heating," *Appl. Energy*, vol. 184, pp. 1374–1388, 2016, doi: 10.1016/j.apenergy.2016.02.144.

[10] R. Mikulandrić *et al.*, "Performance analysis of a hybrid district heating system: A case study of a small town in Croatia," *J. Sustain. Dev. Energy, Water Environ. Syst.*, vol. 3, no. 3, pp. 282–302, 2015, doi: 10.13044/j.sdewes.2015.03.0022.

[11] P. Prebeg, G. Gasparovic, G. Krajacic, and N. Duic, "Long-term energy planning of Croatian power system using multi-objective optimization with focus on renewable energy and integration of electric vehicles," *Appl. Energy*, 2016, doi: 10.1016/j.apenergy.2016.03.086.

[12] M. A. Sayegh *et al.*, "Trends of European research and development in district heating technologies," *Renew. Sustain. Energy Rev.*, vol. 68, pp. 1183–1192, 2017, doi: 10.1016/j.rser.2016.02.023.

[13] H. Ahvenniemi and K. Klobut, "Future services for district heating solutions in residential districts," *J. Sustain. Dev. Energy, Water Environ. Syst.*, vol. 2, no. 2, pp. 127–138, 2014, doi: 10.13044/j.sdewes.2014.02.0012.

[14] S. Buffa, M. Cozzini, M. D'Antoni, M. Baratieri, and R. Fedrizzi, "5th generation

district heating and cooling systems: A review of existing cases in Europe," *Renew. Sustain. Energy Rev.*, vol. 104, no. June 2018, pp. 504–522, 2019, doi: 10.1016/j.rser.2018.12.059.

[15] A. Arabkoohsar and A. S. Alsagri, "Thermodynamic analysis of ultralow-temperature district heating system with shared power heat pumps and triple-pipes," *Energy*, vol. 194, p. 116918, 2020, doi: 10.1016/j.energy.2020.116918.

[16] M. Tańczuk, J. Skorek, and P. Bargiel, "Energy and economic optimization of the repowering of coal-fired municipal district heating source by a gas turbine," *Energy Convers. Manag.*, vol. 149, pp. 885–895, 2017, doi: 10.1016/j.enconman.2017.03.053.

[17] A. Niromandfam, A. S. Yazdankhah, and R. Kazemzadeh, "Modeling Demand Response based on Utility function considering wind profit maximization in the day-ahead market," *J. Clean. Prod.*, 2019, doi: 10.1016/j.jclepro.2019.119317.

[18] G. Li and J. Shi, "Agent-based modeling for trading wind power with uncertainty in the day-ahead wholesale electricity markets of single-sided auctions," *Appl. Energy*, vol. 99, pp. 13–22, 2012, doi: 10.1016/j.apenergy.2012.04.022.

[19] L. Chinmoy, S. Iniyan, and R. Goic, "Modeling wind power investments, policies and social benefits for deregulated electricity market – A review," *Appl. Energy*, vol. 242, no. May 2018, pp. 364–377, 2019, doi: 10.1016/j.apenergy.2019.03.088.

[20] S. S. Reddy, P. R. Bijwe, and A. R. Abhyankar, "Electrical Power and Energy Systems Optimum day-ahead clearing of energy and reserve markets with wind power generation using anticipated real-time adjustment costs," *Int. J. Electr. Power Energy Syst.*, vol. 71, pp. 242–253, 2015, doi: 10.1016/j.ijepes.2015.03.002.

[21] M. Doostizadeh, F. Aminifar, H. Lesani, and H. Ghasemi, "Multi-area market clearing in wind-integrated interconnected power systems: A fast parallel decentralized method," *Energy Convers. Manag.*, vol. 113, pp. 131–142, 2016, doi: 10.1016/j.enconman.2016.01.047.

[22] S. Fogelberg and E. Lazarczyk, "Wind power volatility and its impact on production failures in the Nordic electricity market," *Renew. Energy*, vol. 105, pp. 96–105, 2017, doi: 10.1016/j.renene.2016.12.024.

[23] R. P. Odeh and D. Watts, "Impacts of wind and solar spatial diversification on its market value : A case study of the Chilean electricity market," *Renew. Sustain. Energy Rev.*, vol. 111, no. May, pp. 442–461, 2019, doi: 10.1016/j.rser.2019.01.015.

[24] F. Isaza and S. Botero, "Wind power reliability valuation in a Hydro-Dominated power market : The Colombian case," *Renew. Sustain. Energy Rev.*, vol. 57, pp. 1359–1372, 2016, doi: 10.1016/j.rser.2015.12.159.

[25] M. Pavičević, T. Novosel, T. Pukšec, and N. Duić, "Hourly optimization and sizing of district heating systems considering building refurbishment - Case study for the city of Zagreb," *Energy*, 2016, doi: 10.1016/j.energy.2017.06.105.

[26] J. P. Jiménez Navarro, J. M. Cejudo López, and D. Connolly, "The effect of feed-in-tariff supporting schemes on the viability of a district heating and cooling production system," *Energy*, vol. 134, pp. 438–448, 2017, doi: 10.1016/j.energy.2017.05.174.

[27] T. Falke, S. Krengel, A.-K. Meinerzhagen, and A. Schnettler, "Multi-objective optimization and simulation model for the design of distributed energy systems," *Appl.*

Energy, 2016, doi: 10.1016/j.apenergy.2016.03.044.

[28] D. Wei, A. Chen, B. Sun, and C. Zhang, "Multi-objective optimal operation and energy coupling analysis of combined cooling and heating system," *Energy*, vol. 98, pp. 296–307, 2016, doi: 10.1016/j.energy.2016.01.027.

[29] M. Pirouti, A. Bagdanavicius, J. Ekanayake, J. Wu, and N. Jenkins, "Energy consumption and economic analyses of a district heating network," *Energy*, vol. 57, pp. 149–159, 2013, doi: 10.1016/j.energy.2013.01.065.

[30] N. Lamaison, S. Collette, M. Vallée, and R. Bavière, "Storage influence in a combined biomass and power-to-heat district heating production plant," *Energy*, vol. 186, 2019, doi: 10.1016/j.energy.2019.07.044.

[31] M. Åberg, L. Fälting, D. Lingfors, A. M. Nilsson, and A. Forssell, "Do ground source heat pumps challenge the dominant position of district heating in the Swedish heating market?," *J. Clean. Prod.*, vol. 254, 2020, doi: 10.1016/j.jclepro.2020.120070.

[32] K. Kontu, S. Rinne, and S. Junnila, "Introducing modern heat pumps to existing district heating systems – Global lessons from viable decarbonizing of district heating in Finland," *Energy*, vol. 166, pp. 862–870, 2019, doi: 10.1016/j.energy.2018.10.077.

[33] P. Sorknæs, S. R. Djørup, H. Lund, and J. Z. Thellufsen, "Quantifying the influence of wind power and photovoltaic on future electricity market prices," *Energy Convers. Manag.*, vol. 180, no. November 2018, pp. 312–324, 2019, doi: 10.1016/j.enconman.2018.11.007.

[34] S. Amiri and G. Weinberger, "Increased cogeneration of renewable electricity through energy cooperation in a Swedish district heating system - A case study," *Renew. Energy*, vol. 116, pp. 866–877, 2018, doi: 10.1016/j.renene.2017.10.003.

[35] S. Djørup, J. Z. Thellufsen, and P. Sorknæs, "The electricity market in a renewable energy system," *Energy*, 2018, doi: 10.1016/j.energy.2018.07.100.

[36] B. Felten, "An integrated model of coupled heat and power sectors for large-scale energy system analyses," *Appl. Energy*, vol. 266, no. January, p. 114521, 2020, doi: 10.1016/j.apenergy.2020.114521.

[37] S. Mosquera-lópez and A. Nursimulu, "Drivers of electricity price dynamics : Comparative analysis of spot and futures markets," *Energy Policy*, vol. 126, no. November 2018, pp. 76–87, 2019, doi: 10.1016/j.enpol.2018.11.020.

[38] W. Liu, D. Klip, W. Zappa, S. Jelles, and G. Jan, "The marginal-cost pricing for a competitive wholesale district heating market: A case study in the Netherlands," *Energy*, no. 189, p. 116367, 2019, doi: 10.1016/j.energy.2019.116367.

[39] J. Hennessy, H. Li, F. Wallin, and E. Thorin, "Towards smart thermal grids : Techno-economic feasibility of commercial heat-to-power technologies for district heating," *Appl. Energy*, vol. 228, no. June, pp. 766–776, 2018, doi: 10.1016/j.apenergy.2018.06.105.

[40] D. Wang *et al.*, "Integrated demand response in district electricity-heating network considering double auction retail energy market based on demand-side energy stations," *Appl. Energy*, vol. 248, no. January, pp. 656–678, 2019, doi: 10.1016/j.apenergy.2019.04.050.

[41] Z. Yifan *et al.*, “Power and Energy Flexibility of District Heating System and Its Application in Wide-Area Power and Heat Dispatch,” *Energy*, p. 116426, 2019, doi: 10.1016/j.energy.2019.116426.

[42] J. Wang, Z. Zhou, J. Zhao, J. Zheng, and Z. Guan, “Optimizing for clean-heating improvements in a district energy system with high penetration of wind power,” *Energy*, vol. 175, pp. 1085–1099, 2019, doi: 10.1016/j.energy.2019.03.153.

[43] F. Levihn, “CHP and heat pumps to balance renewable power production: Lessons from the district heating network in Stockholm,” *Energy*, vol. 137, pp. 670–678, 2017, doi: 10.1016/j.energy.2017.01.118.

[44] S. Moser, S. Puschnigg, and V. Rodin, “Designing the Heat Merit Order to determine the value of industrial waste heat for district heating systems,” *Energy*, vol. 200, p. 117579, 2020, doi: 10.1016/j.energy.2020.117579.

[45] J. Wang, S. You, Y. Zong, H. Cai, C. Træholt, and Z. Y. Dong, “Investigation of real-time flexibility of combined heat and power plants in district heating applications,” *Appl. Energy*, vol. 237, no. November 2018, pp. 196–209, 2019, doi: 10.1016/j.apenergy.2019.01.017.

[46] D. Lingfors, J. Olauson, D. Lingfors, and J. Olauson, “Can electricity market prices control power-to-heat production for peak shaving of renewable power generation ? The case of Sweden,” *Energy*, vol. 176, no. 1, pp. 1–14, 2019, doi: 10.1016/j.energy.2019.03.156.

[47] O. Terreros *et al.*, “Electricity market options for heat pumps in rural district heating networks in Austria,” *Energy*, vol. 196, p. 116875, 2020, doi: 10.1016/j.energy.2019.116875.

[48] P. A. Østergaard, J. Jantzen, H. M. Marczinkowski, and M. Kristensen, “Business and socioeconomic assessment of introducing heat pumps with heat storage in small-scale district heating systems,” *Renew. Energy*, vol. 139, pp. 904–914, 2019, doi: 10.1016/j.renene.2019.02.140.

[49] D. Böttger, M. Götz, M. Theofilidi, and T. Bruckner, “Control power provision with power-to-heat plants in systems with high shares of renewable energy sources - An illustrative analysis for Germany based on the use of electric boilers in district heating grids,” *Energy*, vol. 82, pp. 157–167, 2015, doi: 10.1016/j.energy.2015.01.022.

[50] M. Ito, A. Takano, T. Shinji, T. Yagi, and Y. Hayashi, “Electricity adjustment for capacity market auction by a district heating and cooling system,” *Appl. Energy*, vol. 206, no. August, pp. 623–633, 2017, doi: 10.1016/j.apenergy.2017.08.210.

[51] J. Zheng, Z. Zhou, J. Zhao, and J. Wang, “Effects of the operation regulation modes of district heating system on an integrated heat and power dispatch system for wind power integration,” *Appl. Energy*, vol. 230, no. September, pp. 1126–1139, 2018, doi: 10.1016/j.apenergy.2018.09.077.

[52] A. Gravelsins, I. Pakere, A. Tukulis, and D. Blumberga, “Solar power in district heating. P2H flexibility concept,” *Energy*, vol. 181, pp. 1023–1035, 2019, doi: 10.1016/j.energy.2019.05.224.

[53] B. Leitner, E. Widl, W. Gawlik, and R. Hofmann, “A method for technical assessment of power-to-heat use cases to couple local district heating and electrical distribution

grids," *Energy*, vol. 182, pp. 729–738, 2019, doi: 10.1016/j.energy.2019.06.016.

[54] D. F. Dominković, M. Wahlroos, S. Syri, and A. S. Pedersen, "Influence of different technologies on dynamic pricing in district heating systems: Comparative case studies," *Energy*, vol. 153, no. March, pp. 136–148, 2018, doi: 10.1016/j.energy.2018.04.028.

[55] E. Sandberg, J. G. Kirkerud, E. Trømborg, and T. F. Bolkesjø, "Energy system impacts of grid tariff structures for flexible power-to-district heat," *Energy*, vol. 168, pp. 772–781, 2019, doi: 10.1016/j.energy.2018.11.035.

[56] H. Averfalk, P. Ingvarsson, U. Persson, M. Gong, and S. Werner, "Large heat pumps in Swedish district heating systems," *Renew. Sustain. Energy Rev.*, vol. 79, no. May, pp. 1275–1284, 2017, doi: 10.1016/j.rser.2017.05.135.

[57] P. A. Østergaard and A. N. Andersen, "Economic feasibility of booster heat pumps in heat pump-based district heating systems," *Energy*, 2018, doi: 10.1016/j.energy.2018.05.076.

[58] K. Askeland, K. N. Bozhkova, and P. Sorknæs, "Balancing Europe : Can district heating affect the flexibility potential of Norwegian hydropower resources ?," *Renew. Energy*, vol. 141, no. 2019, pp. 646–656, 2020, doi: 10.1016/j.renene.2019.03.137.

[59] M. Swing, J. Are, and E. Dotzauer, "Potential for district heating to lower peak electricity demand in a medium-size municipality in Sweden," *J. Clean. Prod.*, vol. 186, pp. 1–9, 2018, doi: 10.1016/j.jclepro.2018.03.038.

[60] P. Sorknæs *et al.*, "Smart Energy Markets - Future electricity, gas and heating markets," *Renew. Sustain. Energy Rev.*, vol. 119, no. March 2019, 2020, doi: 10.1016/j.rser.2019.109655.

[61] M. A. Mirzaei *et al.*, "Evaluating the impact of multi-carrier energy storage systems in optimal operation of integrated electricity, gas and district heating networks," *Appl. Therm. Eng.*, vol. 176, p. 115413, 2020, doi: 10.1016/j.applthermaleng.2020.115413.

[62] J. Jimenez-Navarro, K. Kavvadias, F. Filippidou, M. Pavičević, and S. Quoilin, "Coupling the heating and power sectors : The role of centralised combined heat and power plants and district heat in a European decarbonised power system," *Appl. Energy*, vol. 270, no. May, 2020, doi: 10.1016/j.apenergy.2020.115134.

[63] H. Dorotić, T. Pukšec, and N. Duić, "Multi-objective optimization of district heating and cooling systems for a one-year time horizon," *Energy*, 2019, doi: 10.1016/j.energy.2018.11.149.

[64] H. Dorotić, T. Pukšec, and N. Duić, "Economical, environmental and exergetic multi-objective optimization of district heating systems on hourly level for a whole year," *Appl. Energy*, vol. 251, p. 113394, Oct. 2019, doi: 10.1016/j.apenergy.2019.113394.

[65] JRC, "PVGIS." [Online]. Available: http://re.jrc.ec.europa.eu/pvgis.html, the last access 28/06/2020

[66] "Renewable ninja." [Online]. Available: https://www.renewables.ninja/, the last access 28/06/2020

[67] P. A. Sørensen, J. E. Nielsen, R. Battisti, T. Schmidt, and D. Trier, "Solar district heating guidelines: Collection of fact sheets," no. August, p. 152, 2012.

[68] “SPF Institut für Solartechnik.” [Online]. Available: http://www.spf.ch/index.php?id=111&L=6, the last access 28/06/2020

[69] S. Frederiksen and S. Werner, *District Heating and Cooling*. 2013.

[70] W. Jakob and C. Blume, “Pareto optimization or cascaded weighted sum: A comparison of concepts,” *Algorithms*, vol. 7, no. 1, pp. 166–185, 2014, doi: 10.3390/a7010166.

[71] M. Dillig, M. Jung, and J. Karl, “The impact of renewables on electricity prices in Germany – An estimation based on historic spot prices in the years 2011 – 2013,” *Renew. Sustain. Energy Rev.*, vol. 57, pp. 7–15, 2016, doi: 10.1016/j.rser.2015.12.003.

[72] “Nord Pool.”

[73] K. Van Den Bergh and E. Delarue, “Cycling of conventional power plants: Technical limits and actual costs,” *Energy Convers. Manag.*, vol. 97, pp. 70–77, 2015, doi: 10.1016/j.enconman.2015.03.026.

[74] “Danish Energy Agency, Technology database.” .

PAPER 6

Evaluation of District Heating with Regard to Individual Systems – Importance of Carbon and Cost Allocation in Cogeneration Units

Hrvoje Dorotić*, Tomislav Pukšec, Daniel Rolph Schneider, Neven Duić

University of Zagreb, Faculty of Mechanical Engineering and Naval Architecture,

Department of Energy, Power Engineering and Environmental Engineering, Ivana Lučića 5, 10002, Zagreb, Croatia

Email: hrvoje.dorotic@fsb.hr

Abstract

Although, district heating has high share in the heating sector of Northern Europe, Central-Eastern European countries often do not utilize full potential for further thermal network expansion. The main reasons for this are relatively low energy market prices, such as natural gas for households, which diminish economic feasibility of the proposed projects. Even though there are numerous optimization methods which can optimize district heating system, they rarely provide cost comparison with individual heating solutions. This paper presents a novel method of evaluating district heating with respect to individual systems by using multi-objective optimization approach coupled with cost and carbon allocations in cogeneration units. Objective functions are defined as minimization of total discounted cost, including environmental impact, and maximization of exergy efficiency. To deal with multi-objective optimization, epsilon-constraint method has been used. The main outcome of this research are energy market prices for which district heating systems have lower environmental impact and exergy destruction than individual natural gas-based heating solutions, while at the same time being economically feasible. Finally, the paper demonstrates that cogeneration-based district heating systems are superior to individual heating, even for low households' natural gas prices.

Keywords: district heating, energy planning, cogeneration, multi-objective optimization, CHP allocation

Abbreviations

CHP	cogeneration
DH	district heating
EH	electrcial heater
HOB	heat-only boiler
HP	heat pump
RES	renewable energy sources
ST	solar thermal

Chemical formulas

CO_2	carbon dioxide

Variables and parameters

A_{ST}	area of solar thermal collectors [m^2]
a_1	first order heat loss coefficient [W/K]
a_2	second order heat loss coefficient [W/K^2]
b	binary variable, technology selection [-]
C	cost [EUR]
$Cost_{CHP}$	total cost of CHP unit [EUR]
$Cost^*_{CHP}$	cost of CHP unit allocated to heat [EUR]
$CO_{2_{CHP}}$	Total carbon emisssions of CHP unit [tonnes of CO_2]
$CO^*_{2_{CHP}}$	Carbon emisssions of CHP unit alocated to heat [tonnes of CO_2]
DEM	district heating demand [MW]
e_{Exe}	exergy factor of the fuel [-]
e_{CO_2}	Speficic carbon emissions of a fuel [tonnes of CO_2/MWh]
E	electrical energy production in CHP unit [MWh]
Ex_{in}	exergy input [MWh]
Ex_{out}	exergy output [MWh]
f_{eco}	ecological objective function [tonnes of CO_2]
f_{econ}	economical objective function (EUR)
f_{exe}	exergetic objective function [-]
$f_{Lorentz}$	Lorentz factor of the heat pump [-]
G	global solar radiation [W/m^2]
P	supply capacity [MW]
Q	thermal energy [MWh]
$r_{up-down}$	ramping limit of technology [h^{-1}]
SOC	state-of-charge [MWh]
T	temperature [°C]
TES	thermal storage
TES_{in-out}	thermal storage charge and discharge [MW]

Greek letters

β_{CHP}	power-loss factor of CHP unit [-]
η	technology efficiency [-]
η_0	optical efficiency of solar thermal collector [-]

ε_{eco}	epsilon constraint for ecological objective function [tonnes of CO_2]
ε_{exe}	epsilon constraint for exergetic objective function [-]
σ_{CHP}	power-to-heat factor of CHP unit [-]

Subscripts

eco	ecological
econ	economical
exe	exergetic
fix	fixed
i	technology type
inv	investment
t	time
var	variable

1. Introduction

District heating (DH) systems will be crucial component in future energy systems with high share of renewable energy sources [1], [2] by utilizing power-to-heat technologies [3] to store excess of electricity as thermal energy [4] in various thermal storage types [5]. In the literature, four generations of district heating systems are defined, each one with lower temperatures and higher thermal network efficiencies than the previous one [6]. Lower temperatures can offer additional possibilities of numerous available heat sources, such as data centres [7], [8], metro stations and other [9]. Ommen et al. have analysed different configurations of booster heat pumps in ultra-low temperature systems [10]. This technical challenge has also been interest of Elmegaard et al. in [11]. In other paper, authors have analysed how temperature reduction in DH supply will affect Danish energy system [12]. All authors agree how heat pumps will play crucial part in these systems, due to their increased efficiency in low temperature systems. However, this will also mainly depend on their positioning in the energy system, as shown in [13]. Buffa et al. have provided the extensive list of already existing ultra-low and neutral temperature DH systems, calling them the 5^{th} generation [14].

Although district heating systems are recognized as economically feasible option of heating in urban areas, their current potential is still left untapped [15]. Additionally, most of the current DH networks still have relatively high supply temperatures [16]. These systems are here to stay until most of the building stock is refurbished and prepared for lower supply temperatures. Besides high temperatures in the district heating, current systems still have high share of natural gas which is not always efficiently utilized through cogeneration (CHP) units. The importance of CHP in the coupled heating and power sector is analysed in [17]. Dominković et al. have studied the impact of natural gas CHP in thermal network expansion [18]. In paper [19], repowering of coal power plant to cogeneration units for district heating system has been analysed. Soltero et al. evaluated the potential of natural gas based cogeneration in order to decarbonize economy of the Spanish continental area [20]. Sun et al. have studied the integration of natural gas based DH system with geothermal renewable energy source [21]. The issue of exergy destruction in natural gas heat-only boiler has been studied in [22], with the combustion chamber being the highest source of irreversibility.

One of the main competitors of district heating in urban areas is still natural gas due to its relatively small price for households in numerous EU countries [23]. Attractiveness of district heating in these countries is reduced due to marginal financial feasibility, while usage of natural gas heat-only boilers is still expanding. Comparison of district heating with individual heating systems has been carried out for some specific cases. Authors are usually focusing on low-energy buildings and low temperature district heating systems. Paper [24] calculated carbon dioxide (CO_2) abatement cost for different district heating technologies which are substituting natural gas individual heating system. Utilization of natural gas and biomass district heating system have negative abatement cost for great range of the CO_2 emissions reduction. Yoon et al. have investigated opinion of final users on different heating options while focusing on district heating and individual boilers. They have concluded that higher-income and more educated consumers prefer district heating while other consumers who currently use power-to-heat appliances prefer individual heating options. The study was carried out for South Korea [25]. Similar survey has been carried out in [26]. Brum et al. analysed benefits of centralized systems providing space heating and domestic hot water for low energy buildings in Northern

California. From the results acquired, the most efficient technology is a district heating ground based heat pump [27]. Hansen et al. analysed the feasibility of district heating in a case of low energy buildings, while focusing on heating demand density. They have compared district heating and individual heating solutions. The paper concludes that percentage of connected customers is crucial factor for the feasibility of the district heating system [28]. Paper [29] provides an overview of the costs and benefits of preparing the existing Danish building stocks for low temperature district heating. From an energy system perspective, simple payback periods are equal to 1.2-4.3 years. The study concludes that it is economically feasible to invest in a system control which will enable lower district heating return temperatures.

One of the biggest challenges in planning of CHP based district heating systems is cost and carbon allocation between heat and electricity production. This issue is crucial for policy makers, energy planners and researchers which are dealing with heating and power sector coupling and district heating system expansion. Numerous methods have already been proposed. Noussan provides detailed overview of different allocation methods in cogeneration units. Paper also analyses allocation methods in different case studies. Obtained results vary greatly depending on the chosen method and different defined boundary conditions [30]. Tereschenko and Nord also provide different methods for the allocation of CO_2 emissions in cogeneration power plant [31]. Six different methods are explained in detail and used to calculate heat allocation factor while using district heating system as the case study. Gao et al. provided exergy and exergoeconomics analysis of the coal-fired cogeneration power plant [32]. By using these results, they have proposed CO_2 allocation factor for heat and electricity part of the cogeneration unit. Obtained results show how 22%-61%, depending on the method, of the CO_2 emissions produced in the unit should be allocated to heat. This results in heat carbon factors equal to 78-210 g/kWh. Pina et al. tackled the issue of allocating economic cost in trigeneration systems which include thermal energy systems. Hourly unit costs of the internal flows and final products were obtained for a day of the year [33]. Wang et al. proposed systematic method (ECAEL) for defining additional allocation equations and calculating the exergy cost of flows in thermal system [34]. The costs of all flows are calculated by solving the exergy consumption and allocation equations with design conditions. The proposed method provides an option to complete the thermoeconomic analysis of multi-product systems. Gao et al [35] carried out CO2 allocation in coal CHP unit based on exergoeconomic modelling. The results show that carbon emissions allocated to heat and electricity are similar, around 950 g/kWh. Paper [36] compares five allocation techniques usually applied in life-cycle analysis studies with three thermoeconomic allocation techniques for different pollutants (CO_2, NOx and SOx) and resources (fuel consumption) in cogeneration systems. Dos Santos et [37] showed how the thermoeconomic models can be adapted to allocate the overall CO_2 emission of four different cogeneration systems to the electricity and heat. They have also determined specific CO_2 emissions (in g/kWh) for each product. Furthermore, other papers provide allocation methods for other industrial processes, such as for syngas and ammonia production plant [38].

One of the most interesting allocation methods is power-loss, or sometimes called Dresden, method. It is based on translating electricity production reduction, due to the heat production, to carbon emissions and operational cost of a CHP unit. As such, it is in line with the idea that the thermal energy coming from CHP units is mostly excess, or waste heat, which would be unexploited if not used in district heating systems. This method has been presented in numerous

reports [39], [40], [41] and research papers [30], [42], [31], [43]. Cost and carbon allocation approach shown in this paper is also based on this method, as explained in Section 2.

District heating systems are often analysed by means of multi-objective optimization approach. In paper [44], genetic algorithm has been used to obtain the Pareto solutions. Ameri et al. have used multi-objective optimization to integrate district heating and cooling [45]. Franco et al. [46] analysed optimal share of cogeneration in the technology mix while considering second law of thermodynamics. Issue of exergy losses minimization is incorporated in many other papers. Di Somma et al. have developed mixed integer linear programming model to maximize exergy efficiency [47]. Their model has been upgraded and presented in [48]. In paper [49], different DH operation strategies have been analysed by taking into account network temperatures and network losses. Mikulandrić et al. examined performance of hybrid district heating system [50]. Huang et al carried out economic analysis of DH systems combined with solar thermal collectors. They used levelized cost of heat as the objective function, while examining different boundary conditions [51]. Pavičević et al develop the method for operation and capacity optimization of DH supply system, however CHP units have not been considered in the model [52]. In paper [53], multi-objective optimization of integrated district heating and cooling systems has been carried out by using LP approach. Cogeneration units have been included as an option. However, CHP allocation has not been proposed and efficiency of optimal solutions has not been calculated. Although Leśko et al proposed detailed optimization of CHP unit operation, integrated with thermal storage, neither cost nor carbon allocation has been carried out in cogeneration system [54]. Furthermore, the modelling covers only single day, i.e. 24 hours. Similar modelling has been carried out by Kazagić et al in [55]. However, they used commercially available tool called energyPRO. Jie et al developed district heating model [56] based on cogeneration, while also taking into account final customers, i.e. existing buildings. They have optimized insulation thickness to obtain minimum annual total cost. Morvaj et al [57] carried out multi-objective optimization of DH system sizing and operation. Objective functions are minimization of total cost and carbon emissions. Epsilon constraint method was also used to deal with multi-objective optimization. Although cogeneration units were considered, no CHP allocation has been implemented. Finally, no comparison with individual solutions has been carried out. Paper [58] deals with optimisation of marginal extension of existing DH system. The model is capable of optimising DH operation and selecting between different CHP units and sizes. The objective function is cost savings maximization or CO_2 emissions minimisation. The method also includes CHP carbon allocation based on the boiler displacement method used in UK industry for energy reporting. However, only CHP carbon factor for electricity is calculated, while cost allocation has not been carried out. Obtained results have not been compared with individual solutions.

According to the carried-out literature review, multi-objective optimization of district heating systems is rarely carried out in combination with cost and carbon allocation in cogeneration units. Secondly, carbon allocation is usually used to provide analysis of already existing district heating systems or to carry out simple calculation carried out on yearly level. Thirdly, carbon allocation is rarely used together with cost allocation in CHP units, while analysis of allocation for integrated district heating and cooling systems has not been carried out so far on this level of detail. Finally, most of the papers dealing with multi-objective optimization of district heating systems do not compare obtained results with individual heating solutions, such as

natural gas. In other words, their economic feasibility and environmental impact are not brought into question.

While considering carried out literature review and gap analysis of the existing papers dealing with multi-objective optimization of district heating systems, scientific contribution of this paper is defined as following:

- Development of the mixed-integer linear programming, hourly based, multi-objective optimization model capable of optimizing supply capacities and system operation for a whole year, while minimizing total cost, carbon emissions and maximizing exergy efficiency of the system;
- Analysis of the Pareto shift caused by carbon and cost allocation based on the power-loss in cogeneration units;
- Systematic comparison of the district and individual heating systems with respect to cost and carbon allocation methods in cogeneration units;
- Analysis of the impact of allocation methods on integrated district heating and cooling systems.

This paper is divided into several sections. Section 2 provides overview of the district heating optimization model, cost and carbon allocation in CHP unit and multi-objective optimization approach. Section 3 displays input data needed to run the model, while Section 4 shows the obtained results and discusses them in detail. Section 5 summarizes the main outputs and concludes the paper. Finally, Appendix shows different hourly input data, displays overview of the district heating system and provides analysis of renewable energy sources share in energy and exergy output.

2. Method

In this section method used in this paper is presented. In Section 2.1, district heating model is shown in detail, while Section 2.2 shows P-Q (power-heat) diagrams approach used for CHP modelling. Section 2.3 displays carbon and cost allocation used in cogeneration units. Section 2.4 defines objective functions used in the optimization approach, while Section 2.5 shows how multi-objective optimization was treated in the paper.

The method developed for the purpose of this paper is based on the model previously developed by the authors [59].

2.1. District heating model

In this section, district heating model is presented in detail. The model involves several technologies such as heat-only boilers, cogeneration units, heat pumps, electrical heaters, solar thermal collectors, including short-term and seasonal thermal storage. Optimization variables are technology capacities P_i, thermal storage capacities TES_{size} and hourly system operation of each supply unit $Q_{i,t}$, including thermal storage charging and discharging $TES_{in-out,t}$. In other words, P_i represents maximum possible load of technology i, i.e. installed nameplate capacity. Hourly load of technology $Q_{i,t}$ represents thermal energy dispatched from the supply unit to the thermal network in a single hour. Its value cannot be higher than installed capacity P_i. Thermal storage units are treated in similar manner. Maximum state-of-charge is equal to TES_{size}, it represents the size of thermal storage expressed in energy equivalent. Thermal storage charging and discharging on hourly level, is represented with variable $TES_{in-out,t}$. It has negative value in case of discharging and positive value when thermal storage is being charged.

As said, proposed model has a time step of one hour, while time horizon is equal to a whole year. Such lengthy time horizon is needed to carry out sizing of the system without using time slices, as done in other papers. Equation (1) presents basic constraint which implies that heating demand DEM_t should be satisfied in every hour of the year by using various supply capacities and storage. Furthermore, it should be noticed that there are two thermal storage units, as shown in Figure 5A of Appendix. Thermal storage 1 serves as a buffer and can be charged with all technologies, except solar thermal. Thermal storage 2 can be charged only with solar thermal collectors and can also serve as a seasonal storage.

$$DEM_t = Q_{HOB,gas,t} + Q_{HOB,biomass,t} + Q_{EH,t} + Q_{HP,t} + Q_{CHP,gas,t} + Q_{CHP,biomass,t} - TES_{1,in-out,t} - TES_{2,in-out,t} \quad (1)$$

Hourly operation of each supply unit is constrained by using Equation (2), i.e. hourly production of the unit cannot be higher than its installed peak capacity.

$$0 \leq Q_{i,t} \leq P_i \quad (2)$$

Since the technology used in the model include natural gas combi-cogeneration and other large units, minimum possible installed capacity is defined. In order to model such constraint, Equation (3) is used, where b_i is binary variable which describes selection of the technology i, while $P_{min,i}$ is predefined minimum possible capacity of technology i.

$$b_i \cdot P_{min,i} \leq P_i \leq b_i \cdot P_{max,i},\ b_i = \{b_i \in \mathbb{Z} | 0 \leq b_i \leq 1\} \quad (3)$$

In order to acquire more realistic operation supply units, ramping limits are integrated in the model by using Equation (4), where $r_{up-down,i}$ is ramping limit expressed as share of the peak capacity of the technology.

$$-r_{up-down,i} \cdot P_i \leq Q_{i,t} - Q_{i,t-1} \leq r_{up-down,i} \cdot P_i \quad (4)$$

Short-term and seasonal storages are modelled similarly by using Equations (5)-(9). SOC_t is state-of-charge in a time step t, while TES_{loss} is hourly self-discharge of the storage, i.e. hourly thermal loss.

$$SOC_{1,t=1} = SOC_{1,t=8760} = SOC_{1,start-end} \cdot TES_{1,size} \quad (5)$$

$$SOC_{1,t} = SOC_{1,t-1} + TES_{1,in-out,t} - SOC_{1,t} \cdot TES_{1,loss} \quad (6)$$

$$SOC_{2,t=1} = SOC_{2,t=8760} = SOC_{2,start-end} \cdot TES_{2,size} \quad (7)$$

$$SOC_{2,t} = SOC_{2,t-1} + TES_{2,in-out,t} - SOC_{2,t} \cdot TES_{loss} + Q_{ST,t} \quad (8)$$

Operation of the solar thermal collectors is acquired by using Equation (9), where A_{ST} is area of the solar field. This is also the only optimization variable related to the solar thermal collectors, since their operation is constrained, as shown in Equation (9). $P_{solar,specific,t}$ is specific solar thermal output which could be calculated by using Equation (10), $\eta_{c,t}$ is solar thermal collector efficiency which is calculated as explained below.

$$Q_{ST,t} = A_{ST} \cdot P_{solar,specific,t} \quad (9)$$

$$P_{solar,specific,t} = \eta_{c,t} \cdot G_t \quad 10)$$

Besides optimization variables, there are various exogeneous variables which are calculated by using meteorological data and district heating network temperatures. Equation (11) shows calculation of the solar thermal collector efficiency by using predefined solar thermal collector parameters η_0, a_1 and a_2. The first parameter, η_0, is called optical efficiency, a_1 is first order thermal loss coefficient and a_2 is second order thermal loss coefficient. $T_{ref,t}$ is hourly outside temperature, G_t is hourly global solar radiation, while $T_{m,t}$ is mean collector fluid temperature. For the purposes of this paper it is equal to mean value of district heating supply and return temperature in respective time step t, already proposed in [60]. Its calculation has been simplified to secure linearity of the model.

$$\eta_{c,t} = \eta_0 - a_1 \frac{\left(T_{m,t} - T_{ref,t}\right)}{G_t} - a_2 \frac{\left(T_{m,t} - T_{ref,t}\right)^2}{G_t} \quad (11)$$

Coefficient of performance of the heat pump (COP) could be calculated by using Equation (12), where f_{Lorenz} presents the ratio between real and ideal heat pump efficiency.

$$\eta_{HP,t} = f_{Lorenz} \cdot \left(\frac{T_{DH,t}}{T_{DH,t} - T_{ref,t}}\right) \quad (12)$$

Illustration of proposed DH system is shown in Figure A5 in Appendix. It shows correlations between all technologies and related optimization variables.

2.2. CHP modelling

To understand allocation methods used in this paper, the CHP modelling approach should firstly be introduced. Cogeneration units used in this paper are steam extraction plants which could operate in three regimes: back-pressure, condensation and steam extraction mode. Possible combinations of CHP's heat and power outputs can be illustrated by using so called P-Q (power-heat) diagram, as shown in Figure 1. However, real P-Q diagrams are more complex since they include minimum technical power and heat outputs, the illustrated lines are not straight, heat capacity is sometimes constrained, etc. For the purpose of this paper, and to secure linearity of the model, technical minimum of the CHP units is neglected. This approach is interesting since complex operation of cogeneration units can be modelled by using two lines – back-pressure and extraction line. The slope of the back-pressure line is called power-to-heat factor and is labelled with σ_{CHP_i}. The slope of the extraction line is called power-loss factor and is marked with β_{CHP_i}. They depend on the numerous parameters, such as cogeneration unit type, extraction temperature, i.e. district heating supply temperature, etc. [61]. Heat ($Q_{CHP_i,t}$) and power ($E_{CHP_i,t}$) cogeneration outputs are correlated according to the Equations (13)-(15). In other words, operating point of the CHP unit could only be inside the region bounded with back-pressure and extraction line. The CHP unit could also operate in the condensation mode. In that case, heat output is equal to zero, i.e. operating point is on the y-axis. However, in that case total efficiency would be the lowest, since it could be assumed that fuel input is constant on the extraction line. CHP modelling based on using P-Q diagrams is fully explained in papers [61] and [62].

$$E_{CHP_i,t} \geq \sigma_{CHP_i} \cdot Q_{CHP_i,t} \tag{13}$$

$$E_{CHP_i,t} \leq P_{el,CHP,i} - \beta_{CHP_i} \cdot Q_{CHP_i,t} \tag{14}$$

$$E_{CHP_i,t} \leq P_{el,CHP,i} \tag{15}$$

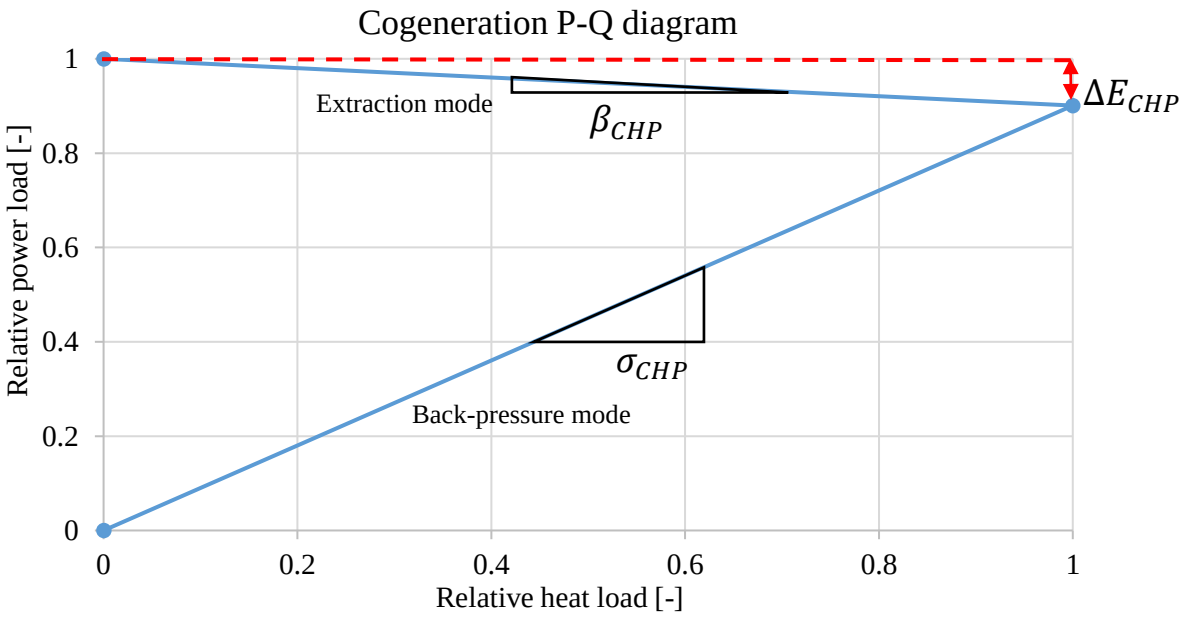

Figure 1 Illustration of cogeneration plant P-Q diagram

2.3. CHP allocation methods

There are various allocation methods proposed by numerous researchers. Allocation method used in this paper is based on the idea that heat output should be treated as a power-loss of the cogeneration unit. Due to this, the method is called power-loss method, or sometimes referred to as Dresden method. It is illustrated in the Figure 1 by using a dashed red line. Power loss due to the heat production in a CHP unit, i.e. $\Delta E_{CHP_i,t}$, could be calculated by using Equation (16). It presents loss of electrical energy production at the expense of thermal energy production in cogeneration units.

$$\Delta E_{CHP_i,t} = \beta_{CHP_i} . Q_{CHP_i,t} \tag{16}$$

Power loss could thus be translated into cost and carbon emissions due to the heat production in a CHP unit. Following subsections explain in detail such approach.

2.3.1. Cost allocation

As already mentioned, cost of CHP unit could be allocated to heat and electricity. Equation (17) shows cost of CHP with no allocation between heat and electricity, $Cost_{CHP_i}$. Cost of the fuel is represented with $c_{fuel,i}$, c_{CO2} represents CO_2 cost, in terms of EUR/ton of CO_2, e_{CO2_i} are specific carbon emissions of the fuel i.e. technology, $c_{var_{CHP_i}}$ are variable operation and maintenance costs of CHP unit, $c_{el,t}$ are power market prices, c_{inv,CHP_i} is specific investment cost of the CHP unit and $c_{fix_{CHP,i}}$ are specific fixed operation and maintenance costs, while CRF_{CHP_i} is capital recovery factor used to discount investment cost. Finally, η_{el,CHP_i} represents electrical efficiency of the CHP unit. It can be noticed how the total cost of CHP is assigned to heat production. The first part of the equation of the right side consists of fuel, variable cost and carbon tax in case of natural gas utilization, second part represents income in terms of electricity production, while the third part is investment and fixed cost of the CHP unit. Allocated cost of CHP $Cost^*_{CHP}$ can be calculated by using Equation (18). In this case operational cost is equal to the electricity market loss due to the heat production, while investment cost is calculated by using c_{conv,CHP_i}, specific investment needed for CHP conversion [61]. This is cost which is needed to upgrade condensation power plant to cogeneration unit. In this case this is theoretical value since it only indicates the share of a CHP investment allocated to heat.

$$\begin{aligned} Cost_{CHP_i} = \sum_i \sum_{t=1}^{t=8760} & (E_{CHP_i,t} + \Delta E_{CHP_i,t}) \cdot \left(\frac{c_{fuel,i} + e_{CO2_i} \cdot c_{CO2}}{\eta_{el,CHP_i}} + c_{var_{CHP_i}} \right) \\ & - E_{CHP,i,t} \cdot c_{el,t} + P_{el,CHP_i} \cdot \left(c_{inv,CHP_i} \cdot CRF_{CHP_i} + c_{fix_{CHP,i}} \right) \end{aligned} \tag{17}$$

$$Cost^*_{CHP} = \sum_i \sum_{t=1}^{t=8760} \Delta E_{CHP_i,t} \cdot c_{el,t} + P_{el,CHP_i} \cdot c_{conv,CHP_i} \cdot CRF_{CHP_i} \tag{18}$$

2.3.2. Carbon allocation

Like cost, carbon allocation in CHP units is also based on power-loss due to the heat production. Total carbon emissions in a CHP unit $CO_{2_{CHP_i}}$ could be calculated by using Equation (19). It can be noticed once again, how all emissions are associated to heat production,

i.e. to district heating system. However, power-loss could be recalculated to carbon emissions. In other words, CO_2 emissions due to the heat production $CO^*_{2_{CHP_i}}$ are equal to the lost power which should be produced in a power plant with the same electrical efficiency unit by using the same fuel. This is also shown in Equation (20).

$$CO_{2_{CHP_i}} = \sum_i \sum_{t=1}^{t=8760} \frac{E_{CHP_i,t} + \Delta E_{CHP_i,t}}{\eta_{el,CHP_i}} \cdot e_{CO2_i} \tag{19}$$

$$CO^*_{2_{CHP_i}} = \sum_i \sum_{t=1}^{t=8760} \frac{\Delta E_{CHP_i,t}}{\eta_{el,CHP_i}} \cdot e_{CO2_i} \tag{20}$$

2.4. Objective functions

Since this paper uses multi-objective optimization approach, more than one objective function must be identified. In this research, three objective functions are defined – minimization of discounted cost, minimization of carbon emissions and maximization of exergy efficiency. Equations (21) show economic objective functions where cost allocation is not implemented, while Equation (22) shows objective function with inclusion of CHP cost allocation.

$$f_{econ} = \sum_i \sum_{t=1}^{t=8760} Q_{i,t} \cdot \left(\frac{c_{fuel,i} + e_{CO2_i} \cdot c_{CO2}}{\eta_i} + c_{var_i} \right) + P_i \cdot (c_{inv,i} \cdot CRF_i + c_{fix,i}) + Cost_{CHP_i} \tag{21}$$

$$f^*_{econ} = \sum_i \sum_{t=1}^{t=8760} Q_{i,t} \cdot \left(\frac{c_{fuel,i} + e_{CO2_i} \cdot c_{CO2}}{\eta_i} + c_{var_i} \right) + P_i \cdot (c_{inv,i} \cdot CRF_i + c_{fix,i}) + Cost^*_{CHP_i} \tag{22}$$

In the similar manner, Equations (23) and (24) show ecological objective function with and without CHP carbon allocation.

$$f_{eco} = \sum_i \sum_{t=1}^{t=8760} \frac{Q_{i,t}}{\eta_i} \cdot e_{CO2_i} + CO_{2_{CHP_i}} \tag{23}$$

$$f^*_{eco} = \sum_i \sum_{t=1}^{t=8760} \frac{Q_{i,t}}{\eta_i} \cdot e_{CO2_i} + CO^*_{2_{CHP_i}} \tag{24}$$

Since exergy efficiency of the system does not depend on the allocation methods in the CHP units, it is calculated as follows. By using Equation (25), exergy input $Ex_{in,i,t}$ could be calculated, while Equation (26) shows how to obtain exergy output $Ex_{out,i,t}$. Finally, exergy efficiency of the system could be calculated by using Equation (27). It is important to notice how this is non-linear equation since exergy input and output contain optimization variables. To deal with this challenge, epsilon constraint method has been used as shown in the following section.

$$Ex_{in,i,t} = \frac{Q_{i,t}}{\eta_i} \cdot e_{Exe,i} \tag{25}$$

$$Ex_{out,i,t} = Q_{i,t} \cdot \left(1 - \frac{T_{ref_t}}{T_{DHN_t}}\right) + E_{CHP,i,t} \tag{26}$$

$$\eta_{exe} = \frac{\sum_{t=1}^{t=8760} \sum_i Ex_{out,i,t}}{\sum_{t=1}^{t=8760} \sum_i Ex_{in,i,t}} \tag{27}$$

It can be noticed that exergy efficiency of the district heating system includes only energy transformation at the location of supply technology i.e. at the boundary with the thermal network. In other words, exergy destruction of the thermal network, building substation and building distribution are not integrated in the objective function. Nevertheless, Section 4.2 shows the impact of exergy destruction in the thermal network and comparison with natural gas-based individual boilers.

2.5. Multi-objective optimization approach

In this paper, multi-objective optimization is handled by using epsilon-constraint method. The main advantage of this approach is that translates multi-objective optimization problem into single objective optimization with additional sets of constraints, called "epsilon constraints" ε_{eco} and ε_{exe}, as shown in Equation (28) [63]. In order to start the procedure, the borders of Pareto front have to be known in order to ensure that assigned epsilon constraints are eligible. In other words, the least-cost, the most environmentally friendly and the solution with the highest exergy efficiency must be known.

$$\min (f_{econ}) \text{ for } f_{eco} \leq \varepsilon_{eco},\ f_{exe} = \varepsilon_{exe} \tag{28}$$

The main drawback of this method is large computational time, since it acquires great number of optimization runs in order to visualize a whole Pareto set, especially in a case of three objective functions.

3. Case study and input data

The developed method was tested on the numerical case study which includes following data: hourly demand, hourly district heating network temperatures and hourly meteorological data. Mentioned distributions are shown in Appendix. Case study is located in Northern Croatia, with continental climate. Minimum temperature reaches -10°C during winter season, while the highest summer temperature reaches more than 35°C, as shown in Figure A1. District heating supply temperature is in direct correlation with outside temperature, as shown in Figure A2. Maximum supply temperature reaches around 115°C. District heating system in this case study covers both space heating and domestic hot water demand, i.e. operates through a whole year as shown in Figure A3. Peak load is around 450 MW, achieved during winter season, while total thermal demand is equal to 808 GWh. In this section, technology input data is displayed, together with district heating network cost. Finally, programming language and optimization solver is presented.

3.1. Technology data

Table 1 shows various technology characteristics, including prices per technology. It also includes thermal storage characteristics such as daily losses. Technology characteristics are based on the information provided by the Danish Energy Agency database for energy plants [64]. Power-to-heat and power-loss factor of cogeneration units are defined by using EC Joint Research Centre (JRC) report [65] and paper [61].

Table 1 Technology data [64], [65]

Technology	Investment cost [€/MW] / [€/m^2] /[€/MWh]	Variable cost [€/MWh]	Fixed cost [€/MW] / [€/m^2] /[€/MWh]	Efficiency/ storage self-discharge [-]	Ramp-up/down [-]	Technical lifetime [years]	Power-to-heat ratio [-]	Power-loss factor [-]
Natural gas boiler	60,000	1,1	2,000	0.89	0.9	25	-	-
Biomass boiler	300,000	1,0	32,000	0.8	0.6	25	-	-
Electrical heater	150,000	0.8	1,100	0.98	0.95	20	-	-
Heat pump	700,000	3.3	2,000	Hourly distribution (avg.2.3)	0.95	25	-	-
Cogeneration (combined cycle) natural gas	1,200,000 (electrical power)	5.5	20,000	0.55 (electrical)	0.6	25	1.17	0.13
Cogeneration biomass	3,000,000 (electrical power)	3.8	45,000	0.45	0.5	25	0.377	0.334
Solar thermal	190 €/m^2	0.2	0.04 €/m^2	Hourly distribution	-	25	-	-
Short term thermal storage	4,500	-	8.6 €/MWh	0.5 %/day	-	40	-	-
Seasonal thermal storage	900	-	3 €/MWh	0.05 %/day	-	20	-	-

Table 2 shows other data related to district heating system optimization such as fuel prices, electricity market prices and electricity network costs. As already mentioned, the model includes carbon tax for natural gas technologies. For the purpose of this paper it is equal to 25 EUR/ton of CO_2. To calculate emissions for respective technologies, emission factors for fuels are defined. It is important to mention that both biomass and electricity have carbon factors, however they are not part of the carbon taxing system. Exergy factors are used to calculate exergy input of the fuel. Finally, CHP conversion cost is used to allocate investment cost between heat and electricity.

Table 3 shows data which data are used for calculation of levelized cost of heat (LCOH) and carbon factor of the natural gas based individual heating, while Table 4 displays cost data for district heating network connection.

Table 2 Other district heating input data [64]

Natural gas price [EUR/MWh]	30
Biomass price [EUR/MWh]	20
Electrical energy price [EUR/MWh]	hourly distribution
Electricity network price [EUR/MWh]	30
CO_2 price [EUR/ton]	25
Natural gas CO_2 factor [tonnes of CO_2/MWh]	0.22
Biomass CO_2 factor [tonnes of CO_2/MWh]	0.042
Electricity CO_2 factor [tonnes of CO_2/MWh]	0.234
Exergy factor biomass [-]	1.2
Exergy factor natural gas [-]	1.04
Cogeneration plant conversion cost [EUR/MW]	300,000

Table 3 Input data for individual gas boilers [64]

Natural gas price for individual customers [EUR/MWh]	30
Natural gas CO_2 factor [ton of CO_2/MWh]	0.22
Natural gas boiler efficiency, individual [-]	0.95
Natural gas price boiler, investment cost	320,000
Lifetime [years]	20

Table 4 Cost data for district heating network connection with a building [64]

District heating network connection pipe investment cost [EUR/MW]	250,000
Lifetime of network connection pipe [years]	50
Building substation investment cost [EUR/MW]	220,000
Lifetime of a substation [years]	25

3.2. District heating network cost calculation

Calculation of district heating network investment cost has been modelled by using information gathered in the Horizon2020 project called STRATEGO. In report [66], relation between heating demand density and thermal network investment cost is presented. This correlation is shown in Figure 2, including the corresponding equation. For higher demand densities, lower specific investment cost is needed. In other words, economic feasibility of a district heating system greatly depends on the heating demand density in a specific area.

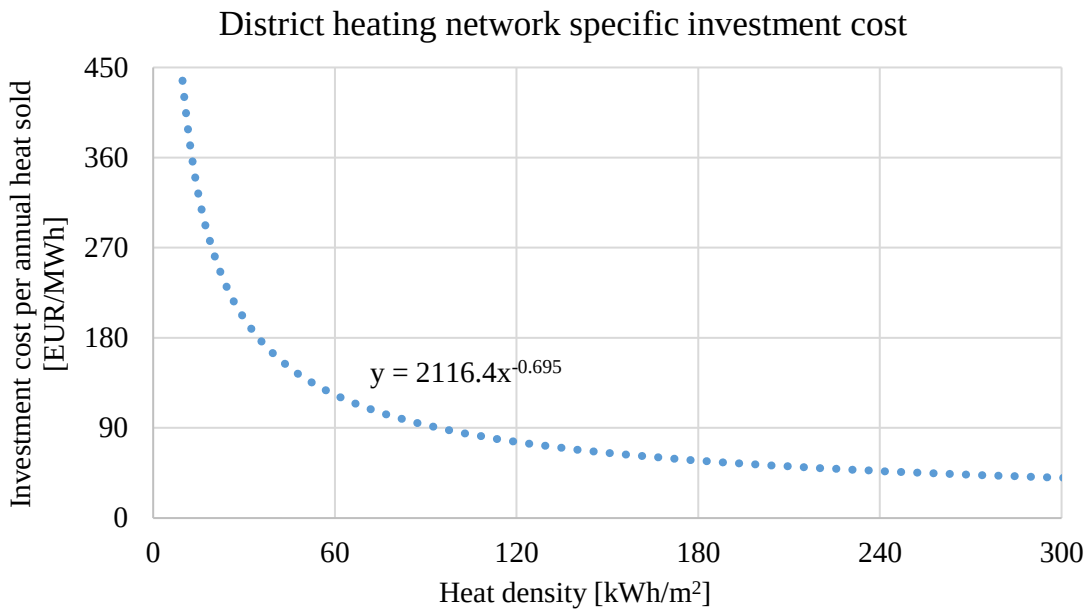

Figure 2 District heating network specific investment cost as a function of heat density [66]

3.3. Programming language and optimization solver

The proposed multi-objective optimization model is written by using free and open-source Julia programming language [67]. The language has been developed for the purpose of increasing computational speed. Julia package, called JuMP [68] is needed in order to create and run optimization model. The optimization problem was solved by using Gurobi [69]. Optimization runs were carried out by using PC workstation with Intel Xeon CPU E5-2623 processor. Single optimization run, i.e. per single set of epsilon constraints, lasted 60 minutes in average.

4. Results and discussion

The results obtained in this paper and related discussions are represented through five sections. Section 4.1 shows Pareto solutions supply technologies, including CHP share with respect to different CHP allocations. In Section 4.2, the acquired results have been compared with individual heating solutions, while focusing on exergy efficiency. In Section 4.3, obtained results are shifted due to the addition of district heating network cost and then compared with natural gas individual heating. Section 4.4 shows the impact of district heating and cooling integration.

Economical objective function is translated to levelized cost of heat (LCOH). It is done by dividing economical objective function value with total heating demand. In the similar manner, environmental objective function is reduced to specific CO_2 emissions, sometimes referred to as a carbon factor. It should be mentioned that in Section 4.4, where district cooling integration is analysed, levelized cost of thermal energy (LCOTE) is used as economical parameter. In this case, economical objective function is divided by total heating and cooling demand.

Finally, it should be mentioned that additional analysis has been carried out, in which share of renewable energy sources in energy and exergy output has been obtained. The results of this analysis are shown in Appendix.

4.1. The impact of different CHP allocations on district heating parameters

In this section, the impact of different CHP allocations on district heating parameters are shown. The focus is put on specific CO_2 emissions, levelized cost of heat and exergy efficiency of the system. Furthermore, optimal technology mix and overall CHP share of selected Pareto solutions is displayed. Each figure shown below consists of six Pareto fronts, constructed for six different exergy efficiency constraints. It should be mentioned how the solutions with the lowest CO_2 emissions, and consequently with the highest cost, are not shown in the diagrams since they are out of scale. It is crucial to mention that exergy efficiency calculation presented in this section includes exergy destruction related to energy transformation on the supply technology level, i.e. exergy destruction of the thermal network has not been considered. Exergy losses of the network are considered and analysed in Section 4.2.

4.1.1. No CHP allocation

The results acquired if no CHP allocation is implemented is shown in Figure 3, where x-axis shows specific CO_2 emissions of the system, while y-axis shows LCOH of the system. For specific points on the diagram, pie charts are developed, indicating technology share in a thermal energy production. The number next to the pie chart indicates CHP share in the technology mix. It should be mentioned that in these results, thermal network cost is not included. For the sake of clarity, third objective function, i.e. exergy efficiency is not plotted on the third axis, but as a parameter. Six Pareto fronts are constructed – five with constrained exergy efficiency, starting with 0.2 and reaching 0.5, and one Pareto front with no constraints put on exergy efficiency. The Pareto front with no constraint put on exergy efficiency reaches the lowest LCOH and CO_2 emissions, i.e. less than 50 EUR/MWh and 0.12 tCO_2/MWh, respectively. These solutions utilize only natural gas and biomass boilers, while CHP share is equal to zero. Similar, but nonetheless higher, system parameters are obtained for Pareto solution with exergy efficiency equal to 0.2. However, to obtain such exergy efficiency, heat

pump must be integrated. For Pareto fronts with exergy efficiency higher than 0.2, CHP share is increased – solutions with lower LCOH and higher emissions utilize natural gas CHP, while solutions with higher cost and lower emissions uses biomass CHP and heat pump. The Pareto front with exergy efficiency equal to 0.5, reaches CO_2 factor of 0.52 tCO_2/MWh, with LCOH in the range of 55-80 EUR/MWH.

It should be noticed how specific trend emerges – solutions with higher CHP share have higher CO_2 emissions and higher system costs. This is also emphasized with the arrow shown in Figure 3. The main reason behind this is allocation in which all carbon emissions and investment, including operational, costs are assigned to heat production. However, heat produced in cogeneration units should be considered as excess, or sometimes called waste, heat and treated as such during system optimization. In the following subsections, we will show how this trend could be influenced by using CHP carbon and cost allocation methods.

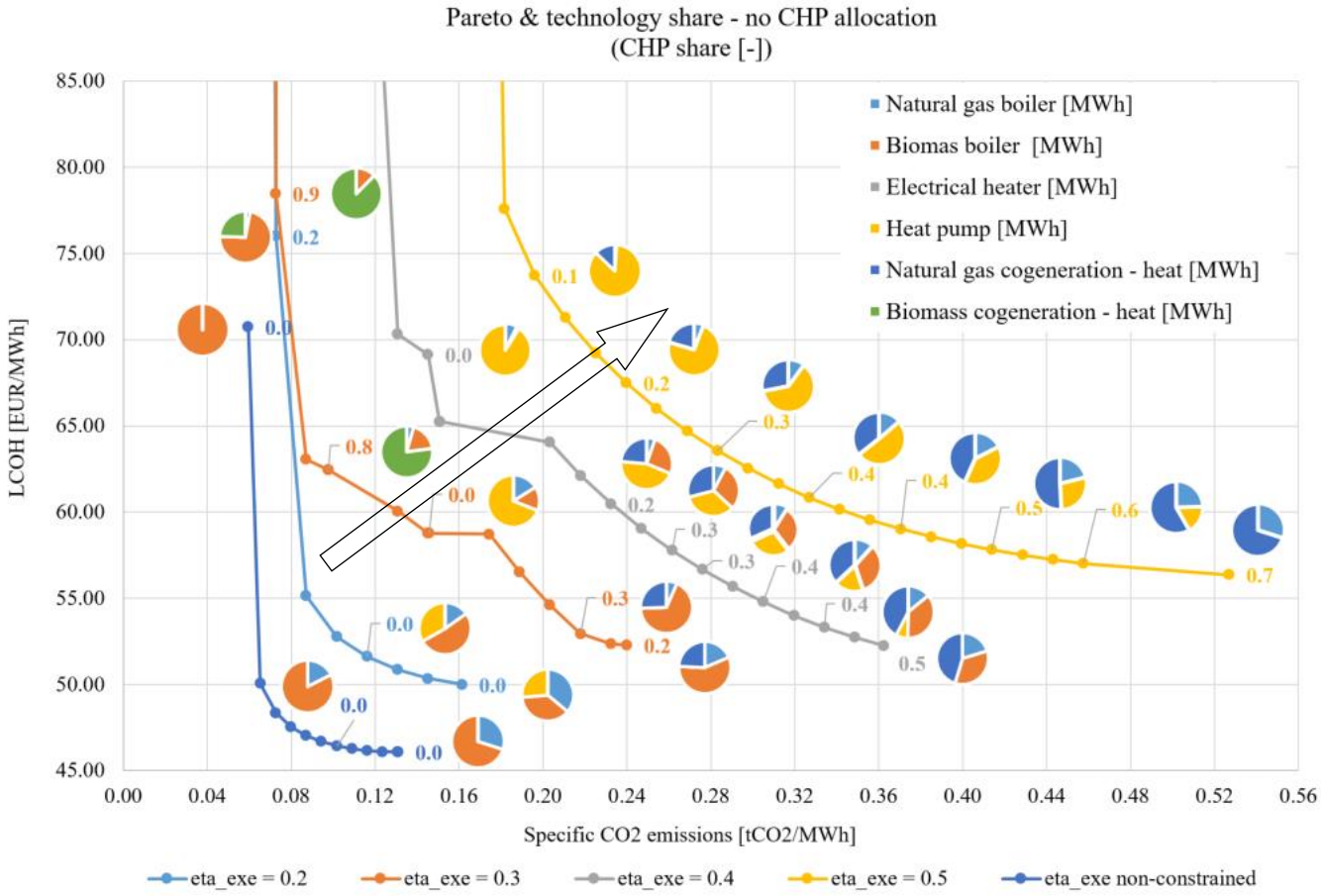

Figure 3 Pareto solutions, technologies and CHP share for no CHP allocations implemented

4.1.2. Cost CHP allocation

Figure 4 shows Pareto results obtained if CHP cost allocation is considered. In this case, the solution with the lowest exergy efficiency, equal to 0.2, reaches highest LCOH (around 40 EUR/MWh) and the lowest carbon emissions (less than 0.1 tCO_2/MWh), while the CHP share is kept relatively low, equal to 0.3. With the increase of exergy efficiency, CHP share is also increased, as already seen in the case when no allocation methods in CHP units are introduced. However, in this case increase of exergy efficiency results in lower LCOH of

the system, reaching around 20 EUR/MWh. This is almost 50% lower than in the first case with no allocation in CHP units. However, the results with the highest share of CHP and high exergy efficiency have the highest carbon factor equal to 0.7 tCO_2/MWh. Thus, the following can be concluded: if cost allocation method is implemented, increase of CHP share results in LCOH reduction and carbon factor increase. In other words, exergy efficiency increase shifts Pareto solutions to the region of high carbon emissions and lower total costs. Once again, this is also emphasized with the arrow shown in Figure 4. It should be mentioned how Pareto front with no constraint put on exergy efficiency is relatively flat, i.e. LCOH reaches values between 25 and 20 EUR/MWh, while carbon factor is in range of 0.1-0.7 tonnes of CO_2/MWh. The highest CO_2 emissions are obtained for natural gas CHP dominated system, while the lowest emissions are reached for biomass-based system.

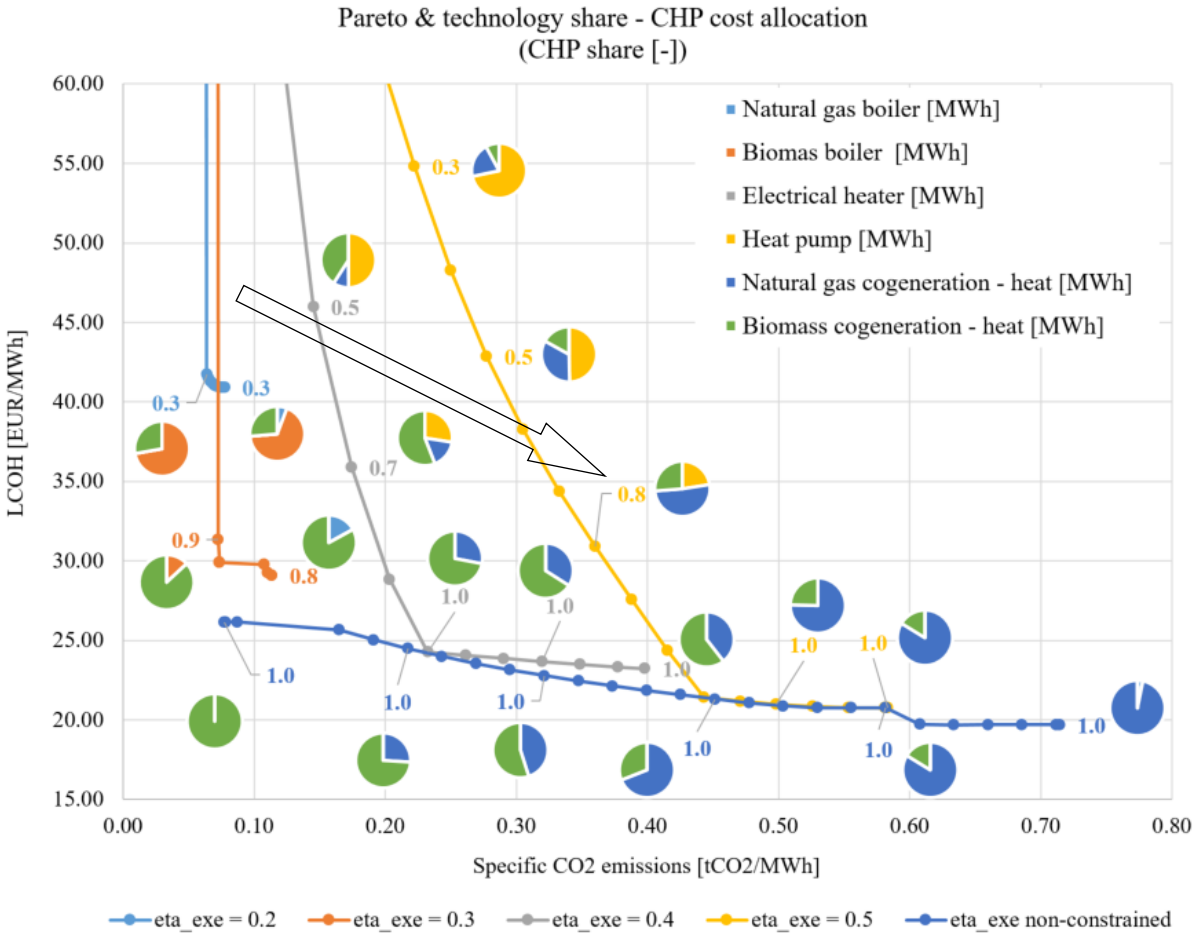

Figure 4 Pareto solutions, technologies and CHP share for cost CHP allocation implemented

4.1.3. Carbon CHP allocation

Pareto solutions with implemented cogeneration carbon allocation is shown in Figure 5. Firstly, it should be noticed that the highest carbon factor of the system is equal to 0.16 tonnes of CO2/MWh, which is relatively low when compared with the first two cases where the highest value reached 0.5 and 0.7 tCO_2/MWh respectively . Solutions with the lowest CO_2 emissions are based on biomass CHP, while natural gas cogeneration causes larger emissions and higher exergy efficiency. Heat pump is rarely part of the optimal solution, only visible for exergy efficiency equal to 0.2. Although all Pareto fronts have different exergy

efficiencies, they are all clustered together, i.e. there is no specific shift of the Pareto solution. However, increase of exergy efficiency (and CHP share) tends to move all Pareto solutions, except those with exergy efficiency equal to 0.5, to the region of lower CO_2 emissions. This is also emphasized with an arrow illustrated in the Figure 4. In other words, carbon allocation allows utilization of CHP in different technology mixes which result in similar carbon emission factor and LCOH values.

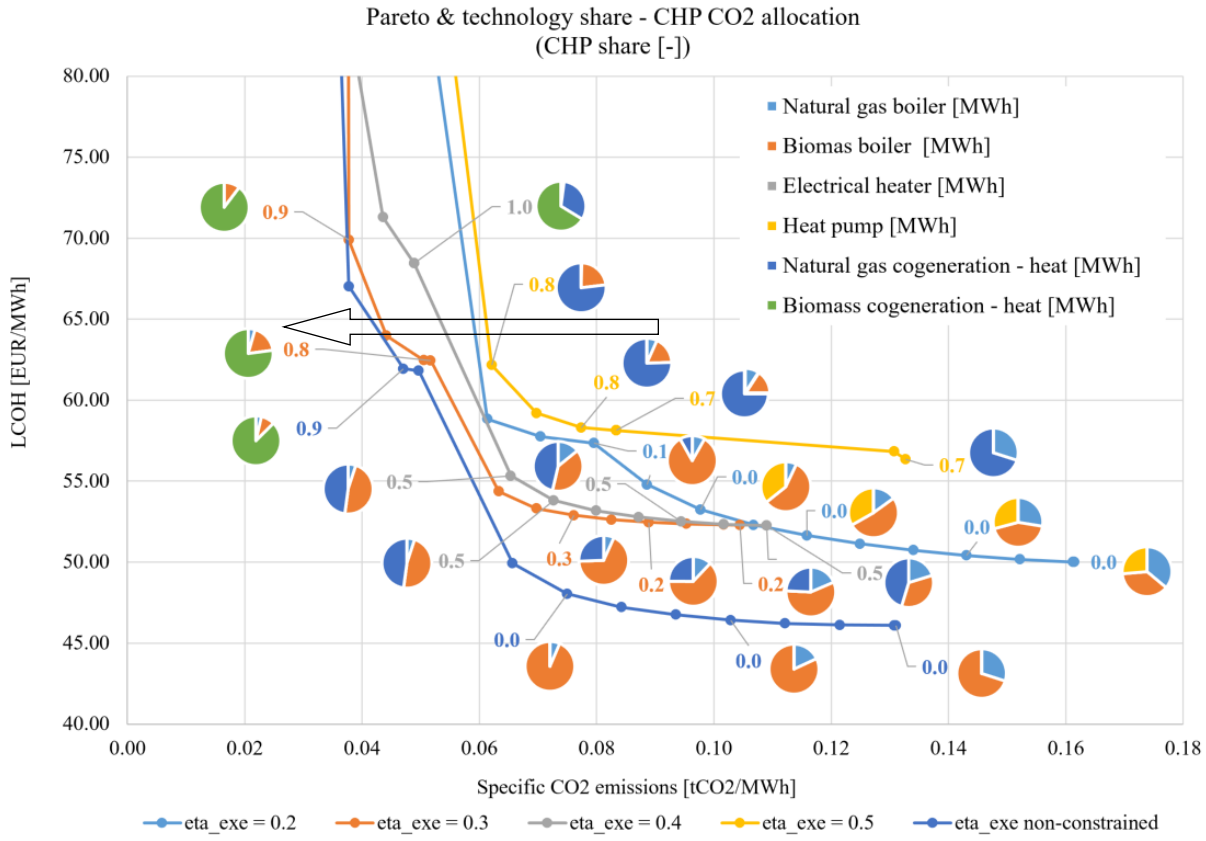

Figure 5 Pareto solutions, technologies and CHP share for carbon CHP allocation implemented

4.1.4. Carbon and cost CHP allocation

Figure 6 shows optimization results for implemented carbon and CHP allocation. It can be noticed how increase of exergy efficiency shifts Pareto solutions to the region of low LCOH and low carbon emissions. This is consequence of a large CHP share and allocation in cogeneration units put both on carbon emissions and cost. This is also displayed with the arrow shown in Figure 6. The largest shift is visible between exergy efficiency increase from 0.2 to 0.3 When exergy efficiency exceeds value of 0.3, all Pareto results have CHP share equal to unity. In these cases, share between natural gas and biomass CHP depends on the position at the Pareto front. It should be mentioned that Pareto front with no constraints put on exergy efficiency coincides with some parts of other Pareto fronts. Simultaneous cost and carbon allocations give the lowest maximum carbon factor with the value equal to 0.08 tonnes of tCO_2/MWh. Values of LCOH are relatively low when compared with previous scenarios since in the most cases stay well below 35 EUR/MWh.

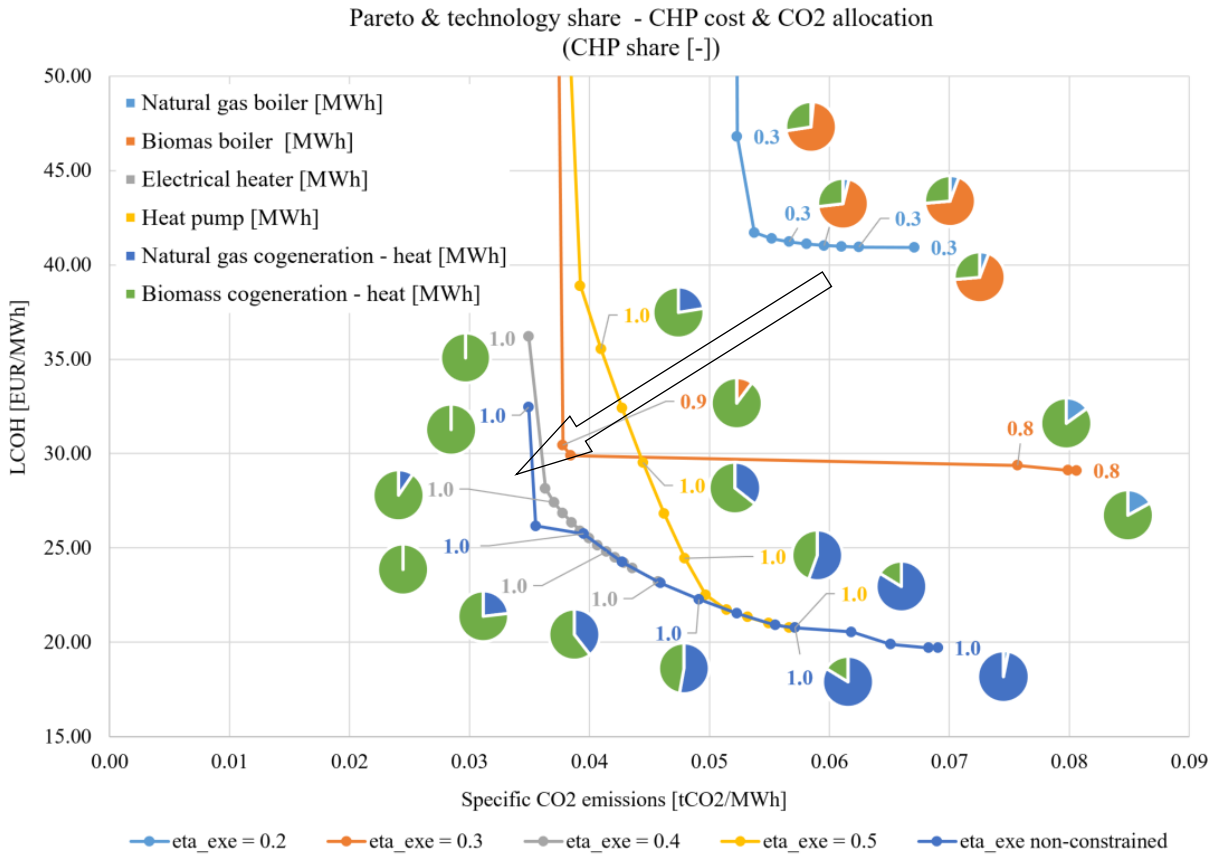

Figure 6 Pareto solutions, technologies and CHP share for cost and carbon CHP allocations implemented

4.2. Comparison with individual heating solutions focusing on exergy efficiency

Figure 7 presents exergy efficiency comparison of a whole DH system (includes supply technology and a thermal network) and individual natural gas boilers. X-axis presents exergy efficiency of the system which consists of supply technologies only (no exergy loss of the thermal network included). This exergy efficiency was obtained during multi-objective optimization and the results were already presented in Section 4.1. Y-axis presents exergy efficiency of the system calculated when exergy losses of the network are included. Exergy losses of the thermal network were obtained by using thermal loss of the network, district heating supply temperatures and temperature of the building substation. Black dotted line presents case for which exergy losses of the thermal network are neglected. The distance between blue dot (exergy efficiency of DH system) and a black dotted line corresponds to the share of exergy losses which are attributed to the thermal network. This is also marked with orange arrow in Figure 7a. Red full line represents exergy efficiency of the natural gas-based individual boiler. District heating systems should have exergy efficiency higher than natural gas-based individual boilers to be superior to individual natural gas-based heating.

Although exergy efficiency of the supply system (x-axis) is equal for many configurations, such as in Figure 7a and Figure 7b, the exergy efficiency of a whole system (which includes exergy destruction of thermal network) varies greatly. It should be mentioned that this difference mainly depends on the amount of electricity production, i.e. on the CHP share of the

system. Although most of the configurations have exergy efficiency of a whole system higher than individual natural gas-based boilers, some solutions do not. They are marked with red circles in Figure 7. These systems are based on heat-only boiler technologies. Although these systems could be economically more feasible and environmentally more friendly than individual solutions, as shown in Section 4.3, they should also be avoided since their exergy efficiency of a whole system is relatively low. In other words, replacement of individual natural gas boilers should not be done by using heat-only boilers, but CHP technologies or heat pumps combined with convenient heat source.

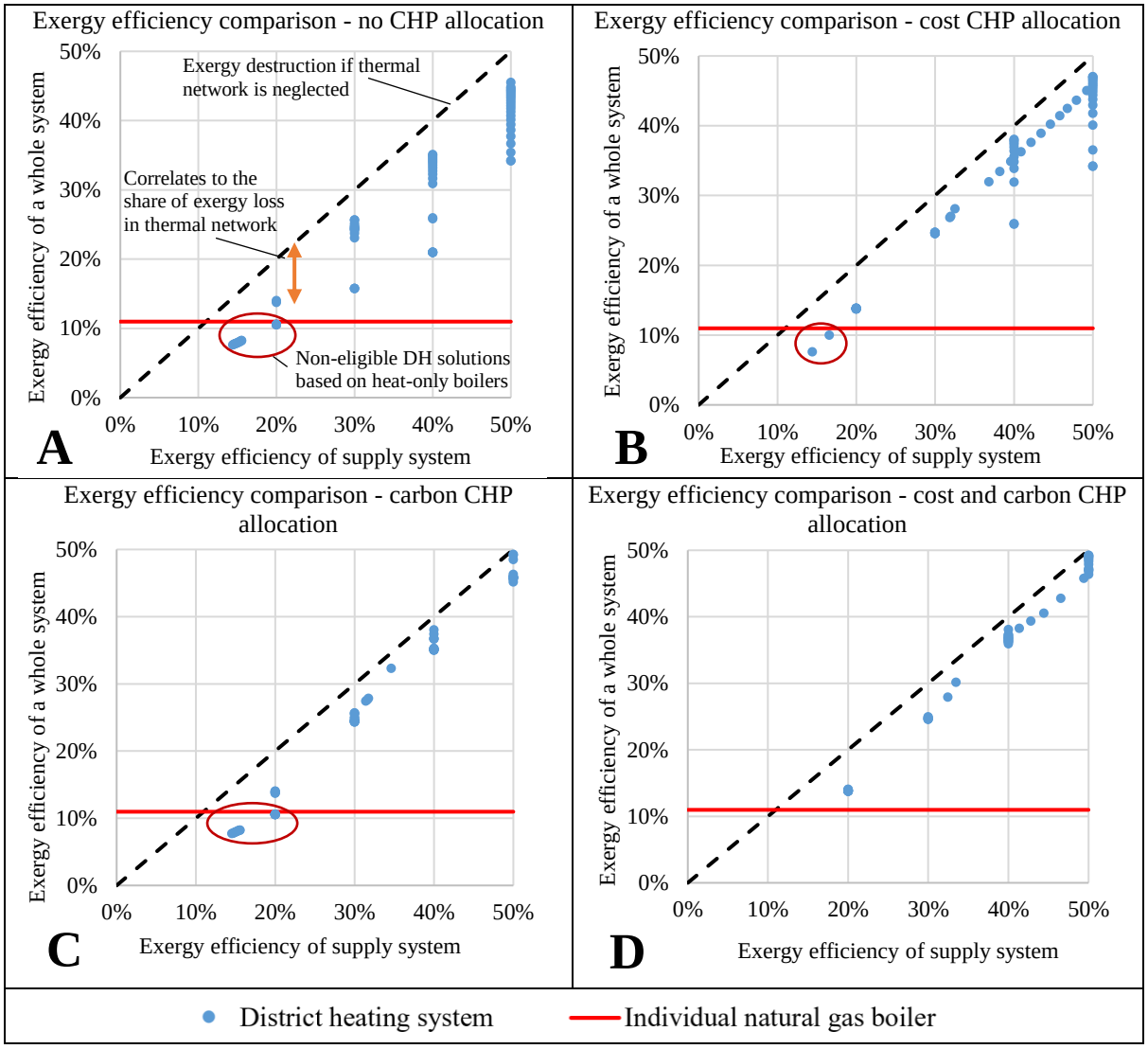

Figure 7 Exergy efficiency comparison between district heating system and individual natural gas-based system (exergy efficiency of the thermal network included): a) no CHP allocation, b) cost CHP allocation, c) carbon CHP allocation, d) cost and carbon allocation

4.3. Comparison with individual heating solutions focusing on cost and carbon emissions

In this section, obtained results are compared with the individual solution based on natural gas, i.e. the case in which predefined demand is covered with individual natural gas boilers. To do so, additional costs should be added to the results obtained by the multi-objective optimization. They are equal to the discounted investment cost of district heating network, individual heating substation and connection pipe between a building and a district heating network. As shown in Section 0, district heating network cost depends on heating demand density. In the following sections, two cases of heating demand densities are used, the first one equal to 50 kWh/m^2 and a second one equal to 200 kWh/m^2. The former represents relatively low, while latter represents relatively high heating demand density. Finally, it is important to notice that discounted costs of installation of natural gas boiler at a building level and installation of district heating substation at building level have similar value, according to the technology database [64].

Since natural gas price for households has crucial impact on the final comparison of results, three natural gas prices have been taken into account: Croatian, Swedish and EU-average, equal to 35, 55 and 95 EUR/MWh respectively [23]. These prices do not include VAT taxes.

4.3.1. No CHP allocation

In this section, multi-objective optimization results with no CHP allocations implemented, which include other district heating network related costs, are compared with individual natural gas boiler solution. The result is shown in Figure 8 and are explained in detail below. Firstly, network cost addition is presented on the example of Pareto front with exergy efficiency equal to 0.5. Three fronts are visible (full, dashed and dotted line). The first one (full) represents the Pareto front with no district heating network cost added, i.e. LCOH is equal to the supply system costs. Second Pareto front (dashed line) represents the solutions which include other district network costs for high heating demand which is equal to 200 kWh/m^2. Similarly, the third Pareto front (dotted line) represents the solutions which include other district heating network cost for low heating demand density, equal to 50 kWh/m^2. Natural gas based individual solutions are illustrated as follows. Carbon factor of individual systems is equal to 0.23 tonnes of tCO_2/MWh, which is represented with vertical dotted black line on the diagram. This means that all solutions left of this line have lower emissions, which is also indicated with horizontal green arrow. Similar illustration can be made for LCOH of individual natural gas boilers. Three black dotted horizontal lines are visible. Each one represents different LCOH obtained for different natural gas prices for households: Croatia, Sweden and EU average. Resulting LCOH of individual natural gas boiler heating system is equal to 54 EUR/MWh for Croatia, 75 EUR/MWh for EU average and 117 EUR/MWh for Sweden. All Pareto solutions which are below these boundaries are better, in economic terms, than natural gas based individual heating in respecting countries. This is also displayed with vertical green arrow. If district heating Pareto solution is inside “the box”, then it can be declared superior, both in carbon emissions and economic terms, to individual heating based on natural gas. According to the results shown in Figure 8 no Pareto results are located inside “the box” for Croatian price conditions. However, for natural gas prices higher than EU average, great part of the Pareto solutions is superior to the individual natural gas-based heating. Furthermore, it should be mentioned that numerous solutions have lower carbon factor than natural gas individual

heating. Nevertheless, it is important to notice how great part of the Pareto solutions with the exergy efficiency higher than 0.4 has higher carbon factor than individual heating.

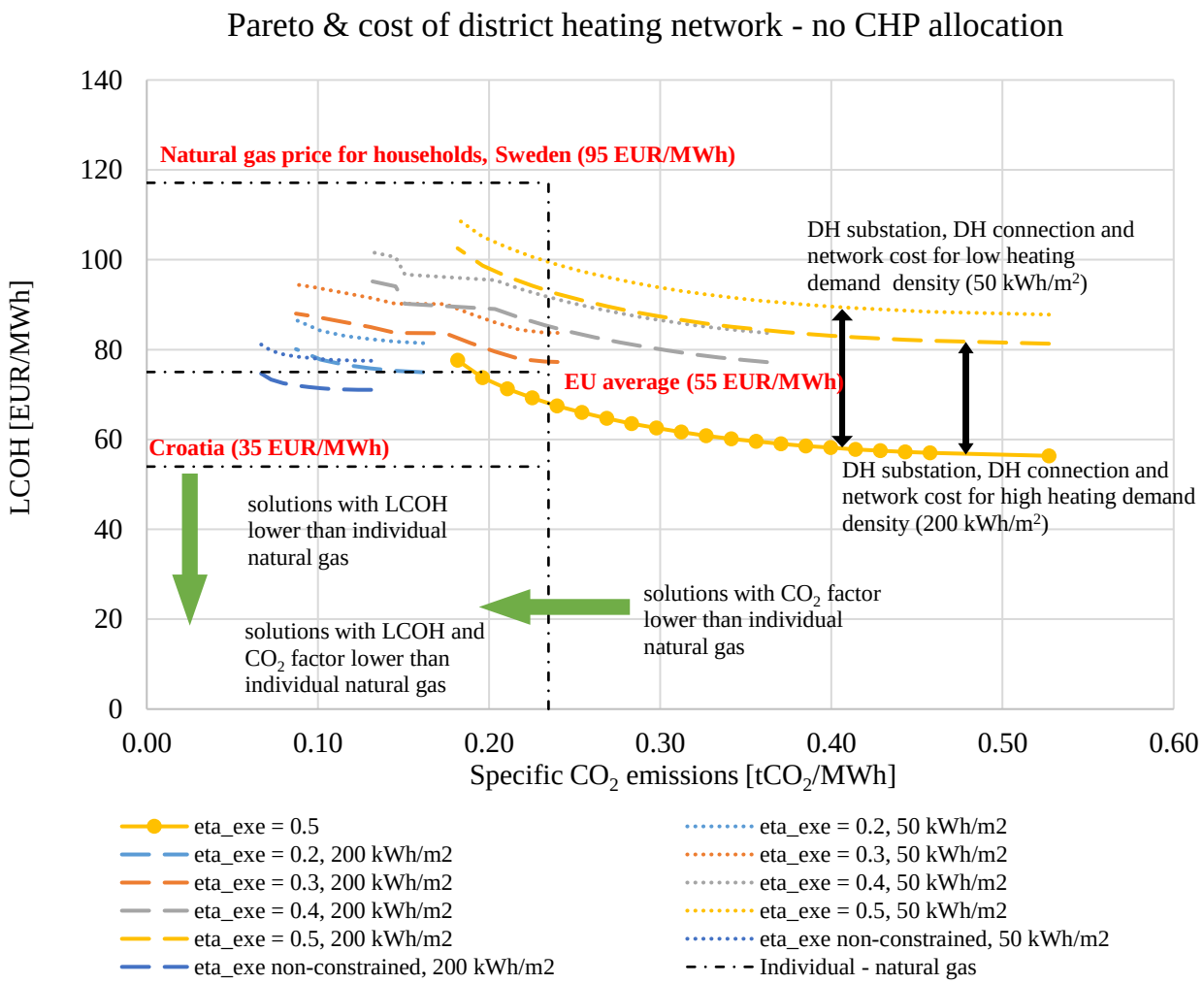

Figure 8 Pareto solutions, including network cost, and comparison with individual natural gas heating for no CHP allocation implemented

From the acquired results, one can conclude that individual natural gas boilers are better solution than cogeneration-based district heating. However, this conclusion heavily depends on the allocation methods used in the cogeneration units. Following sections will demonstrate how CHP based district heating systems are superior to individual natural gas-based heating systems, even for low natural gas price conditions such as in Croatia.

4.3.2. CHP cost allocation

Figure 9 shows comparison of Pareto results with implemented CHP cost and individual heating based on natural gas boilers. All Pareto solutions with exergy efficiency equal or lower than 0.3 are better than individual heating, for EU average natural gas price conditions. It should be noticed how only high demand density solutions with to no constraint put on exergy efficiency are economically better than individual systems for Croatian pricing conditions. As previously shown, this allocation causes great increase of carbon emission factor of the system. Great part of solutions with exergy efficiency higher than 0.4 have carbon emission factor

higher than individual heating systems. For results with the highest exergy efficiency, only the most environmentally friendly solutions are superior to individual heating systems, but for pricing conditions which are higher than the EU average.

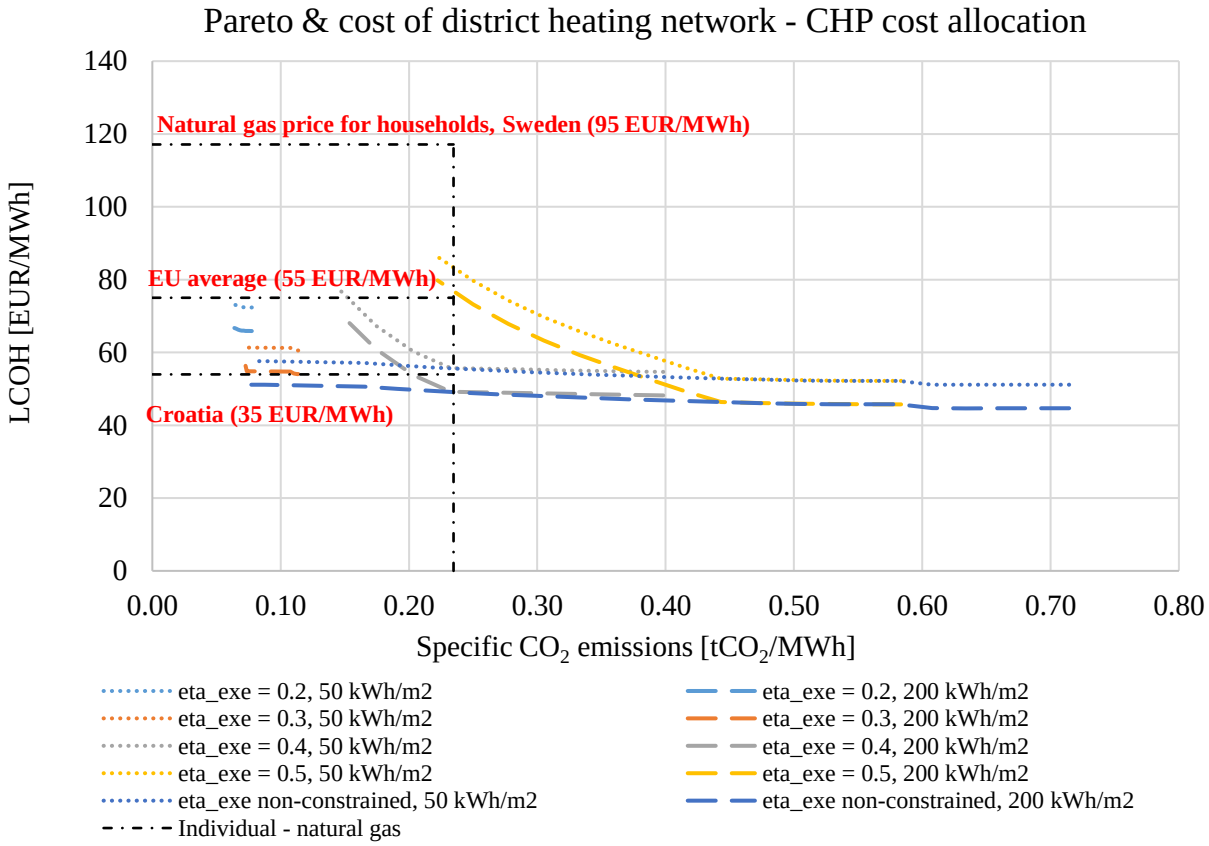

Figure 9 Pareto solutions, including network cost, and comparison with individual natural gas heating for CHP cost allocation implemented

4.3.3. CHP carbon allocation

Comparison of Pareto solutions with implemented CHP carbon allocation and individual heating is shown in Figure 10. All Pareto results have lower carbon factor than individual heating solution based on natural gas. However, all of them also have higher LCOH than individual heating for Croatian and EU average natural gas pricing conditions. Of course, the reason behind this is relatively low natural gas price for individual customers which is equal to 35 EUR/MWh. It should be noticed how all solutions are clustered in the region of carbon emission factor which is around 50% lower than the one for individual heating solutions. To proclaim district heating option economically better than individual heating, natural gas price for households should be higher than 55 EUR/MWh. Finally, it should be noticed that all solutions have relatively similar LCOH values which are in range 80-100 EUR/MWh.

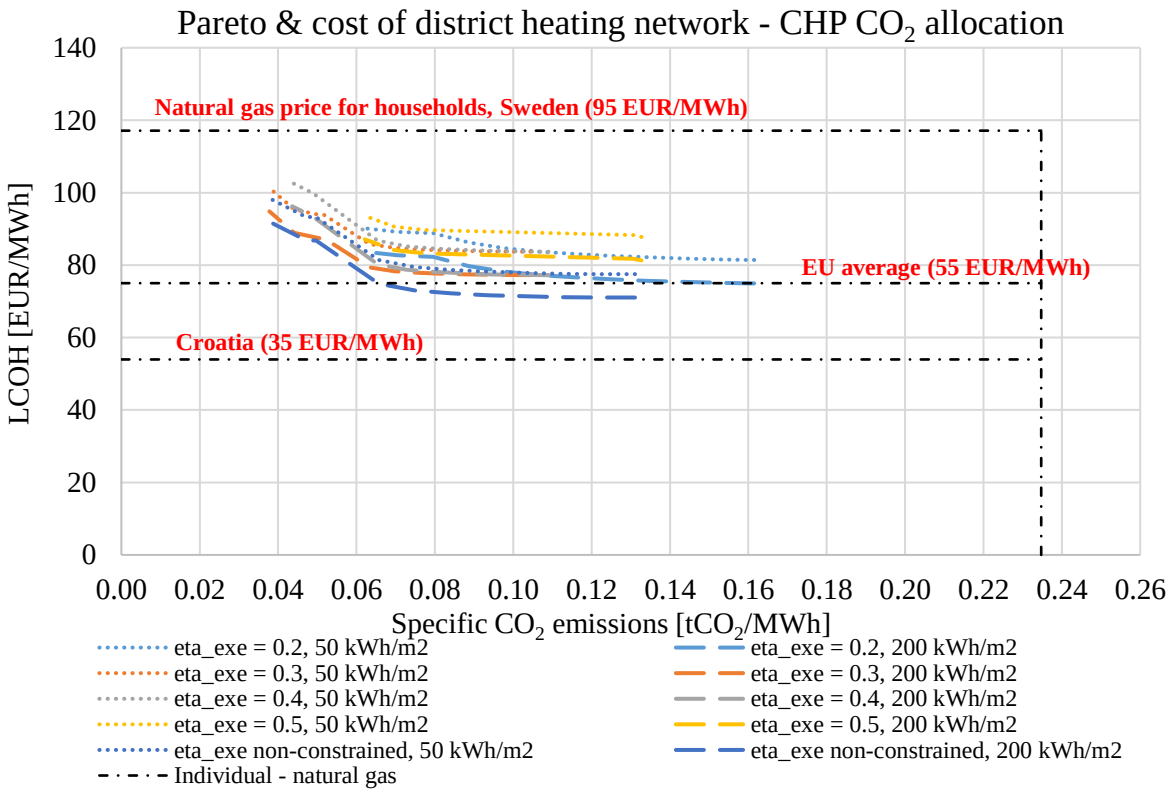

Figure 10 Pareto solutions, including network cost, and comparison with individual natural gas heating for CHP carbon allocation implemented

4.3.4. CHP cost and carbon allocation

Figure 11 shows comparison of Pareto results, for which both allocations are implemented, and individual heating solutions based on natural gas. It is crucial to notice how most of the Pareto solutions are superior to natural gas based individual heating, even for Croatian natural gas pricing conditions. Heating demand density has little-to-no impact. Interestingly, the only Pareto front outside of the box for Croatian conditions, is the one with the exergy efficiency equal to 0.2. On the other hand, all solutions have system LCOH lower than individual heating solutions for EU average natural gas prices. Levelized cost is in range of 45-75 EUR/MWh. In other words, high exergy efficient district heating systems are less expensive option than individual natural gas boilers in the most of EU countries. Finally, it should be noticed how carbon factor for all solutions is almost five times lower than the natural gas based individual heating. Carbon factor of district heating systems is in range 0.04-0.09 tCO_2/MWh.

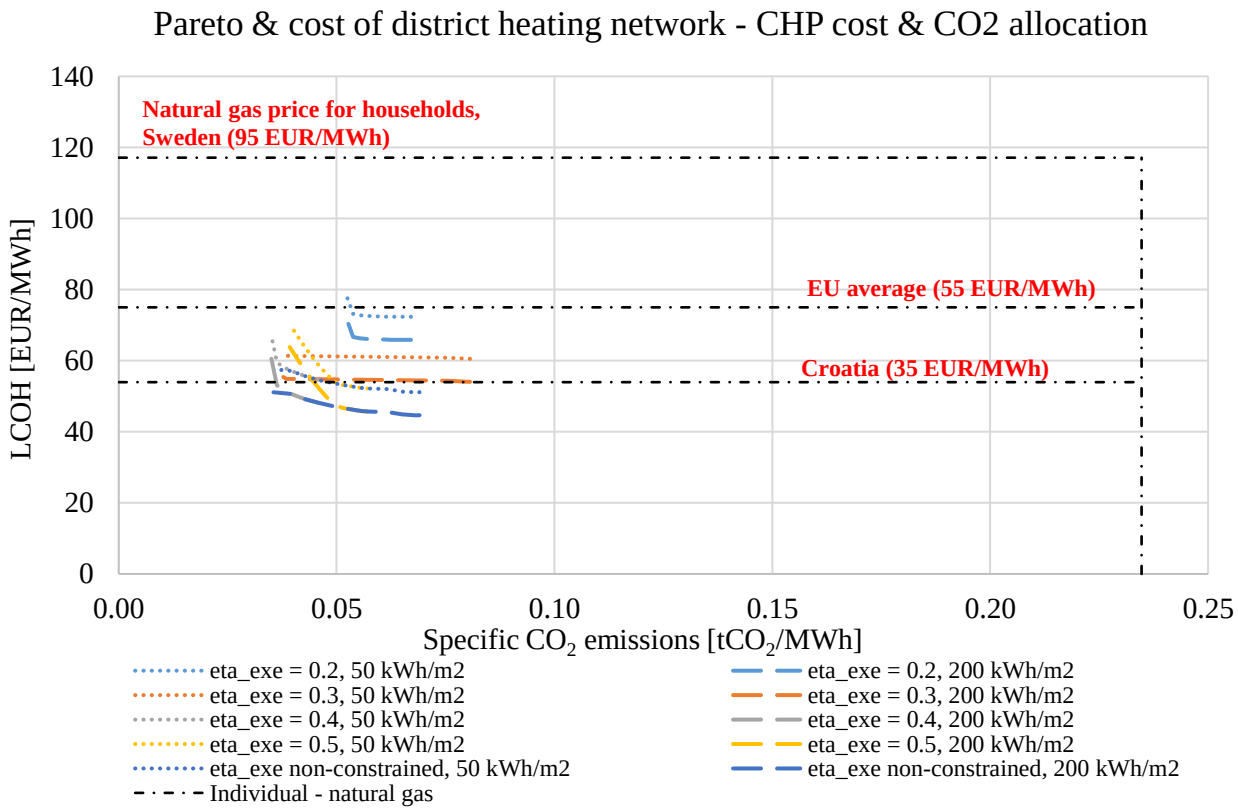

Figure 11 Pareto solutions, including network cost, and comparison with individual natural gas heating for CHP cost and carbon allocation implemented

4.4. District cooling integration

In this section, the impact of integrating of district cooling is analysed. It is connected to district heating by adding absorption heat pump which is utilizing high-temperature heat from heat-only boilers and cogeneration units. It should be mentioned that both absorption heat pump and cooling storage size, including hourly operation on hourly level, are optimization variables. Similar to Section 4.1, four scenarios are developed depending on the allocation used in the CHP units. It should be mentioned that economical objective function is represented by using parameter called levelized cost of thermal energy (LCOTE). It is similar to LCOH, but this time both heating and cooling demand are taken into account.

4.4.1. No CHP allocation

Figure 12 shows the results obtained by integrating district cooling with no CHP allocation used in the CHP units. This figure will also serve as an opportunity to familiarize the reader with the presentation of the results. Once again, Pareto front are plotted for different exergy efficiency values. X-axis represent a carbon factor of the system, while y-axis includes economic parameter called levelized cost of the thermal energy (LCOTE). Pareto fronts with full lines represent the results which include only district heating systems. These Pareto fronts have already been shown in Section 4.1. Dashed Pareto fronts show the results obtained once district cooling is integrated. The difference between the full and dashed Pareto fronts, corresponds to the specific cost difference between the two systems, as illustrated with black arrow in Figure 12. It can be noticed how this difference is relatively low, around 5 EUR/MWh for high carbon emissions. For low exergy efficiency values, integrated district heating and cooling systems even have LCOTE lower than the systems with only district heating option. For high exergy efficiency systems, in the region of low carbon emissions, the difference greatly rises. However, it can be concluded that the cost of the integrated system is kept relatively similar to the DH-only systems. In other words, whenever possible, district cooling should be made available. Nevertheless, it should be mentioned that introduction of district cooling in the buildings is challenging issue due to the distributions systems which should be taken into account. Unfortunately, this analysis is out of the scope of this paper and was not considered.

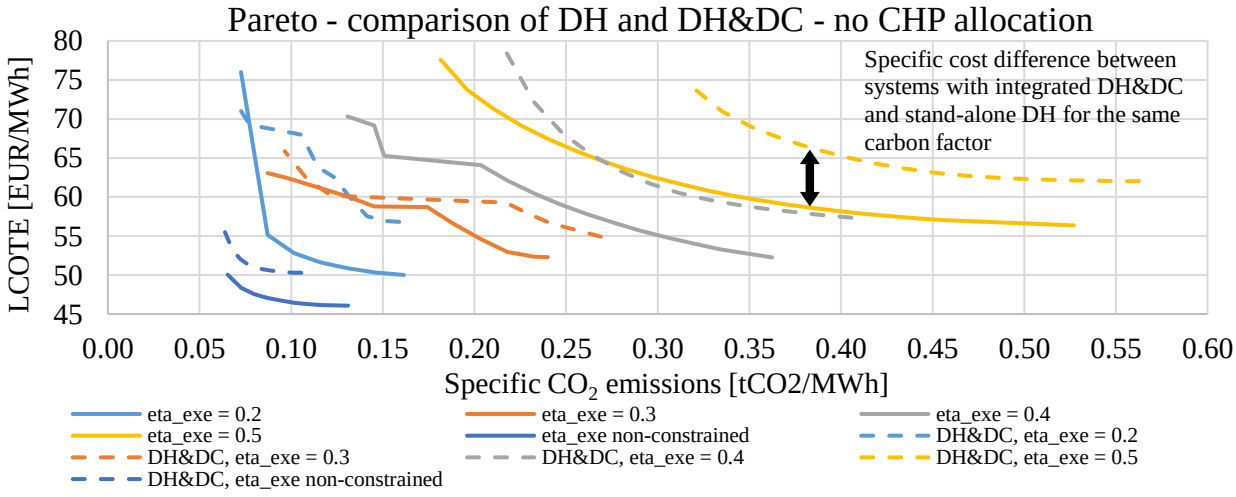

Figure 12 Pareto front comparison for systems with integrated district heating and cooling and a stand-alone district heating system – no CHP allocation implemented

4.4.2. CHP cost allocation

Figure 13 shows the impact of district cooling (DC) integration for CHP cost allocation. Once again, it can be noticed how the cost difference for DH-only and DH-DC integrated systems is relatively small, below 5 EUR/MWh. Low-exergy efficiency solutions have almost identical specific price of the system.

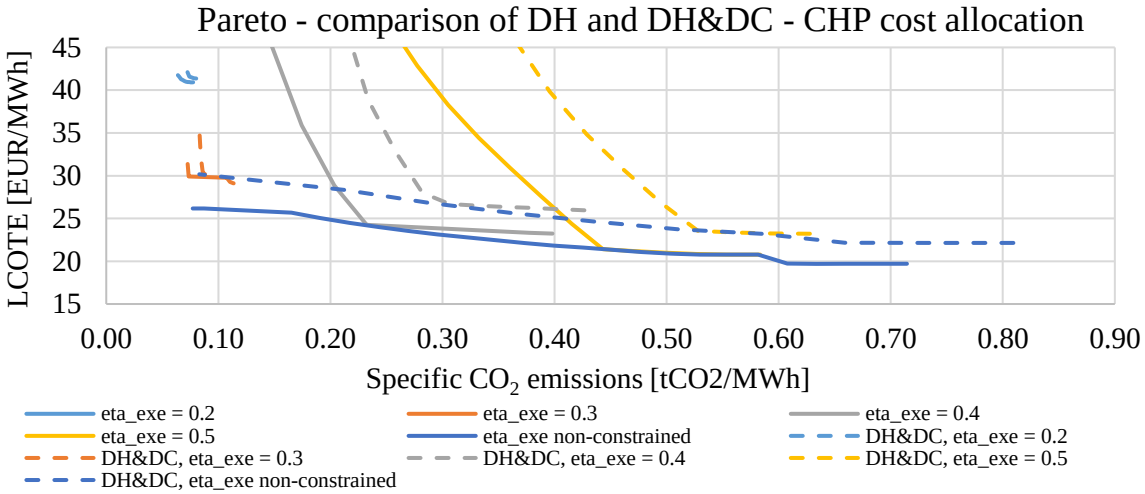

Figure 13 Pareto front comparison for systems with integrated district heating and cooling and a stand-alone district heating system –CHP cost allocation implemented

4.4.3. CHP carbon allocation

Figure 14 shows how district cooling integration behaves under CHP carbon allocation. Once again, the cost difference is relatively low, under 5 EUR/MWh. It should be noticed that full and dashed Pareto fronts are getting closer for low carbon factors. In other words, integration of district heating and cooling systems is more feasible for lower carbon emissions.

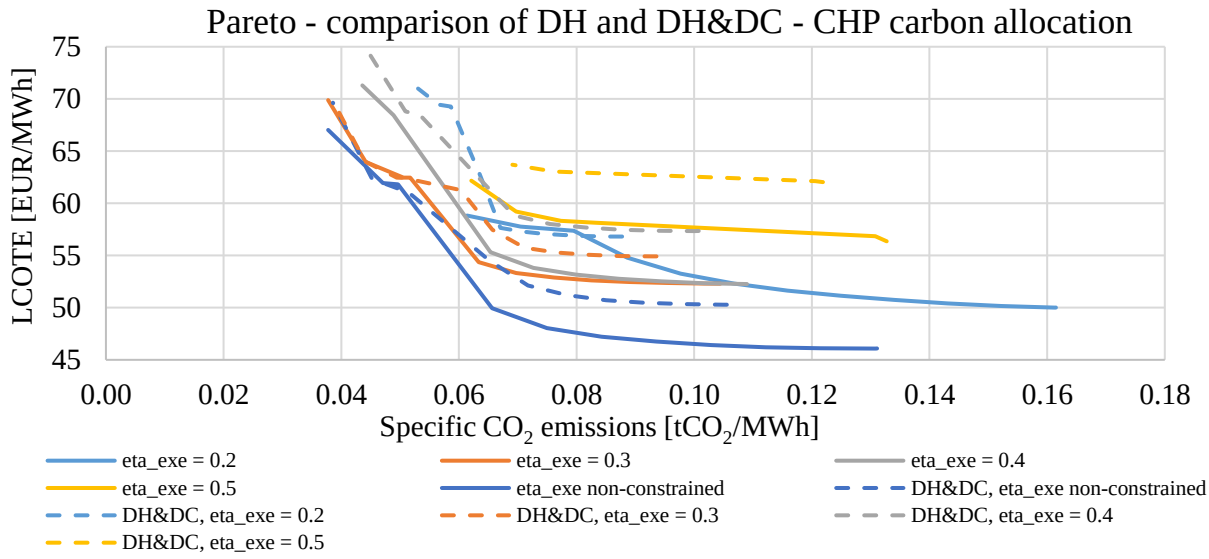

Figure 14 Pareto front comparison for systems with integrated district heating and cooling and a stand-alone district heating system –CHP carbon allocation implemented

4.4.4. CHP cost and carbon allocation

Finally, Figure 15 displays how does district cooling integration influences the results when both cost and carbon allocations are implemented. Cost of difference of 5 EUR/MWh is also kept here. For low exergy efficiencies, the difference is almost equal to zero.

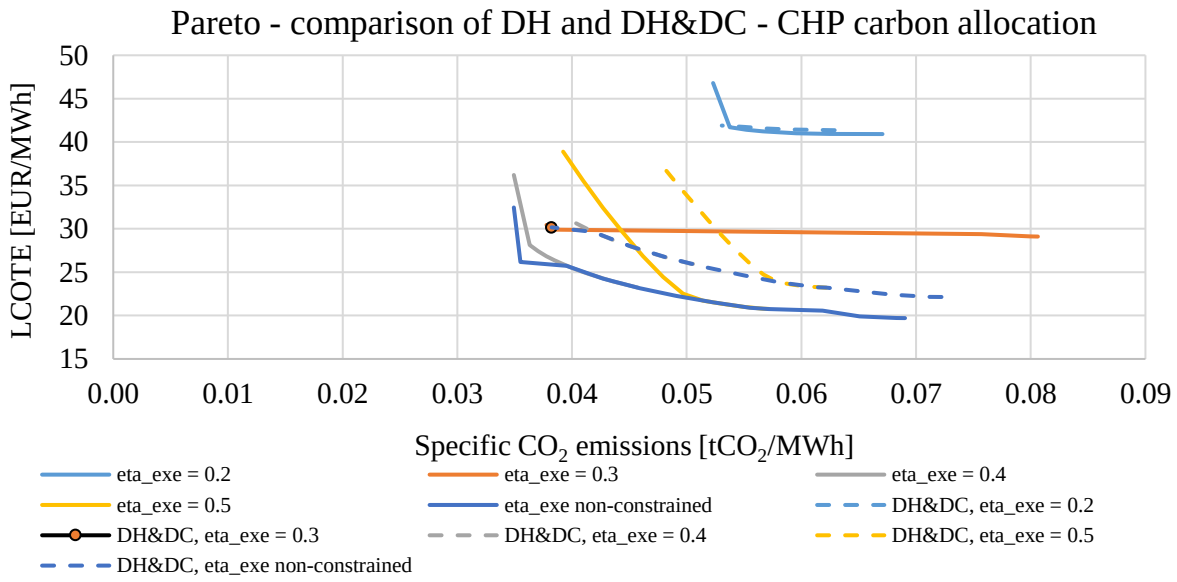

Figure 15 Pareto front comparison for systems with integrated district heating and cooling and a stand-alone district heating system – CHP cost and carbon allocation implemented

5. Conclusion

In this paper, multi objective optimization of district heating, coupled with cogeneration cost and carbon allocation, has been used to provide systematic comparison with individual natural gas-based solutions. The model considers minimization of total cost, carbon emissions and maximization of exergy efficiency. It can optimize supply capacities, including thermal storage, and hourly operation of the system for a whole year. The allocation method is based on translating power-loss, caused by the heat production, to CHP's operational cost and carbon emissions which are allocated to heat production. Obtained results show how increase of exergy efficiency of the system (followed by growth of CHP share) causes rise of system's levelized cost of heat (LCOH) and carbon factor if no allocation in CHP units is implemented. However, once cost and carbon emissions are allocated in CHP units, the results changed drastically. Cost allocation triggered 50% reduction of the system cost, when compared to the reference case, but carbon factor is increased by approximately 30%. Carbon allocation causes great reduction of carbon emissions with no noticeable increase of LCOH. Combined allocation caused simultaneous reduction of carbon factor and LCOH with exergy efficiency increase. These results have also been compared with individual heating based on natural gas. To declare district heating solution superior to the individual heating, it must have lower carbon factor and LCOH. With no implemented heat allocation methods, no district heating solutions are better than individual for low households' natural gas prices. With implemented cost allocation part of the Pareto solutions are superior to individual natural gas heating, however the solutions with the highest exergy efficiency are not. Implementation of carbon allocation positions all district heating solutions in the region with lower carbon factor, however all solutions have higher LCOH when compared to individual heating which utilizes cheap natural gas. Finally, combined cost and carbon allocation makes all district heating solutions, which include CHP, superior to individual systems. In addition to this, analysis of district cooling integration has been carried out. Obtained results show how for small increase of specific cost, cooling energy production could be included in a system.

Appendix

A1 Input data distributions

In this Section, hourly input data are shown. Figure A1 shows meteorological data for a case study – outside temperature and global solar radiation. District heating supply temperature regime is shown in Figure A2. It is assumed that it is in direct correlation with outside temperature. Maximum supply temperature is around 115°C, while minimum supply temperature is 80°C to supply thermal energy needed for domestic hot water production. District heating load is shown in Figure A3. Peak load of the system is around 450 MW. Furthermore, Figure A4 shows hourly power market prices which are used to calculate operational cost of power-to-heat and cogeneration technologies.

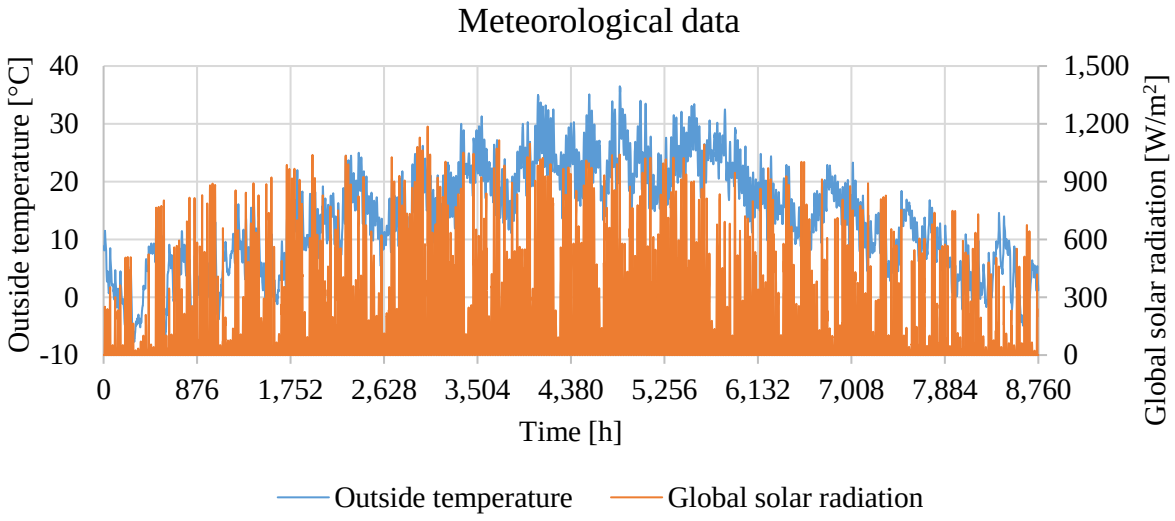

Figure A1 Meteorological data – outside temperature and global solar radiation

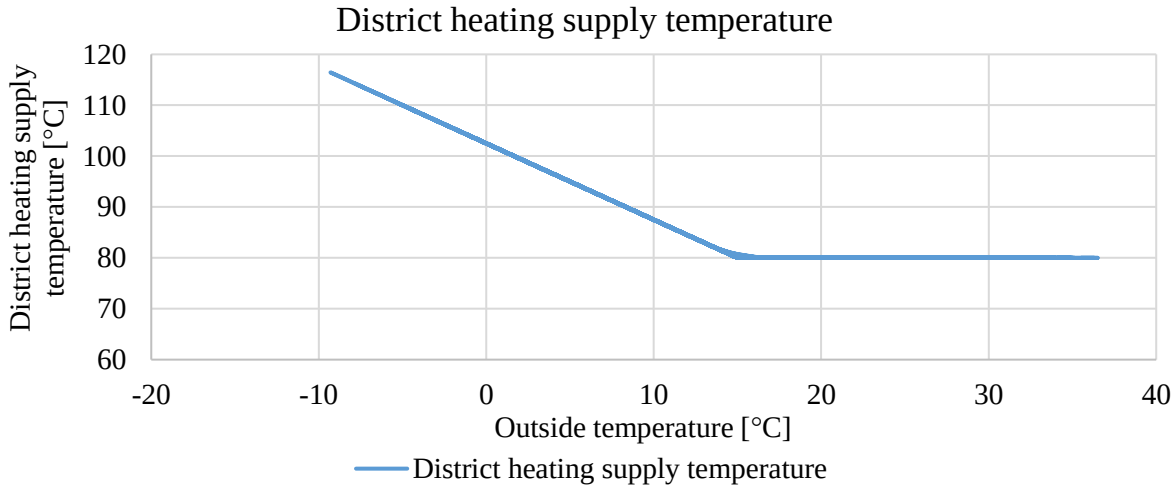

Figure A2 District heating supply network temperature

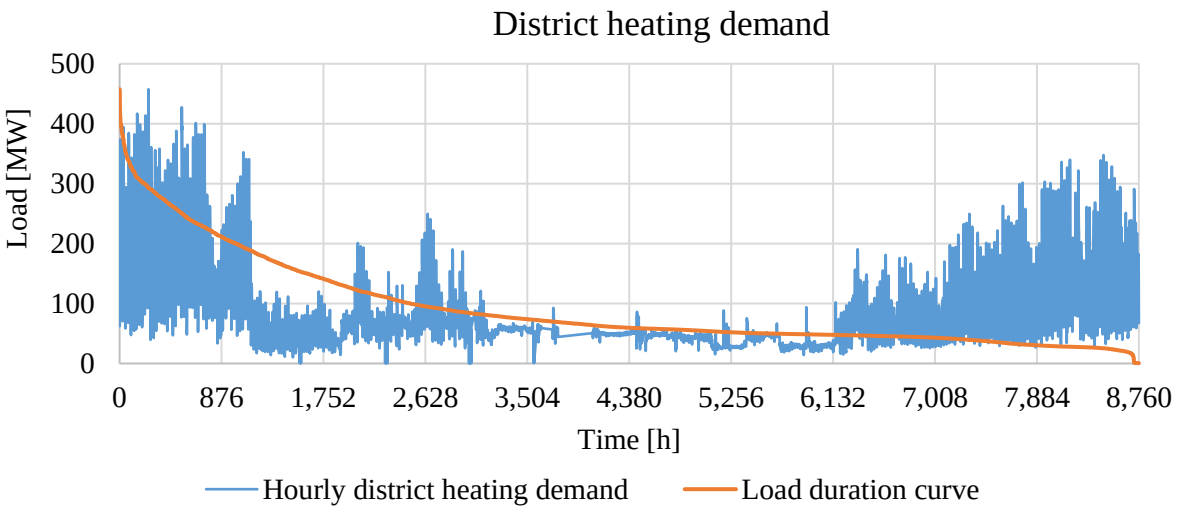

Figure A3 District heating demand – hourly demand and load duration curve

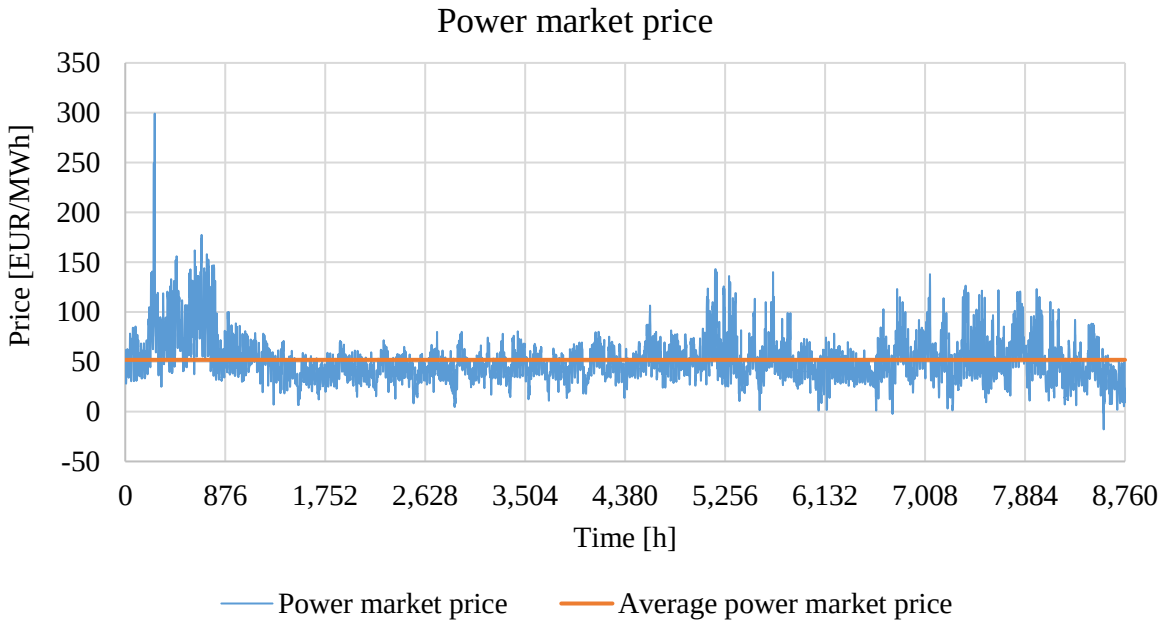

Figure A4 Hourly and average power market price

A2 District heating system overview

Figure A5 illustrates correlation between all technologies and related optimization variables. District heating supply units are supplying district heating demand and are connected to thermal storage units. It should be noticed that only solar thermal collectors are charging seasonal thermal storage. Power-to-heat and cogeneration units are also connected to the power market.

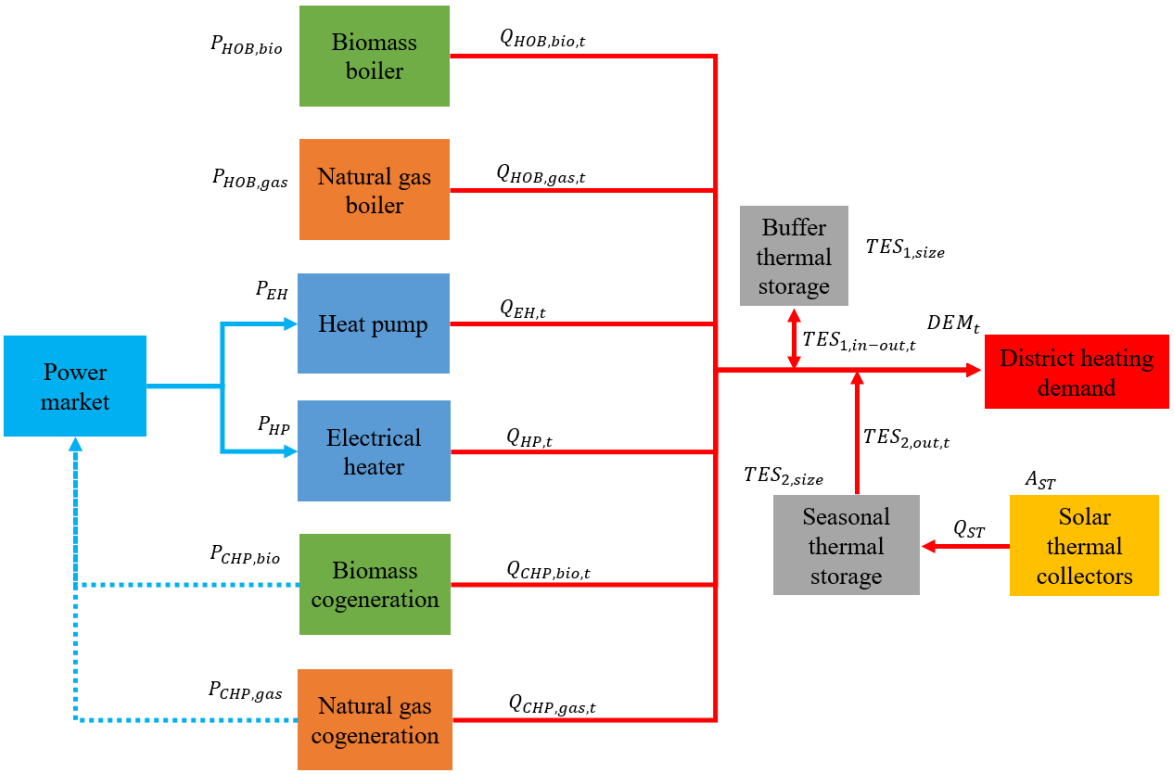

Figure A5 – District heating system overview

A3 Energy and exergy output RES share

This Section presents results of the analysis of energy and exergy output renewable energy sources share. In other words, the obtained results show how much of energy and exergy output is covered by renewable energy in district heating system. It should be mention that this analysis was carried out for different CHP allocation methods. Figure A6 shows the obtained results. In order to simplify visualization, only economic objective function (LCOH) is shown on x-axis, while exergy efficiency of a supply system is plotted as a parameter. Y-axis of diagram shows energy and exergy output RES share. For no CHP allocation, increase of LCOH rapidly increases RES share, as shown in Figure A6a. Furthermore, it should be noticed, that RES share falls down with exergy efficiency increase, due to usage of natural gas CHP. Similar results can be seen in Figure A6b where cost allocation in CHP units is implemented. Figure A6c shows the results with carbon allocation. It should be noticed that low exergy efficiency results have relatively high RES share, due to utilization of biomass. Finally, when both carbon and cost allocation is implemented, increase of exergy efficiency reduces RES share, as shown in Figure A6d.

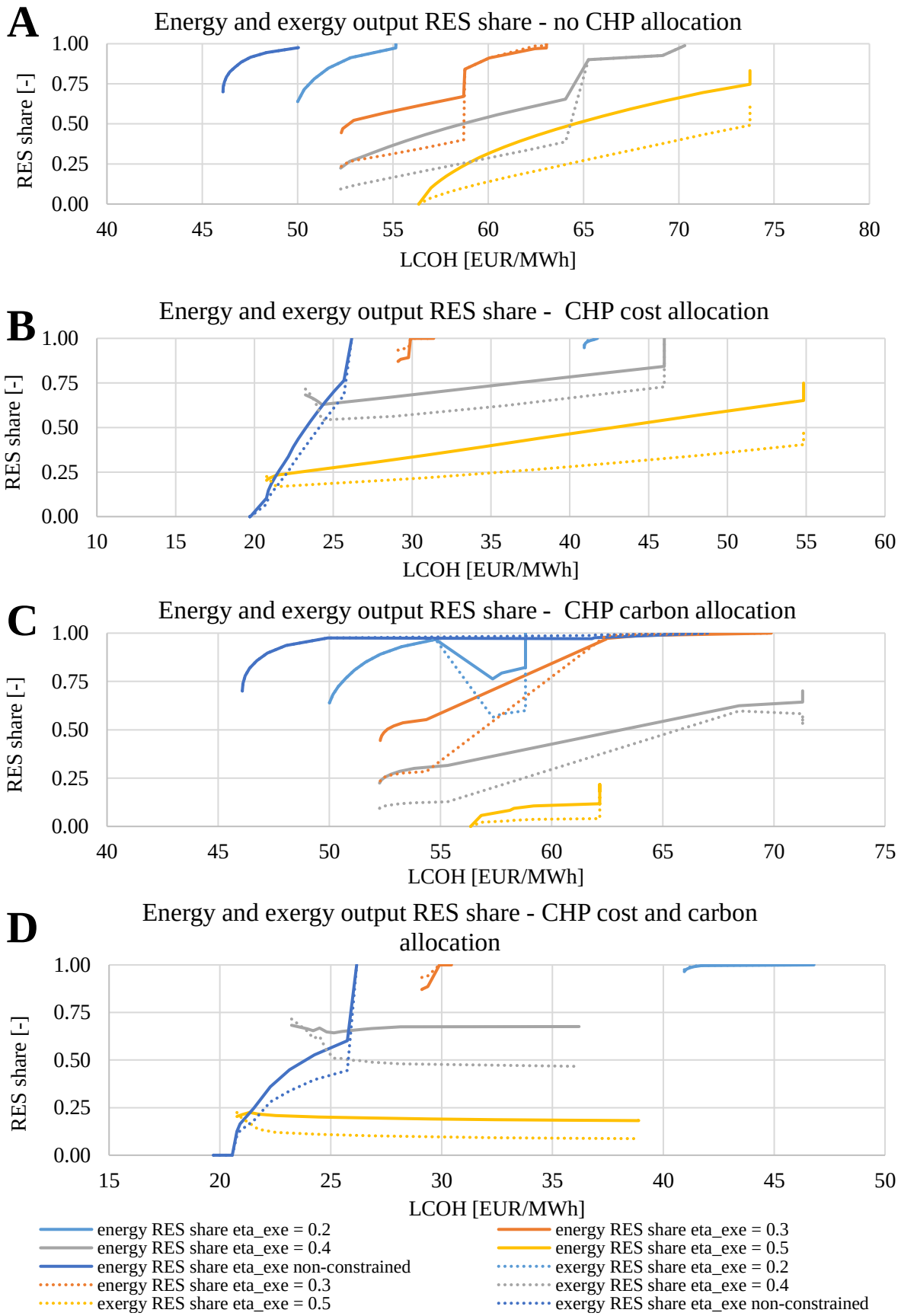

Figure A6 Energy and exergy output share of RES for different CHP allocation methods: A) no allocation, B) cost allocation, C) carbon allocation, D) cost and carbon allocation

References

[1] H. Lund *et al.*, "The Status of 4 th Generation District Heating : Research and Results," *Energy*, 2018, doi: 10.1016/j.energy.2018.08.206.

[2] H. Lund *et al.*, "4th Generation District Heating (4GDH). Integrating smart thermal grids into future sustainable energy systems.," *Energy*, vol. 68, pp. 1–11, 2014, doi: 10.1016/j.energy.2014.02.089.

[3] P. A. Østergaard and A. N. Andersen, "Booster heat pumps and central heat pumps in district heating," *Appl. Energy*, vol. 184, pp. 1374–1388, 2016, doi: 10.1016/j.apenergy.2016.02.144.

[4] B. V. Mathiesen *et al.*, "Smart Energy Systems for coherent 100% renewable energy and transport solutions," *Appl. Energy*, vol. 145, pp. 139–154, 2015, doi: 10.1016/j.apenergy.2015.01.075.

[5] E. Guelpa and V. Verda, "Thermal energy storage in district heating and cooling systems: A review," *Appl. Energy*, vol. 252, no. June, p. 113474, 2019, doi: 10.1016/j.apenergy.2019.113474.

[6] M. A. Sayegh *et al.*, "Trends of European research and development in district heating technologies," *Renew. Sustain. Energy Rev.*, vol. 68, pp. 1183–1192, 2017, doi: 10.1016/j.rser.2016.02.023.

[7] M. Wahlroos, M. Pärssinen, S. Rinne, S. Syri, and J. Manner, "Future views on waste heat utilization – Case of data centers in Northern Europe," *Renew. Sustain. Energy Rev.*, vol. 82, no. July 2017, pp. 1749–1764, 2018, doi: 10.1016/j.rser.2017.10.058.

[8] G. F. Davies, G. G. Maidment, and R. M. Tozer, "Using data centres for combined heating and cooling: An investigation for London," *Appl. Therm. Eng.*, vol. 94, pp. 296–304, 2016, doi: 10.1016/j.applthermaleng.2015.09.111.

[9] "ReUseHeat project, Horizon2020." [Online]. Available: https://www.reuseheat.eu/.

[10] T. Ommen, J. E. Thorsen, W. B. Markussen, and B. Elmegaard, "Performance of ultra low temperature district heating systems with utility plant and booster heat pumps," *Energy*, vol. 137, pp. 544–555, 2017, doi: 10.1016/j.energy.2017.05.165.

[11] B. Elmegaard, T. S. Ommen, M. Markussen, and J. Iversen, "Integration of space heating and hot water supply in low temperature district heating," *Energy Build.*, vol. 124, pp. 255–264, 2016, doi: 10.1016/j.enbuild.2015.09.003.

[12] T. Ommen, W. B. Markussen, and B. Elmegaard, "Lowering district heating temperatures - Impact to system performance in current and future Danish energy scenarios," *Energy*, vol. 94, no. 3, pp. 273–291, 2016, doi: 10.1016/j.energy.2015.10.063.

[13] T. Ommen, W. B. Markussen, and B. Elmegaard, "Heat pumps in combined heat and power systems," *Energy*, vol. 76, pp. 989–1000, 2014, doi: 10.1016/j.energy.2014.09.016.

[14] S. Buffa, M. Cozzini, M. D'Antoni, M. Baratieri, and R. Fedrizzi, "5th generation district heating and cooling systems: A review of existing cases in Europe," *Renew. Sustain. Energy Rev.*, vol. 104, no. June 2018, pp. 504–522, 2019, doi: 10.1016/j.rser.2018.12.059.

[15] H. Averfalk and S. Werner, “Essential improvements in future district heating systems,” *Energy Procedia*, vol. 116, pp. 217–225, 2017, doi: 10.1016/j.egypro.2017.05.069.

[16] S. Werner, “International review of district heating and cooling,” *Energy*, vol. 137, pp. 617–631, 2017, doi: 10.1016/j.energy.2017.04.045.

[17] J. Jimenez-Navarro, K. Kavvadias, F. Filippidou, M. Pavičević, and S. Quoilin, “Coupling the heating and power sectors : The role of centralised combined heat and power plants and district heat in a European decarbonised power system,” *Appl. Energy*, vol. 270, no. May, 2020, doi: 10.1016/j.apenergy.2020.115134.

[18] D. F. Dominković, G. Stunjek, I. Blanco, H. Madsen, and G. Krajačić, “Technical, economic and environmental optimization of district heating expansion in an urban agglomeration,” *Energy*, vol. 197, p. 117243, 2020, doi: 10.1016/j.energy.2020.117243.

[19] M. Tańczuk, J. Skorek, and P. Bargiel, “Energy and economic optimization of the repowering of coal-fired municipal district heating source by a gas turbine,” *Energy Convers. Manag.*, vol. 149, pp. 885–895, 2017, doi: 10.1016/j.enconman.2017.03.053.

[20] V. M. Soltero, R. Chacartegui, C. Ortiz, and R. Velázquez, “Evaluation of the potential of natural gas district heating cogeneration in Spain as a tool for decarbonisation of the economy,” *Energy*, vol. 115, pp. 1513–1532, 2016, doi: 10.1016/j.energy.2016.06.038.

[21] F. Sun, X. Zhao, X. Chen, L. Fu, and L. Liu, “New configurations of district heating system based on natural gas and deep geothermal energy for higher energy efficiency in northern China,” *Appl. Therm. Eng.*, vol. 151, no. April 2018, pp. 439–450, 2019, doi: 10.1016/j.applthermaleng.2019.02.043.

[22] M. Terhan and K. Comakli, “Energy and exergy analyses of natural gas-fired boilers in a district heating system,” *Appl. Therm. Eng.*, vol. 121, no. April, pp. 380–387, 2017, doi: 10.1016/j.applthermaleng.2017.04.091.

[23] “EUROSTAT.” [Online]. Available: https://ec.europa.eu/eurostat/data/database.

[24] L. Björnebo, S. Spatari, and P. L. Gurian, “A greenhouse gas abatement framework for investment in district heating,” *Appl. Energy*, vol. 211, no. June 2017, pp. 1095–1105, 2018, doi: 10.1016/j.apenergy.2017.12.003.

[25] T. Yoon, Y. Ma, and C. Rhodes, “Individual Heating systems vs. District Heating systems : What will consumers pay for convenience ?,” *Energy Policy*, vol. 86, pp. 73–81, 2015, doi: 10.1016/j.enpol.2015.06.024.

[26] H. Ahvenniemi and K. Klobut, “Future services for district heating solutions in residential districts,” *J. Sustain. Dev. Energy, Water Environ. Syst.*, vol. 2, no. 2, pp. 127–138, 2014, doi: 10.13044/j.sdewes.2014.02.0012.

[27] M. Brum, P. Erickson, B. Jenkins, and K. Kornbluth, “A comparative study of district and individual energy systems providing electrical-based heating , cooling , and domestic hot water to a low-energy use residential community,” vol. 92, no. 100, pp. 306–312, 2015.

[28] C. H. Hansen, O. Gudmundsson, and N. Detlefsen, “Cost efficiency of district heating for low energy buildings of the future,” *Energy*, vol. 177, pp. 77–86, 2019, doi: 10.1016/j.energy.2019.04.046.

[29] D. S. Østergaard and S. Svendsen, “Costs and benefits of preparing existing Danish

buildings for low-temperature district heating," *Energy*, vol. 176, pp. 718–727, 2019, doi: 10.1016/j.energy.2019.03.186.

[30] M. Noussan, "Allocation factors in Combined Heat and Power systems – Comparison of di ff erent methods in real applications," *Energy Convers. Manag.*, vol. 173, no. June, pp. 516–526, 2018, doi: 10.1016/j.enconman.2018.07.103.

[31] T. Tereshchenko and N. Nord, "Uncertainty of the allocation factors of heat and electricity production of combined cycle power plant," *Appl. Therm. Eng.*, vol. 76, pp. 410–422, 2015, doi: 10.1016/j.applthermaleng.2014.11.019.

[32] J. Gao, Q. Zhang, X. Wang, D. Song, and W. Liu, "Exergy and exergoeconomic analyses with modeling for CO 2 allocation of coal- fi red CHP plants," *Energy*, vol. 152, pp. 562–575, 2018, doi: 10.1016/j.energy.2018.03.171.

[33] E. A. Pina, M. A. Lozano, and L. M. Serra, "Thermoeconomic cost allocation in simple trigeneration systems including thermal energy storage," *Energy*, vol. 153, pp. 170–184, 2018, doi: 10.1016/j.energy.2018.04.012.

[34] Z. Wang, W. Han, N. Zhang, M. Liu, and H. Jin, "Exergy cost allocation method based on energy level (ECAEL) for a CCHP system," *Energy*, 2017, doi: 10.1016/j.energy.2017.06.015.

[35] J. Gao, Q. Zhang, X. Wang, D. Song, W. Liu, and W. Liu, "Exergy and exergoeconomic analyses with modeling for CO2 allocation of coal-fired CHP plants," *Energy*, vol. 152, pp. 562–575, Jun. 2018, doi: 10.1016/j.energy.2018.03.171.

[36] J. A. M. da Silva, J. J. C. S. Santos, M. Carvalho, and S. de Oliveira, "On the thermoeconomic and LCA methods for waste and fuel allocation in multiproduct systems," *Energy*, vol. 127, pp. 775–785, May 2017, doi: 10.1016/j.energy.2017.03.147.

[37] R. G. dos Santos, P. R. de Faria, J. J. C. S. Santos, J. A. M. da Silva, and D. Flórez-Orrego, "Thermoeconomic modeling for CO 2 allocation in steam and gas turbine cogeneration systems," *Energy*, vol. 117, pp. 590–603, Dec. 2016, doi: 10.1016/j.energy.2016.04.019.

[38] D. Flórez-Orrego and S. de Oliveira Junior, "On the efficiency, exergy costs and CO 2 emission cost allocation for an integrated syngas and ammonia production plant," *Energy*, vol. 117, pp. 341–360, Dec. 2016, doi: 10.1016/j.energy.2016.05.096.

[39] M. Harmelink and L. Bosselaar, "Allocating CO2 emissions to heat and electricity," 2015. [Online]. Available: http://harmelinkconsulting.nl/files/2015-09/harmelinkconsulting-ca8d6d8ab68a5197ace66a1969af4957-allocating-co2-emissions-to-heat-and-ele.pdf.

[40] T. Sander and D. S. Robbi, "Allocation of CO2 -Emissions to Power and Heat from CHP Plants." [Online]. Available: https://tu-dresden.de/ing/maschinenwesen/iet/gewv/ressourcen/dateien/veroefftlg/alloc_co2?lang=en.

[41] Ecoheat4cities, "Technical report on labeling criteria for DHC," 2011. [Online]. Available: https://www.euroheat.org/wp-content/uploads/2016/04/Ecoheat4cities_2.1_Final_Technical-Report.pdf.

[42] T. Tereshchenko and N. Nord, "Energy planning of district heating for future building stock based on renewable energies and increasing supply flexibility," *Energy*, vol. 112,

pp. 1227–1244, 2016, doi: 10.1016/j.energy.2016.04.114.

[43] L. Nordenstam, D. Djuric Ilic, and L. Ödlund, “Corporate greenhouse gas inventories, guarantees of origin and combined heat and power production – Analysis of impacts on total carbon dioxide emissions,” *J. Clean. Prod.*, vol. 186, pp. 203–214, 2018, doi: 10.1016/j.jclepro.2018.03.034.

[44] T. Falke, S. Krengel, A.-K. Meinerzhagen, and A. Schnettler, “Multi-objective optimization and simulation model for the design of distributed energy systems,” *Applied Energy*. 2016, doi: 10.1016/j.apenergy.2016.03.044.

[45] M. Ameri and Z. Besharati, “Optimal design and operation of district heating and cooling networks with CCHP systems in a residential complex,” *Energy Build.*, vol. 110, pp. 135–148, 2016, doi: 10.1016/j.enbuild.2015.10.050.

[46] A. Franco and M. Versace, “Multi-objective optimization for the maximization of the operating share of cogeneration system in District Heating Network,” *Energy Convers. Manag.*, vol. 139, pp. 33–44, 2017, doi: 10.1016/j.enconman.2017.02.029.

[47] M. Di Somma *et al.*, “Operation optimization of a distributed energy system considering energy costs and exergy efficiency,” *Energy Convers. Manag.*, vol. 103, pp. 739–751, 2015, doi: 10.1016/j.enconman.2015.07.009.

[48] M. Di Somma *et al.*, “Multi-objective design optimization of distributed energy systems through cost and exergy assessments,” *Appl. Energy*, vol. 204, pp. 1299–1316, 2017, doi: 10.1016/j.apenergy.2017.03.105.

[49] M. Pirouti, A. Bagdanavicius, J. Ekanayake, J. Wu, and N. Jenkins, “Energy consumption and economic analyses of a district heating network,” *Energy*, vol. 57, pp. 149–159, 2013, doi: 10.1016/j.energy.2013.01.065.

[50] R. Mikulandrić *et al.*, “Performance analysis of a hybrid district heating system: A case study of a small town in Croatia,” *J. Sustain. Dev. Energy, Water Environ. Syst.*, vol. 3, no. 3, pp. 282–302, 2015, doi: 10.13044/j.sdewes.2015.03.0022.

[51] J. Huang, J. Fan, S. Furbo, D. Chen, Y. Dai, and W. Kong, “Economic analysis and optimization of combined solar district heating technologies and systems,” *Energy*, vol. 186, p. 115886, Nov. 2019, doi: 10.1016/j.energy.2019.115886.

[52] M. Pavičević, T. Novosel, T. Pukšec, and N. Duić, “Hourly optimization and sizing of district heating systems considering building refurbishment - Case study for the city of Zagreb,” *Energy*, 2016, doi: 10.1016/j.energy.2017.06.105.

[53] H. Dorotić, T. Pukšec, and N. Duić, “Multi-objective optimization of district heating and cooling systems for a one-year time horizon,” *Energy*, vol. 169, pp. 319–328, Feb. 2019, doi: 10.1016/j.energy.2018.11.149.

[54] M. Leśko, W. Bujalski, and K. Futyma, “Operational optimization in district heating systems with the use of thermal energy storage,” *Energy*, vol. 165, pp. 902–915, Dec. 2018, doi: 10.1016/j.energy.2018.09.141.

[55] A. Kazagic, A. Merzic, E. Redzic, and D. Tresnjo, “Optimization of modular district heating solution based on CHP and RES - Demonstration case of the Municipality of Visoko,” *Energy*, vol. 181, pp. 56–65, 2019, doi: 10.1016/j.energy.2019.05.132.

[56] P. Jie, F. Yan, J. Li, Y. Zhang, and Z. Wen, “Optimizing the insulation thickness of walls

of existing buildings with CHP-based district heating systems," *Energy*, vol. 189, p. 116262, Dec. 2019, doi: 10.1016/j.energy.2019.116262.

[57] B. Morvaj, R. Evins, and J. Carmeliet, "Optimising urban energy systems: Simultaneous system sizing, operation and district heating network layout," *Energy*, vol. 116, pp. 619–636, 2016, doi: 10.1016/j.energy.2016.09.139.

[58] A. Delangle, R. S. C. Lambert, N. Shah, S. Acha, and C. N. Markides, "Modelling and optimising the marginal expansion of an existing district heating network," *Energy*, vol. 140, pp. 209–223, 2017, doi: 10.1016/j.energy.2017.08.066.

[59] H. Dorotić, T. Pukšec, and N. Duić, "Economical, environmental and exergetic multi-objective optimization of district heating systems on hourly level for a whole year," *Appl. Energy*, vol. 251, p. 113394, Oct. 2019, doi: 10.1016/j.apenergy.2019.113394.

[60] B. van der Heijde, A. Vandermeulen, R. Salenbien, and L. Helsen, "Integrated optimal design and control of fourth generation district heating networks with thermal energy storage," *Energies*, vol. 12, no. 14, 2019, doi: 10.3390/en12142766.

[61] J. P. Jiménez Navarro, K. C. Kavvadias, S. Quoilin, and A. Zucker, "The joint effect of centralised cogeneration plants and thermal storage on the efficiency and cost of the power system," *Energy*, vol. 149, pp. 535–549, 2018, doi: 10.1016/j.energy.2018.02.025.

[62] A. Christidis, C. Koch, L. Pottel, and G. Tsatsaronis, "The contribution of heat storage to the profitable operation of combined heat and power plants in liberalized electricity markets," *Energy*, vol. 41, no. 1, pp. 75–82, 2012, doi: 10.1016/j.energy.2011.06.048.

[63] W. Jakob and C. Blume, "Pareto optimization or cascaded weighted sum: A comparison of concepts," *Algorithms*, vol. 7, no. 1, pp. 166–185, 2014, doi: 10.3390/a7010166.

[64] "Danish Energy Agency Technology data." [Online]. Available: https://ens.dk/en/our-services/projections-and-models/technology-data.

[65] S. Grosse, R., Christopher, B., Stefan, W., Geyer, R. and Robbi, "Long term (2050) projections of techno-economic performance of large-scale heating and cooling in the EU," *Publications Office of the European Union*, 2017. [Online]. Available: http://data.europa.eu/89h/jrc-etri-techno-economics-larger-heating-cooling-technologies-2017.

[66] B. Möller and S. Werner, "Quantifying the Potential for District Heating and Cooling in EU Member States, STRATEGO project," 2016. [Online]. Available: http://www.heatroadmap.eu/resources/STRATEGO WP2 - Background Report 6 - Mapping Potenital for DHC.pdf.

[67] "Julia." [Online]. Available: https://julialang.org/.

[68] "JuMP." [Online]. Available: http://www.juliaopt.org/JuMP.jl/0.18/.

[69] "Gurobi." [Online]. Available: https://www.gurobi.com.